THE UNIVERSITY
of EDINBURGH

Investigating the role of Cdc14 in the regulation of the meiosis I to meiosis II transition.

Colette Connor

Thesis presented for the degree of Doctor of Philosophy
The University of Edinburgh
2015

Declaration

I declare that this thesis was composed by myself, that the work contained herein is my own except where explicitly stated otherwise in the text, and that this work has not been submitted for any other degree or professional qualification except as specified.

Colette Connor

Acknowledgements

I would like to thank all the people who have helped me throughout my PhD. While this is by no means an exhaustive list of all the awesome people who have donated their time, expertise and enthusiasm to aid me in my research, hopefully I have remembered to thank the key individuals without whom this work would not be possible.

Foremost, I would like to thank Adèle Marston for giving me the opportunity to undertake my PhD research in her lab. The last four years have been full of frustration, elation, depression and tentative optimism, and without the continuous support, guidance and considerable patience of Adèle, I fear I would have cracked long ago. Thank you to all Marston lab members, past and present, for stimulating discussions, sharing the weekend workload and for reminding me there is always time for cake. Thank you to my PhD committee members, Ken Sawin, Bill Earnshaw and Kevin Hardwick, for their useful suggestions and invaluable comments that have helped shape my project.

Next, I would like to thank a number of people who have aided me with a plethora of technical support. Thank you to Stephen Mitchel, Tom Giddings Jr, Eileen O'Toole, Mary Morphew and Courtney Ozzello for their significant help with sample preparation and EM imaging of my meiotic cells. Thank you to Mark Winey and his lab at the University of Colorado for hosting me during my stay in Boulder. Thank you to Martin Wear for his assistance with protein purification. Thank you to Flavia Alves and Juan Zou for processing my IP samples for Mass Spec., and additionally to Flavia for her excellent training in protein sample

preparation. Thank you to Dave Kelly for letting me use his precious machines and for his stellar expertise, even if he is a Mackem.

Lastly, I would like to express my deepest appreciation to all the people who have kept me sane during the last four years. Thank you to the Minipreps, for always being up for a beer (or five) and for their mediocrity at pub quizzes. Thank you to my family, especially my parents, for the emotional and financial support. Thank you to Simon Fox, for making bad days better.

In addition, I would like to acknowledge the sacrifice of rabbits R3285-3288, affectionately known as Flopsy, Mopsy, Cottontail and Peter, who gave their lives for the pursuit of science.

Abstract

Meiosis is a specialized cell division that produces haploid gametes from a diploid progenitor cell. It consists of one round of DNA replication followed by two consecutive rounds of chromosome segregation. Homologous chromosomes segregate in meiosis I and sister chromatids segregate in meiosis II. Failure to correctly regulate meiosis can result in aneuploidy, where daughter cells inherit an incorrect number of chromosomes. Aneuploidy is usually poorly tolerated in eukaryotes, and is associated with infertility, miscarriages and birth defects.

At the meiosis I to meiosis II transition, DNA replication does not occur between chromosome segregation steps despite the need for Spindle Pole Bodies (SPBs) to be re-licensed in order to build meiosis II spindles. The mechanisms that make this distinction are not yet known.

In budding yeast, the protein phosphatase Cdc14 is essential for the progression of cells into meiosis II. Cdc14 is sequestered for the majority of the cell cycle in the nucleolus by the inhibitor Cfi1/Net, and is only released in anaphase. We have observed Cdc14 localizing to and interacting with SPB components when nucleolar sequestration is inhibited. Through fluorescence microscopy and EM analysis, we have determined that Cdc14 is required for the re-duplication of SPBs after meiosis I. Our data implies a role for Cdc14 in the phospho-regulation of SPB half-bridge component Sfi1. Cdc14 is therefore essential for the re-licensing of SPB duplication, a crucial step necessary to ensure accurate chromosome segregation in meiosis.

Abbreviations

APC - Anaphase Promoting Complex

APS – Ammonium Persulfate

ATP – Adenosine Triphosphate

bp – Base Pairs

CDK - Cyclin Dependent Kinase

DAPI – 4', 6'-diamidino-2-phenylindol

DMSO – Dimethyl Sulfoxide

DNA – Deoxyribonucleic Acid

dNTPs–Deoxyribonucleotides

DTT –Dithiothreitol

ECL – Enhanced Chemiluminescence

EDTA – Ethylenediaminetetraacetic Acid

EM – Electron Microscopy

FEAR – Cdc14 Early Anaphase Release

GAP - GTPase-Activating Protein

GEF - Guanine-nucleotide Exchange Factor

GFP – Green Fluorescent Protein

GTP - Guanosine-5'-triphosphate

HEPES – 4-(2-hydroxyethyl)-1-piperazineethanesulfonic Acid

HRP – Horse Radish Peroxidase

IF – Immunofluorescence

IP – Immunoprecipitation

IPTG - Isopropyl β-D-1-thiogalactopyranosid

kb – Kilo Base Pairs

kDa – KiloDaltons

MEN – Mitotic Exit Network

Mk – Marker

OD – Optical Density

PAGE – Polyacrylamide Gel Electrophoresis

PBS – Phosphate Buffered Saline

PCR – Polymerase Chain Reaction

PEG – Polyethylene Glycol

PMSF - Phenylmethylsulfonyl Fluoride

PP2A – Protein Phosphatase 2A

RNAi - Ribonucleic Acid Interference

SDS – Sodium Dodecyl Sulfate

SPB – Spindle Pole Body

SPO - Sporulation media

SPOC – Spindle Positioning Checkpoint

TCA – Trichloroacetic Acid

TEMED – Tetramethylethylenediamine

UTR - Untranslated Region

Table of Contents

Chapter 1

Introduction

1. Introduction

Eukaryotic cell divisions can be classified into two distinct types termed mitosis and meiosis. Mitosis is a form of asexual reproduction, during which a parental diploid cell divides and segregates sister chromatids to generate two diploid daughter cells that are genetically identical to the parental cell (Fig. 1) (reviewed by Marston and Amon 2004). Meiosis, conversely, is a specialised cell division required for sexual reproduction. Unlike in mitosis, four haploid gametes are produced from a diploid progenitor cell through two consecutive rounds of chromosome segregation (reviewed by Marston and Amon 2004). Homologous chromosomes segregate in meiosis I, referred to as a reductional division since the chromosome number is halved, and sister chromatids segregate in meiosis II in an equational division, analogous to mitosis (Fig. 1).

The transition between meiosis I and meiosis II is unique due to the absence of an intervening S-phase between meiotic chromosome divisions, as is present after every mitotic division (reviewed by Marston and Amon 2004). In mitosis, S-phase is linked to the completion of M-phase through coupling of late anaphase events with the re-firing of DNA origins (reviewed by Petronczki, Siomos et al. 2003). Once cells exit mitosis, the conditions within the cell become permissible for re-replication of DNA. Similarly, the replication of DNA initiates mitotic events. This interdependency between S-phase and M-phase ensures the proper progression of cells through the cell cycle (reviewed by Dalton 1998). Meiotic events, on the other hand, appear to be differently regulated. Despite the lack of a second round of DNA replication following meiosis I, the molecular machinery required for chromosome segregation must be re-set in order to ensure accurate

segregation of sister chromatids in meiosis II (Fig. 1). Failure to do so can lead to aneuploidy, where daughter cells contain an abnormal number of chromosomes. Aneuploidy is poorly tolerated in most animal species, observed through infertility, miscarriage and birth defects such as Down syndrome and Turner syndrome (reviewed by Hassold and Hunt 2001). In humans, the incidence of aneuploidy as a result of meiotic error in live births is only 0.3%, despite the much higher incidence of aneuploidy in conception of ~10% (reviewed by Hassold and Hunt 2001).

Currently, little is known about the regulation of the meiosis I-meiosis II transition. In this study, I set out to determine how the mitotic molecular machinery has been adapted during meiosis to allow for the specialised cell division.

Mitosis

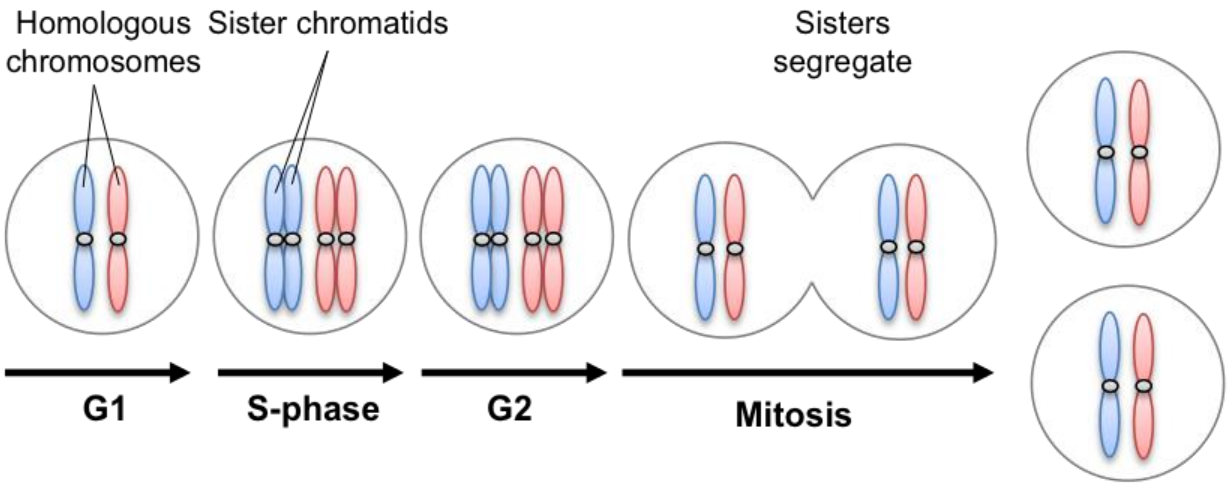

Meiosis

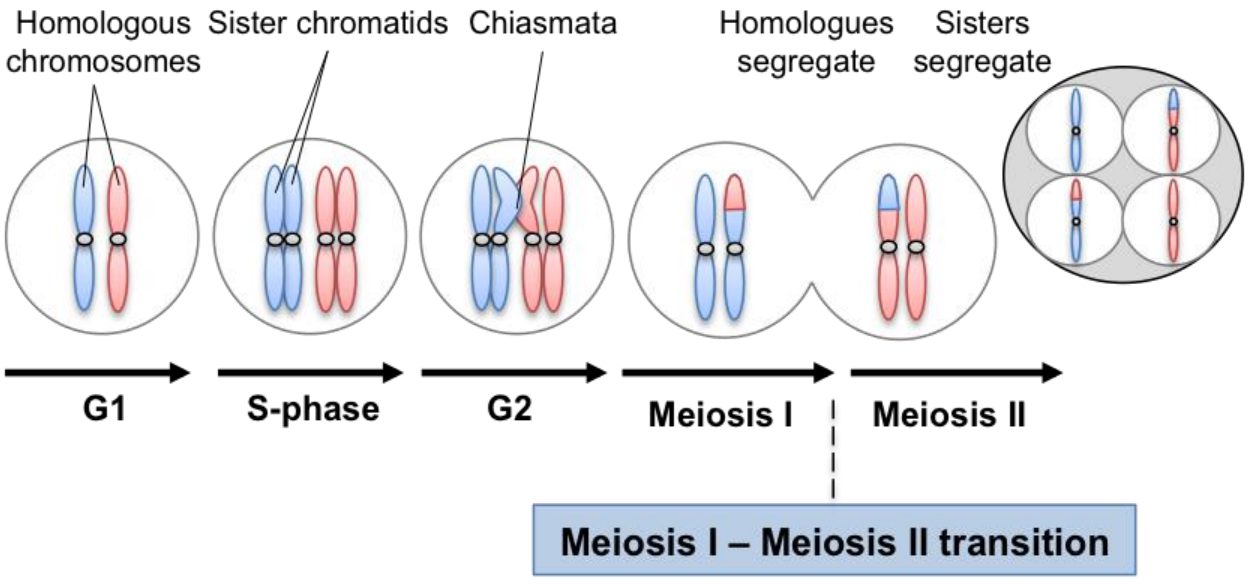

Figure 1: Mitotic versus meiotic divisions. Mitosis occurs in somatic cells and is the process through which a diploid cell duplicates itself to form two identical diploid daughter cells. Meiosis occurs in germ line cells and gives rise to four haploid gametes, which contain half the number of chromosomes of the progenitor cell. Homologous recombination occurs prior to meiotic divisions, resulting in genetic diversity in offspring.

1.1 The mitotic cell cycle

Prior to mitosis, DNA is replicated in S-phase. This chromosome duplication step results in the production of two identical sister chromatids, physically bound together by cohesin ring complexes (Uhlmann and Nasmyth 1998). Whilst cohesin is enriched at centromeres, it is also localised along chromosome arms, ensuring that sister chromatids are paired (Blat and Kleckner 1999, Megee, Mistrot et al. 1999, Tanaka, Cosma et al. 1999, Laloraya, Guacci et al. 2000).

In prophase, cells separate their microtubule organising centres, termed centrosomes, which duplicate in G1-phase but are linked to each other until entry into mitosis (reviewed by Jaspersen and Winey 2004). Following separation, these two centrosomes migrate to opposite sides of the nucleus through the action of interpolar microtubules and microtubules-associated motor proteins (reviewed by Winey and Bloom 2012)(Fig. 1. 1). Microtubules, emanating from centrosomes at opposite poles of the cell, attach to sister kinetochores and exert pulling forces on the chromosomes. This results in the alignment of chromosomes along the metaphase plate and tension across bi-oriented sister chromatids (reviewed by Guo, Kim et al. 2013). Once all sister chromatids have correctly bi-oriented, cells progress into anaphase.

Upon anaphase onset, the anaphase-promoting complex (APC), an E3 ubiquitin ligase, associates with its activator, Cdc20, and APC^{Cdc20} targets the anaphase inhibitor securin for degradation (Cohen-Fix, Peters et al. 1996, Funabiki, Yamano et al. 1996, Zachariae, Schwab et al. 1998). Loss of securin initiates separase activation, which is a protease that cleaves the cohesin complex

between sister chromatids (Fig. 1. 1) (Ciosk, Zachariae et al. 1998, Uhlmann, Lottspeich et al. 1999, Hornig, Knowles et al. 2002, Waizenegger, Gimenez-Abian et al. 2002). Without cohesin to oppose kinetochore microtubule pulling forces, sister chromatids segregate to opposite poles of the cell (Uhlmann, Lottspeich et al. 1999, Uhlmann, Wernic et al. 2000). Interpolar microtubules lengthen, pushing chromosome sets apart and ensuring that each daughter cell receives one copy of each chromosome before nuclear division in late mitosis.

Following the separation of sister chromatids in anaphase, the cell must exit mitosis and re-set itself for entry into a succeeding G1 phase. Mitotic structures, such as the mitotic spindle, must disassemble and mitotic regulators must be inactivated. One key regulator of mitosis that must be down-regulated for mitotic exit is Cdc28, the budding yeast cyclin-dependent kinase (CDK) (Ghiara, Richardson et al. 1991).

Mitosis

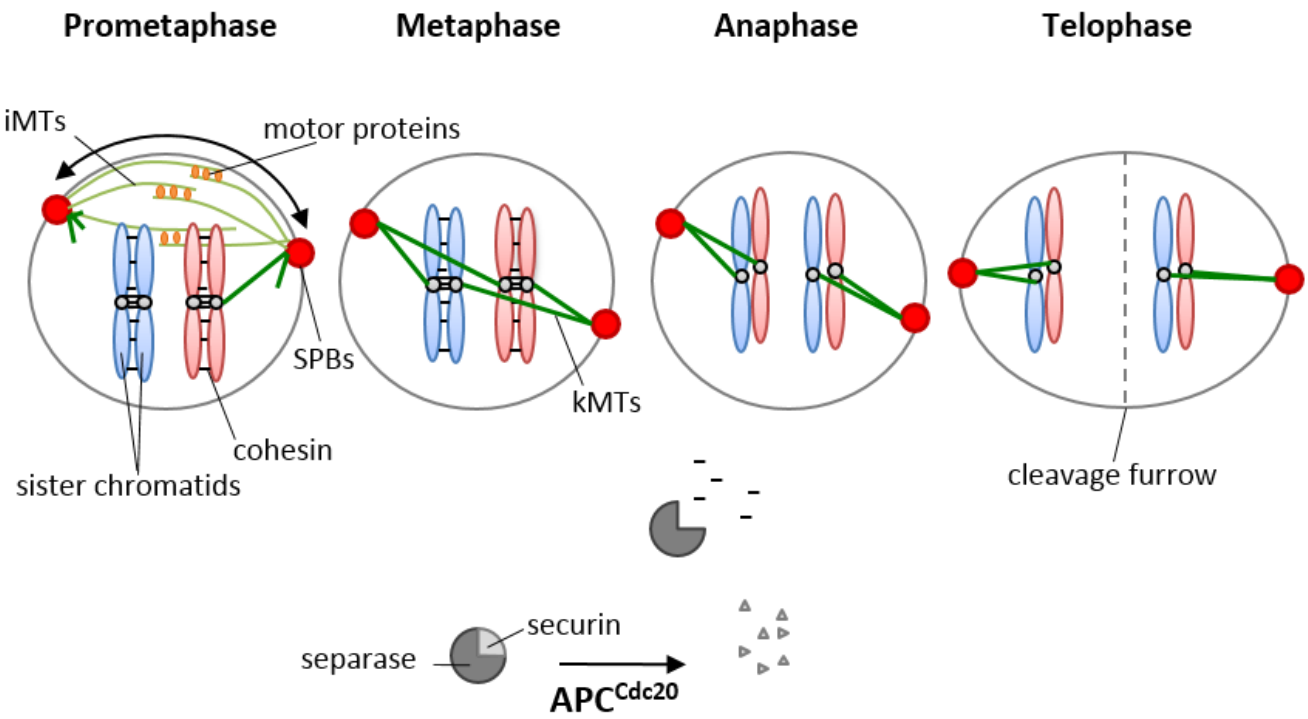

Figure 1.1: Loss of cohesin in anaphase enables sister chromatids to segregate. DNA replication occurs in S-phase, and duplicate sister chromatids are held together by cohesin. SPBs duplicate in G1 then migrate to opposite poles of the nucleus in prometaphase through the action of interpolar microtubules (iMTs) and motor proteins. SPB separation enables mitotic spindle assembly. Microtubules emanating from polar opposite SPBs (kMTs) attach to the kinetochores of sister chromatids in metaphase I, aligning bi-orientated chromatids on the metaphase plate. Upon anaphase onset, securin is degraded by APC^{Cdc20} activity. Separase is then free to cleave cohesin from the chromosomes, allowing for the separation of sister chromatids in anaphase.

1.1.1 CDKs in mitosis

CDKs play a vital role in regulating the cell cycle during mitosis. In budding yeast, multiple CDKs are formed through the association of a sole kinase, Cdc28, with different regulatory cyclin subunits (reviewed by Hartwell 1991, Nasmyth, Dirick et al. 1991). These cyclins can be divided into three main groups based on their timing of expression; G1-phase cyclins, Cln1-3, S-phase cyclins, Clb5-6, and M-phase cyclins, Clb1-4 (Richardson, Wittenberg et al. 1989, Epstein and Cross 1992, Fitch, Dahmann et al. 1992, Schwob and Nasmyth 1993). Cyclin subunits bind to Cdc28 to form cyclin-CDK complexes, which are implicated in distinct stages of the cell cycle and are required for a wide variety of cellular events. CDK-dependent phosphorylation of target proteins can affect substrate activity, localisation and stabilisation to promote the occurrence of specific downstream events at the appropriate stage of the cell cycle. These events include cell budding, spindle pole body (SPB) duplication, DNA replication, mitotic spindle formation and activation of the mitotic exit network (MEN) (reviewed in Mendenhall and Hodge 1998).

Oscillations in stage-specific cyclin levels regulate CDK function and trigger the activation of subsequent cyclins to ensure proper progression of cells through mitosis. For example, in addition to promoting bud emergence and SPB duplication, G1-phase cyclins activate B-type cyclins required in S-phase (Richardson, Wittenberg et al. 1989). G1 cyclins are then repressed by S-phase cyclin-CDK activity, assuring the correct ordering of cell cycle events.

1.1.1.1 Downstream cellular events of CDK phospho-regulation

CDKs are able to recognise multiple substrates and, therefore, are able to coordinate numerous events that occur during each cell cycle phase. In addition, the phase-specific expression of differential cyclins enables multiple cyclin-CDK complexes to drive protein signal transduction pathways throughout the cell cycle.

1.1.1.1.1 SPB duplication

One such CDK-regulated pathway is the SPB duplication pathway (Fig. 1. 1. 1. 1. 1B). SPBs are microtubule-organising centres, functionally comparable to centrosomes in higher eukaryotes (reviewed in Jaspersen and Winey 2004). They are composed of at least 19 proteins, assembled into a cylindrical organelle that is embedded in the nuclear envelope (Rout and Kilmartin 1990)(Fig. 1. 1. 1. 1. 1A). The SPB core, made up of a central, an outer and an inner plaque, traverses the nuclear envelope. It interacts with cytoplasmic and nuclear microtubules via γ-tubulin complexes formed at the outer and inner plaque respectively (Knop and Schiebel 1997, O'Toole, Winey et al. 1999). Membrane proteins, including Ndc1, Mps2 and Bbp1, localise to the SPB periphery, anchoring the SPB within the nuclear envelope (Winey, Hoyt et al. 1993). A half-bridge bilayer, consisting of Kar1, Mps3, Sfi1 and Cdc31, extends from the SPB and acts as the site for new SPB assembly (Baum, Furlong et al. 1986, Rose and Fink 1987, Spang, Courtney et al. 1993, Vallen, Ho et al. 1994, Jaspersen, Giddings et al. 2002, Kilmartin 2003). The SPB is highly phosphorylated (Wigge, Jensen et al. 1998), and many of its components have been identified as Cdc28 substrates

(Ubersax, Woodbury et al. 2003) suggesting that CDK-dependent phosphorylation of the SPB may contribute to its assembly and function.

The compilation of numerous EM studies using SPB mutants has revealed an extensive model for SPB duplication. In G1, SPB duplication is initiated by half-bridge elongation (Byers and Goetsch 1974). Once a full-bridge structure has formed, satellite material is deposited at the distal cytoplasmic tip of the bridge and expands into a duplication plaque, which resembles the cytoplasmic half of a mature SPB (Byers and Goetsch 1974, Adams and Kilmartin 1999). The plaque is then inserted into the nuclear envelope. Following this embedding step, inner plaque proteins assemble at the nuclear face of the newly duplicated SPB (Kilmartin and Goh 1996, Sundberg, Goetsch et al. 1996, Sundberg and Davis 1997). At the close of G1, two duplicated SPBs have fully assembled side-by-side physically connected by a full-bridge (Byers and Goetsch 1974). The bridge is then severed in mitosis, allowing the separation of SPBs and the formation of the mitotic spindle.

Multiple components of the SPB duplication pathway are believed to be phospho-regulated by Cdc28. Cln-CDK activity in G1 has been shown as sufficient to initiate SPB duplication (Haase, Winey et al. 2001). Cdc28 phosphorylates and stabilises another kinase, Mps1. Mps1p, alongside Cdc28, aids the self-assembly of the core SPB component, Spc42, into the higher-order structure required for duplication plaque formation (Jaspersen, Huneycutt et al. 2004).

In S-phase, Clb5- and Clb6-CDK activity promotes the severing of the full-bridge structure and subsequent SPB separation (Fig. 1. 1. 1. 1. 1B). This step is achieved via two mechanisms. Firstly, Cdc28 phosphorylates the bridge component, Sfi1. Phosphorylated Sfi1 is unable to form C-C end terminal dimers, resulting in the splitting of full-bridge structures between the two duplicated SPBs (Avena, Burns et al. 2014, Elserafy, Saric et al. 2014). Secondly, Cdc28-dependent inhibition of APC^{Cdh1} results in the accumulation of Cin8p and Kip1p motor proteins in the cell (Zachariae, Schwab et al. 1998, Crasta and Surana 2006, Crasta, Lim et al. 2008). Cin8 and Kip1 act to cross-link antiparallel non-kinetochore microtubules that exert pushing forces on SPBs, resulting in separation of the poles (Saunders and Hoyt 1992, Geiser, Schott et al. 1997, Hildebrandt and Hoyt 2001). The timely separation of duplicated SPBs is required for the assembly of a bipolar spindle in metaphase (Haase, Winey et al. 2001).

In M-phase, Clb1-4-CDK activity inhibits SPB re-duplication (Haase, Winey et al. 2001). This ensures that SPBs only duplicate once during the cell cycle (Fig. 1. 1. 1. 1. 1B). It has been suggested that Cdc28-dependent phosphorylation of Sfi1 prevents SPBs from re-duplication by preventing the initiation of half-bridge elongation (Avena, Burns et al. 2014, Elserafy, Saric et al. 2014, Bouhlel, Ohta et al. 2015). In order for SPBs to re-duplicate in the following G1-phase, Sfi1 must be dephosphorylated and Clb-CDKs inhibited. Oscillations in CDK activities, therefore, enable multi-step control of SPB duplication.

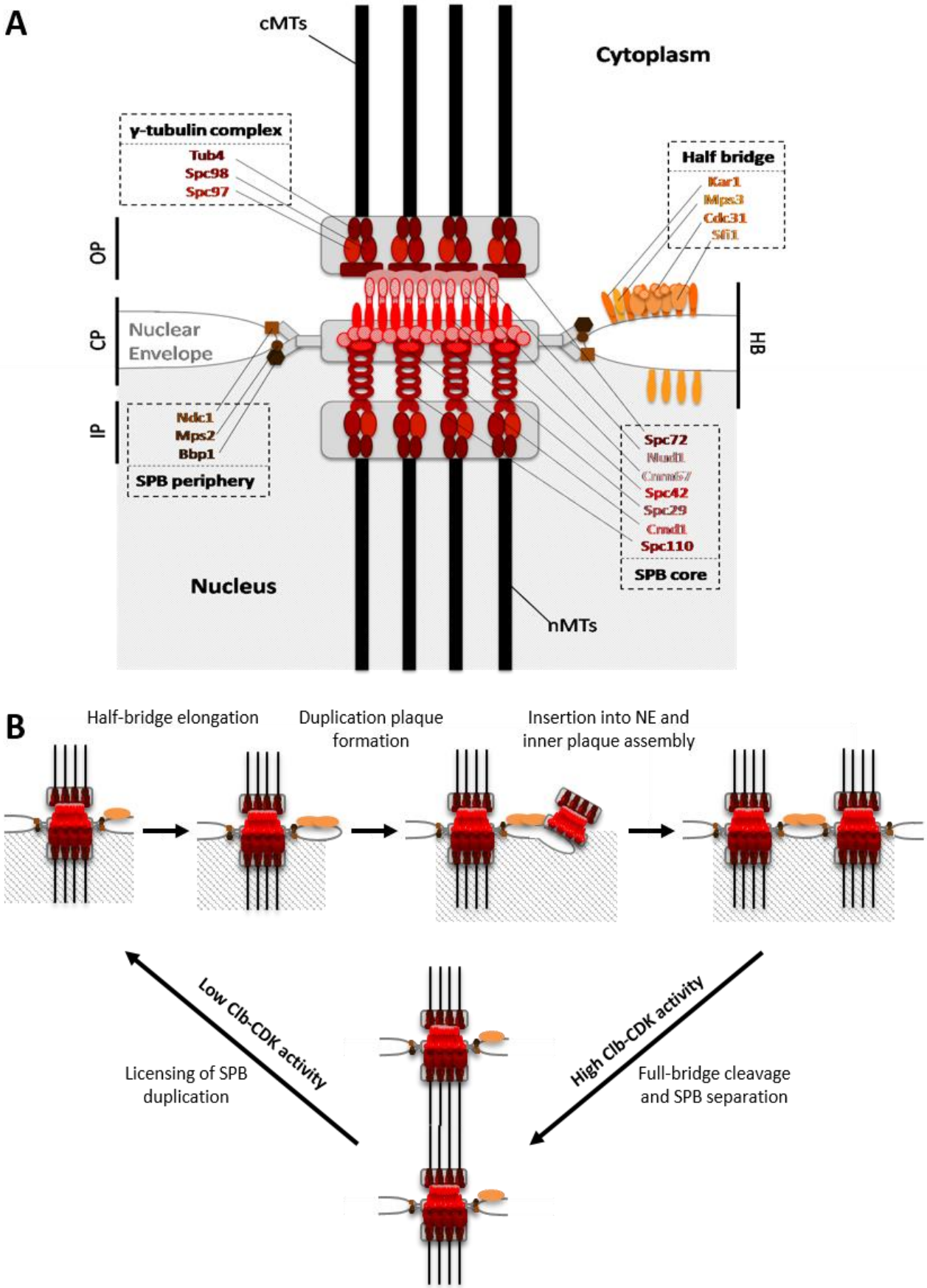

Figure 1.1.1.1.1: CDK-dependent regulation of the SPB duplication pathway. (A) Protein components of the SPB are assembled into intraorganelle structures, as indicated by dashed boxes. SPBs assemble cytoplasmic and nuclear microtubules (cMTs and nMTs) to enable chromosome segregation. Figure modified from Avena, Burns et al. 2014. (B) The SPB duplication pathway can be divided into multiple steps, which are regulated by CDKs.

OP = outer plaque CP = central plaque IP = inner plaque HB = half-bridge NE = nuclear envelope

1.1.1.1.2 DNA replication

Cdc28-dependent phosphorylation is required for both initiation and inhibition of DNA replication (Loog and Morgan 2005). DNA synthesis is licensed in G1-phase by formation of the pre-replicative complex (pre-RC) at origins of replication. Pre-RCs, consisting of Cdh1, Cdc6 and the helicase heterohexamer Mcm2-7, are recruited specifically to origins by origin recognition complexes (ORCs) but remain inactive until S-phase. Clb5- and Clb6-CDKs as well as the Dbf4-Cdc7 kinase (DDK) complex trigger pre-RC activation (reviewed by Labib 2010). Sld3 and the helicase-activating protein, Cdc45, are recruited to Mcm2-7 via DDK-dependent phosphorylation (Heller, Kang et al. 2011). Clb5-CDK phosphorylates replication proteins Sld2 and Sld3, which interact with Cdc45 and lead to the recruitment of Dpb11 at origins. Another complex known as GINS is then recruited. GINS has also been shown to maintain the association of Cdc45 with Mcm2-7 at replication forks (Gambus, Jones et al. 2006). The formation of the Cdc45-Mcm2-7-GINS complex activates the helicase and triggers unwinding of the double-stranded DNA. DNA polymerase can then be recruited, initiating DNA synthesis (Masumoto, Sugino et al. 2000, Masumoto, Muramatsu et al. 2002). Once origins have fired, the pre-RC then disassembles (reviewed by Bloom and Cross 2007).

To restrict DNA replication to once per cell cycle, the formation of the pre-RC must be prevented during mitosis. This is achieved through the phosphorylation of Cdc6, a component of the pre-RC, by Clb-CDKs (Elsasser, Lou et al. 1996). Cdc6p is targeted for ubiquitination and subsequent degradation, resulting in the removal of Cdc6 from origins (Calzada, Sanchez et al. 2000, Mimura, Seki et al.

2004). Additionally, Clb-CDKs phosphorylate other subunits of the pre-RC, Mcm proteins, which leads to their nuclear exclusion and displacement from ORCs (Labib, Diffley et al. 1999, Nguyen, Co et al. 2001)

A further mechanism of premature re-replicative prevention is through inhibition of ORC function. Orc2 and Orc6 are phosphorylated by Clb5-CDK in late G1, after origin firing. In order for re-replication of DNA, these ORC subunits must be hypophosphorylated. This occurs in early G1, when Cln-CDKs are active and Clb-CDK activity is low (Nguyen, Co et al. 2001).

Individually, inhibition of any of these three mechanisms, Cdc6 degradation, Mcm export or ORC phosphorylation, is not sufficient to cause DNA re-replication in cells. However, when all three mechanisms are disrupted, DNA synthesis is initiated (Nguyen, Co et al. 2001). This suggests coordinated, multiple level regulation of DNA replication is required to ensure origin firing once per cell cycle.

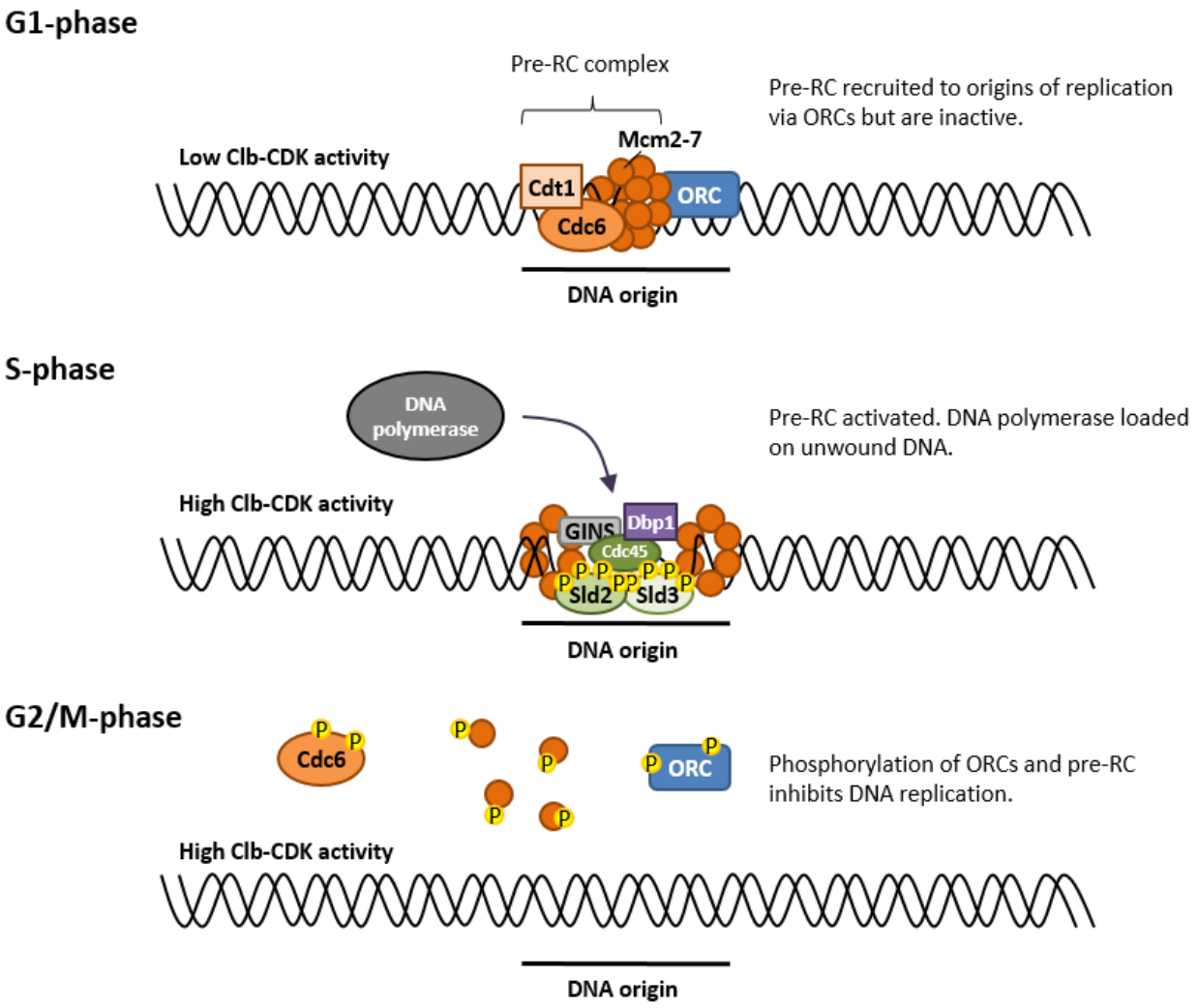

Figure 1.1.1.1.2: CDK-dependent regulation of DNA replication. In G1, low Clb-CDK activity enables the assembly of the pre-RC at DNA origins of replication. Increased Clb-CDK activity in S-phase results in the phosphorylation of replication proteins, initiating the melting of DNA and firing of origins. After origin firing, the pre-RC disassembles and maintained phosphorylation prevents its assembly until Clb-CDK down-regulation.

1.1.1.1.3 Mitotic spindle assembly

SPBs are able to polymerize tubulin and assemble kinetochore microtubules, which attach to centromeric regions of the chromosome and aid the separation of sister chromatids in anaphase. SPBs also assemble astral and interpolar microtubules. It is these interpolar microtubules that play a role in moving SPBs to opposite poles of the cell. Cyclin-CDK complexes have been shown to phosphorylate a number of microtubule-associated proteins (Ubersax, Woodbury et al. 2003), which help regulate the assembly and disassembly of the mitotic spindle.

Ase1 is a microtubule bundling protein that localises at the mitotic spindle mid-zone and is crucial for its integrity (Pellman, Bagget et al. 1995, Schuyler, Liu et al. 2003). Phosphorylation of Ase1 by Clb-CDKs promotes Ase1p recruitment to the spindle, stabilising microtubules to promote spindle elongation. In late anaphase, Ase1 is degraded through APC-mediated proteolysis and spindles disassemble (Juang, Huang et al. 1997), resulting in the exit of cells from mitosis.

Kar9, a cortical protein required for spindle positioning, and Dyn1, cytoplasmic dynein, are also regulated by CDK phosphorylation. Both Kar9p and Dyn1p localise preferentially to the daughter cell-bound SPB (Miller and Rose 1998, Liakopoulos, Kusch et al. 2003, Grava, Schaerer et al. 2006). CDK-mediated asymmetry of microtubule-associated proteins is essential for correct spindle positioning, enabling the formation and elongation of the mitotic spindle.

1.1.1.2 Mechanisms for CDK down-regulation

CDKs are regulated extensively through control of cyclin levels. Cyclins are regulated by two main mechanisms; transcriptional control of cyclin gene expression and cyclin proteolysis.

1.1.1.2.1 Transcriptional regulation

Transcriptional regulation of cyclins is crucial for the differential regulation of G1 and B-type cyclins during the cell cycle. During S-phase, B-type cyclins, primarily Clb5 and Clb6, initiate DNA replication. Following the increase of Clb levels, transcription of G1-specific cyclins is repressed through phosphorylation and inhibition of G1-specific cyclin transcription factors (Amon, Tyers et al. 1993, Siegmund and Nasmyth 1996). Conversely, transcription of G2/M-phase cyclins is increased through phosphorylation and recruitment of distinct transcription factors to Clb promoters, enabling the transition of cells into M-phase (Darieva, Pic-Taylor et al. 2003, Reynolds, Shi et al. 2003). Activation of Clb1-Clb4 subsequently promotes the stimulation of downstream proteins involved in chromosome condensation and mitotic spindle assembly (Fitch, Dahmann et al. 1992, Richardson, Lew et al. 1992, Amon, Tyers et al. 1993).

1.1.1.2.2 Cyclin proteolysis

Ubiquitin-mediated cyclin proteolysis ensures the specific degradation and subsequent inhibition of CDKs. Cyclins are polyubiquitinated by E3 ubiquitin ligases, targeting them for degradation by the 26S proteasome. Two ubiquitin ligases are crucial during the cell cycle. The multi-protein SCF complex is required to mark G1 and G2 cyclins for destruction, to enable the transitions between G1/S-phase and G2/M-phase respectively (Barral, Jentsch et al. 1995, Skowyra, Craig et al. 1997), whereas the APC targets mitotic cyclins for proteolysis (Visintin, Prinz et al. 1997). APC activity can be specifically regulated during mitosis through binding to activating subunits; Cdc20 and Cdh1. APC^{Cdc20} mediates the metaphase-anaphase transition through degradation of the anaphase inhibitor securin and M-phase cyclins (Cohen-Fix, Peters et al. 1996, Funabiki, Yamano et al. 1996). To allow cells to exit from mitosis into a following G1, Clb-CDKs require inactivation through complete M-phase cyclin proteolysis (revieweb by Morgan 1997, Visintin, Prinz et al. 1997, Shirayama, Zachariae et al. 1998). This cyclin degradation step is catalysed by APC^{Cdh1} activity (Zachariae, Schwab et al. 1998). Inhibition of Clb-CDK activity allows for relicensing of replication origins for progression into the next round of DNA replication in S-phase (Holt, Hutti et al. 2007).

1.1.1.2.3 Inhibitor binding

A third mechanism of CDK regulation is through the binding of stoichiometric inhibitors. Clb-CDK activity is repressed when bound to the inhibitor, Sic1 (Schwob, Bohm et al. 1994). In order to alleviate Sic1 inhibitory binding to CDKs, ubiquitin-mediated proteolysis of Sic1 is required. Phosphorylation of Sic1, by Clb-CDKs as well as other kinase, results in its degradation by the SCF complex (Feldman, Correll et al. 1997, Skowyra, Craig et al. 1997, Verma, Annan et al. 1997). This promotes the entry of cells into S-phase. Moreover, in order for complete Clb-CDK inactivation at the end of mitosis, Sic1 must be dephosphorylated by Cdc14 and thus stabilised to enable inhibitory binding of Sic1 to mitotic CDKs (Visintin, Craig et al. 1998).

1.1.2 The conserved phosphatase Cdc14

Cdc14 is a dual-sensitivity protein phosphatase with known roles in mitotic CDK inactivation (reviewed by Morgan 1999). Whilst Cdc14 homologues have been identified in organisms ranging from fission yeast and human cells, its role is best understood in budding yeast.

1.1.2.1 Cdc14 is required for mitotic exit via CDK down-regulation

In budding yeast, Cdc14 is essential for the down-regulation of mitotic CDKs, enabling mitotic exit (Jaspersen, Charles et al. 1998, Visintin, Craig et al. 1998, Zachariae, Schwab et al. 1998). In temperature-sensitive *cdc14* mutants at the restrictive temperature, Clb-CDK activity remains high. Furthermore, mitotic spindles, which disassemble in low Clb-CDK states, persist in *cdc14-1* cells indicating that mitotic exit has not occurred (Culotti and Hartwell 1971, Visintin, Craig et al. 1998).

Activation of Cdc14 during mitosis brings about Clb-CDK inactivation via multiple mechanisms. Firstly, Cdc14 dephosphorylates Cdh1, the late-mitosis APC activator, thereby activating it (Visintin, Craig et al. 1998, Zachariae, Schwab et al. 1998, Jaspersen, Charles et al. 1999). This results in the proteolysis of B-type cyclins, antagonising Clb-CDK activity. Cdc14 also dephosphorylates Sic1, the mitotic CDK inhibitor, and Swi5, the Sic1 transcription factor. These events result in the stabilisation and accumulation of Sic1 in cells, leading to complete Clb-CDK inhibition (Knapp, Bhoite et al. 1996, Toyn, Johnson et al. 1997, Verma, Annan et al. 1997, Visintin, Craig et al. 1998). Furthermore, Cdc14 opposes Clb-CDK activity by reversing the phosphorylation of a number of CDK targets, in

order to re-set the cell for G1 (Bloom, Cristea et al. 2011, Bremmer, Hall et al. 2012, Avena, Burns et al. 2014).

1.1.2.2 Cdc14 activation in early anaphase by FEAR

Cdc14 is tightly regulated throughout mitosis and is only active in anaphase. For the majority of the cell cycle, Cdc14 is kept inactive and sequestered in the nucleolus, bound to the inhibitor Cfi1/Net1 (Shou, Seol et al. 1999, Visintin, Hwang et al. 1999). Upon anaphase onset, Cfi1/Net1becomes phosphorylated (Kerr, Sarkar et al. 2011), causing the dissociation of the complex and the subsequent release of Cdc14 from the nucleolus. This release is maintained until telophase, when Cdc14 is resequestered by its inhibitor (Shou, Seol et al. 1999, Visintin, Hwang et al. 1999, Manzoni, Montani et al. 2010). The phosphorylation and disassociation of Cfi1/Net1 from Cdc14 is believed to be the work of mitotic CDKs, mediated by the Cdc14-Early Anaphase Release (FEAR) network and MEN (Fig. 1. 1. 2. 2.) (reviewed by Stegmeier and Amon 2004).

The FEAR network acts in early anaphase, as a consequence of chromosome segregation (Stegmeier, Visintin et al. 2002). Activation of APC^{Cdc20} results in the destruction of securin and the subsequent activation of separase, a component of FEAR (Pereira, Manson et al. 2002, Stegmeier, Visintin et al. 2002, Yoshida and Toh-e 2002). Separase activation leads to phosphorylation of Cfi1/Net1 through activation of Cdc5, which initiates the transient release of Cdc14 from the nucleolus (Visintin, Stegmeier et al. 2003, Azzam, Chen et al. 2004, Queralt, Lehane et al. 2006). Separase (Esp1), the polo kinase, Cdc5, kinetochore protein, Slk19, and nucleolar protein, Spo12, have all been shown as regulators of Cdc14 release, although how these FEAR components all interact with one another is unclear.

The polo kinase, Cdc5, is essential for Cdc14 release from nucleolar sequestration independent of MEN activation (Pereira, Manson et al. 2002, Stegmeier, Visintin et al. 2002). However, the role of Cdc5 within FEAR is hard to discern due to its function as an activator of MEN (Hu, Wang et al. 2001). Cdc5 appears to promote the phosphorylation of Cdc14 and Cfi1/Net1 in anaphase (Shou, Azzam et al. 2002, Yoshida and Toh-e 2002), although the latter event seems to require MEN function (Visintin, Stegmeier et al. 2003). It also appears to be the main effector of the FEAR network, as over-expression of Cdc5 suppresses Cdc14-release defects observed in *esp1-1* and *slk19Δ* FEAR mutants (Visintin, Stegmeier et al. 2003). In addition, Cdc5 activity contributes to numerous anaphase events. Firstly, Cdc5-dependent phosphorylation of cohesin subunit Scc1 facilitates its cleavage by Esp1 (Alexandru, Uhlmann et al. 2001). Secondly, Cdc5 kinase induces Swe1 degradation, promoting CDK activity (Liang, Jin et al. 2009). Finally, Cdc5-mediated release of Cdc14 plays an important role in proper spindle elongation and progression through anaphase (Park, Park et al. 2008, Roccuzzo, Visintin et al. 2015).

Slk19 and Spo12 also play a role in Cdc14 release, although potentially through parallel pathways (Stegmeier, Visintin et al. 2002, Sullivan and Uhlmann 2003, Visintin, Stegmeier et al. 2003, Tomson, Rahal et al. 2009). Slk19 is a kinetochore protein which forms a complex with Esp1 during anaphase (Fig. 1. 1. 2. 2), the association of which is required for localisation of separase to the spindle midzone and kinetochores (Sullivan and Uhlmann 2003). However, through use of a catalytically inactive separase mutant and a non-cleavable Slk19 mutant, it was shown that Esp1 function in FEAR is independent of protease activity

(Sullivan and Uhlmann 2003). The exact mechanism of Slk19-depedent regulation of initial Cdc14 release has yet to be determined. More recently, Slk9 has been implicated in preventing the movement of FEAR released-Cdc14 from the nucleus to the cytoplasm (Faust, Wong et al. 2013). A Slk19 triple point mutant resulted in the normal release of Cdc14 from the nucleolus into the nucleus during early anaphase but, additionally, caused the premature appearance of Cdc14 in the cytoplasm prior to spindle disassembly. This early movement of Cdc14 to the cytoplasm, which under normal circumstances occurs upon MEN activation, enabled spindle disassembly even within MEN-deficient cells (Faust, Wong et al. 2013). Expression of *SLK19* and *slk19Δ* in *cdc15-2* cells at the restrictive temperature does not prevent a delay in spindle disassembly observed when MEN in inactivated. However, *Slk19^{3R} cdc15-2* cells displayed a partial rescue of the spindle disassembly arrest defect. This suggests that Slk19 is required to couple Cdc14 release from the nucleus with spindle disassembly.

The role of Spo12 in the FEAR network has been partially characterised. Alongside its homologue, Bns1, Spo12 localises to the nucleolus where it interacts with Fob1, a protein required to block replication forks (Stegmeier, Huang et al. 2004). Fob1 is also an inhibitor of FEAR, forming a complex with Cfi1/Net1 to maintain Cdc14 sequestration during metaphase. Spo12 is phosphorylated in anaphase by mitotic CDKs, an event which is dependent on Esp1 and Slk19 function (Tomson, Rahal et al. 2009) despite Spo12 appearing to act in a parallel pathway to separase (Stegmeier, Visintin et al. 2002, Sullivan and Uhlmann 2003, Visintin, Stegmeier et al. 2003). Phosphorylation of Spo12 in anaphase reduces its binding affinity to Fob1 (Stegmeier, Huang et al. 2004),

hinting that the phospho-regulation of Spo12 may play a role in Cdc14 release (Fig. 1. 1. 2. 2). Interestingly, Cdc14 was identified as the phosphatase required for maintaining Spo12 dephosphorylation prior to anaphase, suggesting that Cdc14 may still be active despite sequestration within the nucleolus (Tomson, Rahal et al. 2009).

Although FEAR released-Cdc14 is restricted to the cell nucleus (Faust, Wong et al. 2013), it is able to regulate a number of anaphase events such as mitotic spindle dynamics, correct chromosome structure and segregation, and protein localisation (reviewed by D'Amours and Amon 2004, reviewed by Rock and Amon 2009, Roccuzzo, Visintin et al. 2015). Cdc14 released by FEAR also initiates MEN through dephosphorylation and subsequent activation of Cdc15 (Fig. 1. 1. 2. 2), as well as through inhibition of the spindle positioning checkpoint (SPOC) (Jaspersen and Morgan 2000, Pereira, Manson et al. 2002, Stegmeier, Visintin et al. 2002). Although FEAR is not essential for mitotic progression, its absence has been associated with a significant loss of viability during anaphase. This is indicative of its importance in ensuring accurate separation of rDNA (D'Amours, Stegmeier et al. 2004).

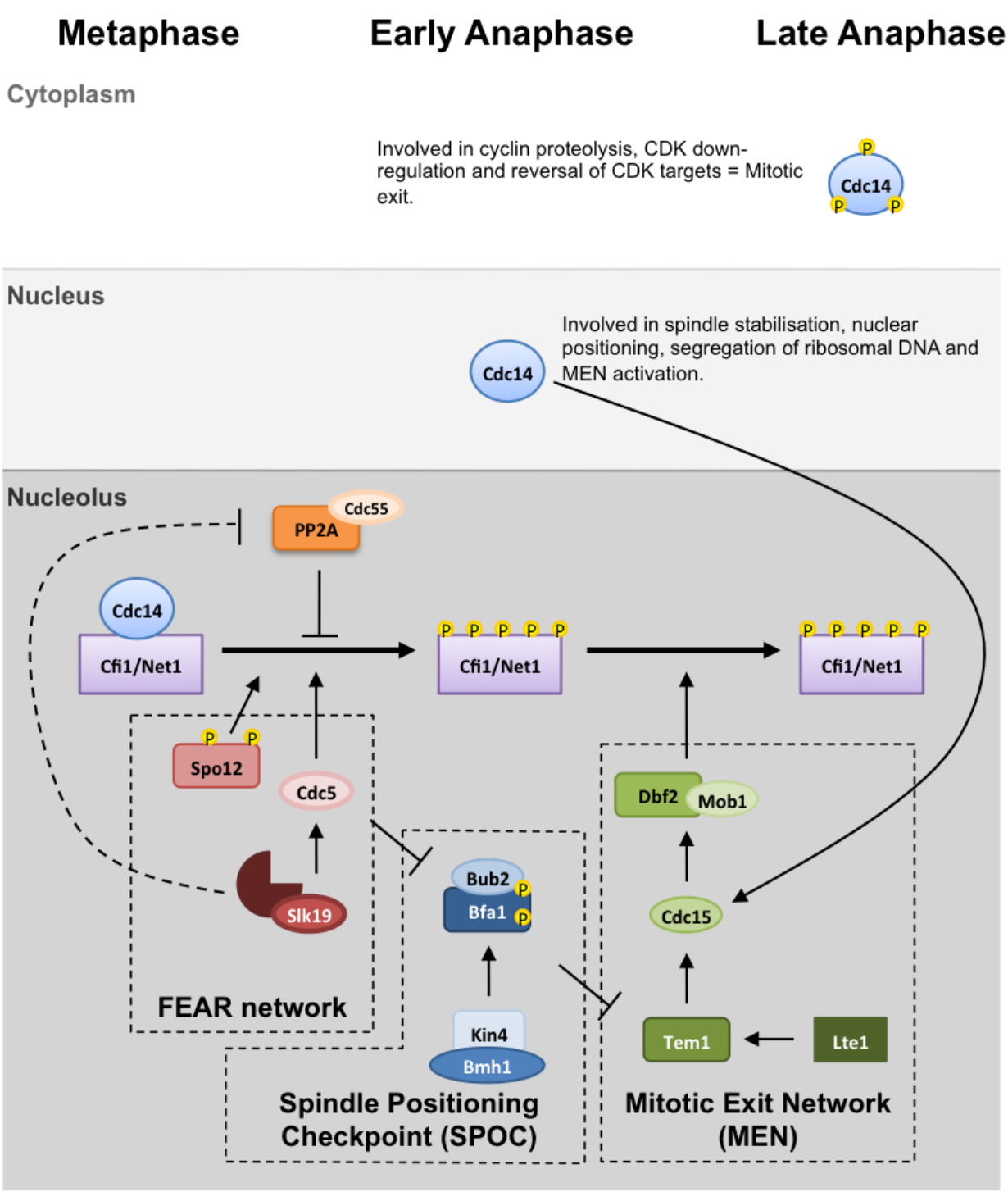

Figure 1.1.2.2: Activation of Cdc14 in mitosis by FEAR and MEN. During the majority of the cell cycle, Cdc14 is kept inactive in the nucleolus through binding to its inhibitor Cfi1/Net1. Upon anaphase onset, Cdc14 is released from inhibition through the activation of two distinct yet interacting protein signalling networks, FEAR and MEN. FEAR-released Cdc14 is required for anaphase events, whereas MEN-released Cdc14 enables mitotic exit. SPOC regulates MEN to ensure that spindles are properly aligned on the mother-bud cell polarity axis.

Dotted inhibition line indicates indirect association.

1.1.2.3 PP2A^{Cdc55} maintains Cdc14 sequestration in the nucleolus

The release of Cdc14 in anaphase results from phosphorylation of the Cfi1/Net1 inhibitor (Queralt, Lehane et al. 2006). In order for Cdc14 resequestration at the end of mitosis, this inhibitory phosphorylation must be reversed. Furthermore, by maintaining the unphosphorylated form of Cfi1/Net1 during the rest of the cell cycle, premature release of Cdc14 is prohibited.

PP2A is a protein phosphatase that is involved in several aspects of the cell cycle (Stark 1996). It can bind to multiple regulatory subunits to enable substrate specificity. PP2A^{Cdc55} has been shown to maintain Cdc14 sequestration in the nucleolus by preventing early phosphorylation of Cfi1/Net1 in metaphase (Queralt, Lehane et al. 2006). Upon anaphase onset, PP2A^{Cdc55} activity is down-regulated by a separase-dependent pathway (Fig. 1. 1. 2. 2). Cfi1/Net1 is then phosphorylated by Clb-CDKs and Cdc5, and Cdc14 is consequently released. Loss of Cdc55 in mitosis results in the ectopic release of Cdc14, as a consequence of premature Cfi1/Net1 phosphorylation (Queralt, Lehane et al. 2006).

1.1.2.4 Cdc14 activation in late anaphase by MEN

Whilst FEAR activation is required to couple chromosome segregation to initiation of mitotic exit, MEN signalling is essential to trigger the irreversible exit of cells from mitosis. MEN activity in late anaphase results in the full activation of Cdc14, maintaining its release from nucleolar sequestration and enabling Cdc14 accumulation in the cytoplasm (Shou, Seol et al. 1999, Visintin, Hwang et al. 1999, Mohl, Huddleston et al. 2009). This sustained release of Cdc14 enables the phosphatase to access and dephosphorylate a number of mitotic substrates, such as Cdh1 and Sic1, which promote the inactivation of Clb-CDKs and exit of cells from mitosis (Visintin, Craig et al. 1998, Zachariae, Schwab et al. 1998, Jaspersen, Charles et al. 1999).

MEN plays an additional role in spindle positioning. Mitotic budding yeast cell divide asymmetrically; the daughter cell-derived bud emerges from the mother cell (reviewed by Li 2013). Cell polarity is needed to establish this specialised budding pattern, and the mitotic spindle aligns along the mother-bud cell polarity axis to ensure the proper inheritance of nuclei in dividing cells (Monje-Casas and Amon 2009). The spindle position checkpoint (SPOC) monitors spindle positioning and acts upon MEN component Tem1 to inhibit the signalling cascade when spindles are misaligned. Consequently, MEN signalling is regulated in a spatial manner (reviewed by Stegmeier and Amon 2004, Caydasi, Ibrahim et al. 2010).

MEN is a GTPase-driven signalling pathway (Fig. 1. 1. 2. 2). When active, the G protein Tem1 is bound to GTP and can promote the activation of the kinase

Cdc15 (Shirayama, Matsui et al. 1994, Jaspersen, Charles et al. 1998, Lee, Frenz et al. 2001, Visintin and Amon 2001). Cdc15 successively activates Dbf2-Mob1. Active Dbf2 kinase, alongside its regulatory partner Mob1, is able to enter the nucleolus and results in the sustained release of Cdc14 (Mohl, Huddleston et al. 2009). This has been theorised to be through phosphorylation of Cdc14 itself, as well as its inhibitor, to ensure the maintained dissociation of Cdc14 and Cfi1/Net1 (Visintin, Stegmeier et al. 2003, Mohl, Huddleston et al. 2009). Simultaneous to its role in MEN, Dbf2 also phosphorylates proteins involved in cytokinesis, thus linking mitotic exit to onset of cell cleavage in telophase (Meitinger, Boehm et al. 2011).

As denoted earlier, MEN activity is driven primarily by temporal and spatial changes in its components (Bardin, Visintin et al. 2000, Pereira, Hofken et al. 2000). The SPB constituent, Nud1, functions as a scaffold for MEN assembly at the SPB (Adams and Kilmartin 2000, Bardin, Visintin et al. 2000, Gruneberg, Campbell et al. 2000, Pereira, Hofken et al. 2000, Visintin and Amon 2001). During mitotic spindle assembly, Tem1 localises preferentially to the daughter cell bound-SPB (Fig. 1. 1. 2. 4A). Bub2 and Bfa1 proteins comprise a GTPase-activating protein complex (GAP), which co-localise with and inhibit Tem1 by promoting the hydrolysis of Tem1-GTP to Tem1-GDP (Bardin, Visintin et al. 2000, Pereira, Hofken et al. 2000). It is believed that, as the mitotic spindle grows, the Tem1-associated SPB enters into the bud and comes into close proximity with the MEN regulator, Lte1, a guanine-nucleotide exchange factor (GEF) (Shirayama, Matsui et al. 1994, Geymonat, Spanos et al. 2009). GEF activity promotes Tem1 activation (reviewed by D'Amours and Amon 2004).

Furthermore, phosphorylation of Bfa1-Bub2 by FEAR component, Cdc5, in early anaphase alleviates the inhibition of Tem1 by the GAP complex. These two regulatory events result in MEN signal cascade activation (Hu, Wang et al. 2001, Geymonat, Spanos et al. 2009). $PP2A^{Cdc55}$ has also been implicated in MEN activation, through counteracting Bfa1 activity (Baro, Rodriguez-Rodriguez et al. 2013).

SPOC monitors spindle positioning and can delay MEN activation when the mitotic spindle is misaligned (Pereira, Hofken et al. 2000, Pereira, Manson et al. 2002). This delay provides time for proper spindle realignment along the mother-bud cell polarity axis. With correct spindle orientation, Bfa1-Bub2 localises preferentially to the daughter cell bound-SPB, where Tem1 is also asymmetrically localised (Fig. 1. 1. 2. 4A) (Pereira, Hofken et al. 2000, Molk, Schuyler et al. 2004). When asymmetrically localised, Bfa1 can achieve maximum phosphorylation by Cdc5 and thus GAP activity is inhibited, enabling Tem1 activation (Hu, Wang et al. 2001, Pereira, Tanaka et al. 2001, Kim, Luo et al. 2012).

Misalignment of spindles, conversely, results in the mother cortex-associated kinase, Kin4, phosphorylating Bfa1 at distinct sites from Cdc5. Kin4-dependent phosphorylation of Bfa1 prevents Cdc5-dependent inhibition of Bfa1-Bub2 (Maekawa, Priest et al. 2007). Therefore, Tem1 inhibition is maintained when SPOC is activated (Pereira, Tanaka et al. 2001, Caydasi and Pereira 2009). Phosphorylation of Bfa1 by Kin4 also enables Bmh1 docking with the GAP complex (Caydasi, Micoogullari et al. 2014). Bmh1 and Kin4 consequently

promote the symmetric localisation of the GAP complex to SPBs through the removal of Bfa1 from the daughter cell bound-SPB (Fig. 1. 1. 2. 4B) (Caydasi and Pereira 2009, Monje-Casas and Amon 2009). Decreased residence of Bfa1-Bub2 at the daughter SPB has been proposed to inhibit Tem1 targeting to SPBs (Valerio-Santiago and Monje-Casas 2011, Caydasi, Lohel et al. 2012). Decreased Tem1-SPB localisation would inhibit MEN activity, promoting mitotic arrest and preventing sustained Cdc14 release.

The protein phosphatase Cdc14 has also been shown to localise asymmetrically to SPBs in mitosis, localising preferentially to the MEN-bound SPB. This co-localisation is dependent on Bfa1-Bub2, and Cdc14 has been shown to dephosphorylate and reactivate the GAP complex at mitotic exit (Pereira, Manson et al. 2002, Yoshida, Asakawa et al. 2002). Similarly, Cdc14 is required for the dephosphorylation and removal of Cdc15 from SPBs at the time of cytokinesis (Cenamor, Jimenez et al. 1999, Jaspersen and Morgan 2000, Xu, Huang et al. 2000). As such, Cdc14 appears to play a role in restoring the SPB environment to a pre-mitotic state.

Interestingly, the asymmetry of SPOC and MEN components does not appear to be a requisite for mitotic exit. It has been reported that a constitutively active Tem1 mutant shows increased symetric localisation to SPBs and impairs Bub2 asymmetry (Scarfone, Venturetti et al. 2015). Despite enhancing Cdc15 loading at SPBs, the timing of mitotic exit remains unaffected, suggesting additional mechanisms other than SPOC exist downstream of Tem1 to control MEN activity.

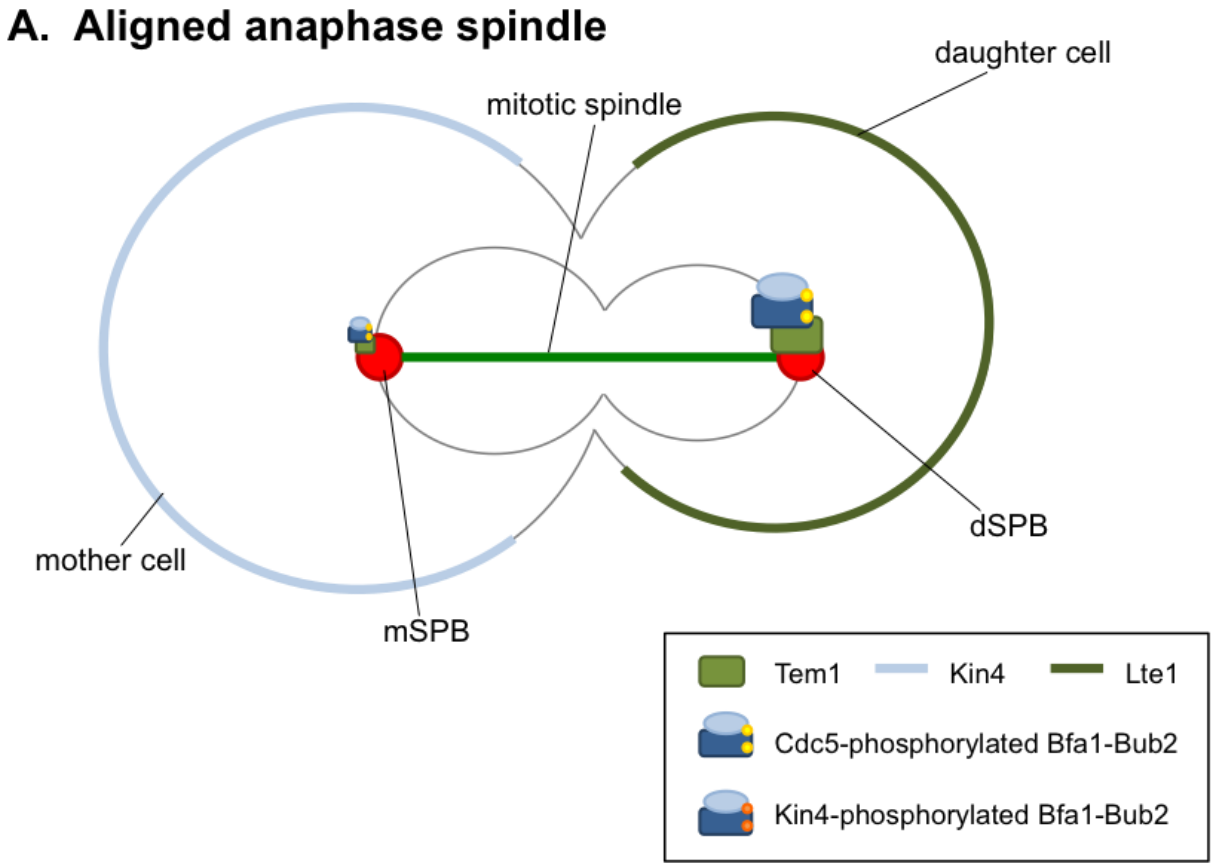

Figure 1.1.2.4: Spindle positioning and SPOC activation. (A) When mitotic spindles are correctly aligned, Tem1, Bfa1 and Bub2 are asymmetrically localised to daughter SPBs (dSPBs). Cdc5-depedent phosphorylation of Bfa1-Bub2 inhibits GAP activity, enabling Tem1 activation by daughter cortical GEF, Lte1. (B) When mitotic spindles are misaligned, Tem1, Bfa1 and Bub2 are symmetrically localised to SPBs. Mother cell cortex protein, Kin4, phosphorylates Bfa1-Bub2 to prevent inhibition by Cdc5, thus Tem1 is inactive.

1.1.2.5 The role of Cdc14 orthologs in other organisms

Cdc14 in budding yeast (*S. cerevisiae)*, hereafter referred to as *Sc*Cdc14, has been extensively studied and its role in CDK down-regulation and mitotic exit is well documented. However, ScCdc14 is a member of a family of highly conserved dual-specificity phosphatases that have been identified in many other organisms. Despite sharing sequence similarities, *Sc*Cdc14 ortholog in other species do not always share a conserved function in cell cycle regulation.

1.1.2.5.1 Fission yeast

In fission yeast (*S. pombe*), a non-essential ortholog of Cdc14 was identified, termed Clp1/Flp1. *Sp*Clp1/Flp1 antagonises mitotic CDK activity, similar to *Sc*Cdc14, but functions mainly in mitotic entry and coordinating cytokinesis, and is not essential for mitotic exit (Cueille, Salimova et al. 2001, Trautmann, Wolfe et al. 2001). Whilst *Sc*Cdc14 acts mainly through cyclin proteolysis, *Sp*Clp1/Flp1 inhibits mitotic CDKs by promoting the inhibitory phosphorylation of Cdc2, the fission yeast homologue to Cdc28 (reviewed by Morgan 1997). *Sp*Clp1/Flp1 dephosphorylates and inactivates Cdc25, a phosphatase required to ensure Cdc2 is not phosphorylated by the protein kinase Wee1. Once active, Wee1 can phosphorylate a highly conserved tyrosine residue (Tyr15) on Cdc2, which results in the inactivation of the mitotic CDK (Mueller, Coleman et al. 1995, Cueille, Salimova et al. 2001).

*Sp*Clp1/Flp1 is predominately sequestered in the nucleolus for the majority of the cell cycle (Wolfe, McDonald et al. 2006). However, it is released in early mitosis instead of late and, upon release, localises not only to SPBs but along the

mitotic spindle and to the medial ring as well (Cueille, Salimova et al. 2001). The co-localisation of *Sp*Clp1/Flp1 with SPBs is also observed prior to mitotic release of the phosphatase, suggesting that a pool of *Sp*Clp1/Flp1 remains associated with SPBs throughout the cell cycle.

The mitotic release of *Sp*Clp1/Flp1 is promoted through a MEN-like pathway involved in septum formation, which contains MEN ortholog (reviewed by Bardin and Amon 2001). This so-called septation initiation network (SIN) is driven by a GTPase switch, Spg1, and initiates a conserved signalling cascade similar to the Tem1-dependent activation of MEN. The SPB acts as a scaffold for SIN signalling (Krapp, Schmidt et al. 2001) and inactivation of Cdc2 is sufficient to activate SIN (Dischinger, Krapp et al. 2008). *Sp*Clp1/Flp1 was found to regulate the localisation of SIN components to the SPB following Cdc2 inactivation, indicating that *Sp*Clp1/Flp1 is both an activator and target of SIN signalling (Dischinger, Krapp et al. 2008). However, since *Sp*Clp1/Flp1 is not essential, another phosphatase is likely involved in SIN activation. Interestingly, FEAR orthologs are not required for the release of *Sp*Clp1/Flp1 from the nucleolus (Chen, Peli-Gulli et al. 2006).

In addition to CDK down-regulation, *Sp*Clp1/Flp1 appears to regulate the mitotic spindle through dephosphorylation of Ase1 and kinesin-6 motor Klp9 to promote spindle elongation, analogous to *Sc*Cdc14 function (Fu, Ward et al. 2009, Khmelinskii, Roostalu et al. 2009). More recently, *Sp*Clp1/Flp1 has been shown to regulate SPB duplication through dephosphorylation of half-bridge

component Sfi1 after anaphase to enable the re-setting of SPBs for the subsequent G1 phase (Bouhlel, Ohta et al. 2015).

These findings suggest that *Sc*Cdc14 and *Sp*Clp1/Flp1 have similar functions in budding yeast and fission yeast respectively. They both promote mitotic CDK down-regulation, albeit through differential mechanisms. They are also both involved in the stabilisation of mitotic spindles, the re-duplication of SPBs and the initiation of cytokinesis events. However, *Sc*Cdc14 and *Sp*Clp1/Flp1 release from nucleolar sequestration differs in both timing and mechanism, and the role of *Sc*Cdc14 in mitotic exit appears unique to budding yeast. One proposed reason for this is that mitotic CDK activity is high in budding yeast anaphase, unlike in other organisms where CDK activity is inhibited upon anaphase onset (Chen, Peli-Gulli et al. 2006). This could explain why *Sc*Cdc14-dependent dephosphorylation of mitotic CDK targets is so crucial in anaphase to ensure that mitotic CDK activity is sufficiently low for entry into G1.

1.1.2.5.2 Non-mammalian eukaryotes

Relatively little is known about Cdc14 function in higher eukaryotes. In *C.elegans*, Cdc14 has been shown to localise to the spindle midzone in anaphase and to the midbody of the cell in telophase (Gruneberg, Glotzer et al. 2002), analogous to *Sp*Clp1/Flp1 localisation. Similarly, *Ce*Cdc14 has also been observed at SPBs (Saito, Perreault et al. 2004). However, the function of *Ce*Cdc14 has not been determined, as RNAi experiments in different studies contradict one another (Gruneberg, Glotzer et al. 2002, Saito, Perreault et al. 2004).

In *Xenopus* cells, two isoforms of Cdc14 have been identified; *X*Cdc14A and *X*Cdc14B (Kaiser, Nachury et al. 2004, Krasinska, de Bettignies et al. 2007). Whilst the role of *X*Cdc14B has yet to be determined, *X*Cdc14A localises to the centrosome in interphase and the cell midbody in late mitosis. It appears to be involved in cytokinesis and the dephosphorylation of Cdc25, likely resulting in the inhibitory tyrosine phosphorylation of Cdc2 by conserved Wee1 (Mueller, Coleman et al. 1995, Krasinska, de Bettignies et al. 2007).

A novel function of Cdc14 has also been identified in zebrafish, where it was found to regulate ciliogenesis (Clement, Solnica-Krezel et al. 2011). Zebrafish have three Cdc14 genes, which are expressed throughout embryogenesis. Through inhibition of phosphatase function in a Cdc14B homolog during early stage development, it was shown that Cdc14 activity was pivotal to establish left-right (LR) asymmetry (Clement, Solnica-Krezel et al. 2011). LR asymmetry is required for the non-symmetrical placement of internal organs, such as the heart, liver and brain (Levin 2005). Whilst the exact mechanism of this LR

asymmetry defect is unclear, it was observed that several types of cilia were affected in a Cdc14B loss of function mutant. Cilia tended to be significantly shorter when CDC14B phosphatase activity was abolished, suggesting that CDC14B is required to phospho-regulate an as yet unknown substrate in order to regulate cilia length (Clement, Solnica-Krezel et al. 2011).

1.1.2.5.3 Vertebrates

Human cells contain two orthologs of ScCdc14, *h*Cdc14A and *h*Cdc14B (Li, Ernsting et al. 1997). Similar to *Sc*Cdc14 and *Sp*Clp1/Flp1, *h*Cdc14 can promote CDK inactivation (Li, Ljungman et al. 2000, Listovsky, Zor et al. 2000), the mechanisms of which appears to be through promoting inhibitory tyrosine phosphorylation of Cdk1 (Ovejero, Ayala et al. 2012). Phosphorylation of Cdk1 on Tyr-15 is catalysed by the kinases Wee1 and Myt1 (reviewed by Marston and Amon 2004).

Mammalian Cdc14A localises to centrosomes throughout the majority of the cell cycle, similar to *Sp*Clp1/Flp1. This localisation is facilitated through active nuclear export and is required for accurate centrosome separation and subsequent chromosome segregation (Kaiser, Zimmerman et al. 2002, Mailand, Lukas et al. 2002). It has also been shown to prevent the premature entry of cells into mitosis by inhibiting mitotic CDKs (Sacristan, Ovejero et al. 2011).

*h*Cdc14B function, on the other hand, is tightly regulated via nucleoli sequestration and is released in early mitosis with a similar timing to *Sp*Clp1/Flp1 (Mailand, Lukas et al. 2002, Nalepa and Harper 2004). Once released from the nucleoli, *h*Cdc14B localises to the spindle midzone in anaphase and later to the cell midbody in telophase. It has been shown to cause the bundling and stabilisation of microtubules, suggesting that mammalian Cdc14B is important for mitotic spindle assembly and disassembly (Nalepa and Harper 2004, Cho, Liu et al. 2005).

Many other roles for *h*Cdc14B have been suggested, including centriole duplication (Wu, Cho et al. 2008), mitotic exit (Dryden, Nahhas et al. 2003, Rodier, Coulombe et al. 2008), nuclear organisation (Nalepa and Harper 2004) and regulation of the tumour suppressor p53 (Li, Ljungman et al. 2000). However, studies have thus far been carried out using RNAi and over-expression of *h*Cdc14, and not knockouts. Inexplicably, deletion of either *h*Cdc14A or *h*Cdc14B in human somatic cells appears not to display the same defects observed when *h*Cdc14 is depleted (Berdougo, Nachury et al. 2008, Mocciaro, Berdougo et al. 2010). Potential substrates of *h*Cdc14 therefore need validated *in vivo* and *in vitro* to establish if defects observed in RNAi experiments are physiologically true.

1.2 The meiotic cell cycle

Unlike in mitosis, meiotic cells undergo two consecutive rounds of chromosome segregation. The separation of homologues in meiosis I is a unique event, as it is sister chromatids that segregate in both mitosis and meiosis II. Meiosis I, therefore, must be differently regulated from mitosis to ensure proper chromosome segregation.

Meiosis I differs from mitosis in three key ways. Firstly, homologous chromosomes, composed of paired sister chromatids, attach to microtubules emanating from opposite SPBs. Kinetochores of sister chromatids, therefore, attach to microtubules growing from the same SPB (mono-orientation) instead of to microtubules from opposite poles (bi-orientation), as is observed during mitosis or meiosis II (reviewed by Duro and Marston 2015). Secondly, these homologue pairs must be physically linked to one another by chiasmata, formed by reciprocal recombination, to ensure that homologues correctly bi-orientate on the meiosis I spindle. Thirdly, cohesin between sister chromatids is maintained throughout meiosis I to prevent their premature separation (reviewed by Duro and Marston 2015).

The cohesin ring complex, which holds sister chromatids together in mitosis until its cleavage in anaphase, is removed from chromosomes in a stepwise manner during meiosis (Klein, Mahr et al. 1999). Cohesin is removed by separase from chromosome arms in meiosis I but is retained at the area surrounding the centromere, termed the pericentromere, until meiosis II (Fig. 1. 2). Protection of pericentromeric cohesin during meiosis I is a result of shugoshin (Sgo1)

localisation to this region (Katis, Galova et al. 2004, Kitajima, Kawashima et al. 2004, Marston, Tham et al. 2004).

Sgo1 is a conserved tension-sensing protein. During metaphase I, bi-orientated homologous chromosomes align at the metaphase plate. Sister chromatids are mono-orientated and Sgo1 is retained at the pericentromeres through an as yet unidentified mechanism (Nerusheva, Galander et al. 2014). Sgo1 recruits $PP2A^{Rts1}$ (Kitajima, Sakuno et al. 2006, Riedel, Katis et al. 2006), which prevents the phosphorylation and subsequent cleavage of meiotic cohesin subunit Rec8 (Brar, Kiburz et al. 2006, Ishiguro, Tanaka et al. 2010, Katis, Lipp et al. 2010). Recruitment of PP2A to the pericentromere is sufficient to prevent cleavage of Rec8, as was demonstrated through the artificial tethering of PP2A to chromosome arms, which resulted in aberrant cohesin protection during meiosis I (Riedel, Katis et al. 2006). Since no cohesin protection mechanism is usually present at chromosome arms in meiosis I, when separase is released from inhibition in anaphase I through APC^{Cdc20} activation, only cohesin at arm sites is cleaved. Resolution of chiasmata hence enables the separation of homologous chromosomes in meiosis I.

Once meiosis I is completed, cells then progress into meiosis II to separate sister chromatids in a mitosis-like segregation step. SPBs require re-duplication, so that a total of four SPBs are present in cells to assemble two meiosis II spindles (Fig. 1. 2) (Moens and Rapport 1971). At this point, sister chromatids become bi-oriented and under tension. Tension across sister chromatids likely contributes to the removal of the cohesin-protector Sgo1 from pericentromeres, although the

exact mechanism is not yet known (Nerusheva, Galander et al. 2014). Upon anaphase I onset, separase is able to degrade pericentromeric cohesin, enabling the separation of sister chromatids. Since an intervening S-phase between meiosis I and meiosis II is bypassed, these two consecutive rounds of chromosome segregations result in the production of four haploid daughter cells at the end of meiosis.

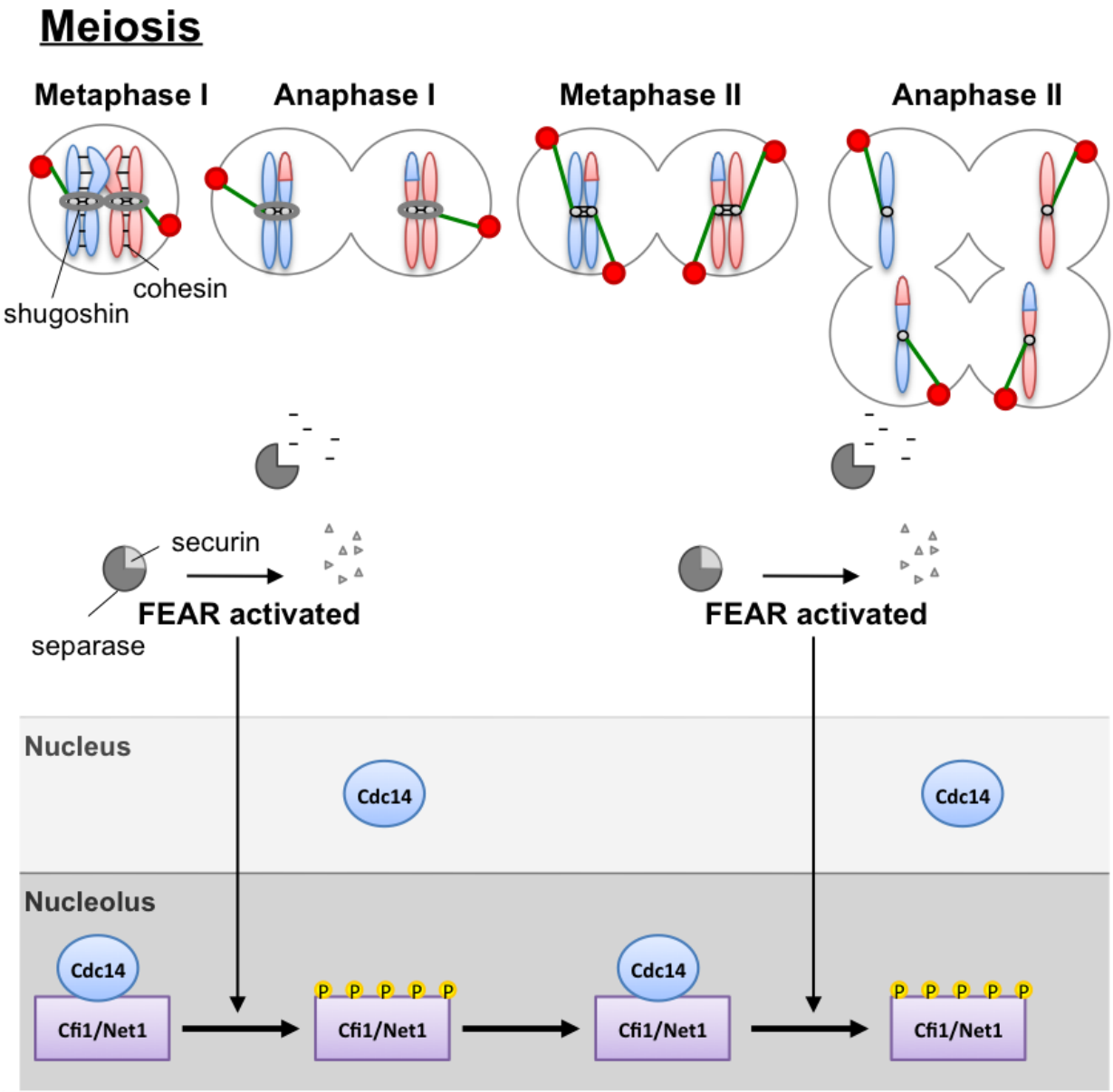

Figure 1.2: Stepwise loss of cohesin in meiosis ensures homologous chromosomes segregate in meiosis I. Chiasmata are resolved in anaphase I when active separase cleaves arm cohesin. Peri-centromeric cohesin is protected by Shugoshin (Sgo1), ensuring that sister chromatids mono-orientate. In anaphase II, Sgo1 is removed to allow for the segregation of sister chromatids upon separase release. Degradation of securin in anaphase I and anaphase II promotes the activation of FEAR, resulting in two waves of Cdc14 release from the nucleolus.

1.2.1 CDKs in meiosis

Budding yeast cells undergo meiosis as a response to nutritional stress. As such, meiosis can be induced through starvation of cells, grown in the absence of glucose and other nutritional factors (reviewed by Honigberg and Purnapatre 2003). Transcription of the meiotic inducer gene *IME1*initiates the transcription of genes involved in sporulation (Kassir, Granot et al. 1988, reviewed by van Werven and Amon 2011), including *IME2,* which regulates early meiotic genes (Smith, Su et al. 1990, Yoshida, Kawaguchi et al. 1990). Ime2 is required for the destruction of Sic1, which in turn activates Clb5- and Clb6-CDKs for progression through S-phase (Dirick, Goetsch et al. 1998). In combination, Ime1 and Ime2 up-regulate *NDT80* expression, required for the expression of meiotic cyclins Clb1- and Clb3-6 (Chu and Herskowitz 1998). As such, CDK activity plays a vital role in regulating meiotic progression.

Like in mitosis, Clb-CDK complexes regulate key meiotic events. Clb5- and Clb6-CDK are essential to initiate S-phase (Dirick, Goetsch et al. 1998, Stuart and Wittenberg 1998), with an additional role in triggering homologous recombination (Henderson, Kee et al. 2006). Clb1-, Clb3- and Clb4-CDK activities are vital during meiosis (Dahmann and Futcher 1995, Benjamin, Zhang et al. 2003), as they drive cells through two successive meiotic divisions. In contrast to mitosis, the major mitotic cyclin, Clb2, is not expressed during meiosis (Dahmann and Futcher 1995).

Regulation of Clb-CDK activities during meiosis occurs through a diverse range of mechanisms. Clb1-CDK activity is restricted to meiosis I through a post-

translational modification other than Clb1 degradation (Carlile and Amon 2008). Potential phosphorylation of Clb1, observed as a slower migrating form of Clb1, is evident during meiosis I and is associated with Clb1-CDK activity (Carlile and Amon 2008, Tibbles, Sarkar et al. 2013). CDK-dependent re-localisation of Clb1 to the nucleus promotes FEAR activation in anaphase I (Tibbles, Sarkar et al. 2013), after which the slower migrating form of Clb1 disappears and Clb1-CDK becomes inactive (Carlile and Amon 2008).

Clb3 cyclin is expressed only in meiosis II via translational repression during meiosis I. This limits Clb3-CDK activity to the second meiotic division (Carlile and Amon 2008), where it can regulate late meiotic events such as spore morphogenesis. The 5' UTR of *CLB3* prevents the accumulation of Clb3 by decreasing translational efficiency in meiosis I (Carlile and Amon 2008). This is through the association of Rim4, an RNA-binding protein, with the 5'UTR during meiosis I. Upon entry into meiosis II, increased Ime2 activity promotes a decrease in Rim4 protein levels and thus its inhibitory binding to *CLB3* is alleviated (Berchowitz, Gajadhar et al. 2013).

Clb4 cyclin is present throughout meiosis and is required after prophase exit to initiate spindle assembly (Kim, Meyer et al. 2013), although Clb4-CDK activity is down-regulated after metaphase II through an unknown mechanism (Carlile and Amon 2008). Clb5, as described earlier, is essential in S-phase. However, Clb5 protein abundance peaks in metaphase I and then again in metaphase II (Carlile and Amon 2008). Clb5 protein levels correlate with its kinase activity. This

suggests that Clb5-CDK may be acting early in meiosis II, although its role has yet to be determined.

1.2.2 Regulating CDKs at meiosis I exit

At the meiosis I to meiosis II transition, meiotic I spindles must disassemble to enable the subsequent assembly of spindles in meiosis II (Woodruff, Drubin et al. 2012). This requires a state of low Clb-CDK activity (Juang, Huang et al. 1997). However, to avoid re-duplication of the DNA, origins of replication must not be reset, which necessitates the maintenance of high Clb-CDK activity (Elsasser, Lou et al. 1996, Nguyen, Co et al. 2001). These opposing requirements hint that mitotic CDK activity must be down-regulated to a sufficient level that is permissive for meiotic spindle disassembly but is still admissible to restrict the formation of the preRC on DNA origins (reviewed by Marston and Amon 2004). Partial inactivation of CDKs, as has been observed in frog oocytes at meiosis I exit (Furuno, Nishizawa et al. 1994, Iwabuchi, Ohsumi et al. 2000), regulated by Cdc14 has been hypothesised (D'Amours and Amon 2004).

In *Xenopus*, the retention of CDK activity between meiosis I and meiosis II is ensured through regulation of cyclin B (reviewed by Marston and Amon 2004). After meiosis I, the APC inhibitor Emi1 binds to the APC co-activator Cdc20 to prevent complete APC activation and subsequent cyclin B destruction (Reimann and Jackson 2002, Schmidt, Rauh et al. 2006). Residual CDK activity is thought to inhibit Wee1 activation, whereas the *Xenopus* polo kinase Plx1 has been proposed to inhibit Myt1 kinase activity (Palmer, Gavin et al. 1998), thereby preventing Cdc2 inactivation. Since Cdc14 regulates the Wee1 *S. cerevisiae* ortholog Swe1 and the polo kinase *S. cerevisiae* ortholog Cdc5 regulates Cdc14 nucleolar release, it is possible Cdc14 does ensure partial down-regulation of CDKs at the meiosis I-meiosis II transition in budding yeast.

1.2.3 Cdc14 in meiosis

Cdc14 is essential for progression of cells from meiosis I to meiosis II (Buonomo, Rabitsch et al. 2003, Marston, Lee et al. 2003). It is released from nucleolar sequestration twice during meiosis; in anaphase I and, again, in anaphase II after its intermediate re-sequestration in metaphase II (Fig. 1. 2). Whilst the FEAR network plays a vital role in release of Cdc14 in anaphase I, MEN is dispensable (Buonomo, Rabitsch et al. 2003, Marston, Lee et al. 2003, Kamieniecki, Liu et al. 2005) and does not appear to be active until anaphase II (Attner and Amon 2012).

Similar to mitosis, $PP2A^{Cdc55}$ is required for maintaining the association of Cdc14 with Cfi1/Net1. $PP2A^{Cdc55}$-dependent inhibition of Cdc14 activity in early meiosis is essential for meiosis I spindle assembly (Bizzari and Marston 2011, Kerr, Sarkar et al. 2011). Depletion of Cdc55during meiosis, achieved through putting Cdc55 under the control of the mitosis-specific *CLB2* promoter (Clift, Bizzari et al. 2009), results in impaired nuclear division and prevents the formation of meiotic spindles (Bizzari and Marston 2011, Kerr, Sarkar et al. 2011).

Upon activation of the FEAR network during anaphase I, $PP2A^{Cdc55}$ is inhibited, enabling the phosphorylation of Cfi1/Net1 and subsequent release of Cdc14 from the nucleolus (Yellman and Burke 2006, Bizzari and Marston 2011, Kerr, Sarkar et al. 2011). When Cdc14 activity is impaired, cells undergo a single meiotic division, where a normal reductional division occurs in meiosis I. No tetranucleate cells are formed (Sharon and Simchen 1990a, Sharon and Simchen 1990b, Buonomo, Rabitsch et al. 2003, Marston, Lee et al. 2003). Meiotic

progression is similarly affected when Cdc14 release is impaired, as is observed in *slk19Δ* and *spo12Δ* FEAR mutants (Buonomo, Rabitsch et al. 2003, Marston, Lee et al. 2003).

Initially, it was reported that Cdc14 activity was required for meiotic spindle disassembly, since meiosis I spindle breakdown appeared delayed in temperature-sensitive *cdc14-1* cells at the restrictive temperature after the separation of homologues (Marston, Lee et al. 2003). However, upon visualisation of GFP-tagged tubulin in live cells, it became clear that meiosis I spindles do disassemble in *cdc14-1* mutants (Marston, Lee et al. 2003, Bizzari and Marston 2011). This is in contrast to observations in mitosis. Interestingly, 10-15% of *cdc14-1* cells re-fuse their nuclei upon spindle disassembly and then attempt to separate sister chromatids in a following equational segregation step but on a single meiosis II spindle (Bizzari and Marston 2011). This explains why previous studies believed that meiosis I spindles persist in cells where Cdc14 activity is impaired, since cell populations and not individual cells were analysed (Buonomo, Rabitsch et al. 2003, Marston, Lee et al. 2003). As a result of some cells having undergone a meiosis I-like segregation and others having undergone a meiosis II-like segregation, analysis of *cdc14-1* binucleate cells reveals a mixed segregation phenotype (Sharon and Simchen 1990a, Sharon and Simchen 1990b, Kamieniecki, Shanks et al. 2000). This mixed segregation phenotype is also observed when Cdc14 release is inhibited in anaphase I, as is seen when FEAR components *SLK19* and *SPO12* are deleted (Marston, Lee et al. 2003). Cdc14 activity, therefore, is essential for the formation of two meiosis II spindles and tetranucleate cells.

Despite the fact that *cdc14-1* mutants form only one meiosis II spindle and commit a single nuclear division, several molecular events characteristic of two rounds of chromosome segregation are still observed. Securin (Pds1) undergoes two rounds of accumulation and degradation, indicative of two FEAR activation events (Bizzari and Marston 2011). Furthermore, cohesin (Rec8) is removed from chromosomes in a stepwise manner, from chromosome arms in meiosis I and from pericentromere during meiosis II when Cdc14 release is impaired (Kamieniecki, Shanks et al. 2000).

The role of Cdc14 during the meiosis I to meiosis II transition has yet to be fully determined. Preliminary data from an incomplete analysis of CDKs in meiosis has suggested that at least a one major cyclin-CDK complex in meiosis is normally regulated independently of Cdc14 activity (Bizzari and Marston 2011). Clb1 does not appear to be prematurely degraded when Cdc14 is ectopically released from inhibition, nor is it stabilised when Cdc14 activity impaired. This would appear to contradict the theory that Cdc14 had a CDK-inhibitory role during meiosis, as is observed in mitotic exit. However, Clb1 analysis cannot disprove the possibility that Cdc14 is required for the down-regulation of other mitotic CDKs at the meiosis I-meiosis II transition. Further analysis of Clb-CDKs in meiosis is required.

1.3 Aim of this study

In this study, I will attempt to discern the role of Cdc14 in the meiosis I to meiosis II transition using budding yeast as a model organism. To date, how meiotic cells are able to undergo two consecutive rounds of chromosome segregation without entering an intermediate round of DNA duplication has yet to be determined. Understanding the mechanics of meiotic regulation is essential to establish how and why chromosome segregation errors occur. Aneuploidy in human meiotic cells mostly results in the spontaneous termination of a developing foetus, and any offspring that survive until birth often exhibit birth defects such as Down Syndrome and Turner syndrome. I hope that my work could provide insight into possible causes of infertility, miscarriage and birth defects that arise in humans.

Chapter 2

Materials and Methods

2. Materials and Methods

2.1 General Information

2.1.1 Supplier information

Chemicals used in this study were purchased from G.E. Healthcare, Life Technologies, Roche, Sigma, Starlab, Thermo Fisher Scientific, Qiagen and VWR International, unless stated otherwise. Formedium, Difco and Sigma provided growth medium components. New England BioLabs supplied restriction enzymes.

2.1.2 Sterilisation

Most solutions used were sterilised by filtration using a 0.45 µm bottle top (Nalgene) or syringe (Millipore) filters. Growth media was autoclaved at 120°C and 15 pounds/inch^2 for 15 min. All glassware was sterilised by baking at 250°C for 16 h.

2.2 Bacterial methods

2.2.1 *E. coli* strains

DH5α electrocompetent cells were used for cloning and propagation of plasmids.

Strain name	Genotype
DH5α	*F- φ80lacZΔM15 Δ(lacZYA-argF)U169 deoR recA1 endA1 hsdR17(rk-, mk+) phoA supE44 thi-1 gyrA96 relA1 λ*
BL21 (EC76)	*F- dcm ompT hsdS (r_B- m_B-) gal [malB$^+$]$_{K-12}$ (λ^S)*
EC77	BL21 containing AMp943 (*PGK1-GST*)
EC78	BL21 containing AMp945 (*PGK1-MBP*)
EC79	BL21 containing AMp949 (*KAR2-GST*)
EC80	BL21 containing AMp951 (*KAR2-MBP*)

Table 2. 2. 1: *E. coli* strains used in this study.

2.2.2 *E. coli* media

LB (Luria-Bertani): 1% (w/v) Bactotryptone

0.5% (w/v) Bacto-yeast extract

0.5% (w/v) NaCl

pH adjusted to 7.2 with NaOH

2% (w/v) agar was added for solid media.

2.2.3 *E. coli* growth conditions

Bacteria were typically grown on solid LB medium at 37°C or in liquid LB at 37°Cwith shaking. All plasmids used in this study carry an ampicillin resistance marker. For plasmid selection and maintenance, Amp was used within medium at a final concentration of 100 µg/ml.

2.2.4 Storage of *E. coli*

Bacterial cells were typically kept on LB-Amp plates at 4°C for 1-2 weeks. For long-term storage, bacterial strains were resuspended in 20% glycerol in cyrotubes and frozen at -80°C.

2.2.5 *E. coli* transformation by electroporation

Electrocompetent DH5α cells were thawed slowly on ice. 40 µl of cells were aliquoted into pre-chilled electroporation curvettes (Cell Projects, 2 mm gap). An appropriate amount of plasmid DNA (0.5 – 5 µl depending on plasmid concentration) was added to the cells and mixed. Electroporation was performed using a Bioread Gene Pulser II at 2.5 V, 200 Ω and 2.5 µF. Immediately following electroporation, 1 ml of 37°C LB media was added and transferred with the reaction to a glass tube for incubation at 37°C for 1 h. After the incubation, cultures were transferred to 1.5 ml eppendorf tubes and spun at 3000 rpm for 3 mins. The majority of the supernatant was aspirated leaving ~150 µl with which to resuspend and plate cells onto pre-warmed LB-Amp solid media. Reactions were incubated o/n at 37°C.

2.3 Budding yeast methods

2.3.1 Budding yeast strains

All yeast strains used in this study were diploid and derived from SK1, unless otherwise stated.

Strain number	Genotype
1835	*MATa/MATα*
3560	*MATa/MATα* *cdc20::pCLB2-3HA-CDC20::KanMX6/cdc20::pCLB2-3HA-CDC20::KanMX6*
6770	*MATa/MATα* *CLB1-9MYC::TRP1/CLB1-9MYC::TRP1* *GAL-NDT80::TRP1/GAL-NDT80::TRP1* *ura3::pGPD1-GAL4(848).ER::URA3/ura3::pGPD1-GAL4(848).ER::URA3*
6961	*MATa/MATα* *CLB1-9MYC::TRP1/CLB1-9MYC::TRP1* *cdc55::KanMX6::PCLB2-3HA-CDC55/cdc55::KanMX6::PCLB2-3HA-CDC55* *GAL-NDT80::TRP1/GAL-NDT80::TRP1* *ura3::pGPD1-GAL4(848).ER::URA3/ura3::pGPD1-GAL4(848).ER::URA3*
7815	*MATa/MATα* *CLB1-9MYC::TRP1/CLB1-9MYC::TRP1* *cdc14::KanMX6/cdc14::KanMX6* *trp1::cdc14-1::TRP1::LEU2/trp1::cdc14-1::TRP1::LEU2* *GAL-NDT80::TRP1/GAL-NDT80::TRP1* *ura3::pGPD1-GAL4(848).ER::URA3/ura3::pGPD1-GAL4(848).ER::URA3*
7816	*MATa/MATα* *CLB1-9MYC::TRP1/CLB1-9MYC::TRP1* *cdc14::KanMX6/cdc14::KanMX6* *trp1::cdc14-1::TRP1::LEU2/trp1::cdc14-1::TRP1::LEU2* *cdc55::KanMX6::PCLB2-3HA-CDC55/ cdc55::KanMX6::PCLB2-3HA-CDC55* *GAL-NDT80::TRP1/GAL-NDT80::TRP1* *ura3::pGPD1-GAL4(848).ER::URA3/ura3::pGPD1-GAL4(848).ER::URA3*

Table 2. 3. 1: *S. cerevisiae* strains used in this study.

Strain number	Genotype
8776	*MATa/MATα* *his3::HIS3p-GFP-TUB1-HIS3/his3::HIS3p-GFP-TUB1-HIS3* *SPC42-tdTomato::NAT/SPC42-tdTomato::NAT*
9004	*MATa/MATα* *CLB3-3HA::KANR/CLB3-3HA::KANR* *GAL-NDT80::TRP1/GAL-NDT80::TRP1* *ura3::pGPD1-GAL4(848).ER::URA3/ura3::pGPD1-GAL4(848).ER::URA3*
9005	*MATa/MATα* *CLB4-3HA::KANMX6/CLB3-3HA::KANMX6* *GAL-NDT80::TRP1/GAL-NDT80::TRP1* *ura3::pGPD1-GAL4(848).ER::URA3/ura3::pGPD1-GAL4(848).ER::URA3*
9006	*MATa/MATα* *CLB5-3HA::HIS3MX6/CLB5-3HA::HIS3MX6* *GAL-NDT80::TRP1/GAL-NDT80::TRP1* *ura3::pGPD1-GAL4(848).ER::URA3/ura3::pGPD1-GAL4(848).ER::URA3*
9007	*MATa/MATα* *CLB3-3HA::KANR/CLB3-3HA::KANR* *cdc55::KanMX6::PCLB2-3HA-CDC55/cdc55::KanMX6::PCLB2-3HA-CDC55* *GAL-NDT80::TRP1/GAL-NDT80::TRP1* *ura3::pGPD1-GAL4(848).ER::URA3/ura3::pGPD1-GAL4(848).ER::URA3*
9024	*MATa/MATα* *CLB4-3HA::KANMX6/CLB4-3HA::KANMX6* *cdc55::KanMX6::PCLB2-3HA-CDC55/cdc55::KanMX6::PCLB2-3HA-CDC55* *GAL-NDT80::TRP1/GAL-NDT80::TRP1* *ura3::pGPD1-GAL4(848).ER::URA3/ura3::pGPD1-GAL4(848).ER::URA3*
9025	*MATa/MATα* *CLB5-3HA::HIS3MX6/CLB5-3HA::HIS3MX6* *cdc55::KanMX6::PCLB2-3HA-CDC55/cdc55::KanMX6::PCLB2-3HA-CDC55* *GAL-NDT80::TRP1/GAL-NDT80::TRP1* *ura3::pGPD1-GAL4(848).ER::URA3/ura3::pGPD1-GAL4(848).ER::URA3*

Table 2. 3. 1 (Continued): *S. cerevisiae* strains used in this study.

Strain number	Genotype
9065	*MATa/MATα* *CLB3-3HA::KANR/CLB3-3HA::KANR* *cdc14::KanMX6/cdc14::KanMX6* *leu2::cdc14-1::LEU2::TRP1/ leu2::cdc14-1::LEU2::TRP1* *GAL-NDT80::TRP1/GAL-NDT80::TRP1* *ura3::pGPD1-GAL4(848).ER::URA3/ura3::pGPD1-GAL4(848).ER::URA3*
9066	*MATa/MATα* *CLB4-3HA::KANMX6/CLB4-3HA::KANMX6* *cdc14::KanMX6/cdc14::KanMX6* *leu2::cdc14-1::LEU2::TRP1/leu2::cdc14-1::LEU2::TRP1* *GAL-NDT80::TRP1/GAL-NDT80::TRP1* *ura3::pGPD1-GAL4(848).ER::URA3/ura3::pGPD1-GAL4(848).ER::URA3*
9067	*MATa/MATα* *CLB5-3HA::HIS3MX6/CLB5-3HA::HIS3MX6* *cdc14::KanMX6/cdc14::KanMX6* *leu2::cdc14-1::LEU2::TRP1/leu2::cdc14-1::LEU2::TRP1* *GAL-NDT80::TRP1/GAL-NDT80::TRP1* *ura3::pGPD1-GAL4(848).ER::URA3/ura3::pGPD1-GAL4(848).ER::URA3*
9068	*MATa/MATα* *CLB3-3HA::KANR/CLB3-3HA::KANR* *cdc14::KanMX6/cdc14::KanMX6* *leu2::cdc14-1::LEU2::TRP1/leu2::cdc14-1::LEU2::TRP1* *cdc55::KanMX6::PCLB2-3HA-CDC55/cdc55::KanMX6::PCLB2-3HA-CDC55* *GAL-NDT80::TRP1/GAL-NDT80::TRP1* *ura3::pGPD1-GAL4(848).ER::URA3/ura3::pGPD1-GAL4(848).ER::URA3*
9178	*MATa/MATα* *CLB5-3HA::HIS3MX6/CLB5-3HA::HIS3MX6* *cdc14::KanMX6/cdc14::KanMX6* *leu2::cdc14-1::LEU2::TRP1/leu2::cdc14-1::LEU2::TRP1* *cdc55::KanMX6::PCLB2-3HA-CDC55/cdc55::KanMX6::PCLB2-3HA-CDC55* *GAL-NDT80::TRP1/GAL-NDT80::TRP1* *ura3::pGPD1-GAL4(848).ER::URA3/ura3::pGPD1-GAL4(848).ER::URA3*

Table 2. 3. 1 (Continued): *S. cerevisiae* strains used in this study.

Strain number	Genotype
9212	*MATa/MATα* *CLB4-3HA::KANMX6/CLB4-3HA::KANMX6* *cdc14::KanMX6/cdc14::KanMX6* *leu2::cdc14-1::LEU2::TRP1/leu2::cdc14-1::LEU2::TRP1* *cdc55::KanMX6::PCLB2-3HA-CDC55/cdc55::KanMX6::PCLB2-3HA-CDC55* *GAL-NDT80::TRP1/GAL-NDT80::TRP1* *ura3::pGPD1-GAL4(848).ER::URA3/ura3::pGPD1-GAL4(848).ER::URA3*
9319	*MATa/MATα* *CDC14-SZZ(TAP)::KanMX6/CDC14-SZZ(TAP)::KanMX6* *cdc55::KanMX6::PCLB2-3HA-CDC55/cdc55::KanMX6::PCLB2-3HA-CDC55*
9434	*MATa/MATα* *CDC14-SZZ(TAP)::KanMX6/CDC14-SZZ(TAP)::KanMX6*
9459	*MATa/MATα* *cdc55::KanMX6::PCLB2-3HA-CDC55/cdc55::KanMX6::PCLB2-3HA-CDC55*
11517	*MATa/MATα* *CDC14-GFP-LEU2/CDC14-GFP-LEU2* *SPC42-tdTomato::NAT/SPC42-tdTomato::NAT* *GAL-NDT80::TRP1/GAL-NDT80::TRP1* *ura3::pGPD1-GAL4(848).ER::URA3/ura3::pGPD1-GAL4(848).ER::URA3*
11443	*MATa/MATα* *SPC42-3FLAG-KANMX6/SPC42-3FLAG-KANMX6* *cdc14::KanMX6/cdc14::KanMX6* *trp1::cdc14-1::TRP1::LEU2/trp1::cdc14-1::TRP1::LEU2*
11444	*MATa/MATα* *SPC42-3FLAG-KANMX6/SPC42-3FLAG-KANMX6*
12329	*MATa/MATα* *SFI1-6HA::KanMX6/SFI1-6HA::KanMX6* *GAL-NDT80::TRP1/GAL-NDT80::TRP1* *ura3::pGPD1-GAL4(848).ER::URA3/ura3::pGPD1-GAL4(848).ER::URA3*
12330	*MATa/MATα* *SFI1-6HA::KanMX6/SFI1-6HA::KanMX6* *cdc14::KanMX6/cdc14::KanMX6* *trp1::cdc14-1::TRP1::LEU2/trp1::cdc14-1::TRP1::LEU2* *GAL-NDT80::TRP1/GAL-NDT80::TRP1* *ura3::pGPD1-GAL4(848).ER::URA3/ura3::pGPD1-GAL4(848).ER::URA3*

Table 2. 3. 1 (Continued): *S. cerevisiae* strains used in this study.

Strain number	Genotype
13123	*MATa/MATα* *CDC14-GFP-LEU2/CDC14-GFP-LEU2* *SPC42-tdTomato::NAT/SPC42-tdTomato::NAT* *cdc55::KanMX6::PCLB2-3HA-CDC55/cdc55::KanMX6::PCLB2-3HA-CDC55* *GAL-NDT80::TRP1/GAL-NDT80::TRP1* *ura3::pGPD1-GAL4(848).ER::URA3/ura3::pGPD1-GAL4(848).ER::URA3*
13989	*MATa/MATα* *SPC42-tdTomato::NAT/SPC42-tdTomato::NAT* *GAL-NDT80::TRP1/GAL-NDT80::TRP1* *ura3::pGPD1-GAL4(848).ER::URA3/ura3::pGPD1-GAL4(848).ER::URA3*
14709	*MATa/MATα* *CDC14-SZZ(TAP)::KanMX6/CDC14-SZZ(TAP)::KanMX6* *cdc55::KanMX6::PCLB2-3HA-CDC55/cdc55::KanMX6::PCLB2-3HA-CDC55* *cdc20::pCLB2-3HA-CDC20::KanMX6/cdc20::pCLB2-3HA-CDC20::KanMX6*
14939	*MATa/MATα* *CDC14-SZZ(TAP)::KanMX6/CDC14-SZZ(TAP)::KanMX6* *cdc20::pCLB2-3HA-CDC20::KanMX6/cdc20::pCLB2-3HA-CDC20::KanMX6*
15024	*MATa/MATα* *cdc55::KanMX6::PCLB2-3HA-CDC55/cdc55::KanMX6::PCLB2-3HA-CDC55* *cdc20::pCLB2-3HA-CDC20::KanMX6/cdc20::pCLB2-3HA-CDC20::KanMX6*
15543	*MATa/MATα* *CDC14-GFP-LEU2/CDC14-GFP-LEU2* *SPC42-tdTomato::NAT/SPC42-tdTomato::NAT* *bub2Δ::NAT/bub2Δ::NAT* *GAL-NDT80::TRP1/GAL-NDT80::TRP1* *ura3::pGPD1-GAL4(848).ER::URA3/ura3::pGPD1-GAL4(848).ER::URA3*
15984	*MATa/MATα* *SPC42-tdTomato::NAT/SPC42-tdTomato::NAT* *cdc55::KanMX6::PCLB2-3HA-CDC55/cdc55::KanMX6::PCLB2-3HA-CDC55* *GAL-NDT80::TRP1/ GAL-NDT80::TRP1* *ura3::pGPD1-GAL4(848).ER::URA3/ura3::pGPD1-GAL4(848).ER::URA3*

Table 2. 3. 1 (Continued): *S. cerevisiae* strains used in this study.

Strain number	Genotype
15985	*MATa/MATα* *his3::HIS3p-GFP-TUB1-HIS3/his3::HIS3p-GFP-TUB1-HIS3* *PDS1-tdTomato-KITRP1/PDS1-tdTomato-KITRP1* *spo12Δ::LEU2/spo12Δ::LEU2* *GAL-NDT80::TRP1/GAL-NDT80::TRP1* *ura3::pGPD1-GAL4(848).ER::URA3/ura3::pGPD1-GAL4(848).ER::URA3*
16019	*MATa/MATα* *SPC42-tdTomato::NAT/SPC42-tdTomato::NAT* *bfa1Δ::NAT/bfa1Δ::NAT* *GAL-NDT80::TRP1/GAL-NDT80::TRP1* *ura3::pGPD1-GAL4(848).ER::URA3/ura3::pGPD1-GAL4(848).ER::URA3*
16020	*MATa/MATα* *SPC42-tdTomato::NAT/SPC42-tdTomato::NAT* *slk19Δ::KANMX6/slk19Δ::KANMX6* *GAL-NDT80::TRP1/GAL-NDT80::TRP1* *ura3::pGPD1-GAL4(848).ER::URA3/ura3::pGPD1-GAL4(848).ER::URA3*
16021	*MATa/MATα* *SFI1-6HA::KanMX6/SFI1-6HA::KanMX6* *cdc55::KanMX6::PCLB2-3HA-CDC55/cdc55::KanMX6::PCLB2-3HA-CDC55* *GAL-NDT80::TRP1/GAL-NDT80::TRP1* *ura3::pGPD1-GAL4(848).ER::URA3/ura3::pGPD1-GAL4(848).ER::URA3*
16064	*MATa/MATα* *SPC42-tdTomato::NAT/SPC42-tdTomato::NAT* *spo12Δ::LEU2/spo12Δ::LEU2* *GAL-NDT80::TRP1/GAL-NDT80::TRP1* *ura3::pGPD1-GAL4(848).ER::URA3/ura3::pGPD1-GAL4(848).ER::URA3*
16065	*MATa/MATα* *his3::HIS3p-GFP-TUB1-HIS3/his3::HIS3p-GFP-TUB1-HIS3* *PDS1-tdTomato-KITRP1/PDS1-tdTomato-KITRP1* *GAL-NDT80::TRP1/GAL-NDT80::TRP1* *ura3::pGPD1-GAL4(848).ER::URA3/ura3::pGPD1-GAL4(848).ER::URA3*

Table 2. 3. 1 (Continued): *S. cerevisiae* strains used in this study.

Strain number	Genotype
16066	*MATa/MATα* *his3::HIS3p-GFP-TUB1-HIS3/his3::HIS3p-GFP-TUB1-HIS3* *PDS1-tdTomato-KITRP1/PDS1-tdTomato-KITRP1* *cdc14::KanMX6/cdc14::KanMX6* *leu2::cdc14-1::LEU2::TRP1/leu2::cdc14-1::LEU2::TRP1* *GAL-NDT80::TRP1/GAL-NDT80::TRP1* *ura3::pGPD1-GAL4(848).ER::URA3/ura3::pGPD1-GAL4(848).ER::URA3*
16077	*MATa/MATα* *cdc14::KanMX6/cdc14::KanMX6* *leu2::cdc14-1::LEU2::TRP1/leu2::cdc14-1::LEU2::TRP1* *GAL-NDT80::TRP1/GAL-NDT80::TRP1* *ura3::pGPD1-GAL4(848).ER::URA3/ura3::pGPD1-GAL4(848).ER::URA3*
16078	*MATa/MATα* *GAL-NDT80::TRP1/GAL-NDT80::TRP1* *ura3::pGPD1-GAL4(848).ER::URA3/ura3::pGPD1-GAL4(848).ER::URA3*
16079	*MATa/MATα* *CDC14-GFP-LEU2/CDC14-GFP-LEU2* *SPC42-tdTomato::NAT/SPC42-tdTomato::NAT* *bfa1Δ::NAT/bfa1Δ::NAT* *GAL-NDT80::TRP1/GAL-NDT80::TRP1* *ura3::pGPD1-GAL4(848).ER::URA3/ura3::pGPD1-GAL4(848).ER::URA3*
16080	*MATa/MATα* *SPC42-tdTomato::NAT/SPC42-tdTomato::NAT* *bub2Δ::NAT/bub2Δ::NAT* *GAL-NDT80::TRP1/GAL-NDT80::TRP1* *ura3::pGPD1-GAL4(848).ER::URA3/ura3::pGPD1-GAL4(848).ER::URA3*
16108	*MATa/MATα* *SPC42-tdTomato::NAT/SPC42-tdTomato::NAT* *sfi1::KanMX6::PCLB2-3HA-SFI1/sfi1::KanMX6::PCLB2-3HA-SFI1* *GAL-NDT80::TRP1/GAL-NDT80::TRP1* *ura3::pGPD1-GAL4(848).ER::URA3/ura3::pGPD1-GAL4(848).ER::URA3*
16110	*MATa/MATα* *his3::HIS3p-GFP-TUB1-HIS3/his3::HIS3p-GFP-TUB1-HIS3* *PDS1-tdTomato-KITRP1/PDS1-tdTomato-KITRP1* *slk19Δ::TRP/slk19Δ::TRP* *GAL-NDT80::TRP1/GAL-NDT80::TRP1* *ura3::pGPD1-GAL4(848).ER::URA3/ura3::pGPD1-GAL4(848).ER::URA3*

Table 2. 3. 1 (Continued): *S. cerevisiae* strains used in this study.

Strain number	Genotype
16163	*MATa/MATα* *SPC42-tdTomato::NAT/SPC42-tdTomato::NAT* *cdc14::KanMX6/cdc14::KanMX6* *trp1::cdc14-1::TRP1::LEU2/trp1::cdc14-1::TRP1::LEU2* *GAL-NDT80::TRP1/GAL-NDT80::TRP1* *ura3::pGPD1-GAL4(848).ER::URA3/ura3::pGPD1-GAL4(848).ER::URA3*
16198	*MATa/MATα* *cdc55::KanMX6::PCLB2-3HA-CDC55/cdc55::KanMX6::PCLB2-3HA-CDC55* *GAL-NDT80::TRP1/GAL-NDT80::TRP1* *ura3::pGPD1-GAL4(848).ER::URA3/ura3::pGPD1-GAL4(848).ER::URA3*
17134	*MATa/MATα* *CDC14-GFP-LEU2/CDC14-GFP-LEU2* *SPC42-tdTomato::NAT/SPC42-tdTomato::NAT* *kin4Δ::NAT/kin4Δ::NAT* *GAL-NDT80::TRP1/GAL-NDT80::TRP1* *ura3::pGPD1-GAL4(848).ER::URA3/ura3::pGPD1-GAL4(848).ER::URA3*
17270	*MATa* *SPC42-GFP::KanMX6*
17341	*MATa/MATα* *CDC14-GFP-LEU2/CDC14-GFP-LEU2* *SPC42-tdTomato::NAT/SPC42-tdTomato::NAT* *bmh1Δ::NAT/bmh1Δ::NAT* *GAL-NDT80::TRP1/GAL-NDT80::TRP1* *ura3::pGPD1-GAL4(848).ER::URA3/ura3::pGPD1-GAL4(848).ER::URA3*
17537	*MATα* *CDC14-GBP-mRFP::HIS3*
17740	*MATa/MATα* *Bfa1-tdTomato::NAT/Bfa1-tdTomato::NAT* *SPC42-CFP::TRP1/SPC42-CFP::TRP1* *CDC14-GFP-LEU2/CDC14-GFP-LEU2* *GAL-NDT80::TRP1/GAL-NDT80::TRP1* *ura3::pGPD1-GAL4(848).ER::URA3/ura3::pGPD1-GAL4(848).ER::URA3*

Table 2. 3. 1 (Continued): *S. cerevisiae* strains used in this study.

Strain number	Genotype
17904	*MATa/MATα* *SPC42-tdTomato::NAT/SPC42-tdTomato::NAT* *cdc14::KanMX6/cdc14::KanMX6* *trp1::cdc14-1::TRP1::LEU2/trp1::cdc14-1::TRP1::LEU2* *cdc55::KanMX6::PCLB2-3HA-CDC55/cdc55::KanMX6::PCLB2-3HA-CDC55* *GAL-NDT80::TRP1/GAL-NDT80::TRP1* *ura3::pGPD1-GAL4(848).ER::URA3/ura3::pGPD1-GAL4(848).ER::URA3*

Table 2. 3. 1 (Continued): *S. cerevisiae* strains used in this study.

2.3.1.1 Yeast strain construct and origin

pCLB2-3HA-CDC55 (cdc55mn) was described in (Clift, Bizzari et al. 2009). *CLB1-9MYC* was described in (Buonomo, Rabitsch et al. 2003). c*dc20mn* was described in (Lee and Amon 2003). *GAL-NDT80* and *pGPD1-GAL4(848).ER* were described in (Benjamin, Zhang et al. 2003). *CLB1-9Myc, cdc14-1, slk19Δ* and *spo12Δ* were described in (Marston, Lee et al. 2003). *CDC14-GFP, PDS1-tdTomato* and *GFP-TUB1* were described in (Matos, Lipp et al. 2008). *SPC42-tdTomato* was described in (Fernius and Hardwick 2007). A one-step PCR method was used to generate *pCLB2-3HA-SFI1* (sfi1mn) (Lee and Amon, 2003), *CDC14-SZZ(TAP), SPC42-3FLAG, SPC42-GFP, CDC14-GBP, SFI1-6HA, BFA1-tdTomato, bub2Δ, bfa1Δ, kin4Δ, bmh1Δ* (Longtine et al., 1998) strains. The S*PC42-CFP* strain was obtained by integrating the AMp267 plasmid at the *SPC42* locus.

2.3.2 Budding yeast media

YPDA:	2% (w/v) Bacto-peptone
	1% (w/v) Bacto-yeast extract
	2% (w/v) Glucose
	0.3 mM Adenine
YPG:	2% (w/v) Bacto-peptone
	1% (w/v) Bacto-yeast extract
	2.5% (w/v) Glycerol
4%-YPDA:	2% (w/v) Bacto-peptone
	1% (w/v) Bacto-yeast extract
	4% (w/v) Glucose
BYTA:	2% (w/v) Bacto-peptone
	1% (w/v) Bacto-yeast extract
	1% (w/v) Potassium Acetate
	50 mM Potassium Phthalate
Sporulation media:	0.3% (w/v) Potassium acetate (pH 7)

For making solid media plates, 2% (w/v) agarose was added to liquid solutions prior to autoclaving.

2.3.3 Drugs

2.3.3.1 G418

Used for KanMX6 selection in solid media. G418 powder was dissolved in sterile water, filter sterilised and added to cooled melted agar-media at a final concentration of 300 μg/ml.

2.3.3.2 Hygromycin

Used for HPHMX6 selection in solid media. Hygromycin solution (50 mg/ml) was added to cooled melted agar-media at a final concentration of 300 μg/ml.

2.3.3.3 Clonat

Used for NatMX4 selection in solid media. Clonat stock solution (200 mg/ml) was added to cooled melted agar-media at a final concentration of 100 μg/ml.

2.3.4 Budding yeast growth conditions

Details of individual experiments are given in figure legends.

2.3.4.1 Preparation of cells for sporulation

For meiotic experiments, diploid strains were removed from -80°C storage onto YPG solid media plates and grown overnight (~16 h), The following day, cells were patched to 4%YPDA plates. On the third consecutive day, YPDA liquid cultures were inoculated with yeast strains and grown overnight. Cells were then diluted to OD_{600} =0.2 in BTYA liquid culture and grown to OD_{600} = 6-10. On the fifth day, cells were washed once in sterile water and resuspended in SPO liquid media at OD_{600} = 1.8-3. Meiosis was performed at 30°C.

2.3.4.2 GAL-NDT80 block and release method for synchronous meiosis

Diploid strains homozygous for *GAL-NDT80* and *GAL4(848)-ER* arrest in pachytene (Carlile and Amon 2008). Strains prepared for sporulation are left in SPO for 6 h before the addition of 1 μM of β-estradiol to induce transcription of *NDT80.* Samples were taken every 15 mins for 3 h, then every 30 mins for an additional 3 h after that.

2.3.4.3 Temperature sensitive alleles

Cells were G1-arrested at the permissive temperature (25°C) and released at the restrictive temperature (30°C).

2.3.4.4 Depletion of proteins in meiosis

To specifically deplete proteins during meiosis, the native promoter of the relevant gene was replaced with *pCLB2*, a mitosis-specific promoter (Lee and Amon 2003).

2.3.5 Budding yeast storage

For long-term storage of strains, yeast were resuspended in 20% glycerol in cryotubes and stored at -80°C.

2.3.6. High efficiency transformation

LiTE:	0.1 M LiAc
	10 mM Tris.HCl (pH 7.5)
	1 mM EDTA

40% PEG	0.1 M LiAc
	40% PEG 4000
	10 mM Tris.HCl (pH 7.5)
	1 mM EDTA

50 ml YPDA yeast cultures were grown overnight to OD_{600} =>6. Cultures were diluted the following morning to OD_{600} = 0.2 then grown to OD_{600} = 0.7-1. Cells were spun down at 3000 rpm for 3 mins, washed twice with sterile water and transferred to a 1.5 ml eppendorf tube. Cells were washed once in 1 ml LiTE and resuspended in 250 µl LiTE. 50 µl of yeast suspension was used per transformation reaction and mixed with ~10 µl DNA, 300 µl 40% PEG and 10 µl ssDNA. Reactions were incubated at 30°C for ~1 h then heat shocked at 42°C for 15 mins. Tubes were spun down at 3000 rpm for 3 mins, cell pellets were resuspended in 200 µl water and plated out on YPDA solid media.

2.3.7 Crossing strains

To cross strains, MATa and MATα haploids were mated, and the resulting diploids were selected for plating onto sporulation plates. To improve mating efficiency, a small amount of one strain containing a unique selectable marker was mixed with an excess of another strain of the opposite mating type on YPDA solid media and left to mate overnight. The mating was streaked on a selection plate and incubated until single colonies appear. The majority of these single colonies are diploids, which are picked and patched onto a sporulation plate and left for 2-3 days until tetrad formation occurs.

2.3.8 Tetrad dissection

Tetrads formed from crosses were checked from sporulation plates using a light microscope. A small amount of tetrads were resuspended in 20 µl of zymolase (1 mg/ml) and incubated for 7-8 mins. 1 ml of sterile water was used to dilute zymolase mixture, from which 20 µl were spread on a YPDA solid media plate. Tetrads were dissected using a Nikon Eclipse 50i microscope equipped with micromanipulator and incubated until spore proliferate to form colonies.

2.4 Microscopy methods

2.4.1 General Information

Imaging of fixed cells or live cells at isolated time-points was carried out using a Zeiss Axio Imager Z1 and a Photometrics EMCCD camera. Images were taken using Micro-Manager 1.4 and processed using ImageJ software. For the generation of microfluidics movies, a Deltavision® Elite live cell imaging system was utelised with an Olympus IX-71 microscope and a Photometrics EMCCD Cascade II camera. Multi-point images were taken using SoftWoRx, movies were assembled in Image-Pro Plus and processed further in ImageJ. For transmission EM, images were collected using a Philips CM120 Transmission electron microscope and a Gatan Orius CCD camera.

2.4.2 Whole cell Immunofluorescence (IF) for meiotic spindle analysis

Sorbitol-citrate:	1.2 M Sorbitol
	0.1 M K_2HPO_4
	36 mM Citric acid
PBS-BSA:	1% (w/v) BSA
	40 mM K_2HPO_4
	10 mM KH_2PO_4
	0.15 M NaCl
	0.1% NaN_3

DAPI mount:	9 mM *p*-phenylenediamine
	40 mM K_2HPO_4
	10 mM KH_2PO_4
	0.15 M NaCl
	0.1% NaN_3
	50 ng/ml DAPI
	90% (w/v) Glycerol

200 µl of culture from meiotic cell cycle time-course was spun down at 13000 rpm for 1 min and the cell pellet was resuspended in 1 ml of 3.7% formaldehyde in 0.1 M K Phosphate buffer (pH 6.4). Cells were fixed overnight at 4°C. The following day, cells were washed three times in 1 ml 0.1 M K Phosphate buffer and once in 1 ml sorbitol-citrate before resuspension in 200 µl sorbitol-citrate with 100 µg/ml zymolase 100T and 10% glusulase (Perkin Elmar). Cells were digested for 2 h at 37°C, and sufficient digestion was judged using a light microscope. Digested cells were then spun at 3000 rpm for 3 mins, washed twice in 1 ml sorbitol-citrate and resuspended in ~50 µl of sorbitol citrate. 5 µl of cells per well were placed onto multi-well polylysine slides and left for 10 mins. Excess liquid was aspirated, cell density per well was checked via light microscopy before slides were fixed. Fixation was carried out by submerging slides in methanol for 3 mins followed immediately by acetone for 10 secs before being left to dry. 5 µl of primary antibody solution (Table 2. 4. 1) was added per well and incubated for 2 h at room temperature in a dark moisture chamber. After incubation, cells were washed five times with 5 µl PBS-BSA and then 5 µl of secondary antibody solution (Table 2. 4. 1) was added per well. Slides were

incubated for 2 h in a moisture chamber at room temperature. Cells were washed five times with 5 µl PBS-BSA then 3 µl of DAPI-mount was added per well. A glass coverslip was placed on top of each slide, which were then sealed with clear nail polish and stored long term at -20°C before and after spindle analysis.

Protein	Fixation time	Primary antibody	Secondary antibody
Tubulin	Overnight (4°C)	rat α-TUB 1:50	α-rat FITC 1:100

Table 2. 4. 1: Fixation times and antibody dilutions for whole cell IF. Antibodies diluted in PBS-BSA.

2.4.3 Fluorescence analysis of fixed cells

100 µl of culture from a meiotic cell cycle time-course was added to eppendorf tubes containing 10 µl of 37% formaldehyde. Cells were fixed for 8-10 mins at room temperature. Tubes were spun down at 13000 rpm for 2 mins, washed with 1 ml of 80% ethanol and the cell pellet was resuspended in 20 µl of 1 µg/ml DAPI. Typically, 7 µl of cells were placed onto superfrost slides (BDH) and covered with a glass coverslip before microscopy. In addition to DAPI staining, fluorescently-tagged (-GFP, -tdTomato, -CFP) proteins can also be visualised using this method.

2.4.4 Fluorescence analysis of live cells using agarose pads

A lowered flat surface (~1mm in depth) was created on superfrost slides by taping both ends of the slide. 15-20 µl of melted 2% agarose was added to the centre of the lowered surface and compressed with a coverslip. Agarose was

allowed to cool and solidify before the coverslip was removed. 100 µl of culture from a meiotic cell cycle time-course was spun down at 13000 rpm for 2 mins and resuspended in 5µl of liquid media. 2-3 µl of cell suspension was added to each agarose pad. The slide was covered with a glass coverslip and sealed with a molten mixture of vasoline:lamalin:paraffin (1:1:1) before microscopy.

2.4.5 Fluorescence analysis of live cells using Microfluidics

Live-cell meiotic movies were generated using CellASIC® ONIX Y04D Microfluidics plates (Merck Millipore). All chambers on the plate were washed three times with 500 µl of sporulation media before 200 µl of sporulation media plus 1mM β-estradiol was added to chambers 1-6. Plates were then pre-incubated at 30°□□□□□ 30 mins. After incubation, 200 µl of an individual culture of pachytene-arrested cells was loaded into chamber 8. A total of four different strains can be imaged on a single plate. The microfluidics plate was attached via a low-profile manifold to the CellASIC® ONIX Microfluidic Platform Control System, and the assembly was placed on a Deltavision Elite microscope. Cells were loaded, visualised, washed with β-estradiol-containing sporulation media and imaged.

2.4.6 Quantification of fluorescence signal

Quantification of fluorescence signal was performed as described in (Hoffman, Pearson et al. 2001) In brief, the following equations were used:

$F_{Bk} = (F_O - F_i) * (A_i / (A_O - A_i))$ $F_x = F_i - F_{Bk}$

O and I represent outer and inner regions respectively. The inner region (I) contained ~90% of the signal measured. The outer region (O) was at least twice

the area of the inner region, and was used to calculate the surrounding background (Bk) signal. F signifies integrated fluorescence signal, calculated from Raw Integrated Densities, and A is area of the boxes (Table 2. 4. 6).

	Area of Inner Box (A_i)	**Area of Outer Box (A_O)**
Single images	16 pixels	64 pixels
Microfluidics movies	0.000544 inches	0.002 inches

Table 2. 4. 6: Areas used for quantification of fluorescence signal in this study.

2.4.7 Electron microscopy (EM)

3 ml of culture from meiotic cell cycle time-course per freezing event was vacuum filtered through a 0.45 µm Millipore filter. The cell paste was rapidly frozen under high pressure in a Wohlwend Compact 02 High Pressure Freezer (Boulder Electron Microscopy Services, University of Colorado, USA). Multiple freezing events were performed per time-point, and samples were kept in liquid nitrogen until the time-course was completed. Frozen cell pellets were then freeze substituted in acetone containing 2% (w/v) osmium tetroxide and 0.1% (w/v) uranyl acetate at -80°C. Samples were slowly warmed to room temperature over 3 days. After washing cells twice in acetone, samples were embedded in Epon 812 resin (Hexion) through multiple changes of diluted resin with acetone (1:3, 1:1 and 3:1). Three more changes using undiluted Epon 812 resin were carried out over 2 days before resin was polymerised at 60-70°C overnight. Epon blocks were serially sectioned at a thickness of 70 nm and stained with 2% (w/v) uranyl acetate in sterile water for 8 mins then in Reynolds' lead citrate for 3 mins. Sections were viewed on a Philips CM120

transmission electron microscope (EM Facility, University of Edinburgh) and images were collected with a Gatan Orius CCD camera. Help freezing cells was received from Tom Giddings Jr of the University of Colorado (Boulder). Sectioning was carried out by Eileen O'Toole, Mary Morphew and Courtney Ozzello of the University of Colorado (Boulder), and Stephen Mitchel of the University of Edinburgh.

2.5 Protein analysis

2.5.1 TCA protein extraction preparation

Trichloroacetic acid (TCA) protein extraction method was used for protein analysis from cell cycle cultures for rapid protein precipitation and preservation of protein phosphorylation.

TE:	10 mM Tris-HCl (pH 7.5)
	1 mM EDTA
3x SDS sample buffer:	187 mM Tris (pH 6.8)
	6% (w/v) β-mercaptoethanol
	30% (w/v) Glycerol
	9% (w/v) SDS
	0.05% (w/v) Bromophenol blue

5 ml of culture from cell cycle time-course was spun down in 15 ml falcon tubes at 4000 rpm for 3 mins. Cell pellets were resuspended in 5 ml of 5% TCA and incubated on ice for 10 mins. Tubes were spun down at 4000 rpm for 3 mins at 4°C, the majority of the supernatant was discarded and the pellet was transferred to 2 ml Fastprep tubes (MP Biomedicals) using residual supernatant. Tubes were spun down briefly at 14000 rpm before complete removal of supernatant, and cell pellets were snap-frozen in liquid nitrogen before storage at -80°C. Pellets were then resuspended in 1 ml of acetone via vortexing, spun down at 14000 rpm for 7 mins and the acetone was removed. Cell pellets were air dried in a fume hood for 2-3 h. Dried pellets were then resuspended in 100 µl of ice-cold TE with 2.75 µl of 1 M DTT and 1x Roche EDTA-free protease

inhibitors and a small quantity of glass beads (Sigma). Cells were disrupted using a Fastprep Bio-pulveriser FP120, subjecting tubes to 3 x 45 secs disruption at speed 6.0. 50 µl of 3x SDS sample buffer was added and extracts boiled at 100°C for 5 mins. Tubes were spun down at 14000 rpm for 5 mins and eluted protein was transferred to a new eppendorf before loading onto a gel.

2.5.2 Protein extraction preparation without TCA

When phosphorylation preservation is not essential, protein preparation without TCA was utilised. 10 ml cultures were grown overnight to saturation. Cultures were spun down at 4000 rpm for 3 mins, cell pellets were resuspended in 1 ml of ice-cold 10 mM Tris (pH 7.5) and transferred to Fastprep tubes. Tubes were spun down briefly at 4°C, the supernatant was discarded and cell pellets were snap-frozen in liquid nitrogen for storage at -80°C. Thawed pellets were then resuspended in 100 µl of ice-cold TE with 2.75 µl of 1 M DTT and 1x Roche EDTA-free protease inhibitors and a small quantity of glass beads (Sigma). Cells were disrupted using a Fastprep Bio-pulveriser FP120, subjecting tubes to 3 x 45 secs disruption at speed 6.0. 50 µl of 3x SDS sample buffer was added and extracts boiled at 100°C for 5 mins. Tubes were spun down at 14000 rpm for 5 mins and eluted protein was transferred to a new eppendorf before loading onto a gel.

2.5.3 SDS Polyacrylamide Gel Electrophoresis (SDS-PAGE)

4x Separation buffer:	1.5 M Tris
	0.4% (w/v) SDS
	pH adjusted to 8.8 with glacial acetic acid

2x Stacking buffer:	0.25 M Tris
	0.2% (w/v) SDS
	pH adjusted to 8.8 with glacial acetic acid

Two glass plates were assembled with 1 .5mm gap and the edges sealed with 1% agarose. Polyacrylamide separation gels were prepared according to Table 2. 5. 3 and were poured between the glass plates. The gel was topped with isopropanol to level off the gel, which was then allowed to polymerise. After polymerisation, the isopropanol was removed, the stacking gel (Table 2. 5. 3) was poured on top and a comb of 20 wells was inserted into the stacking gel for setting. Large gels were run using Biometra V15.17 electrophoresis apparatus in 1 x running buffer at 65 mA until samples reached the separation gel layer, when they were then ran at 12mA overnight. Small gels were run on a Mini Trans-Blot Electrophoretic Transfer Cell (Biorad) at 65 mA for ~3 h. A prestained protein marker (GE Healthcare or NEB) was loaded alongside samples.

	10% Separation buffer	**6% Separation buffer**	**4% Stacking buffer**
30% acrylamide (National Diagnostics)	10ml	6 ml	2 ml
4 x Separation buffer	7.5 ml	7.5 ml	-
2 x Stacking buffer	-	-	7.5 ml
10% APS	450 µl	450 µl	150 µl
TEMED	30 µl	30 µl	15 µl
Water	12.5 ml	16.5 ml	5.3 ml

Table 2. 5. 3: Polyacrylamide gel recipes (amounts per one large gel).

2.5.4 Western blotting

Transfer buffer: 25 mM Tris

1.5% (w/v) Glycine

0.02% (w/v) SDS

10% (v/v) Methanol

Ponceau S: 0.47% (w/v) Ponceau S

3% (w/v) TCA

1% (v/v) Acetic acid)

PBS-T: 0.1% Tween-20 in PBS

Following electrophoresis, gels were transferred onto protran BA 85 nictrocellulous membranes (Whatmann). Large gels were transferred using an Amersham TE70 semi-dry transfer unit and small gels were transferred using a Mini Trans-Blot Electrophoretic Transfer Cell. The membrane and blotting paper (Amersham) were soaked in transfer buffer prior to transfer at 1 mA/cm^2 for 2.5 h. After transfer, membranes were stained with Ponceau S then blocked with 2% dry milk in PBS-T. Membranes were incubated with primary antibody (Table 2. 5. 4) overnight at 4°C. Membranes were then washed three times for 15 mins in PBS-T and incubated with secondary antibody (Table 2. 5. 4). After final incubation, membranes were washed twice with PBS-T for 15 mins then a final time with PBS for ~1 h before developing.

<table>
<tr><th></th><th>Primary antibody</th><th>Secondary antibody for ECL</th><th>Secondary antibody for LiCor</th></tr>
<tr><td>-HA/-6HA</td><td>mouse α-12CA5 (Roche) 1:1000</td><td rowspan="2">α-mouse 1:5000</td><td rowspan="2">IRDye® 800CW Donkey α-mouse 1:10000 (LiCor® Bioscience)</td></tr>
<tr><td>-9Myc</td><td>mouse α-9E10 (Roche) 1:1000</td></tr>
<tr><td>-SZZ(TAP)</td><td colspan="2">mouse α-PAP (Thermo Fisher) 1:1000</td><td>-</td></tr>
<tr><td>KAR2</td><td>rabbit α-KAR2 (laboratory stock) 1:5000</td><td rowspan="2">α-rabbit 1:5000</td><td rowspan="2">IRDye® 680RD Donkey α-rabbit 1:10000 (LiCor® Bioscience)</td></tr>
<tr><td>PGK1</td><td>rabbit α-PGK1 (laboratory stock) 1:10000</td></tr>
</table>

Table 2. 5. 4: Antibodies used for western blots in this study. Antibodies were diluted with 2% milk in PBS-T.

2.5.4.1 Western blot analysis using ECl

The ECL detection method was utilised to analyse faint protein signals since ECL offers increased sensitivity. Membranes were subjected to chemiluminescence using the SuperSignal West Pico chemiluminescent kit (Thermo scientific) according to manufactorers instructions. For Sfi1-6HA analysis, SuperSignal West Femto chemiluminescent kit was additionally used. Membranes were wrapped in Saran wrap and exposed to Kodak Bio-Max light film and developed using a Konica-Minolta SRX-101A developer.

2.5.4.2 Western blot analysis using LiCor®

LiCor was utilised for quantification of protein signal. LiCor IRDyes® secondary antibodies are labelled with fluorescent dyes which can be visualised under different wavelengths. The LiCor Odyssey® Quantitative Fluorescence Imager was used to scan membranes at 700nm and 800nm wavelengths. Odyssey® Infrared Imaging software was used to quantify protein signal.

2.5.5 Immunoprecipitation

Hyman buffer:	50 mM Bis-Tris propane (pH 7)
	100 mM KCl
	5 mM EGTA
	10% (v/v) Glycerol
SPB buffer:	20 mM Na-Hepes (pH 7.4)
	300 mM NaCl

Meiotic cells were harvested and washed with sterile water by centrigation at 4000 rpm for 6 mins. Cells were resuspended in 0.2x cell volume of sterile water before drop-freezing in liquid nitrogen. Cells were ground five times in a Retsch Mixer Mill MM400. The yeast lysate were then thawed in Hyman or SPB buffer plus inhibitors (Table 2. 5. 5), depending on pulldown experiment. Hyman buffer was used for Cdc14-TAP immunoprecipitations, whereas SPB buffer was used for Spc42-3FLAG IPs and was adapted from (Niepel, Strambio-de-Castillia et al. 2005). Triton X-100 was added to a final concentration of 1% (w/v) before sonication at 39% amplitude for 1 x 30 secs per 10 ml of lysate. Lysates were centrifuged at 4000 rpm for 5 mins at 4°C and supernatant was transferred to a new 50 ml falcon tube. Immunoprecipitation was performed by adding 5 mg of rabbit IgG-coupled Dynabeads or 18 mg of M2 αFLAG-coupled Dynabeads per 30 g lysed yeast, and rotating at 4°C for 2 h. Lysates were then washed five times in cold buffer without inhibitors and then transferred to a 1.5 ml eppendorf tube with 1ml buffer. Residual buffer was removed and 25 µl of 1x NuPAGE® LDS sample buffer was added to tubes before boiling at 100°C for 5 mins. Samples were transferred to new eppendorfs, removing the Dynabeads. 5 µl of β-mercaptoethanol was added to samples, boiled for another 5 mins then spun down at 13000 rpm for 5 mins before loading onto a precast NuPAGE® 8-12% Bis-Tris gel (Novex).

Inhibitor	Final concentration	Notes
CLAAPE	1x	From 2000x CLAAPE: Chymostatin, Leupeptin, Antipain, Pepstatin A, E-64 Protease inhibitor (all 10 mg/ml)
AEBSF (Pefabloc)	4 mM	
Benzamidine	2 mM	
PMSF	2 mM	
LR microcystin	0.4 μM	
N-ethylmaleimide (NEM)	2 mM	
Sodium orthovanadate	0.8 mM	From 20x phosphatase inhibitor solution
β-glycerophosphate	8 mM	
Sodium pyrosphosphate	4 mM	
Sodium fluoride	20 mM	

Table 2. 5. 5: Protease and phosphatase inhibitors used in immunoprecipitations.

2.5.5.1 Silver Staining

Silver staining was performed using a Silver Staining kit (Thermo Scientific) according to manufacturer's instructions.

2.5.5.2 Coomassie Staining

Coomassie staining was performed using a Colloidal Blue Staining kit (Novex) according to manufacturer's instructions.

2.5.5.3 In-gel tryptic digestion of proteins

Protein bands were excised from Coomassie-stained NuPAGE® 8-12% Bis-Tris gels and washed alternatingly with 50 mM ammonium bicarbonate and acetonitrile solutions until Coomassie staining was removed. Gel pieces were treated with 10 mM DTT in 50 mM ammonium bicarbonate for 30 mins at 37°C then DTT was removed and samples were washed with acetonitrile. 55 mM iodoacetamide in 50 mM ammonium bicarbonate was added to gel slices and incubated at room temperature in the dark for 20 mins. After washing again with 50 mM ammounium bicarbonate and acetonitrile, gel pieces were incubated with trypsin for 15 mins on ice then samples were transferred to 37°C for overnight digestion. The following morning, digestion reactions were treated with 0.1% (w/v) trifluoroacetic acid and left for 15 mins to allow peptides to diffuse from the gel. Samples were then passed through an equilibrated StageTip consisting of two layers of Empore Disks C18 within a pipette tip. A single StageTip was used per sample, as peptides within samples bind to StageTips. Peptides were later eluted for analysis via Mass Spectrometry.

2.5.5.4 Mass Spectrometry (MS)

Mass Spectrometry was performed by Flavia Alves and Juan Zao in the Juri Rappsilber lab (University of Edinburgh). MS data was compiled in MaxQuant 1.4.1.2 and quantitative analysis was performed using Perseus 1.5.1.6 software.

2.5.6 Production of polyclonal antibodies

2.5.6.1 Protein expression

E. coli strains EC77-80 were streaked on LB with ampicillin solid media and single colonies selected to inoculate 5 ml LB with ampicillin starter culture, grown overnight at 37°C. The next day, cells were diluted 1:100 in LB with ampicillin and grown again overnight. The following morning, cells were diluted 1:100 in LB with ampicillin in a 1 L volume and grown to OD = 0.4-0.8. A 5 ml sample was removed as a non-induced control before IPTG was added to the culture at a final concentration of 1 mM to induce protein expression. Cells were grown for 4 h at 37°C before harvesting via ultracentrifugation at 4°C for 10 mins at 3500 rpm.

2.5.6.2 Preparation of inclusion bodies

Lysis buffer:	20 mM Tris (pH 8.0)
	1 mM EDTA
	5 mM $MgCl_2$
	0.3 mM PMSF
	8 U/ml Benzonase
	400 µg/ml lysozyme
Resuspension buffer:	50 mM Tris (pH 8.0)
	300 mM NaCl
	1 mM EDTA
	1% (w/v) Triton X-100

Cells were resuspended in ~9 cell volumes of lysis buffer, ensuring that lumps are removed. Reactions were incubated for 20 mins at room temperature to enable Benzonase activity then reactions were ran through a Constant system 1.1 kW TS cell disruptor (EPPF, University of Edinburgh) on 39kPSI. The disruptor was washed through between samples with ddH_2O, 10% Deacon and HCl. A total cell extract was removed from samples for later comparison. 300 mM of NaCl and 1% (w/v) of Triton X-100 was added to protein samples, and resuspension buffer of an equal volume to that of the sample was also added. Reactions were vortexed briefly and spun down at 4°C for 20 mins at 10000 rpm. A soluble sample was taken from the supernatant and the rest was discarded. Cell pellets were washed three times in 10-20 cell volumes of resuspension buffer before finally resuspension in 1 ml resuspension buffer. 100 µl sample was removed to test the inclusion body fraction, and the rest of the sample was snap-frozen in liquid nitrogen for long-term storage. 3x SDS sample buffer was added to non-induced (NI), total cell extract (TCE), soluble (SOL) and inclusion body (IB) samples, boiled at 100°C for 5 mins and spun down at 14000 rpm for 5 mins. The eluted protein was transferred to a new eppendorf before loading onto a 10% SDS gel (Section 2. 5. 3) alongside BSA standards to visualise protein expression and determine concentration.

2.6 Nucleic Acids

2.6.1 Plasmids

Plasmid number	Name	Description	Origin
AMp195	*pFA6a-kanMX6*	Described in (Longtine, McKenzie et al. 1998)	Mark Longtine
AMp197	*pFA6a-GFP(S65T)-kanMX6*	Described in (Longtine, McKenzie et al. 1998)	Mark Longtine
AMp199	*pFA6a-GFP(S65T)-His3MX6*	Described in (Longtine, McKenzie et al. 1998)	Mark Longtine
AMp267	*PXH133/Spc42-CFP*	Described in (He, Asthana et al. 2000)	Peter Sorgen
AMp296	*pFA6a-GFP(S65T)-kanMX6 derivative*	AMp197 GFP gene mutated to F64L and S65T for brighter signal	Adele Marston
AMp348	*pFA6a-pCLB2-3HA-kanMX6*	Described in (Lee and Amon 2003)	Brian Lee
AMp495	*pFA6a-6HA-kanMX6*	6HA cloned into AMp195	Brian Lee
AMp636	*pFA6a-SZZ(TAP)-kanMX6*	SZZ(TAP) cloned into AMp195	
AMp683	*pFA6a-NAT*	Described in (Hentges, Van Driessche et al. 2005)	Kevin Hardwick

Table 2. 6. 1: Plasmids used in this study.

Plasmid number	Name	Description	Origin
AMp751	*pFA6a-tdTomato-NAT*	Described in (Taxis, Maeder et al. 2006)	
AMp795	*pDONR201*		Invitrogen
AMp796	*pDEST-GST*		Invitrogen
AMp797	*pDEST-INT*		Invitrogen
AMp798	*pDEST-MBP*		Invitrogen
AMp894	*pFA6a-3FLAG-kanMX6*	3FLAG cloned into AMp195	Robin Allshire
AMp934	*pCUP1-GBP-mRFP*		Peter Thorpe
AMp935	*pDONR201-PGK1*	PGK1 cloned into AMp795	This study
AMp942	*pDONR201-KAR2*	KAR2 cloned into AMp795	This study
AMp943	*pDEST-PGK1-GST*	PGK1 from AMp935 cloned into AMp796	This study
AMp944	*pDEST-PGK1-INT*	PGK1 from AMp935 cloned into AMp797	This study
AMp945	*pDEST-PGK1-MBP*	PGK1 from AMp935 cloned into AMp798	This study
AMp949	*pDEST-KAR2-GST*	KAR2 from AMp942 cloned into AMp796	This study

Table 2. 6. 1 (Continued): Plasmids used in this study.

Plasmid number	Name	Description	Origin
AMp950	*pDEST-KAR2-INT*	KAR2 from AMp942 cloned into AMp797	This study
AMp951	*pDEST-KAR2-MBP*	KAR2 from AMp942 cloned into AMp798	This study
AMp960	*pFA6a-GBP-mRFP-His3MX6*	GBP-mRFP amplified from AMp934 and cloned into AMp199 at GFP site	Kitty Verzijlbergen

Table 2. 6. 1 (Continued): Plasmids used in this study.

2.6.2 *E. coli* plasmid mini-prep

GTE solution:	50 mM glucose
	10 mM EDTA
	25 mM Tris (pH 7.5)
Alkaline SDS:	200 mM NaOH
	1 % (w/v) SDS
High salt buffer:	2.5 M potassium acetate (pH 4.8)

2 ml of LB-Amp was inoculated with *E. coli* and incubated at 37°C overnight. The cells were then spun down at 3000 rpm for 3 mins in a 1.5 ml eppendorf tube and the pellet was resuspended in 100 µl of GTE by vortexing. 150 µl of alkaline SDS was added and mixed via inversion. 150 µl of cold high salt buffer was then

added and mixed via inversion before incubation on ice for 15 mins. The reaction was then spun down at 14000 rpm for 5 mins and the supernatant was transferred to a new eppendorf containing 900 µl of cold ethanol. The reaction was then spun down at 14000 rpm for 5 mins, the pellet was washed with 200 µl of 70% ethanol, air dried then resuspended in 50 µl of TE.

2.6.3 Genomic DNA extraction from yeast

DNA breakage buffer:	2% (w/v) Triton X-100
	1% (w/v) SDS
	100 mM NaCl
	10 mM Tris.HCl (pH 8.0)
	1 mM EDTA

A toothpick of yeast cells from a solid media plate was suspended in 200 µl of DNA breakage buffer in an eppendorf tube, along with a scoop of glass beads and 200 µl phenol chloroform. The mixture was vortexed for 1-2 min and then spun down at 14000 rpm for 5 mins. The upper aqueous layer was transferred to a new eppendorf containing 1 ml of cold ethanol. The reaction was mixed via inversion then spun down at 14000 rpm for 5 mins. The supernatant was discarded and the pellet was air dried then suspended in 50 µl of TE.

2.6.4 Agarose gel electrophoresis

TAE buffer:	40 mM Tris
	1 mM EDTA
	0.11% (v/v) acetic acid

1% (w/v) agarose gels were used to analyse DNA with ethidium bromide staining. Agarose was dissolved in TAE buffer by microwaving. After cooling, ethidium bromide was added to the gel at a final concentration of 0.5 μg/ml. DNA samples were mixed with 1 x Orange G DNA loading buffer (NEB) and run at a voltage of 90-140 V. 1 kb DNA ladder (NEB) was ran alongside samples to determine band sizes. DNA was visualised using a UV transilluminator system.

2.6.5 PCR

PCR was performed using a Bio-Rad DNAEngine Thermal Cycler.

2.6.5.1 Polymerase Chain Reaction

10x PCR buffer:	100 mM Tris-HCl (pH 8.3)
	500 mM KCl
	20 mM $MgCl_2$
	0.1% (w/v) gelatin
PCR reaction:	10-500 ng template DNA
	1 μM of each oligonucleotide primer
	0.2 mM dNTPs
	1x PCR buffer
	DNA polymerase
	Sterile distilled water

For most applications, Taq polymerase purified in the lab was used. For reactions where sequence fidelity was essential, ExTaq DNA polymerase

(TaKaRa) was used with 10x PCR buffer and dNTPs provided by the manufacturer. PCR programmes varied depending on the size of the expected product and the annealing temperature of primers used (Fig. 2. 6. 5. 1).

Segment	Cycles	Temperature	Time
1	1	95°C	5 mins
2	24	95°C	30 secs
		55°C	30 secs
		72°C	1 min/kb
3	1	72°C	5 mins
4	1	10°C	forever

Table 2. 6. 5. 1: Template PCR programme.

2.6.5.2 Yeast colony PCR

A fraction of yeast colony DNA was added to 0.2 ml PCR tubes containing 20 µl of PCR reaction. PCR programmes varied depending on the annealing temperature of primers used (Fig. 2. 6. 5. 2).

Segment	Cycles	Temperature	Time
1	1	95°C	10 mins
2	30	95°C	30 secs
		55°C	30 secs
		72°C	1 min
3	1	72°C	5 mins
4	1	10°C	forever

Table 2. 6. 5. 2: Colony PCR programme.

2.6.6 Cloning

2.6.6.1 Restriction digest

Restriction digests were performed using NEB restriction enzymes and buffers according to manufacturer's instructions. Digests were subject to agarose gel electrophoresis to quickly confirm the identity of plasmids.

2.6.6.2 Gateway® cloning

Genes desired for cloning were amplified using PCR with primers to introduce *attB* flanking regions (Section 2. 6. 5. 1). PCR products were inserted into Donor Vector AMp795 using Gateway® Cloning kit containing BP Clonase™ following manufacturer's instructions. BP reactions were transformed into DH5α cells via electroporation (Section 2. 2. 5). Entry clones were isolated from *E. coli* via mini-prep reactions (Section 2. 6. 2). Genes were transferred into destination vectors

AMp796-798 containing epitope tags using LR Clonase™ following manufacturer's instructions.

2.6.6.3 Sequencing

Sequencing reaction: 1-2 µl mini-prep DNA

2 µl Big Dye v3.1

0.5 µl primer (5 µM)

2 µl 5x Big Dye buffer

3.5-4.5 µl sterile water

DNA samples were sequenced using the Big Dye Terminator kit v3.1 (Applied Biosystems; Table 2. 6. 6. 3) and analysed by GenePool (Edinburgh Genomics Sequencing Service, University of Edinburgh) on a ABI 3730 DNA analyser.

Segment	Cycles	Temperature	Time
1	1	95°C	30 secs
2	30	95°C	30 secs
		55°C	15 secs
		60°C	4 mins
3	1	72°C	5 mins
4	1	10°C	forever

Table 2. 6. 6. 3: Sequencing PCR programme.

Chapter 3

Cdc14 is not essential for cyclin degradation during meiosis I

3. Cdc14 is not essential for cyclin degradation during meiosis I

3.1 Introduction

Key eukaryotic cell cycle events, such as DNA replication and chromosome segregation, are driven by cyclin-dependent kinases (CDKs) (reviewed by Morgan 1997). In budding yeast, a single CDK, Cdc28, is activated through binding to different stage-specific cyclins. Progression of cells through S-phase and M-phase requires activation of Cdc28 by Clb1-Clb6 cyclins (Richardson, Lew et al. 1992, Schwob and Nasmyth 1993) whereas in G1 phase Cdc28 associates with Cln1-3 cyclins (Richardson, Wittenberg et al. 1989). Exit from mitosis is achieved through the inactivation of Clb-CDKs, creating permissive conditions for Cln-CDK activities and enabling cells to enter G1 (Amon, Irniger et al. 1994).

The protein phosphatase Cdc14 is essential for mitotic exit in budding yeast (Visintin, Craig et al. 1998). Cdc14 accomplishes mitotic CDK down-regulation through Clb proteolysis and activation of the CDK inhibitor, Sic1 (Jaspersen, Charles et al. 1998, Visintin, Craig et al. 1998, Zachariae, Schwab et al. 1998). It also reverses CDK-dependent phosphorylation (Bremmer, Hall et al. 2012), thus resetting the cell for the next round of DNA duplication.

One hallmark of CDK inactivation is spindle disassembly (Woodruff, Drubin et al. 2012). Cdc14 activates the anaphase-promoting complex (APC) through dephosphorylation of the regulatory subunit, Cdh1. In addition to initiating cyclin proteolysis, APC-dependent degradation of microtubule-stabilising proteins occurs. Degradation of spindle regulators, such as Ase1 (Juang, Huang et al. 1997), Fin1 (Woodbury and Morgan 2007) and Cin8 (Hildebrandt and Hoyt 2001, Roccuzzo, Visintin et al. 2015), results in

microtubule depolymerisation and disassembly of the mitotic spindle . Incomplete spindle disassembly in mitosis inhibits the subsequent assembly of spindles in the following cell cycle (Woodruff, Drubin et al. 2012).

The activity of protein phosphatase Cdc14 is tightly regulated during mitosis through differential subcellular localisation (Shou, Seol et al. 1999, Visintin, Hwang et al. 1999). During prophase and metaphase, Cdc14 is rendered inactive through binding to the inhibitor Cfi1/Net1 in the nucleolus. Upon anaphase onset, Cdc14 is released from nucleolar sequestration allowing it to dephosphorylate substrates and thereby enable mitotic progression. This nucleolar release is achieved through the phosphorylation of Cfi1/Net1 (Shou, Azzam et al. 2002, Yoshida and Toh-e 2002), which reduces its affinity for Cdc14.

Two distinct but interacting pathways regulate the release of Cdc14 in anaphase; the Cdc14 early anaphase release (FEAR) network and the Mitotic Exit Network (MEN). FEAR promotes the transient release of Cdc14 in early anaphase, promoting spindle stability, spindle elongation and activation of MEN (Pereira, Manson et al. 2002, Stegmeier, Visintin et al. 2002, Marston, Lee et al. 2003, Higuchi and Uhlmann 2005, Mohl, Huddleston et al. 2009). In late anaphase, MEN activation provides a complete and sustained release of Cdc14 that drives mitotic exit (Jaspersen, Charles et al. 1998, Shou, Seol et al. 1999, Azzam, Chen et al. 2004, Queralt, Lehane et al. 2006).

During meiosis, Cdc14 is released from nucleolar sequestration in anaphase I through activation of FEAR but not MEN (Kamieniecki, Liu et al. 2005, Attner and Amon 2012). MEN is in fact dispensable for meiosis I exit, suggesting that FEAR alone is sufficient for

anaphase I spindle disassembly (Marston, Lee et al. 2003). CDK activity must be reduced to a sufficient level to allow meiosis I spindles to disassemble. However, complete CDK inactivation would be expected to cause relicensing of DNA origins of replication. It is believed that meiotic CDKs are only partially down-regulated to prevent an intervening S-phase from occurring between meiosis I and meiosis II (Bizzari and Marston 2011). After meiosis I spindle breakdown, Cdc14 is then re-sequestered in metaphase II before a second release occurs in anaphase II (Bizzari and Marston 2011). Both FEAR and MEN activity in anaphase II ensures the complete inactivation of meiotic cyclin-CDKs and exit of cells from meiosis II (Attner and Amon 2012).

In a *cdc14-1* mutant at the restrictive temperature, Cdc14 is present in cells but the phosphatase allele is largely inactive (Marston, Lee et al. 2003). Impairment of Cdc14 activity during meiosis results in cells undergoing a single meiotic division, where homologous chromosomes are segregated normally on an anaphase I spindle (Sharon and Simchen 1990, Bizzari and Marston 2011). Tetranucleate cells are not formed. Initial analysis of fixed cells from poorly synchronised populations observed an increased fraction of cells with long spindles resembling anaphase I (Marston, Lee et al. 2003), suggesting a problem with anaphase I spindle breakdown. Later, live cell imagining revealed that anaphase I spindles do disassemble in *cdc14-1* mutants but 10-15% of cells then re-fuse nuclei and segregate sister chromatids on a single anaphase II spindle (Marston, Lee et al. 2003, Bizzari and Marston 2011). This leads to production of binucleate *cdc14-1* cells where some chromosomes have undergone a meiosis I-like segregation and others have undergone a meiosis II-like segregation. This mixed segregation phenotype is also observed when Cdc14 release is inhibited in anaphase I,

as is seen when FEAR components *SLK19* and *SPO12* are deleted (Marston, Lee et al. 2003).

Even though *cdc14-1* mutants are unable to assemble two meiosis II spindles and commit only a single nuclear division, a number of molecular events indicative of two rounds of chromosome segregation still occur. Pds1, the inhibitor of separase, undergoes two rounds of accumulation and degradation (Bizzari and Marston 2011). Cohesin subunit Rec8 is also lost from chromosomes in a stepwise manner (Kamieniecki, Shanks et al. 2000). It is therefore unclear what role Cdc14 plays in the transition between meiosis I and meiosis II. I set out to address this question, taking cues from what is known of Cdc14 function during mitosis.

I hypothesise that Cdc14 enables the partial down-regulation of meiotic CDK activity during the meiosis I-meiosis II transition. This hypothesis predicts that during late meiosis I, inactivation of Cdc14 would prevent CDK inactivation. The effect of Cdc14 on CDK down-regulation can be monitored through cyclin proteolysis. Inactivation of Cdc14 would lead to stabilisation of cyclins whereas early activation of Cdc14 would result in premature cyclin degradation. Spindle disassembly would also be affected if CDK inactivation were inhibited. Whilst Cdc14 is not required for spindle breakdown in meiosis (Bizzari and Marston 2011), a delay in anaphase I spindle disassembly could affect the subsequent assembly of a second meiosis II spindle perhaps through sequestration of tubulin monomers or by throwing meiosis out of synchrony. This could perhaps explain why a fraction of *cdc14-1* cells separate sister chromatids on a single meiosis II spindle and why *cdc14-1* mutants fail to produce tetranucleate cells.

3.2 Results

3.2.1 Rate of spindle disassembly is significantly affected when Cdc14 activity is impaired

To ascertain whether Cdc14 is required for timely breakdown of anaphase I spindles, I monitored spindle disassembly in live cells during meiosis. Pds1 degradation was used as a marker for entry into anaphase I. The time taken for the meiosis I spindle to completely disassemble after Pds1 proteolysis was measured in individual cells. In the wild type example (Fig. 3. 2. 1A), meiotic spindles break down 40 mins after entry into anaphase I. Following this, metaphase II spindles assemble. Pds1-tomato does not accumulate in live cells during prophase II. This observation is consistent with findings made previously using Pds1-tdTomato and Pds1-RFP constructs, and is believed to be due to a delay in fluorophore maturation (Katis, Lipp et al. 2010, Miller, Unal et al. 2012, Nerusheva, Galander et al. 2014).

In ~82% of *cdc14-1* cells, anaphase I spindles break down and a new spindle does not assemble (Fig. 3. 2. 1A). Similarly, *slk19Δ* and *spo12Δ* cells, which retain Cdc14 in the nucleolus (Stegmeier, Visintin et al. 2002, Marston, Lee et al. 2003), disassemble anaphase I spindles with a timing comparable to wild type cells. The individual rates of spindle disassembly for >67 cells were compiled to calculate a mean rate for all four strains (Fig. 3. 2. 1B). On average, wild type cells took 45.7 ± 2.32 mins to completely disassemble anaphase I spindles. In *cdc14-1* cells, a modest increase in the time taken to disassemble spindles (52.2 ± 1.97 mins) is observed. This increase is statistically significant (p=0.04). However, deletion of *SLK19* and *SPO12* also do not affect spindle breakdown timing, with mean rates of 43.8 ± 4.06 mins and 41.9 ± 2.86 mins respectively. These rates are not statistically significant from wild type cells (p=0.73

and 0.41). Taken together, this data suggests that the release of active Cdc14 may play a role in the timely disassembly of meiosis I spindles but by a FEAR-independent mechanism.

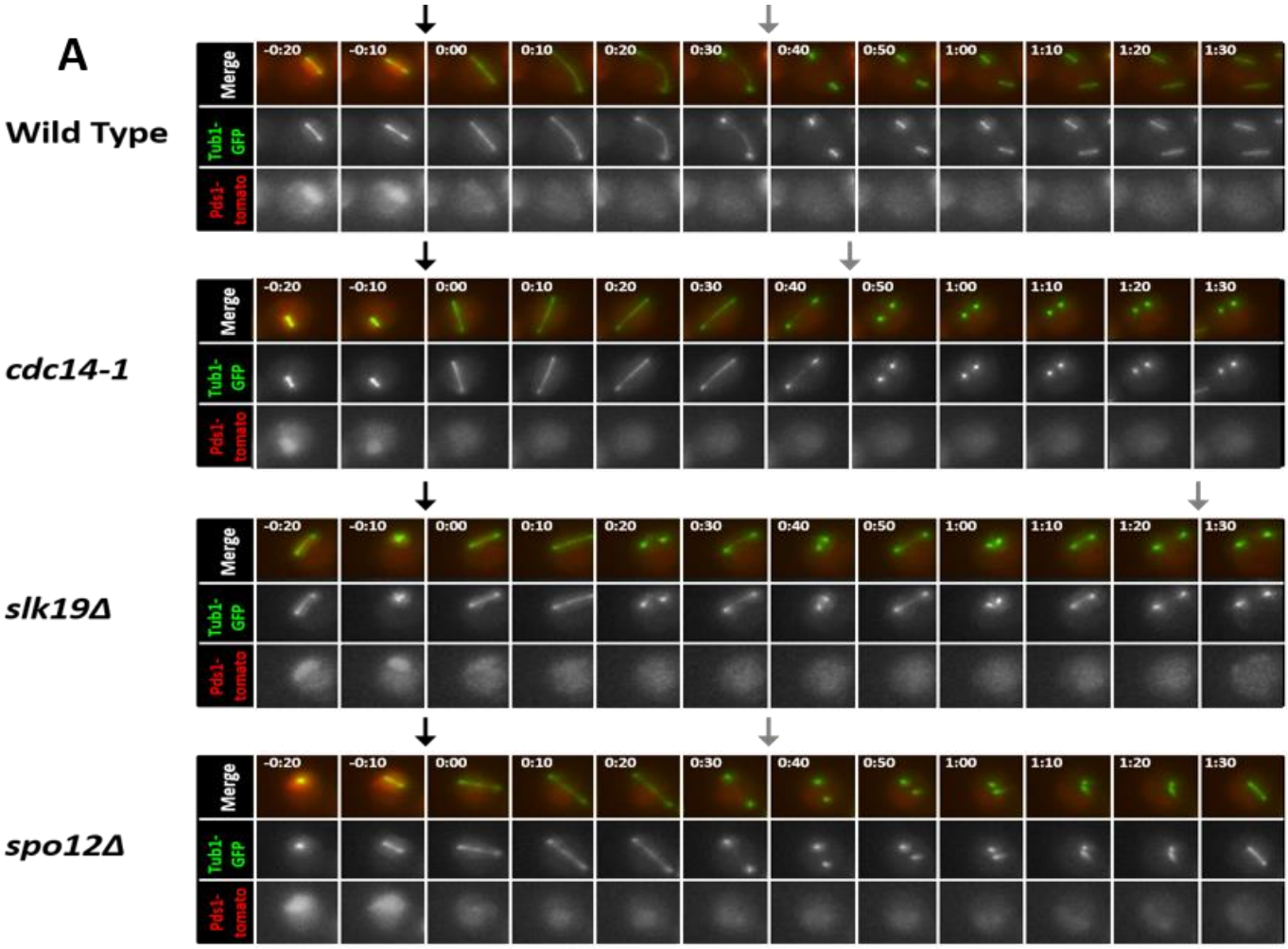

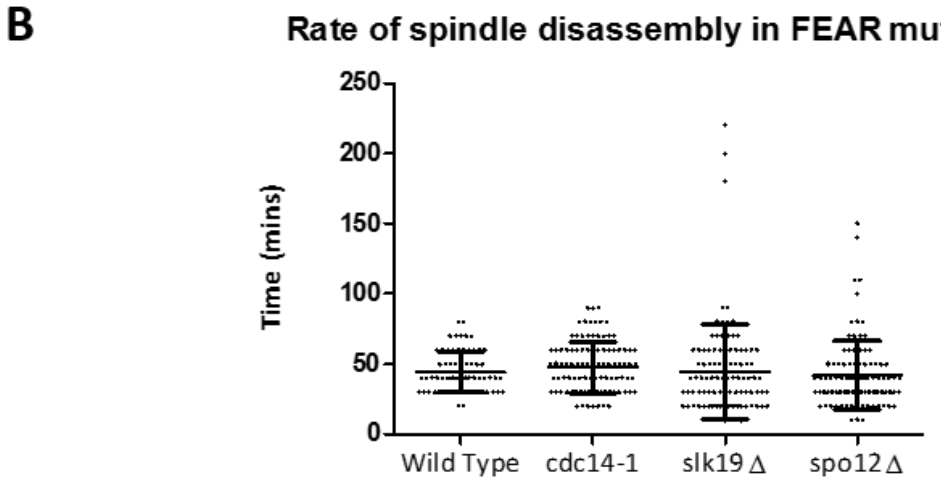

Figure 3.2.1: Cdc14 is required for timely meiosis I spindle disassembly. (A) Wild type (AM16065), *cdc14-1* (AM16066), *slk19Δ* (AM16110) and *spo12Δ* (AM15985) cells carrying *CDC14-GFP* and *PDS1-tomato* were induced to sporulate, released from *GAL-NDT80* block and imaged at 10 minute intervals for a total of 12 hours using microfluidics. Time-lapse examples of individual cells show spindle assembly and disassembly during meiosis. The black arrow denotes Pds1 degradation, marking entry of cells into anaphase I. The grey arrow marks complete spindle break down. (B) The time taken for complete spindle disassembly after Pds1 degradation was recorded for individual cells. Rate of spindle disassembly for a total of 67 wild type cells and 100 *cdc14-1, slk19Δ* and *spo12Δ* cells were plotted. Mean rates of spindle breakdown are shown, with error bars representing standard deviation. The two-tailed Student's *t*-test was used to calculate significance.

3.2.2 Aberrant spindle dynamics observed upon deletion of FEAR components

From the quantification of spindle disassembly in live cells, a number of outliers were present in both *slk19Δ* and *spo12Δ* cell populations. This is reflective of the dynamic nature of the meiotic spindle in FEAR mutants. The cells that entered meiosis were further categorised. As noted earlier, many *cdc14-1, slk19Δ* and *spo12Δ* mutants (82%, 57% and 39% respectively) disassemble anaphase I spindles, leaving two Tub1-GFP foci that do not extend microtubules (Fig. 3. 2. 2). However, 14% of *cdc14-1* cells do extend microtubules and elongate a second meiosis I-like spindle. This phenotype is emphasized further in the FEAR mutants, with 27% and 53% of cells respectively reassembling spindles after the initial anaphase I spindle breakdown (Fig. 3. 2. 1A & Fig. 3. 2. 2). A further 4-16% of FEAR mutants display multiple rounds of microtubule elongation and collapse on the same spindle before spindle disassembly.

The fact that microtubules undergo several round of elongation then collapse in FEAR mutants prior to spindle disassembly indicates that Cdc14 may be required for stablilisation of meiotic spindles. This is concurrent with mitotic data, where Cdc14 has been shown to dephosphorylate the kinetochore component Ask1 in anaphase, which contributes to the silencing of microtubule turnover (Higuchi and Uhlmann 2005). However, since spindle disassembly is only slightly delayed upon Cdc14 inactivation, it is likely that Cdc14 has additional functions in executing the meiosis I-meiosis II transition.

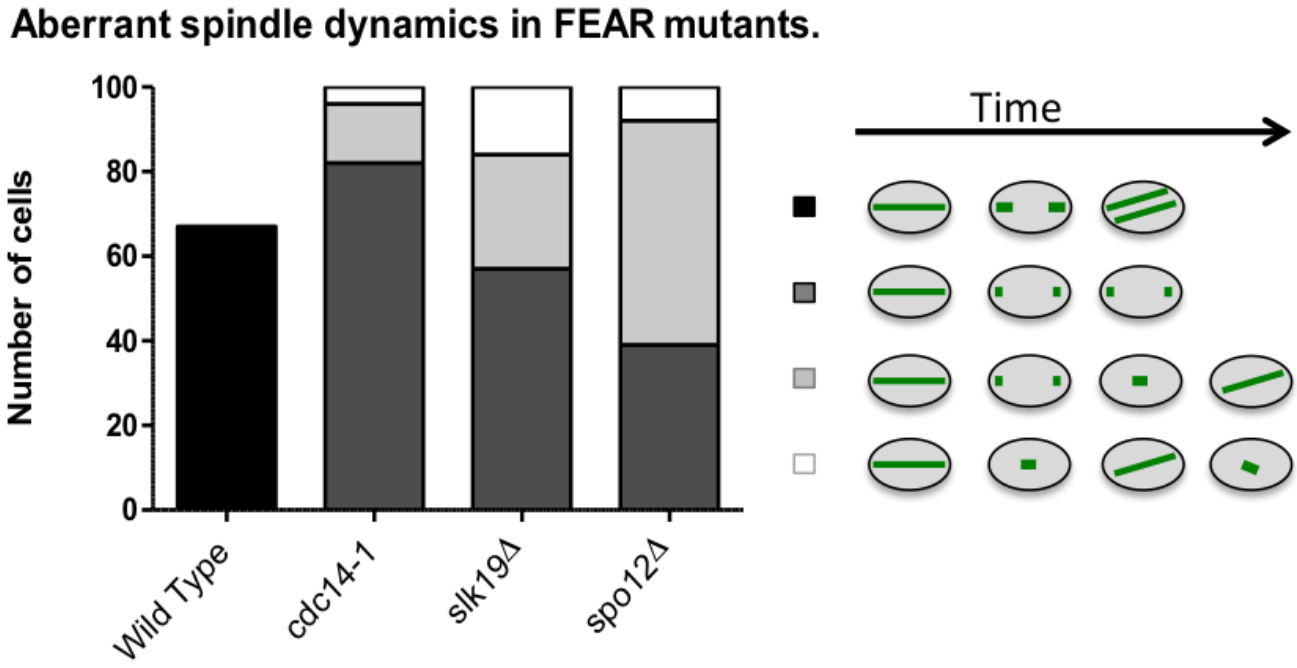

Figure 3.2.2: Inactivation of Cdc14 results in abnormal microtubule dynamics. Wild type (AM16065), *cdc14-1* (AM16066), *slk19Δ* (AM16110) and *spo12Δ* (AM15985) cells imaged in Fig. 3.1.1 were categorised by spindle morphology. Bar chart legend illustrates possible spindle phenotypes observed: two meiosis II spindles assemble after anaphase I spindle disassembly (black), no new spindles assemble after anaphase I spindle disassembly (dark grey), a single meiosis II spindle assembles after anaphase I disassembly (light grey) and anaphase I spindle collapses and elongates multiple times before complete spindle breakdown (white).

3.2.3 Cyclin proteolysis in meiosis is not dependent on Cdc14 activity

To determine whether Cdc14 is required for CDK down-regulation at the meiosis I-meiosis II transition, cyclin protein levels were measured throughout meiosis. During meiosis, Cdc28 is activated through binding to several different meiotic cyclins (Fig. 3. 2. 3). These different CDK complexes are regulated either by protein degradation or posttranslational mechanisms, which confine their activity to specific stages in meiosis (Bloom and Cross 2007, Carlile and Amon 2008).

Clb1-CDK activity is restricted to meiosis I, despite Clb1 protein persisting in cells until exit from meiosis II (Fig. 3. 2. 3). A slower migrating form of Clb1, believed to be phosphorylated Clb1 (Tibbles, Sarkar et al. 2013), is associated with Clb1-CDK activity and is evident in meiosis I indicating that a posttranslational modification other than protein degradation inhibits Clb1-CDK activity (Carlile and Amon 2008). Clb3-CDK activity is meiosis II-specific. Clb3 protein is confined to meiosis II through translational control (Carlile and Amon 2008). Clb4-CDK activity is down-regulated after metaphase II through an unknown mechanism, whilst Clb5-CDK activity is correlated to Clb5 protein abundance (Carlile and Amon 2008).

If Cdc14 phosphatase is required for partial down-regulation of CDKs at the meiosis I to meiosis II transition, its inactivation would lead to stabilisation of meiotic cyclins. I decided to analyse the levels of each individual cyclin throughout meiosis in wild type and *cdc14-1* mutant cells.

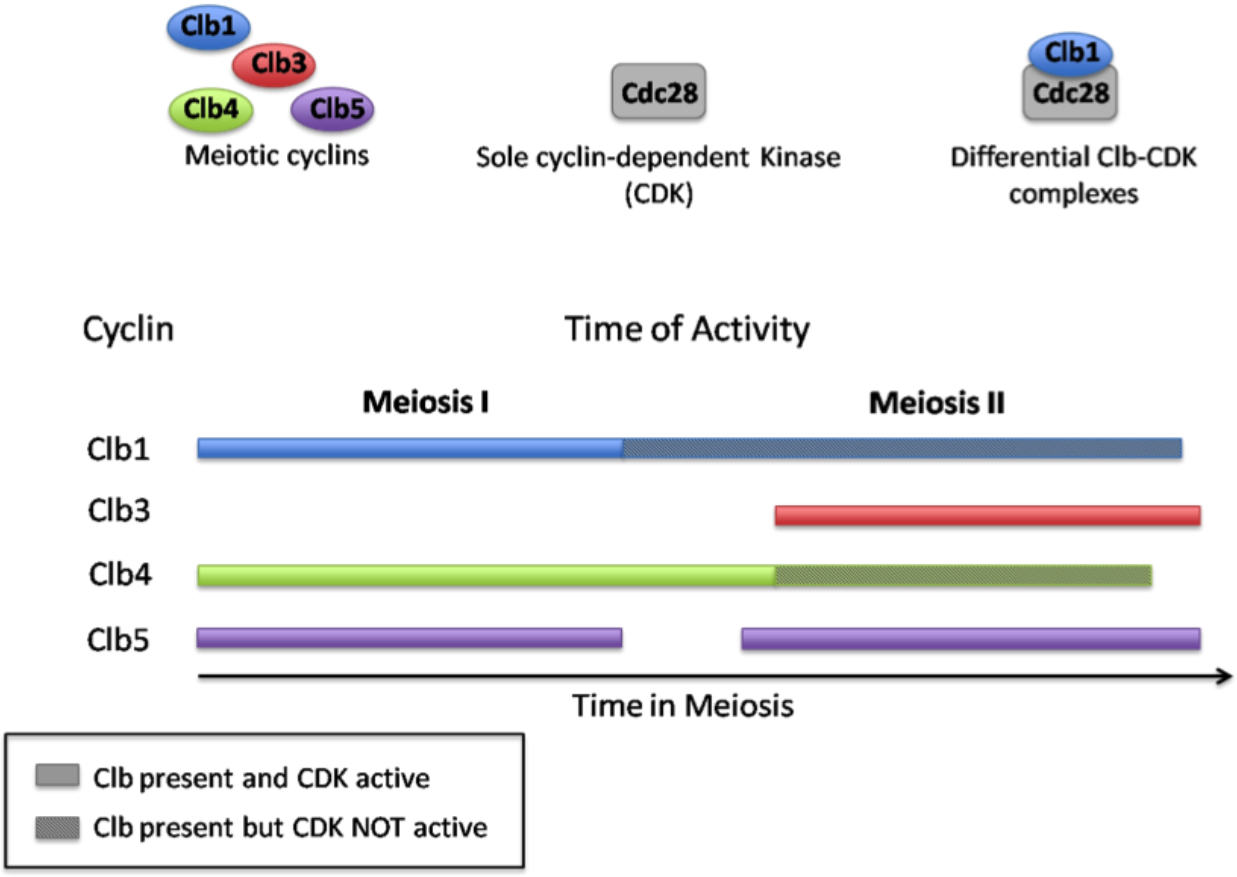

Figure 3.2.3: Schematic of meiotic cyclin-CDK activities: Different B-type meiotic cyclins bind to and activate a single cyclin-dependent kinase (Cdc28 in budding yeast). Each Clb-CDK complex is active at different stages of meiosis and are differentially regulated, either through cyclin proteolysis or posttranslational modifications of cyclin-CDK complexes. Figure based on Carlile & Amon, 2008.

3.2.3.1 Production of polyclonal antibodies for Pgk1 and Kar2 loading controls to allow quantification of target protein levels

Accurate quantification of cyclin protein levels required a new approach for Western blot analysis. Enhanced chemiluminescence (ECL) is a common technique used for the detection of biomolecules on Western blots. A protein of interest is identified through labelling an immunoglobin, which specifically recognizes the molecule, with horseradish peroxidase (HRP) (Towbin, Staehelin et al. 1979). The enzyme complex catalyzes the oxidation of a commercially available enhanced chemiluminescent substrate. This reaction emits a light that is detectable by exposure of photographic film, the intensity of which is indicative of HRP activity and therefore protein abundance.

Whilst ECL can enable the generation of clear and reliable data, the technique has a number of drawbacks (LiCor Biosciences 2015). Firstly, numerous exposures are typically required to capture optimal protein signals and avoid saturation to film. For multiplex detection, where multiple protein targets are detected, the membrane must be stripped and re-probed. Quantification and direct comparison of biomolecules is consequently imprecise. Finally, signal stability is usually restricted to ~30 minutes, after which time the signal begins to fade. This short duration can make comparisons between multiple membranes processed consecutively less accurate.

LiCor® has developed the Odyssey Sa system, which utilizes fluorescence detection of biomolecules (LiCor Biosciences 2015). The secondary antibody is labelled with a near-infrared (NIR) fluorescent dye. Membranes are scanned using Odyssey software to detect fluorescent molecules bound to the target. Signal intensity is indicative of protein abundance. NIR - fluorescence detection is preferable to ECL for a number of reasons. It

is cheaper, gives greater signal sensitivity, allows for both weak and strong signals to be detected on the same membrane with minimized saturation and is a direct detection of target proteins instead of the HRP signal from which depends on enzyme activity. The greatest benefit of fluorescence over chemiluminescence is the ability to detect two target proteins simultaneously on the same membrane, eliminating the need to strip and re-probe. This provides increased accuracy of quantification and comparison.

Loading controls are essential for correct Western blot analysis. By measuring the level of protein loading, the abundance of a target protein can be calibrated. If both protein of interest and loading control are detected on the same membrane, this normalization can be more precise. In order to employ multiplex detection and quantification, target protein and loading control must be recognized by primary antibodies that have been produced from different organisms. LiCor® secondary antibodies labelled with divergent fluorescent dyes can then be used to identify the different proteins via two-colour detection. Since the majority of target proteins regularly used in the laboratory are recognized by mouse-generated antibodies, the antibodies specific to loading controls need to be generated from a different organisms.

I set out to generate polyclonal antibodies specific for Pgk1 and Kar2 in rabbits. These loading controls were chosen as previous experiments have shown that their levels do not change significantly during the cell cycle or meiosis (Clift, Bizzari et al. 2009, Bizzari and Marston 2011).

3.2.3.1.1 Cloning and expression of tagged recombinant Pgk1 and Kar2 in *E. coli* derivative BL21 cells

I tagged Pgk1 and Kar2 with a number of different affinity tags in order to determine which clone would give optimal expression and purification levels. Glutathione-S-transferase (-GST), Intein (-INT) and Maltose binding protein (-MBP) tags were attached to the C-termini of Pgk1 and Kar2 through Gateway Cloning. Clones were sequenced, to confirm no mutations had been introduced into the genes, and transformed into BL21 cells. Since recombinant proteins often show large variability in expression levels and solubility, a small-scale expression test was carried out to determine which derivative clone should be purified (Fig. 3. 2. 3. 1. 1). Protein expression was induced by addition of 1mM IPTG, and cells were lysed with benzonase to degrade nucleic acids in purified protein samples. Soluble and insoluble fractions were run against a non-induced fraction to compare protein expression levels.

Over-expression of Pgk1-GST (~71kDa), Pgk1-MBP (~87kDa), Kar2-GST (~100kDa) and Kar2-MBP (~116kDa) was evident predominately in the insoluble fraction lanes (Fig. 3. 2. 3. 1. 1). INT-fusion proteins achieved poor levels of expression and so were not taken any further.

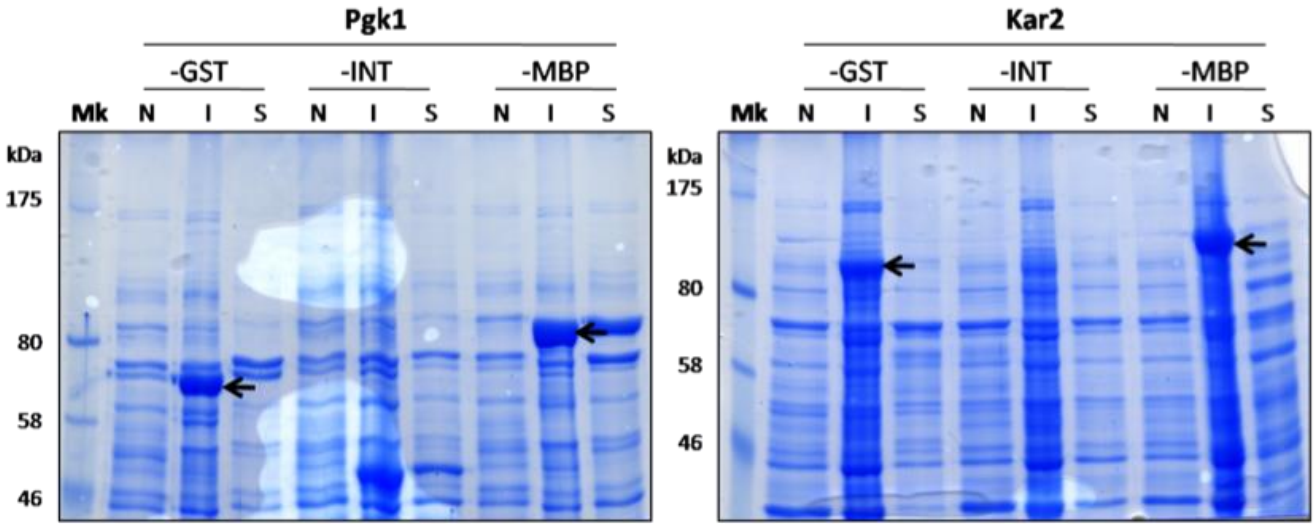

Figure 3.2.3.1.1: Comparison of affinity tags for Pgk1 and Kar2 protein purification in *E. coli*: Small-scale test expression of GST-, INT- and MBP-tagged recombinant proteins in BL21 cells induced by addition of 1mM IPTG. Non-induced (N), induced insoluble (I) and induced soluble (S) fractions were compared and revealed Pgk1-GST (~71kDa), Pgk1-MBP (~87kDa), Kar2-GST(~100kDa) and Kar2-MBP (~116kDa) enriched with insoluble proteins (indicated by black arrows).

Mk = Marker

3.2.3.1.2 Purification of Inclusion Bodies

Inclusion bodies (IB) are *in vivo* protein aggregates formed during protein folding, commonly associated with over-expression of recombinant proteins (Fink 1998). It is unclear whether the proteins contained within IBs resemble native forms or are the result of mis-folding. There is evidence to suggest that proteins may partially retain their native structures (Tsumoto, Umetsu et al. 2003, Umetsu, Tsumoto et al. 2005). However, since the recombinant proteins are only required as antigens for the generation of polyclonal antibodies, protein solubility and correct protein folding are not essential.

I prepared IBs from the bacterial strains containing Pgk1-GST, Pgk1-MBP, Kar2-GST and Kar2-MBP. Dilutions of IB samples were compared to known BSA standards in order to determine protein concentration (Fig. 3. 2. 3. 1. 2). Results suggest that total Pgk1-GST and Kar2-GST purified in IB fractions were ~ 70mg and ~ 18mg respectively. Both MBP-tagged recombinants also purified well but at slightly decreased concentrations.

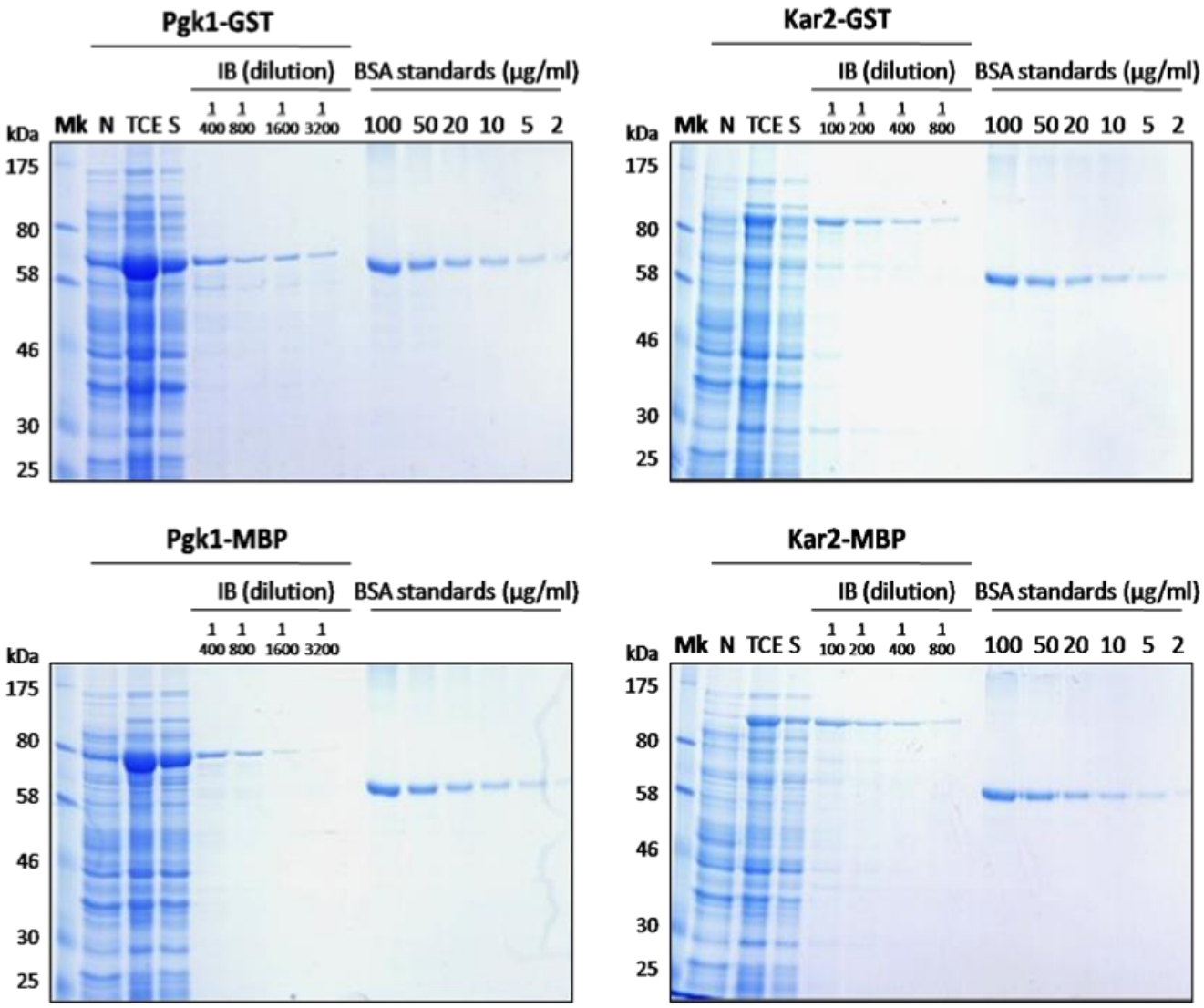

Figure 3.2.3.1.2: Inclusion Body purifications of recombinant Pgk1 and Kar2 proteins: Non-induced (N), total cell extract (TCE) and induced soluble (S) fractions were ran alongside inclusion body (IB) dilutions to show effectiveness of protein purification. Comparison to BSA standards enabled the calculation of recombinant protein concentrations. Pgk1-GST (~72mg), Pgk1-MBP (~58mg), Kar2-GST (~18mg) and Kar2-MBP (~9mg)

3.2.3.1.3 Generation of Pgk1 and Kar2 polyclonal antibodies

Purified Pgk1-GST and Ka2-GST antigens were injected into pre-screen rabbits R3285-R3288 (Fig. 3. 2. 3. 1. 3A). Production of Pgk1 and Kar2 antibodies by host rabbits were monitored in sera isolated from animals prior to each immunization. Final exsanguinations of rabbit revealed each antiserum contained polyclonal antibodies specific to Pgk1 and Kar2 loading controls (Fig. 3. 2. 3. 1. 3A).

Simultaneous detection of two targets is now achievable. Mps3-6HA and loading controls are recognised by primary antibodies isolated from mice and rabbits, respectively. Secondary LiCor® antibodies labelled with spectrally distinct IRDye fluorescent dyes specifically bind to these antigens and are detected in independent fluorescent channels 700nm and 800nm (Fig. 3. 2. 3. 1. 3B). αMouse secondary and αKar2 shows a slight cross-reactive band of the expected size for Kar2 but in the 800nm channel. However, this is extremely faint with respect to the band observed in the 700nm channel. Ultimately, Pgk1 and Kar2 antibodies proved successful for utilisation in multiple detection.

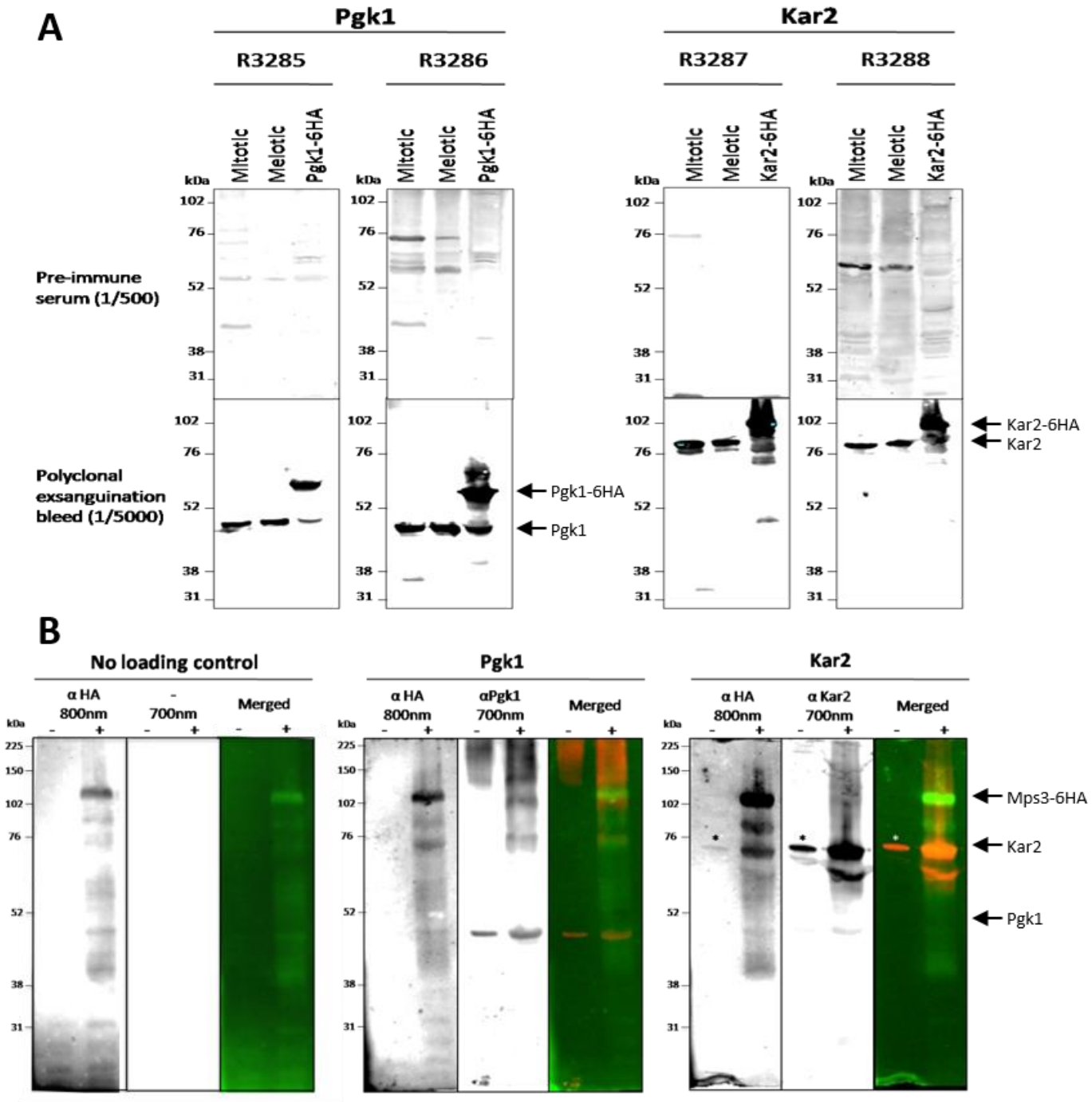

Figure 3.2.3.1.3: Production of Pgk1 and Kar2 polyclonal antibodies in rabbit hosts: (A) Sera taken from host rabbits (R3285-R3288) prior to injection with Pgk1-GST and Kar2-GST antigens (pre-immune serum) and from the final exsanguinations. Sera diluted in PBS-T with 2% dry milk for 1° antibody. Li-Cor 2°αRabbit (1/10000) immunolabeling revealed rabbit hosts did not illicit a strong endogenous immune response. Bands detected were not the appropriate size for Pgk1 or Kar2 until after multiple injection with antigens. Mitotic and meiotic samples contained unmodified Pgk1 and Kar2. Motility shift observed in 6HA-variants confirmed polyclonal antibodies produced were specific to loading controls. (B) Multiplex detection of proteins on western blots. Mps3 (-) and Mps3-6HA (+) samples were incubated with 1° αHA (1/1000) and αPgk1 (1/10000) or αKar2 (1/5000) then 2° αMouse (1/10000) and αRabbit (1/10000). Two-colour detection of target protein and loading controls using fluorescence channels 700nm and 800nm showed evidence of slight cross-reactivity between αMouse and αKar2 (*).

3.2.3.2 Analysis of cyclin degradation in meiosis using multiplex Western blotting

To investigate the role of Cdc14 in meiotic cylin degradation, the protein levels of each Clb was analysed individually during meiosis. The role of Cdc14 in Clb1 degradation had previously been reported by (Bizzari and Marston 2011). Their findings indicate that ectopic release of Cdc14 does not lead to premature degradation of Clb1. Furthermore, they showed that the slower migrating form of Clb1, observed only in meiosis I and associated with Clb1-CDK activity (Carlile and Amon 2008), correlated with nuclear localisation of Clb1. Localisation of Clb1 was unaffected when Cdc14 activity was impaired, suggesting that the posttranslational mechanism regulating Clb1-CDK activity was not dependent of Cdc14 function.

I repeated this experiment and validated these findings. Cdc14 is not required for the formation of a slower migrating form of Clb1 in meiosis I. As metaphase I spindles form in both wild type and *cdc14-1* cells, unmodified Clb1 is detected. The appearance of the slower migrating form of Clb1 correlates with the appearance of anaphase I spindles in both strains. Cdc14 activity is also not a requisite for proteolysis of Clb1, which occurs in both wild type and *cdc14-1* cells when meiotic spindles disassemble (Fig. 3. 2. 3. 2A). Similarly, early release of Cdc14 in *cdc55mn* cells does not result in premature degradation of Clb1. Instead, accumulation of the slow migrating form of Clb1 is observed. As meiotic spindles do not assemble in *cdc55mn* cells, the timing of Clb1 appearance is difficult to determine. However, early release of Cdc14 does not appear to inactivate nor degrade Clb1 as is predicted by my earlier hypothesis.

Clb3-CDK activity is restricted to meiosis II through translational control of *CLB3* transcription (Carlile and Amon 2008). I confirmed that Clb3 is only observed in wild

type cells during meiosis II. Clb3 is then degraded when cells exit meiosis II (Fig. 3. 2. 3. 2B). When Cdc14 activity is impaired, the timing of Clb3 accumulation and degradation appears unaffected. Early activation of Cdc14 in *cdc55mn* cells also does not elicit premature Clb3 degradation, excluding the probability that Cdc14 is required for Clb3 proteolysis.

Clb4 and Clb5 protein degradation during spindle disassembly appears unaffected by inactivation of Cdc14 (Fig. 3. 2. 3. 2C-D). Likewise, neither Clb4 nor Clb5 is degraded early when Cdc14 is released prematurely from the nucleolus. Thus, Cdc14 activity is not essential for Clb4 and Clb5 degradation.

This data suggests that the main role of Cdc14 at the meiosis I- meiosis II transition is not to regulate cyclin proteolysis. However, western blot analysis of *cdc14-1* mutants does seem to show evidence of Clb1 and Clb 3 proteins persisting in cells later than is observed in wild type cells, albeit at greatly reduced levels. Cdc14 may, therefore, be required to degrade these residual cyclins.

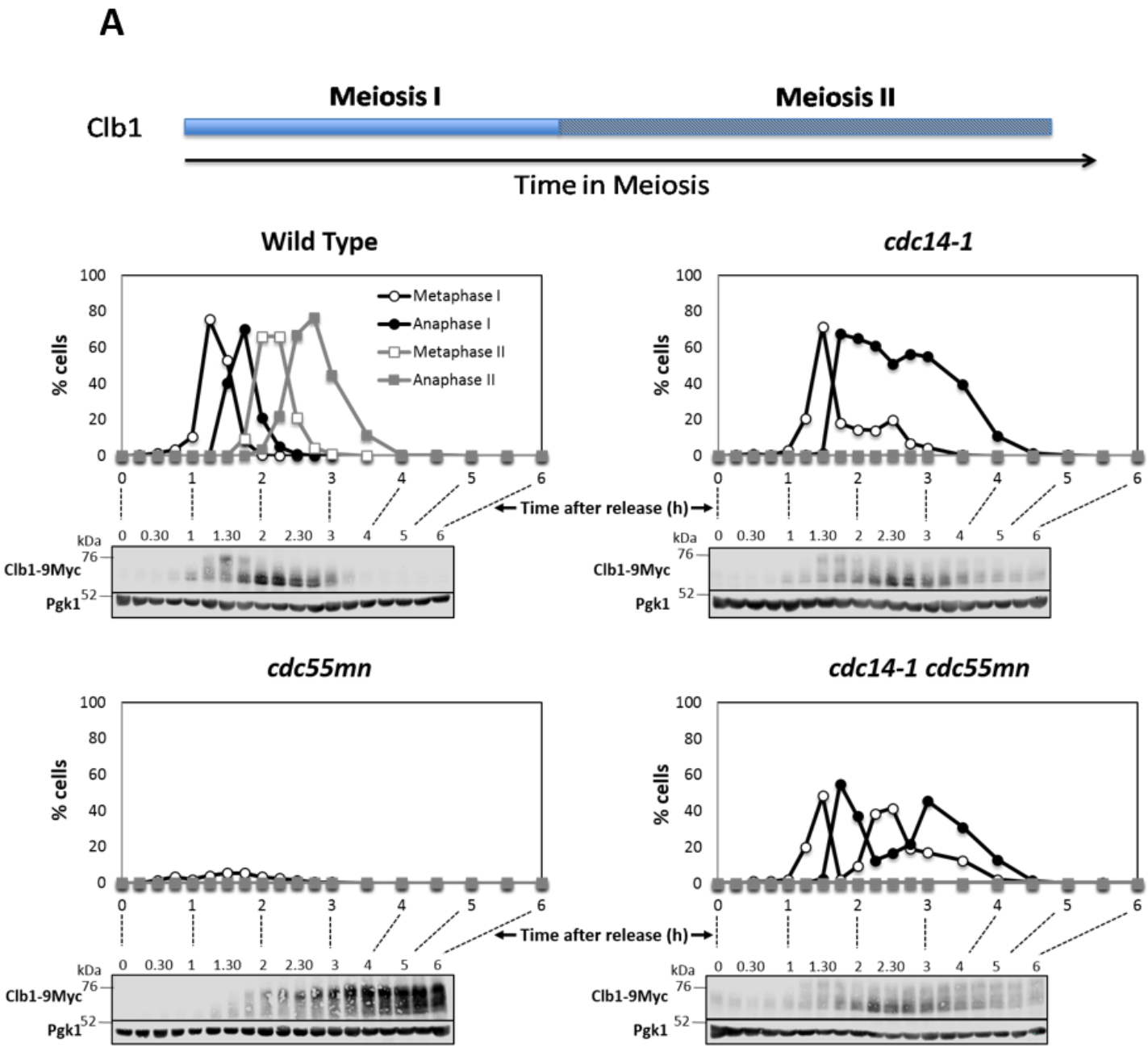

Figure 3.2.3.2: Protein levels of meiotic cyclins in Cdc14 inactive and hyperactive mutants: (A-D) Wild type, *cdc14-1, cdc55mn* and *cdc14-1 cdc55mn* mutants containing *CLB1-9Myc* (AM6770, AM7815, AM6961, AM7816; A), *CLB3-HA* (AM9004, AM9065, AM9007, AM9068; B), *CLB4-HA* (AM9005, AM9066, AM9024, AM9212; C) or *CLB5-3HA* (AM9006, AM9067, AM9025, AM9178; D) were induced to sporulate and released from *GAL-NDT80 block.* The percentage of cells with indicated spindle morphology was determined to show meiotic progression. α HA/Myc immunoblots show Clb protein abundance and timing of degradation can be compared to illustrative figures of meiotic cyclin presence (top). Blots and spindle counts are representative.

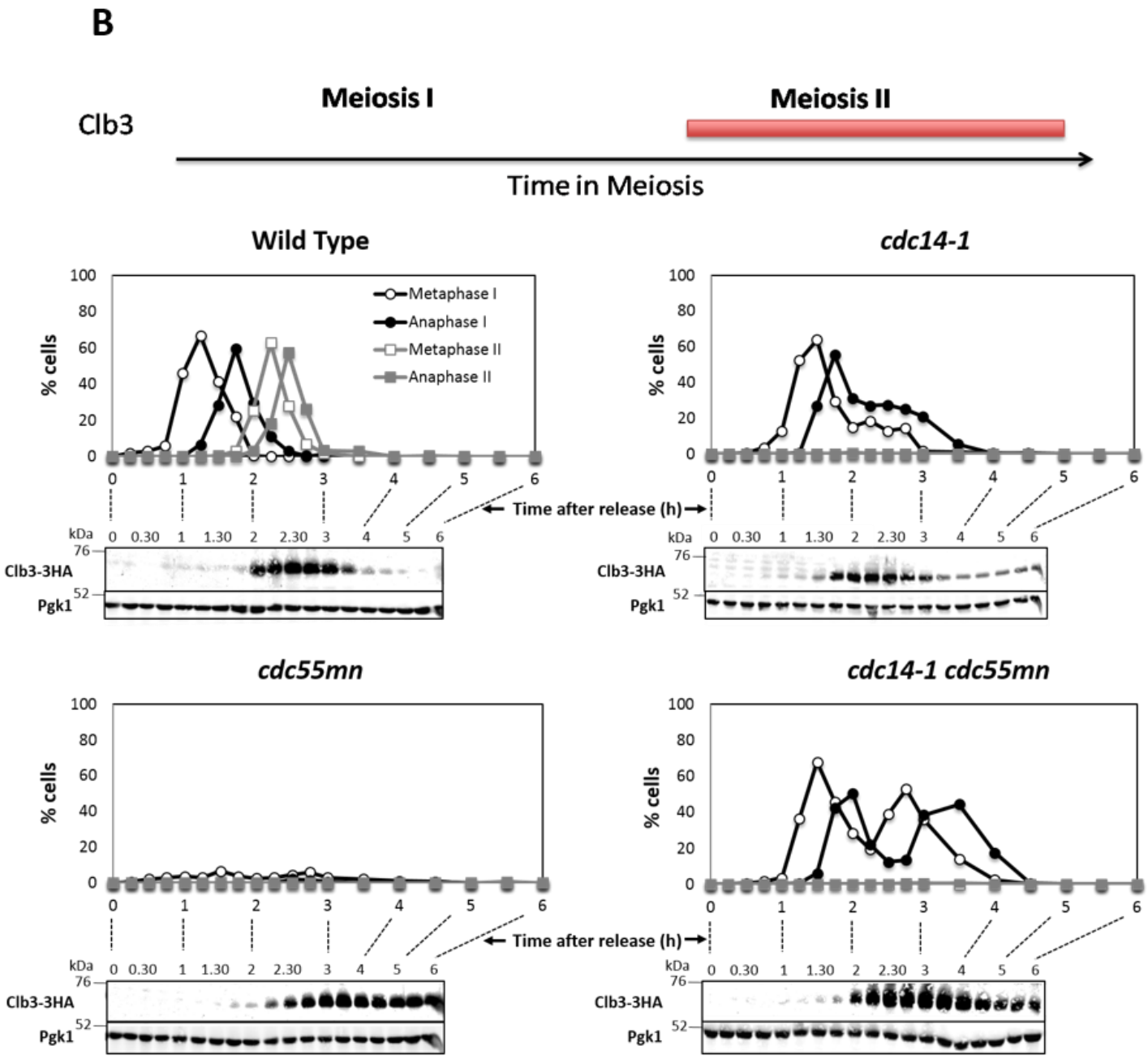
B
Clb3
Meiosis I
Meiosis II
Time in Meiosis
Wild Type
cdc14-1
cdc55mn
cdc14-1 cdc55mn
% cells
Metaphase I
Anaphase I
Metaphase II
Anaphase II
Time after release (h)
kDa
Clb3-3HA
Pgk1
76
52

C

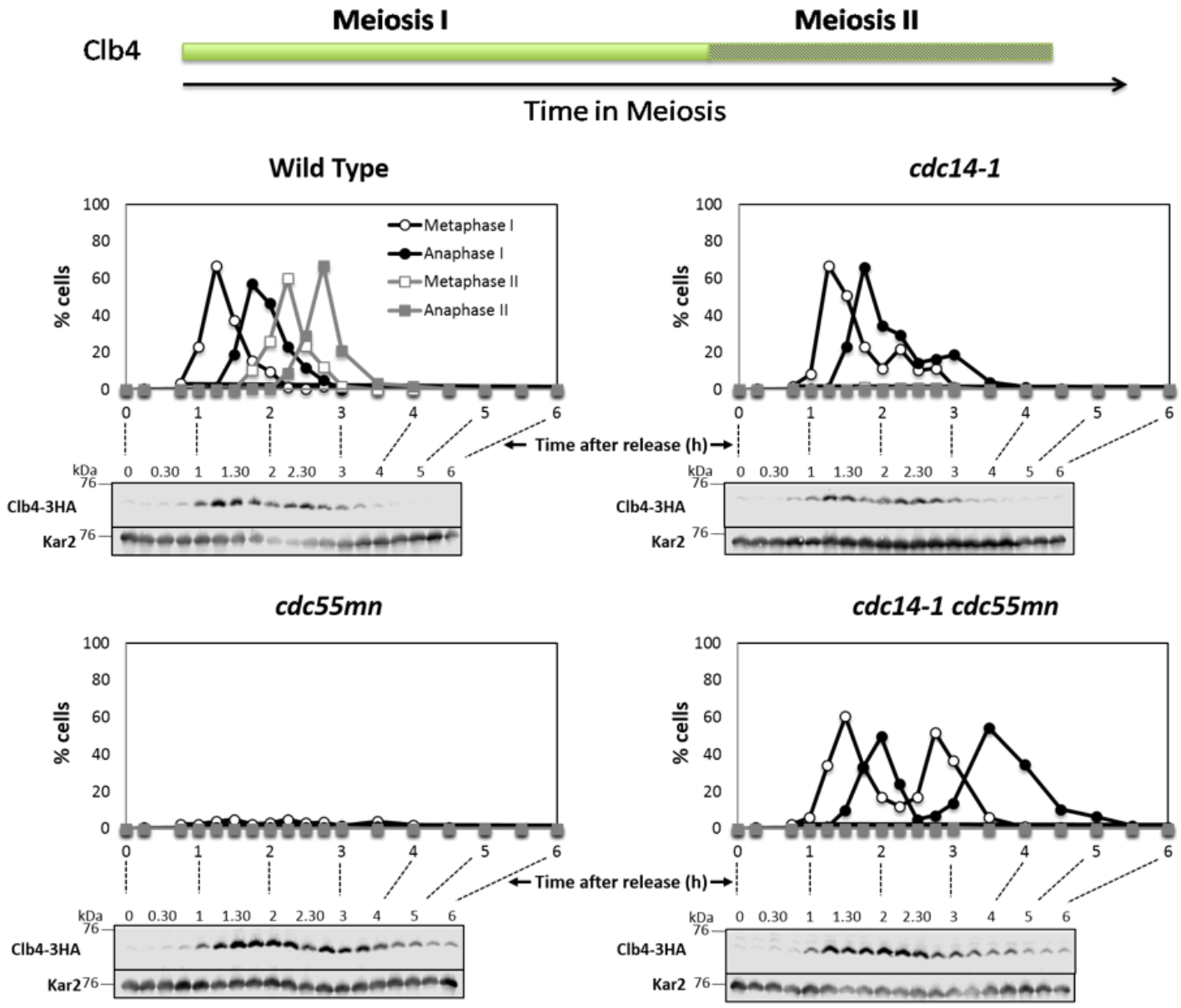
Meiosis I
Meiosis II
Clb4
Time in Meiosis
Wild Type
cdc14-1
cdc55mn
cdc14-1 cdc55mn
% cells
Metaphase I
Anaphase I
Metaphase II
Anaphase II
Time after release (h)
kDa
Clb4-3HA
Kar2

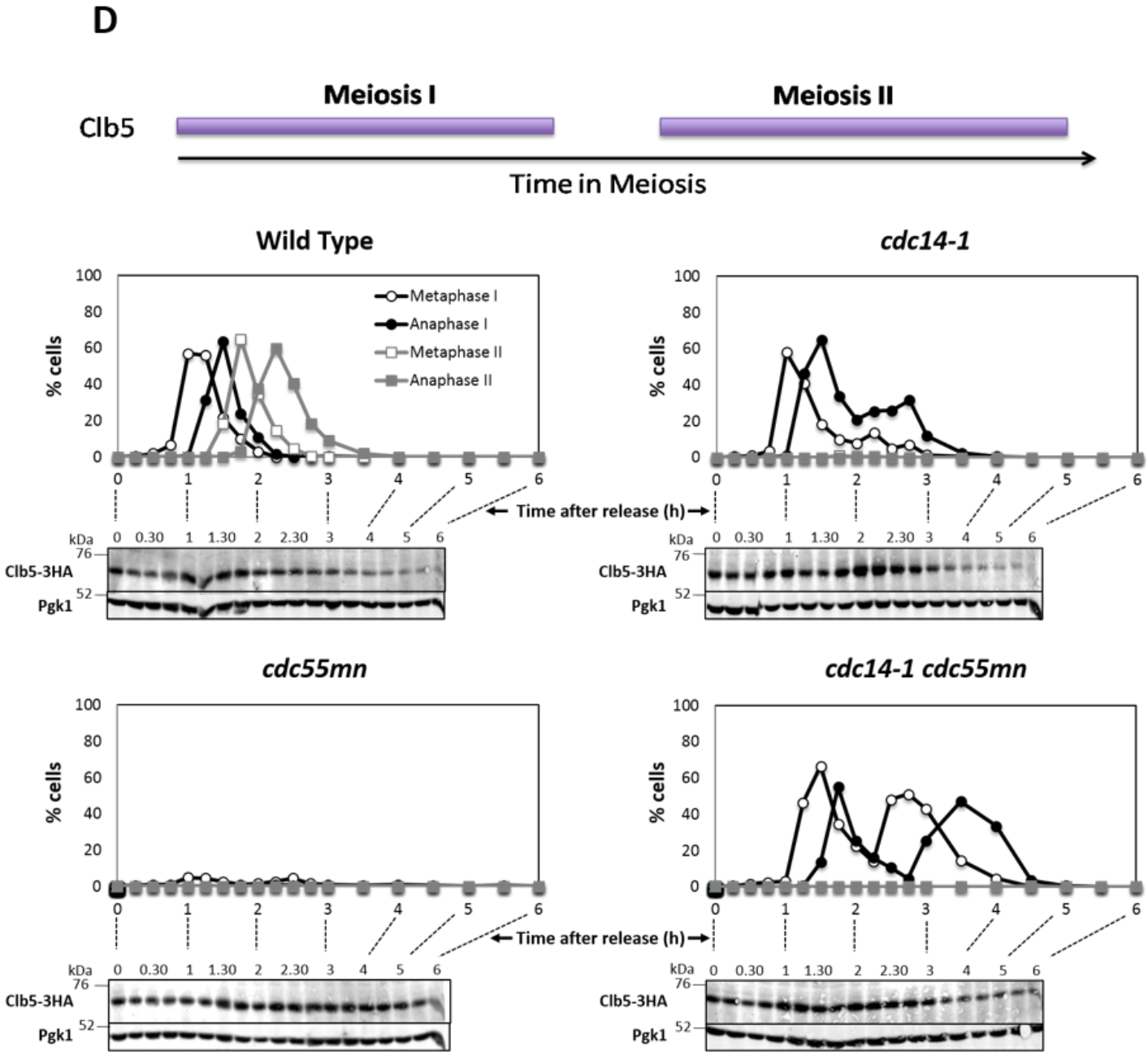
D
Meiosis I
Meiosis II
Clb5
Time in Meiosis
Wild Type
cdc14-1
cdc55mn
cdc14-1 cdc55mn
% cells
Metaphase I
Anaphase I
Metaphase II
Anaphase II
Time after release (h)
kDa
Clb5-3HA
Pgk1

3.2.3.2.1 Quantification of meiotic cyclin levels

To further assess degradation of cyclins in meiosis, the immunoblots generated in Fig. 3. 2. 3. 2A-D can be analysed through quantification of protein signal. Relative meiotic cyclin levels were determined through quantification of each Clb signal, normalising these values against the respective loading control signal. The proteolysis of cyclins in wild type and *cdc14-1* cells can be compared to identify if inactivation of Cdc14 prevents the complete destruction of cyclins.

From qualitative western blot analysis alone, Clb1 and Clb3 proteins appear to persist in *cdc14-1* cells longer than is observed in wild type cells (Fig. 3. 2. 3. 2A,C). However, when the relative abundances of meiotic cyclins were plotted, it is clear that Clb1, Clb3, Clb4 and Clb5 values all decrease in *cdc14-1* mutants to levels comparable to wild type cells (Fig. 3. 2. 3. 2. 1). The timing of Clb1 and Clb3 proteolysis appears delayed by ~30mins when Cdc14 activity is impaired. However, delayed entry of these cells into meiosis, as is illustrated by *cdc14-1* spindle morphology (Fig. 3. 2. 3. 2A-B), could explain this postponement in cyclin degradation. Clb4 abundance may be reduced when Cdc14 is inactivated but the pattern of Clb4 quantification does not seem affected (Fig. 3. 2. 3. 2. 1). Cdc14 is, therefore, unlikely to be involved in cyclin degradation.

To further test whether Cdc14 is required for cyclin degradation, the abundance of meiotic cyclins in *cdc55mn* cells were quantified. If Cdc14 were required for cyclin proteolysis in meiosis, early release of Cdc14 would lead to premature degradation of cyclins in *cdc55mn* mutants.

Clb1, Clb3 Clb4 and Clb5 proteins are not reduced ahead of wild type cells when Cdc14 is released from inhibition early (Fig. 3. 2. 3. 2. 1). On the contrary, cyclin levels appear increased in *cdc55mn* mutants with respect to wild type and c*dc14-1* cells late in meiosis. This finding is consistent with previous data (Bizzari and Marston 2011). There is a slight delay in the appearance of Clb1 and Clb3 protein in *cdc55mn* cells with respect to wild type and *cdc14-1* cells. However, as noted previously, due to a lack of meiotic spindle formation it is difficult to accurately determine the timing of meiosis in these mutants. Since cyclin levels are not prematurely degraded, it is likely that the spindle assembly defect observed in *cdc55mn* mutants is not due to failure of cells to accumulate cyclins at the appropriate stage of the cell cycle.

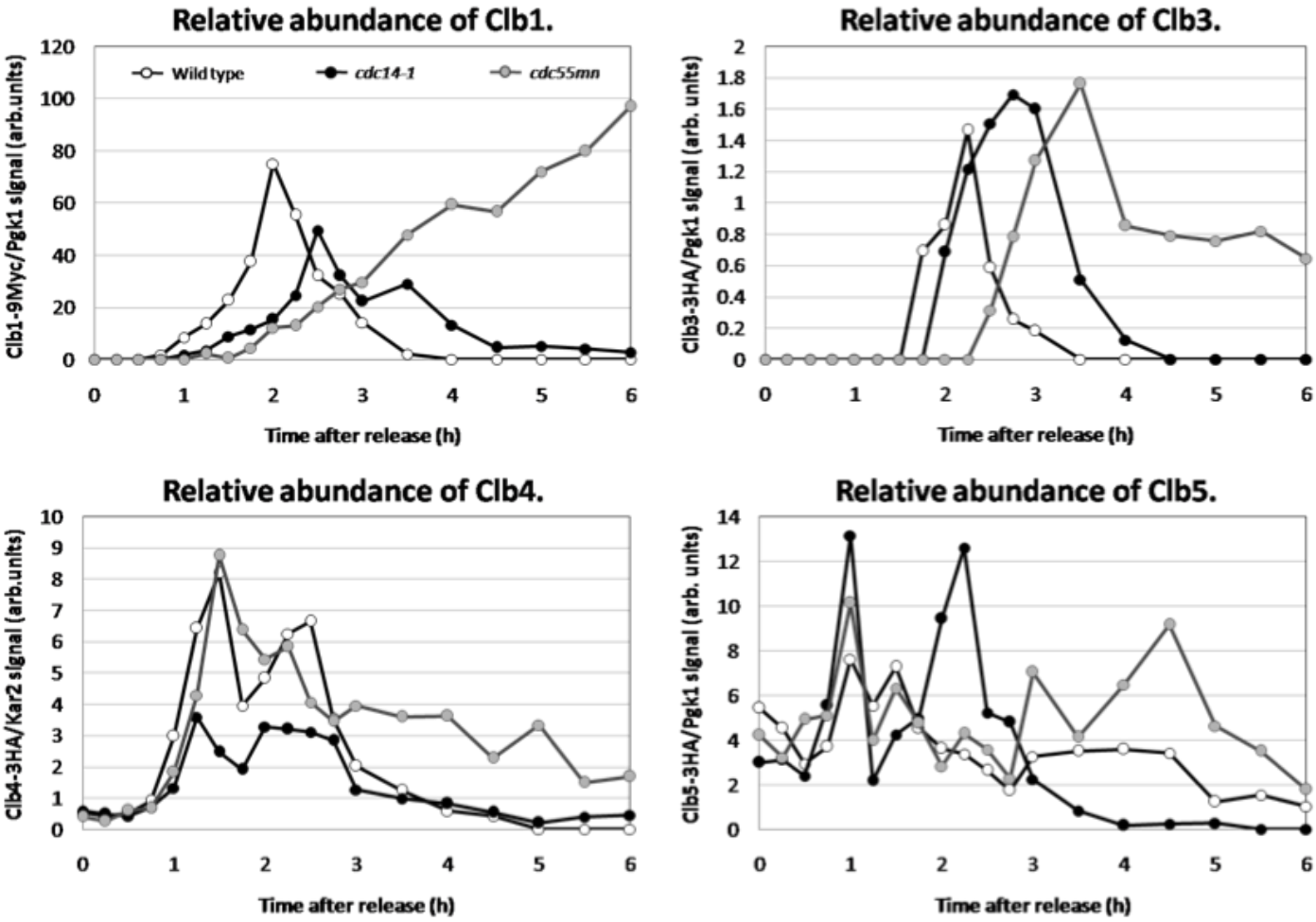

Figure 3.2.3.2.1: Relative protein abundance of meiotic cyclins is not notably affected by Cdc14 inactivation or early activation: Wild type, *cdc14-1* and *cdc55mn* immunoblots for *CLB1-9Myc* (AM6770, AM7815, AM6961), *CLB3-3HA* (AM9004, AM9065, AM9007), *CLB4-3HA* (AM9005, AM9066, AM9024) and *CLB5-3HA* (AM9006, AM9067, AM9025) analysis were quantified using Li-Cor Odyssey Sa software. Western blots analysed were from the representative experiments shown in Fig.3.2.3.2. Levels of meiotic cyclins were determined by calculating the ratio of Clb signal over loading control signal. Values were plotted against time in meiosis.

3.3 Discussion

In mitosis, differential binding of the ubiquitin ligase to two activators regulates APC-dependent proteolysis of cyclins, Cdc20 and Cdh1. APC^{Cdc20} is active when mitotic CDK activity is high in early anaphase (Yeong, Lim et al. 2000). Upon initial cyclin degradation and subsequent CDK down-regulation, APC^{Cdh1} becomes activated in late anaphase to carry out complete cyclin degradation (Visintin, Prinz et al. 1997). Cdh1 activation is believed to be a result of MEN-mediated release of Cdc14 (Jaspersen, Charles et al. 1998, Visintin, Craig et al. 1998). Since MEN is not active during the meiosis I-meiosis II transition (Kamieniecki, Lu et al. 2005), I hypothesised that Cdc14 activation in anaphase I enabled the partial but not complete down-regulation of meiotic CDK activity.

To test this theory, I investigated the role of Cdc14 on timely spindle disassembly, a marker of CDK down-regulation, and on cyclin proteolysis. I discovered that Cdc14 activity did have a minor effect on the timely breakdown of the anaphase I spindle. However, cyclin degradation occurred independent of Cdc14 activity. These observations led me to reject the initial hypothesis. Instead, Cdc14 must play another role in regulating the meiosis I-meiosis II transition.

Whilst it is possible that Cdc14 may down-regulate CDK activity through another mechanism other than cyclin degradation, it is doubtful. Clb3-CDK and Clb5-CDK activities correlate to cyclin protein abundance (Carlile and Amon 2008) and neither is greatly affected by Cdc14 inactivation. Clb1-CDK activity is associated with the slow migrating form of the cyclin (Carlile and Amon 2008, Bizzari and

Marston 2011). This modified form of Clb1 is still present in *cdc14-1* cells during meiosis I. Finally, although the mechanism that regulates Clb4-CDK activity has yet to be identified (Carlile and Amon 2008), Clb4-CDK down-regulation occurs during meiosis II. It is, therefore, unlikely that Cdc14 is essential for Clb4-CDK inhibition at meiosis I exit.

Surprisingly, ectopic release of Cdc14 led to stabilisation, not premature degradation, of meiotic cyclins. This is further evidence against the hypothesis that Cdc14 is required for cyclin proteolysis. Since spindle assembly is inhibited when Cdc14 is active early in meiosis, the majority of kinetochores are not attached to microtubules in *cdc55mn* cells. As a result, the spindle assembly checkpoint (SAC) is likely activated. SAC activation blocks anaphase entry through inhibition of the APC. Cyclins degradation is inhibited to prevent further progression through meiosis (Musacchio and Hardwick 2002). Deletion of a SAC component, such as Mad1 or Mad2, could help investigate this further.

An alternative mechanism proposed for uncoupling DNA replication and spindle formation events in meiosis, other than Cdc14-dependent partial down-regulation of CDKs, is through the activity of an auxiliary kinase. Ime2 has been shown to phosphorylate CDK substrates, including Cdh1 and CDK inhibitor Sic1, but at distinct sites that are resistant to Cdc14-dependent dephosphorylation (Holt, Hutti et al. 2007). Ime2 activity may consequently prevent DNA re-replication and complete cyclin degradation during meiosis independent of Cdc14 activity. This could explain why impairment of Cdc14 activity showed little effect on meiotic cyclin proteolysis.

If Cdc14 does not regulate the meiosis I-meiosis II transition through cyclin degradation, it may be required to dephosphorylate CDK-dependent substrates. Reversal of CDK-dependent phosphorylation is necessary to reset the cell for a new round of nuclear division (Manzoni, Montani et al. 2010). Potential meiotic substrates of Cdc14 need to be identified in order to discern why impairment of Cdc14 activity prevents the formation of tetranucleate cells.

Chapter 4

Cdc14 is required for re-duplication of SPBs after meiosis I

4. Cdc14 is required for reduplication of SPBs after meiosis I

4.1 Introduction

Since Cdc14 does not appear to regulate the meiosis I to meiosis II transition through degradation of meiotic cyclins, it may be required for the reversal of CDK-dependent phosphorylation. In mitosis, Cdc14 dephosphorylates CDK substrates to reset the cell in preparation for the following round of cell division (Visintin, Craig et al. 1998). Upon completion of meiosis I, meiotic CDK targets will presumably also need resetting to restore them to their initial phosphorylation states, enabling cells to enter a second meiotic division. The phosphatase Cdc14 may be acting likewise during meiosis to oppose CDK phosphorylation.

Global analysis of Cdc14 targets in mitotic cells identified several SPB components as Cdc14 associated proteins (Bloom, Cristea et al. 2011, Kao, Wang et al. 2014). Following meiosis I, SPBs must be re-duplicated to undergo a second meiotic division. In this chapter, I hypothesise that Cdc14 acts on the SPBs to allow the assembly of duplicated meiosis II spindles, thereby ensuring the production of tetranucleate cells.

The spindle pole body (SPB) is the microtubule organising centre in budding yeast, functionally comparable to the centrosome in higher eukaryotes (Moens and Rapport 1971, Byers and Goetsch 1974). It consists of at least 19 different components assembled into an organised structure, which is embedded in the nuclear envelope and interacts with cytoplasmic and nuclear microtubules via the γ-tubulin complex (Jaspersen and Winey 2004). The SPB is highly

phosphorylated (Wigge, Jensen et al. 1998), and a number of its components contain multiple consensus Cdc28-phosphoryltaion sites (Ubersax, Woodbury et al. 2003). Phospho-regulation of the SPB has been shown to affect SPB assembly (Adams and Kilmartin 1999), microtubule nucleation (Vogel, Drapkin et al. 2001) and SPB duplication (Vallen, Ho et al. 1994, Kilmartin 2003, Avena, Burns et al. 2014, Elserafy, Saric et al. 2014).

I hypothesise that, upon release from nucleolar sequestration in anaphase I, Cdc14 is required to dephosphorylate SPBs. This dephosphorylation enables re-duplication of SPBs to allow for the proper segregation of sister chromatids in meiosis II. Impairment of Cdc14 activity would therefore result in hyper-phosphorylated SPBs that are unable to re-duplicate after meiosis I. This could explain why *cdc14-1* mutants are unable to properly assemble two meiosis II spindles and form tetranucleate cells.

4.2 Results

4.2.1 Cdc14 interacts with SPBs when released from the nucleolus

To understand how Cdc14 regulates the meiosis I to meiosis II transition, I sought to identify its substrates during meiosis. I decided to IP Cdc14 from meiotic cells. Since Cdc14 is bound to its inhibitor, Cfi1, in the nucleolus for the majority of the cell cycle, I also performed the IP in cdc55mn cells. Upon depletion of Cdc55 from cells, the Cdc14-Cfi1/Net1 association is inhibited and Cdc14 is ectopically released from the nucleolus (Bizzari and Marston 2011, Kerr, Sarkar et al. 2011). Therefore, I anticipated that Cdc14 substrates would be enriched in this IP.

4.2.1.1 Cdc14 immunoprecipitates with all SPB components when released for Cfi1/Net1

I immunoprecipitated Cdc14-TAP (tandem affinity purification tag) (Rigaut, Shevchenko et al. 1999) in wild type and *cdc55mn* cells harvested in anaphase I. Meiotic progression was monitored by counting binucleate and tetranucleate cell populations (Fig. 4. 2. 1. 1A). Cells were harvested~ 4h after induction in sporulation media, where binucleate but not tetranucleate cells were present in wild type samples. This ensures that cells have progressed into meiosis I but have not completed meiosis II. The Cdc14-TAP fusion protein retains the meiotic functions of the endogenous protein, since there was no dramatic change in nuclear division efficiency or timing during meiosis (Fig. 4. 2. 1. 1A).

SDS-PAGE analysis and silver staining of immunoprecipitates (Fig. 4. 2. 1. 1B) reveals a band corresponding to Cdc14-TAP (~82kDa) in both tagged-strain lanes but, crucially, was absent from both no-tag control lanes. This indicates that Cdc14-TAP is enriched in these lanes. Another band, approximately the expected height for Cfi1/Net1 (129~kDa), was present in the wild type IP sample. Cfi1/Net1 band intensity was greatly reduced in *cdc55mn* cells. This observation is in agreement with the phenotype of *cdc55mn* mutants, where Cdc14-Cfi1/Net1 binding is inhibited (Kerr, Sarkar et al. 2011).

IP samples were digested with trypsin and mass spectrometry (MS) was performed by our collaborators, Flavia Alves and Juri Rappsilber. MaxQuant software was used to identify peptides pulled-down with Cdc14. Compiled MS data was sorted by total peptide number. Proteins recognized by comparison to

a data set of routinely occurring contaminants were disregarded, as were proteins that appeared with high peptide numbers in the no tag control samples (Table A1- page 223).

As expected, both Cdc14 and Cfi1 were identified in Cdc14-TAP pulldowns from wild type and cdc55mn cells (Fig. 4. 2. 1. 1C). Interestingly, the number of Cfi1 peptides was reduced in cdc55mn cells compared to wild type, from 43 to 29 peptides. Although this is not quantitative, it is consistent with the fact that Cdc14 tends to reside outside the nucleolus in cdc55mn cells, as shown by imaging methods.

Components of the SPB were highly abundant in both wild type and *cdc55mn* Cdc14-TAP IP samples. This was expected, since greater numbers of Cdc14 proteins are released from Cfi1/Net1-dependent nucleolar sequestration. In depth analysis of SPB constituents confirmed the presence of all proteins from the SPB core, the SPB periphery, the half-bridge and γ-tubulin complex (Fig. 4. 2. 1. 1D). This data suggests that Cdc14 associates with the SPB when released from nucleolar sequestration.

During meiosis II, the SPB is modified through replacement of the outer plaque component Spc72 with Mpc52, and later Spo21, to initiate spore formation (Knop and Strasser 2000). A small number of Mpc52 peptides were identified in wild type but not *cdc55mn* cells, whilst Spo21was not identified in either IP (Fig. 4. 2. 1. 1D). Cells harvested for use in the IP experiment were not synchronous so it is possible that a small fraction of wild type cells entered meiosis II. However,

the lack of Mpc52 in *cdc55mn* mutants suggests that the ectopic release of Cdc14 may prevent meiosis II-specific modification of the SPB.

Another meiotic specific SPB-associated protein, Ndj1, was identified in both wild type and *cdc55mn* pulldowns (Table A1). Ndj1 has recently been identified as a regulator of SPB separation during meiosis, and is absent from SPBs in mitosis (Li, Shao et al. 2015). The presence of this protein in *cdc55mn* samples confirms that mutant cells have entered meiosis, despite an inability to form meiotic spindles.

A

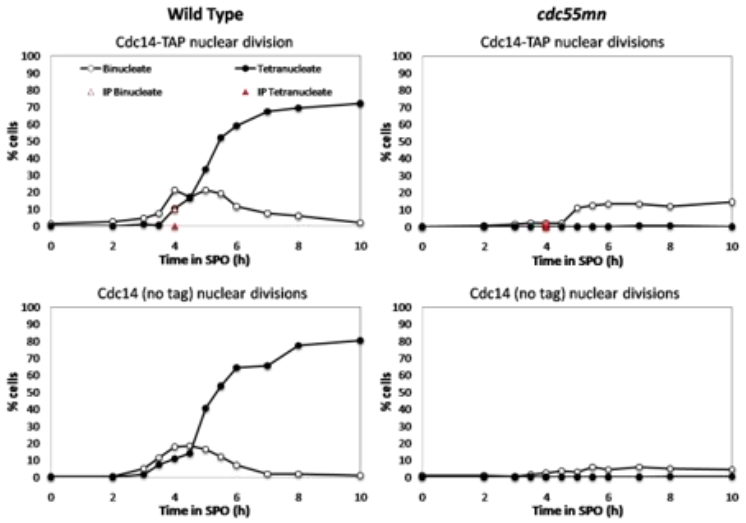

B

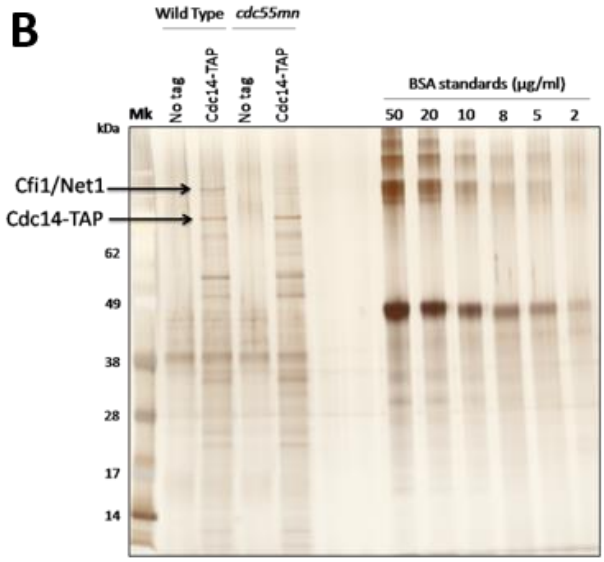

C

Name	Function	Wild Type	*cdc55mn*
Spc110	SPB component	73	89
Cnm67	SPB component	45	53
Pom152	NPC component	52	51
Spc42	SPB component	36	40
Cfi1/Net1	Cdc14 inhibitor	43	29
Bfa1	GTPase activator	42	37
Cdc14	Protein phosphatase	30	28
Spc97	SPB component	28	38
Spc29	SPB component	20	31
Spc72	SPB component	27	30
Spc98	SPB component	25	30
Faa2	Acyl-CoA synthetase	21	33
Acc1	Acetyl-CoA carboxylase	23	22
Mps3	SPB component	26	20
Mps2	SPB component	19	26
Hsl7	Arginine N-methyltransferase	25	23
Bbp1	SPB component	22	18
Hsp82	Hsp90 chaperone	20	23
Ady3	Cnm67 paralogue	18	24
Bub2	GTPase activator	16	17

Figure 4.2.1.1: Cdc14 IPs with SPB components when released from nucleolar sequestration. (A) Wild type and *cdc14-1* cells containing *CDC14* (AM1835, AM9459) and *CDC14-TAP* (AM9434,AM9319) were induced to sporulate and the percentages of binucleate and tetranucleate cells were determined. Cells were harvested after 4h in SPO for immunoprecipitation of Cdc14-TAP. (B) 15µl of all samples and BSA standards loaded onto a Bis/Tris gel. Silver-stained SDS-PAGE showed Cdc14 band appeared in tagged strains lanes only. Cfi1/Net1 band was reduced in *cdc55mn* cells. (C) MS analysis of peptides identified in IP samples recognised strong association of Cdc14 with components of the SPB complex. Numbers indicate peptide numbers identified. (D) Further analysis of data identified all SPB components pulled-down with Cdc14. Schematic of SPB and functions of components were based on Jaspersen & Winey, 2004.

D

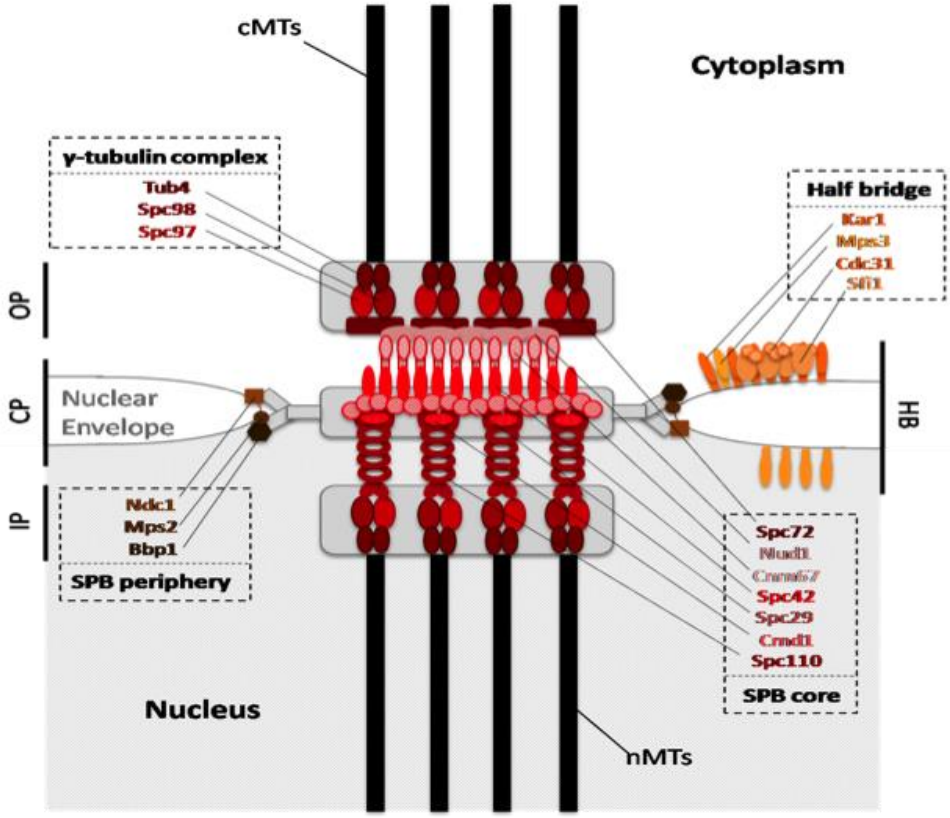

Name	SPB localisation	Role in SPB function	Wild Type	*cdc55mn*
Cdc14			30	28
Tub4	γ-tubulin complex	MT nucleation	14	16
Spc98	γ-tubulin complex	MT nucleation	25	30
Spc97	γ-tubulin complex	MT nucleation	28	38
Spc72	SPB core	γ-tubulin binding protein	27	30
Nud1	SPB core	MEN signaling	8	9
Cnm67	SPB core	Anchors outer plaque to central plaque	45	53
Spc42	SPB core	Structural SPB core	36	40
Spc29	SPB core	Structural SPB core	20	31
Cmd1	SPB core	Structural Spc110 binding protein	9	8
Spc110	SPB core	γ-tubulin binding protein	73	89
Ndc1	SPB periphery	SPB insertion into NE	18	18
Mps2	SPB periphery	SPB insertion into NE	19	26
Bbp1	SPB periphery	SPB core and HB linker to membrane	22	18
Kar1	Half bridge	SPB duplication	17	18
Mps3	Half bridge	SPB duplication	26	20
Cdc31	Half bridge	SPB duplication	12	15
Sfi1	Half bridge	SPB duplication	15	16
Mpc54	Meiotic plaque	Replaces Spc72 in meiosis II	8	0
Spo21	Meiotic plaque	Replaces Spc72 in meiosis II	0	0

4.2.1.2 Retention of Cdc14 in the nucleolus reduces Cdc14-SPB interactions

The association of Cdc14 with the SPB complex in Fig. 4. 2. 1. 1D appears to correlate with Cdc14 release from nucleolar sequestration. Retention of Cdc14 by Cfi1/Net1 should consequently inhibit Cdc14-SPB interactions.

To test this theory, I pulled down Cdc14-TAP in metaphase-arrested cells. During metaphase I, Cdc14 is bound to Cfi1/Net1, thus the association of Cdc14 with SPB components should be impaired. The metaphase arrest was achieved through construction of a Cdc20 meiotic-depletion strain. Cdc20 is an activator of the APC (Visintin, Prinz et al. 1997). Depletion of Cdc20 hence results in inhibition of anaphase I entry.

Metaphase-arrested Cdc14-TAP IP samples were processed, sent for MS and compiled in MaxQuant (Table A2.1 – page 230). Peptide numbers identified for SPB subunits were compared to those observed in the previous IP, where cells were allowed to progress in meiosis (Fig. 4. 2. 1. 2). These are termed as "metaphase I" and "meiosis I" cells respectively.

Cdc14 peptide numbers recovered in both wild type samples were comparable between the two experiments (Fig. 4. 2. 1. 2). An increase in Cfi1/Net1 peptide numbers in the "metaphase I" cells from 43 to 54 peptides may fit well with the idea that Cdc14 was retained in the nucleolus when entry into anaphase I was prohibited. A clear reduction in SPB-Cdc14 association was also evident in these cells, suggesting that inhibition of Cdc14 by nucleolar sequestration may restrict interaction with the SPB.

The number of Cdc14 peptides identified in *cdc55mn* "metaphase I" cells was slightly reduced compared to the wild type situation in the same experiment. Because of this, SPB peptide values were normalised in each IP with respect to Cdc14 peptide numbers to better compare all the samples across both experiments (Table A2.2). These normalised values were then further analysed.

Ratios of wild type/*cdc55mn* normalised peptides values showed that a greater number of SPB components were enriched in *cdc55mn* samples when cells were arrested in metaphase I than when meiotic progression was permitted (Fig. 4. 2. 1. 2). This hints that release of Cdc14 from inhibition is conducive to SPB interaction. However, the total number of SPB peptides pulled-down in *cdc55mn cdc20mn* cells was considerably reduced when compared to those achieved in "meiosis I". This is unanticipated, as the metaphase-arrest should not affect early release of Cdc14 from the nucleolus in c*dc55mn cells*.

It is unclear why SPB and Cfi1/Net1 peptide numbers are so diminished in the "metaphase I" *cdc55mn* sample compared to the "meiosis I" IP. One possible explanation is that Cdc14 failed to pull-down interactors as effectively in this IP. If that were the case, far greater values of SPB peptides would be expected. As a consequence, the enrichment of SPB peptides in the *cdc55mn* sample observed would be further emphasised.

Both Cdc14-TAP IP experiments, using metaphase-arrested cells and meiotic-progressing cells, were performed only once. As such, the MS data generated are not quantitative. Furthermore, some SPB peptides are identified in metaphase-arrested

wild type cells, where Cdc14 is retained in the nucleolus. However, the data imply that enrichment of Cdc14-SPB association likely requires the release of Cdc14 from nucleolar sequestration.

		Meiosis I			Metaphase I		
Name	**SPB localisation**	**Wild Type**	***cdc55mn***		**Wild Type**	***cdc55mn***	
Cdc14		30	28	1.00	27	23	1.00
Cfi1/Net1		43	29	1.38	54	6	7.67
Tub4	γ-tubulin complex	14	16	0.82	1	3	0.28
Spc98	γ-tubulin complex	25	30	0.78	0	2	0.00
Spc97	γ-tubulin complex	28	38	0.69	2	2	0.85
Spc72	SPB core	27	30	0.84	5	7	0.61
Nud1	SPB core	8	9	0.83	2	2	0.85
Cnm67	SPB core	45	53	0.79	24	45	0.45
Spc42	SPB core	36	40	0.84	27	31	0.74
Spc29	SPB core	20	31	0.60	13	16	0.69
Cmd1	SPB core	9	8	1.05	1	2	0.43
Spc110	SPB core	73	89	0.77	35	45	0.66
Ndc1	SPB periphery	18	18	0.93	3	4	0.64
Mps2	SPB periphery	19	26	0.68	7	15	0.40
Bbp1	SPB periphery	22	18	1.14	3	6	0.43
Kar1	Half bridge	17	18	0.88	0	1	0.00
Mps3	Half bridge	26	20	1.21	4	3	1.14
Cdc31	Half bridge	12	15	0.75	3	6	0.43
Sfi1	Half bridge	15	16	0.88	0	0	1.00
Mpc54	Meiotic plaque	8	0	3E+06	0	2	0.00
Spo21	Meiotic plaque	0	0	1.00	0	13	0.00

Figure 4.2.1.2: Comparison of SPB peptide numbers identified in Cdc14 IPs from anaphase I and metaphase I-arrested cells. Wild type *cdc20mn* and *cdc55mn cdc20mn* cells containing *CDC14* (AM3560, AM15024) and *CDC14-TAP* (AM14939, AM14709) were induced to sporulate. Cells were harvested after 4h growth for immunoprecipitation of Cdc14-TAP. Peptide numbers generated by MS analysis of IP samples in metaphase I-arrested cells (metaphase I) were compared to previous Cdc14-TAP IP experiment (meiosis I). The peptide numbers of SPB components identified in each IP were normalised to Cdc14 peptide values (data not shown). The ratio of wild type to *cdc55mn* normalised peptide values were calculated to determine the effect of Cdc14 release from inhibitory binding on SPB association.

Ratios <0.8 indicate enrichment of protein in *cdc55mn* sample (red).

Ratios >1.2 indicate enrichment of protein in wild type sample (green).

4.2.1.3 Cdc14 localises asymmetrically to SPBs in anaphase I

Since Cdc14 appears to associate with the SPB when released from inhibitory binding to Cfi1/Net1, it is reasonable to expect that Cdc14 localises to SPBs in anaphase I. To investigate the localisation of Cdc14 during meiosis, I visualised wild type cells undergoing synchronous meiosis after release from prophase I arrest, where Cdc14 was tagged with GFP (Cdc14-GFP) and the core SPB component, Spc42, was tagged with tdTomato (Spc42-tdTomato). To measure Cdc14 association with the SPB, I quantified the amount of Cdc14-GFP signal, normalising Cdc14-GFP signal intensity at the SPB to that of Spc42-tdTomato. Average relative intensity of Cdc14 per SPB was calculated for 50 cells in each meiotic phase. The meiotic cell cycle stage was determined by the analysis of the number and positioning of SPBs, and the nucleolar sequestration state of Cdc14.

This analysis showed that, in anaphase I, Cdc14 is significantly enriched at SPBs with respect to metaphase I, increasing from 0.08 arbitrary units (a.u) to 0.37 a.u. (Fig. 4. 2. 1. 3A). This confirms that Cdc14 co-localises with SPBs when released from nucleolar sequestration in meiosis I. The SPB-associated pool of Cdc14 observed in anaphase I is not detected in metaphase II, and Cdc14-GFP signal reappears in the nucleolus. This suggests that Cdc14 at SPBs may be re-sequestered in the nucleolus upon meiosis II entry, as evident from the restoration of metaphase I-like Cdc14/SPB relative intensities (0.06 a.u.).

Upon anaphase II entry, there is a modest increase in Cdc14-SPB co-localisation during this second wave of Cdc14 release. However, the increase observed is not statistically significant ($p = 0.67$). This suggests that simply the release of Cdc14 from nucleolar

sequestration is not the only mechanisms regulating Cdc14-SPB localisation. As it is the meiosis I-meiosis II transitional role of Cdc14 that is of interest, I decided to focus on this aspect of Cdc14 localisation and function, and did not further analyse meiosis II.

The images of meiosis I cells were examined further to analyse the localisation of Cdc14 at the SPB. Cells were categorised as either metaphase I or anaphase I based upon release of Cdc14 from the nucleolus and SPB positioning. The co-localisation of Cdc14 with SPBs was scored, discriminating between no SPB localisation, localisation to one SPB (asymmetric) and localisation to both SPBs (symmetric).

During metaphase I, when Cdc14 is retained in the nucleolus, 98.5% of cells exhibited no detectable co-localisation of Cdc14 with SPBs (Fig. 4. 2. 1. 3B). As expected, when Cdc14 is released from inhibition, a pool of Cdc14 is evident at SPBs in 97% of anaphase I cells. This is in accord with the Cdc14-SPB quantification data. Strikingly, this localisation is predominately asymmetric (Fig. 4. 2. 1. 3B).

Using the same Cdc14-GFP strain, I released cells into a synchronous meiosis and imaged the live cells on a microfluidics plate to follow the same cell throughout meiosis. It is apparent that the asymmetric localisation of Cdc14 is maintained throughout anaphase I (Fig. 4. 2. 1. 3C). The pool of SPB-associated Cdc14 remains only at one SPB and there is no evidence of Cdc14 transitioning between the two poles.

It is unclear whether the pool of Cdc14 observed at SPBs is active. However, since Cdc14 interacts with SPBs, it is likely that the complex or one of its components is a target for Cdc14-dependent dephosphorylation.

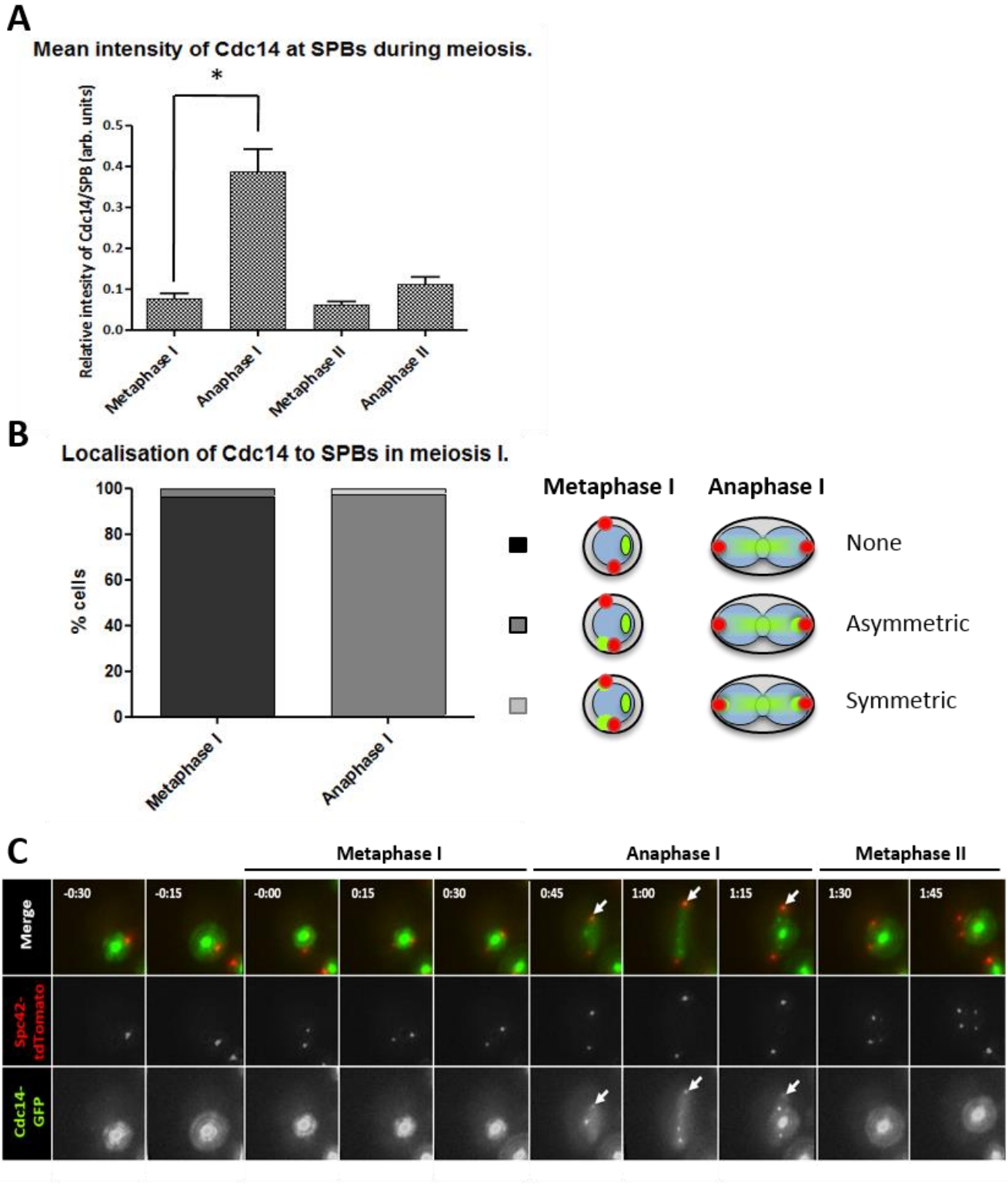

Figure 4.2.1.3: Cdc14 localises asymmetrically to SPBs in anaphase I . (A) Wild type cells containing *CDC14-GFP* and *SPC42-tdTomato* (AM11517) were induced to sporulate, released from *GAL-NDT80* block and imaged at 30 minute intervals using agarose pads. Cdc14-GFP/Spc42-tomato signal per SPB per cell was quantified, with error bars representing standard error. Cells were classified into different meiotic stages through markers such as number of SPB foci, distance between SPBs and Cdc14 nucleolar sequestration. The two-tailed Student's *t*-test was used to calculate significance. * indicates $p<0.001$. n = 50 cells. (B) Co-localisation of Cdc14 with SPBs was scored in meiosis I cells. Cdc14 appears to localise to SPBs asymmetrically in anaphase I. n = 100 cells. (C) Live cells were imaged at 15 minute intervals for a total of 12 hours using microfluidics. A time-lapse example shows Cdc14 remains only at one SPB throughout anaphase I (white arrow) before re-sequestration into the nucleolus in metaphase II.

4.2.1.4 Cdc14 localises to SPBs in *cdc55mn* mononucleate cells

To determine whether ectopically released Cdc14 prematurely associates with the SPB, I analysed Cdc14-GFP localisation in *cdc55mn* mutants. In meiotic wild type cells, Cdc14 is released from nucleolar sequestration in anaphase I (Fig. 4. 2. 1. 3A). When Cdc55 is depleted in meiosis, Cdc14 prematurely exits the nucleolus prior to SPB separation in metaphase I. After 3h in meiosis, 52% of Cdc55-depleted cells show partial or complete release of Cdc14 from the nucleolus (Fig. 4. 2. 1. 4A-B).

Cells were grouped into three distinct categories based on their Cdc14 localisation phenotype. Group 1 cells retain Cdc14 within the nucleolus and display no detectable co-localisation of Cdc14 with SPBs (Fig. 4. 2. 1. 4C). Group 2 cells exhibit a partial release of Cdc14. Whilst a portion of the GFP signal is retained in the nucleolus, a diffuse cloud of Cdc14 is observed emerging from the nucleolar spot. This released Cdc14 cloud co-localises with SPBs in 69% of group 2 cells, although the intensity with which Cdc14 signal localises to the SPB ranges from a mild to strong association. In group 3 cells, Cdc14-GFP signal completely dissipates from the nucleolus. 95% of these cells exhibit strong Cdc14-SPB co-localisation (Fig. 4. 2. 1. 4C), indicating that release of Cdc14 from the nucleolus correlates with SPB co-localisation.

These findings confirm that the early release of Cdc14 in c*dc55mn* mutants results in the premature localisation of Cdc14 to SPBs, prior to meiosis I. This is consistent with MS data, where Cdc14-SPB association is enriched in *cdc55mn* cells (Fig. 4. 2. 1. 2).

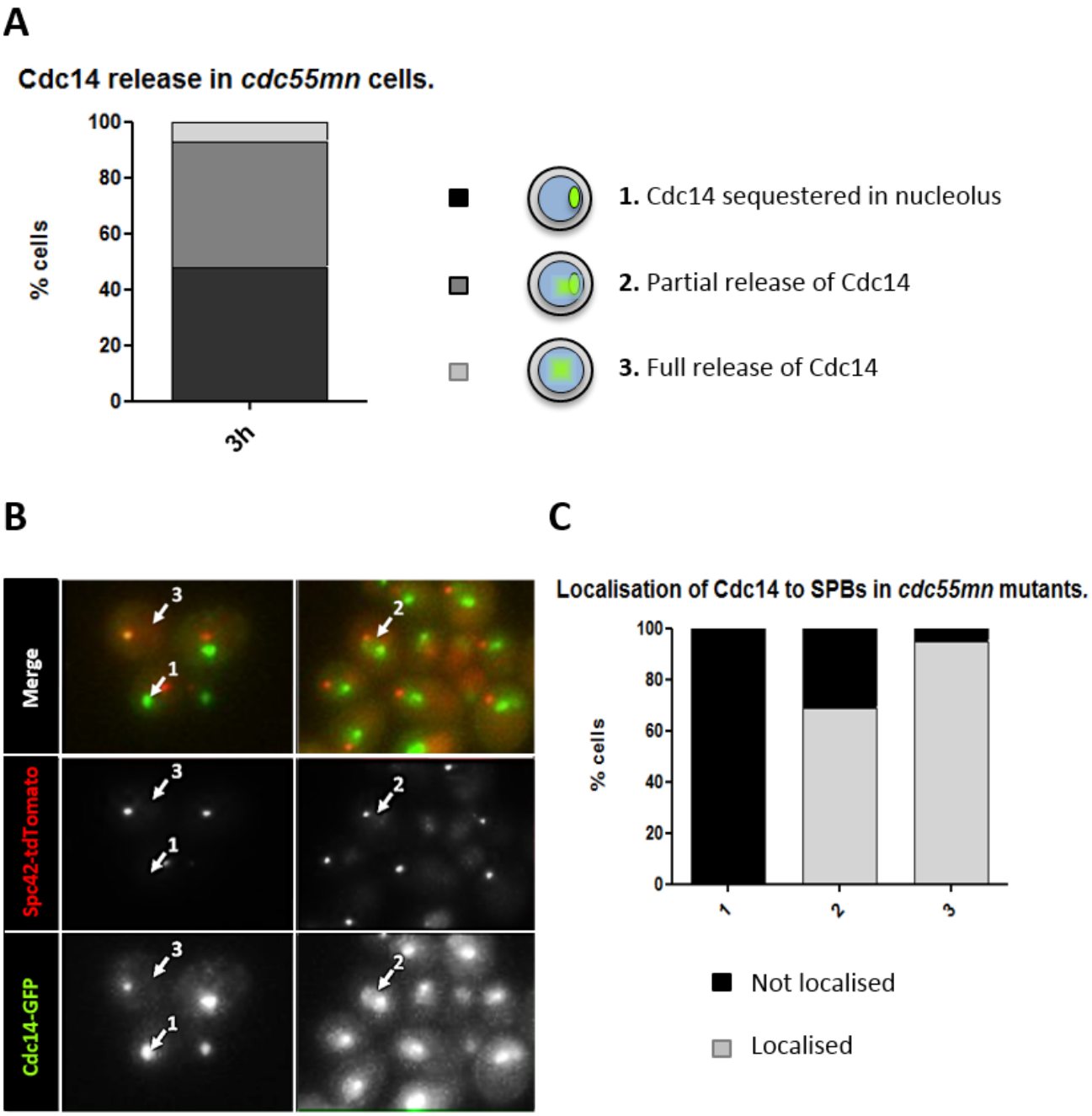

Figure 4.2.1.4: Cdc14 localises prematurely to SPBs in *cdc55mn* mutants . (A) *cdc55mn* cells containing *CDC14-GFP* and *SPC42-tdTomato* (AM13123) were induced to sporulate, released from *GAL-NDT80* block and imaged after 3h using agarose pads. Cdc14 localisation was classified into three categories; sequestered in nucleolus (1), partially released from nucleolus (2) and completely released from nucleolus (3). n = 100 cells. (B) Example images of Cdc14 localisation phenotypes observed in *cdc55mn* cells indicated by arrows. (C) Co-localisation of Cdc14 with SPBs was analysed for each Cdc14 release-phenotype. n = 100 cells.

4.2.2 Cdc14 plays a role in regulating the SPB duplication pathway

For cells to properly assemble meiosis II spindles, a total of four SPBs are required. If inactivation of Cdc14 prevents or impairs SPB duplication, *cdc14-1* cells would not contain the appropriate number of SPBs necessary for nuclear division in meiosis II. This could explain the mixed segregation phenotype observed when Cdc14 activity is inhibited. *cdc14-1* mutants might be unable to properly duplicate the machinery required for a second chromosome segregation step, and so attempt an equational segregation but on a single anaphase I spindle.

To test this hypothesis, the role of Cdc14 in SPB duplication in meiotic cells needed to be investigated.

4.2.2.1 Investigating SPB duplication by SPB focus analysis

To investigate the role of Cdc14 on SPB duplication, I analysed wild type, *cdc14-1, cdc55mn, slk19Δ, spo12Δ* and *cdc14-1 cdc55mn c*ells containing *SPC42-tdTomato.* Spc42 is an essential component of the SPB complex (Donaldson and Kilmartin 1996) and, consequently, the tomato-tagged construct can be used as a marker for presence of the SPB, as was utilised in the Cdc14-SPB localisation experiment (Fig. 4. 2. 1. 3A-C). I released the cells into a synchronous meiosis and counted the percentages of binucleates and tetranucleates at regular time intervals to monitor cell cycle progression. The number of SPB foci per cell was also scored.

Anaphase I and anaphase II entry is indicated by the appearance of binucleate and tetranucleate cells respectively. In wild type cells, the appearance of two or four SPB foci precedes each chromosome segregation steps by ~15 mins (Fig. 4. 2. 2. 1), corresponding to the timing of metaphase I and metaphase II respectively. When Cdc14 activity is impaired, binucleate cells accumulate and persist. Tetranucleate cells are not produced. The same phenotype is observed when Cdc14 is restricted to the nucleolus in *slk19Δ* and *spo12Δ* mutants. These binucleates contains only two SPB foci, suggesting that Cdc14 activity is required for the production of four distinct SPBs.

Early activation of Cdc14 in c*dc55mn* mutants prevents meiosis I nuclear division, resulting in mononucleate cells with ~90% containing a single SPB focus (Fig. 4. 2. 2. 1). A further ~10% of *cdc55mn* mononucleates contain two SPBs. These SPB foci are usually in close proximity to one another, suggesting that SPB separation is impaired through ectopic release of Cdc14. When the prematurely released Cdc14 is inactive in a *cdc14-1 cdc55mn* mutant, SPB separation is partially rescued and two SPBs are

observed, as is seen in a *cdc14-1* single mutant (Fig. 4. 2. 2. 1). This confirms that it is the early activity of Cdc14 in meiosis that impedes proper regulation of the SPB duplication pathway.

Due to the limitations in resolution of conventional light microscopy, it is unclear whether a singular SPB focus observed in cells is an unduplicated SPB or two SPBs that are duplicated but unable to separate from one another, remaining in close association. This distinction must be made in order to identify the stage of SPB duplication that Cdc14 regulates.

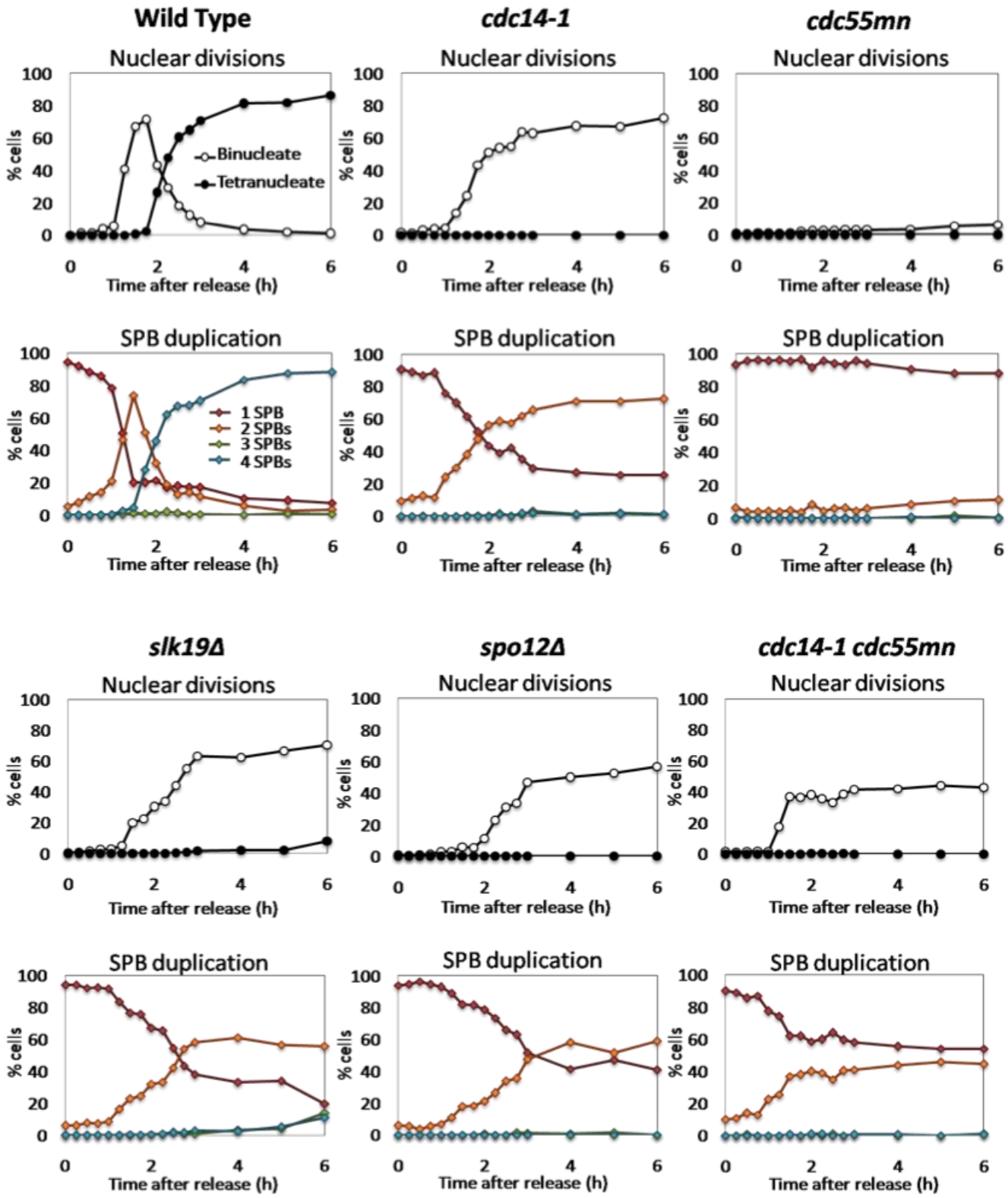

Figure 4.2.2.1: Active Cdc14 is required for cells to form four distinct SPB foci in meiosis . Wild type (AM13989), *cdc14-1* (AM16163), *cdc55mn* (AM15984), *slk19Δ* (AM16020) *spo12Δ* (AM16064) and *cdc14-1 cdc55mn* (AM17904) cells containing *SPC42-tomato* were induced to sporulate and released from *GAL-NDT80* block. The percentages of binucleate and tetranucleate cells were determined. The percentages of cells that contained one, two, three and four SPB foci per cell were also calculated. n = 200 cells.

4.2.2.2 Investigating SPB duplication by quantification of total SPB fluorescence

Total SPB fluorescence can be used to determine the quantity of Spc42 protein in cells. As SPBs duplicate, the fluorescence signal of the SPB focus increases two-fold. I measured F_i (integrated fluorescence intensity minus background) of individual SPBs using a method previously described by Hoffman, Pearson *et al.,* 2001, following SPB duplication in individual cells during meiosis. F_i values for cells of each strain were aligned in time with respect to entry into metaphase I (appearance of two SPBs). The mean total F_i per cell was calculated for each strain and plotted.

Wild type cells initially contain one SPB focus. After the SPB focus splits in metaphase I to two foci, the mean total F_i increases slightly from 3.4 to 3.8 a.u. (Fig. 4. 2. 2. 2A). This is consistent with the expectation that SPBs have already undergo the first round of duplication at the start of the experiment, when cells are arrested in prophase I. On entry into meiosis II, SPBs duplicate and separate into four SPBs with a total F_i of 6.9 a.u. per cell. This value corresponding to four SPBs is approximately double the F_i of two SPBs, indicating that the second round of SPB duplication can be detected using this method. I conclude that quantification of Spc42-tomato signal can be used as an indicator of SPB duplication and separation.

In *cdc14-1* cells, when Cdc14 activity is impaired, four SPBs are not observed. Quantification of the two SPB foci seen in cells show that total SPB F_i is 3.4 a.u. (Fig. 4. 2. 2. 2A-B). This value is close to the 3.9 a.u. measured when wild type cells contain only two SPBs. If SPBs were duplicated but unable to separate from one another in *cdc14-1* mutants, this value should be approximately 6.9 a.u. Therefore, it would appear inactivation of Cdc14 prevents re-duplication of SPBs after meiosis I.

When Cdc14 is prematurely released from nucleolar sequestration, ~90% of mononucleates contain one SPB (Fig. 4. 2. 2. 1). This single SPB focus has a mean F_i of 2.9 a.u. throughout the time course (Fig. 4. 2. 2. 2A-B), reflective of the value observed in both wild type and c*dc14-1* cells prior to entry into metaphase I. It is, therefore, probable that the single focus observed in *cdc55mn* cells after prophase I is actually two adjacent SPBs duplicated side-by-side, since SPBs are known to duplicate after mitosis in G1/S-phase (Jaspersen, Giddings et al. 2002).

To confirm that SPBs are duplicated prior to the prophase I arrest stage, wild type, *cdc14-1* and *cdc55mn* cells were induced to sporulate but were maintained in the *GAL-NDT80* block arrest for 6h (Fig. 4. 2. 2. 2C). Mean SPB intensities were quantified for 100 cells per strain. Total F_i per cell increases in all strains from ~180 to ~290 a.u. These results suggest that Spc42 protein abundance almost doubles before cells arrest in prophase I, implying that SPB duplication occurs and that *cdc55mn* cells contain two duplicated but un-separated SPBs during meiosis.

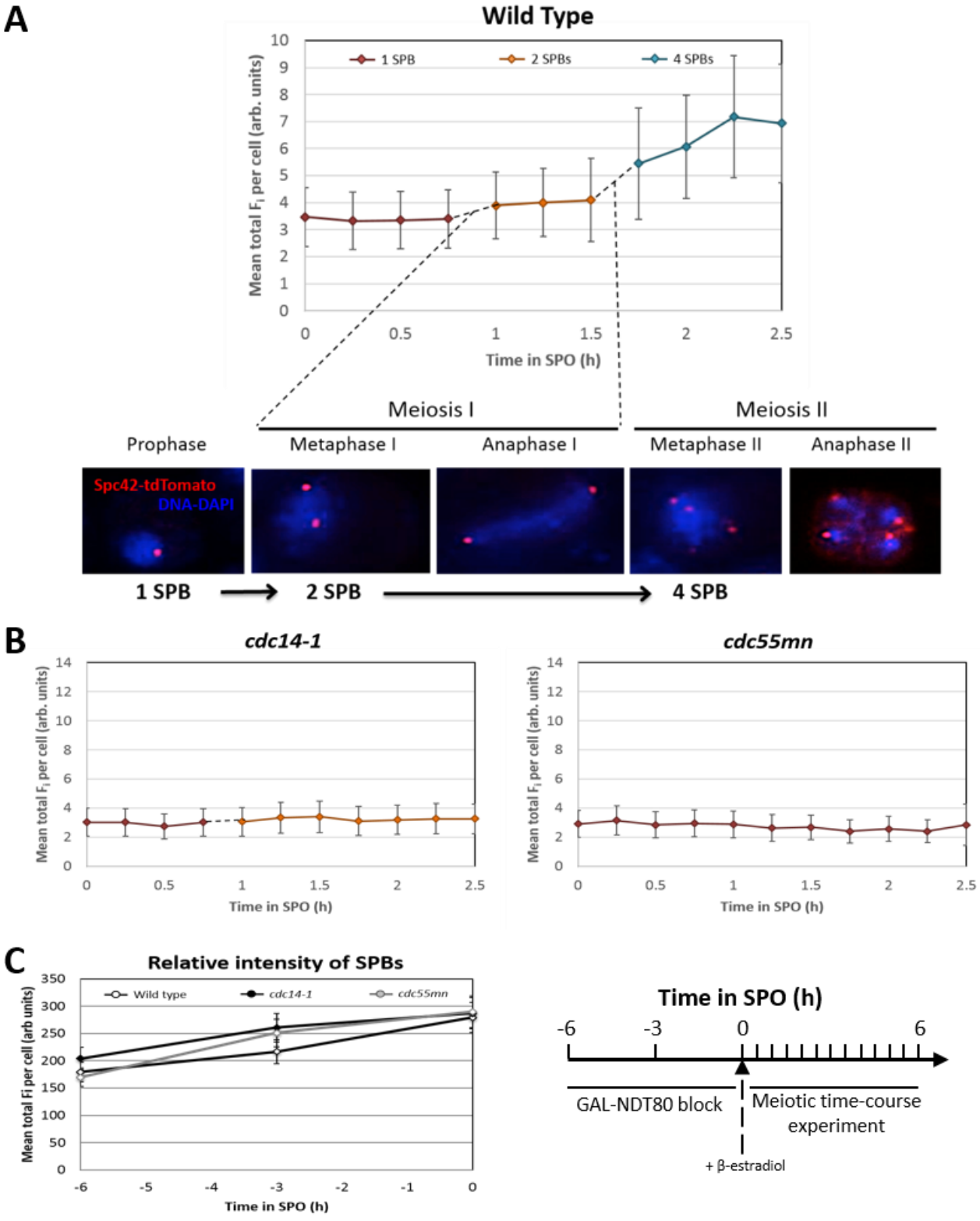

Figure 4.2.2.2: Quantitative analysis of SPB foci in meiosis . (A-B) Wild type (AM13989), *cdc14-1* (AM16163), and *cdc55mn* (AM15984) cells containing *SPC42-tomato* were induced to sporulate, released from *GAL-NDT80* block and imaged at 15 minute intervals for a total of 12 hours. Individual SPB foci were quantified and mean total SPB fluorescence intensity (F_i) per cell was plotted, with error bars representing standard error. Representative images of a wild type cell in (A) used as illustration of SPB duplication and separation. n = 10 cells. (C) Wild type, *cdc14-1* and *cdc55mn* strains were added to SPO and arrested by *GAL-NDT80* block for 6 hours. Cells were imaged at 3 hour intervals using agarose pads. Mean F_i per SPB was plotted for each strain, with error bars for standard error. n = 100 cells

4.2.2.3 Investigating SPB duplication by EM analysis

Quantification of SPBs using fluorescence microscopy suggests that Cdc14 activity is required for the re-duplication of SPBs after meiosis I, and that early release of Cdc14 prevents initial SPB separation in metaphase I. However, to unequivocally establish the stage at which the SPB cycle is blocked, it is necessary to observe their ultrastructure using electron microscopy (EM).

I used cryo-immobilisation, via high pressure freezing (HPF), freeze substitution and subsequent embedding of *cdc14-1* and *cdc55mn* cells to fix mutant meiotic cells for visualisation. Epon blocks were sectioned, stained and serial sections were analysed by transmission EM.

When Cdc14 activity is impaired in meiosis, only two SPB foci are observed in binucleate cells using fluorescence microscopy (Fig. 4. 2. 2. 1). As a result, binucleate *cdc14-1* cells were specifically targeted for analysis via EM. In all cases where SPBs were observed in *cdc14-1* binucleates (n = 7), two SPBs are embedded in the nuclear envelope at polar opposite ends of the cell with a long bipolar spindle assembled between them (Fig. 4. 2. 2. 3A). The SPB structures appear completely unduplicated, as there is no evidence of half bridge elongation or outer plaque assembly at either SPB.

Despite the fact that Cdc14 activity is required for the production of four SPBs in meiosis II, *cdc14-1* mutants are still able to modify their unduplicated SPBs in a meiosis II-specific manner. The meiotic plaque components Mpc54 and Spo21 replace Spc72 during meiosis II, enabling vesicle docking and pro-spore membrane formation (Knop and Strasser 2000). In wild type cells, diffuse Spo21 signal starts to weakly associate

with SPBs in late meiosis I. This signal becomes more pronounced at all four SPBs in the late stages of meiosis II (Marston, Lee et al. 2003). When Cdc14 activity is impaired, cells enter a sustained anaphase I-arrest. At early time points, Spo21 signal appears unaltered from wild type localisation in meiosis I. However, at later time points, Spo21 signal accumulates at SPBs in a meiosis II-like manner. (Marston, Lee et al. 2003).

I show that in c*dc14-1* mutants, a double-membrane sheet, termed the pro-spore membrane (Moens and Rapport 1971), is clearly visible around SPBs (Fig. 4. 2. 2. 3A-B). Serial section images reveal vesicle recruitment to the cytoplasmic side of the SPB, coalescing into the pro-spore membrane (Fig. 4. 2. 2. 3A). This membrane then expands during meiosis II to completely enclose the nucleus anchored to the SPB (Fig. 4. 2. 2. 3B). Pro-spore membrane formation at SPBs appears to be asymmetric, assembling and expanding at one SPB prior to assembly at the other SPB (n = 3). Cdc14, therefore, is not required for meiosis II-specific SPB modification or pro-spore membrane formation.

Ectopic release of Cdc14 results in mononucleate cells containing predominately one SPB focus (Fig. 4. 2. 2. 1). Quantitative fluorescence analysis suggests that this single focus is actually two un-separated SPBs. EM analysis of *cdc55mn* mutants confirms this theory. Two SPBs are visible, embedded into the nuclear envelope in *cdc55mn* cells (Fig. 4. 2. 2. 3C). These SPBs are physically connected to one another by a bridge structure emanating from the central plaque of each SPB (n = 6), visible on both sides of the nuclear envelope. Short nuclear and cytoplasmic microtubules assemble at both SPBs but, since SPBs do not separate and migrate to opposite poles of the cell, are unable to assemble meiosis spindles in EM images.

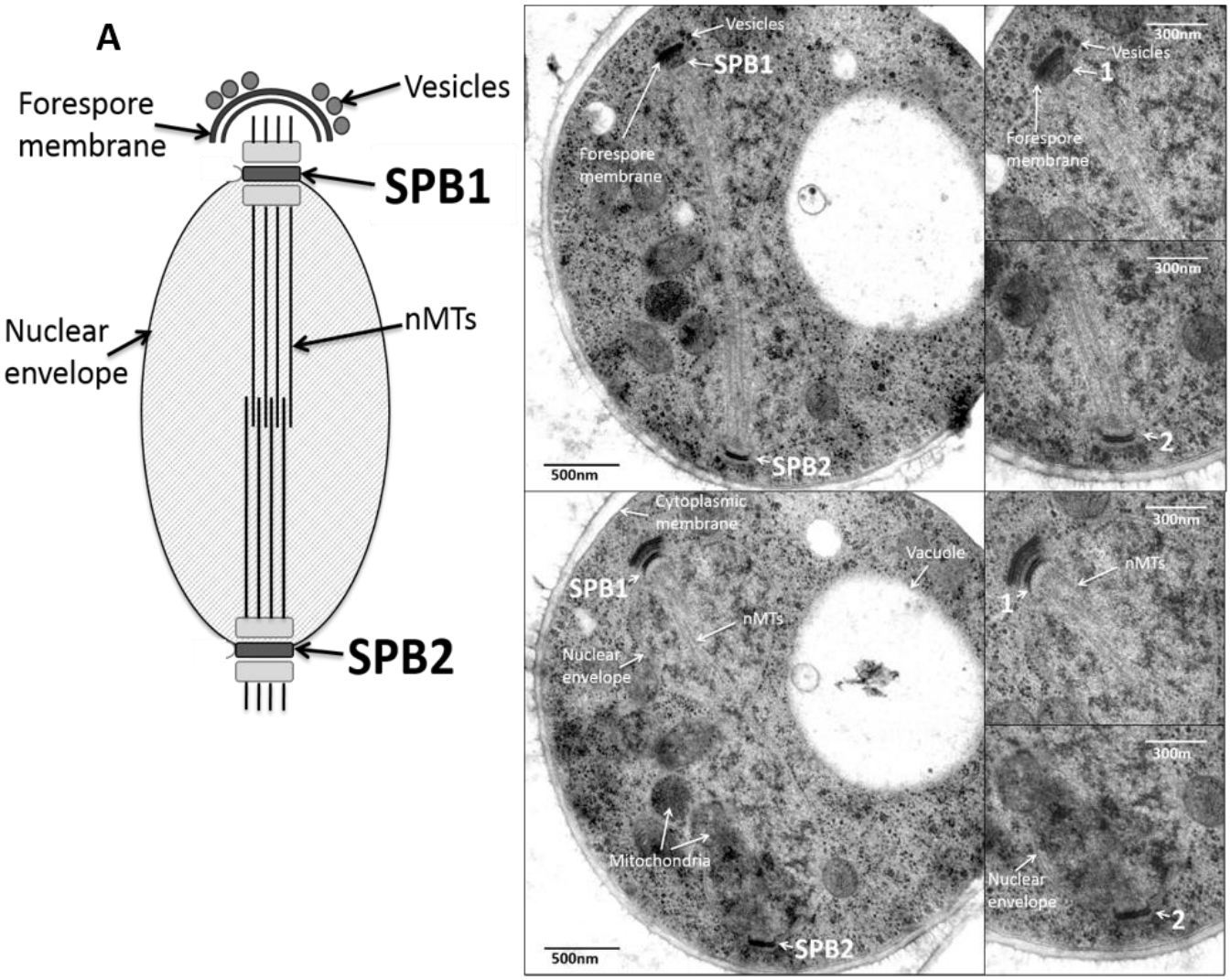

Figure 4.2.2.3: EM analysis of SPBs in meiosis . (A-B) c*dc14-1* (AM16077) and (C) *cdc55mn* (AM16198) cells were induced to sporulate, released from *GAL-NDT80* block and prepared for EM. Serial sections were examined. Left panel shows entire cell image. Right panels show higher magnification of SPBs in the same cell. Model illustrates in dark grey the cellular structures visible in EM images. (A) Multiple sections of the same representative *cdc14-1* cell (n= 7) containing a long bipolar spindle with two unduplicated SPBs (1,2) embedded in the nuclear envelope. Pro-spore wall formation observed around SPB1 and secretory vesicle recruitment is evident. (B) Representative c*dc14-1* cell (n = 3) containing two unduplicated SPBs (1,2). Full spore wall assembled from SPB1 enclosing nucleus. Pro-spore wall forming at SPB2. (C) Representative *cdc55mn* cell (n = 6) containing two SPBs connected via a bridge structure.

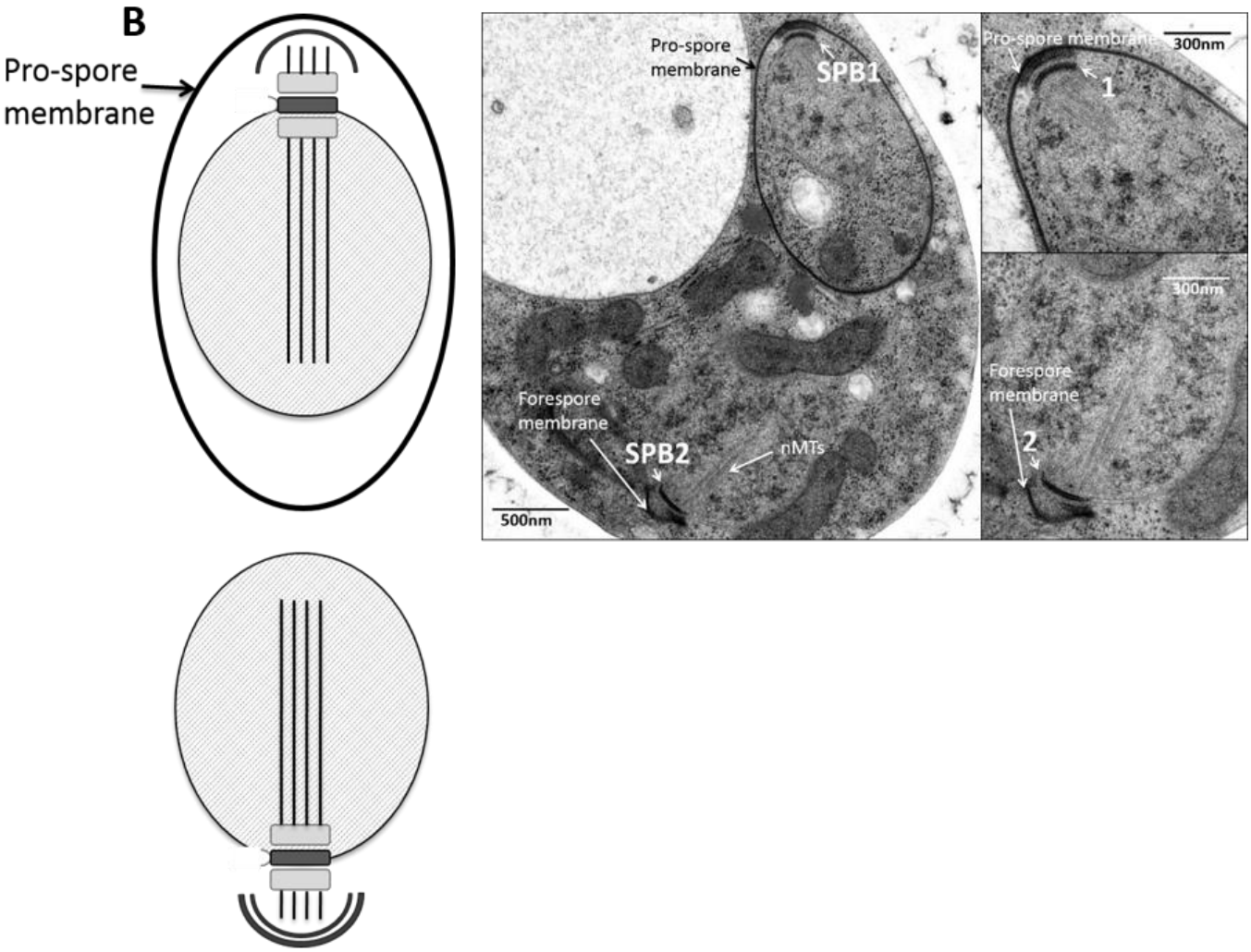
B
Pro-spore membrane
Pro-spore membrane
SPB1
Forespore membrane
SPB2
nMTs
500nm
Pro-spore membrane
1
300nm
300nm
Forespore membrane
2

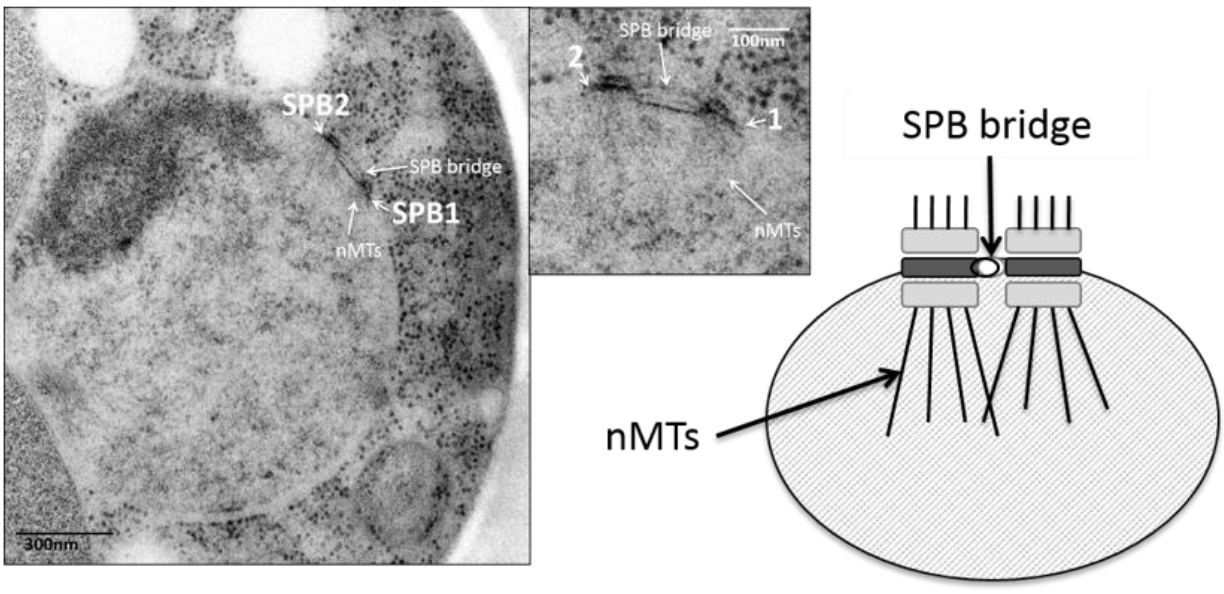
C
SPB2
SPB bridge
SPB1
nMTs
300nm
SPB bridge
100nm
2
1
nMTs
SPB bridge
nMTs

4.2.3 Bfa1-Bub2-dependent location of Cdc14 to SPBs is important for timely SPB re-duplication in meiosis

During mitosis, budding yeast cells divide asymmetrically. To ensure proper segregation of sister chromatids in anaphase, the mitotic spindle must align correctly on the mother-bud cell polarity axis, enabling spindle elongation and insertion into the budding daughter cell. Failure to properly align spindles results in activation of the spindle position checkpoint (SPOC) (Pereira, Hofken et al. 2000, Pereira, Manson et al. 2002, Kim, Luo et al. 2012) and delayed mitotic exit. The SPB acts as a scaffold for MEN signalling (Bardin, Visintin et al. 2000, Visintin and Amon 2001, Pereira, Manson et al. 2002), components of which assemble preferentially at the daughter cell-bound SPB (Menssen, Neutzner et al. 2001, Valerio-Santiago and Monje-Casas 2011, Kim, Luo et al. 2012).

Bfa1-Bub2 form a GTPase activating protein (GAP) complex that activates Tem1 and initiates MEN signalling (Bardin, Visintin et al. 2000, Pereira, Hofken et al. 2000). Bfa1-Bub2 localisation is regulated by SPOC components Kin4 and Bmh1, which ensures that GAP activity is restricted to daughter SPB when mitotic spindles are correctly aligned. In contrast, spindle misalignment results in activation of SPOC and symmetric localisation of Bfa1-Bub2 (Caydasi, Micoogullari et al. 2014). Asymmetric localisation of MEN is required for timely mitotic exit (Kim, Luo et al. 2012). Cdc14 has also been show to localise asymmetrically to the daughter pole in a Bub2-dependent manner (Yoshida, Asakawa et al. 2002).

Meiosis is a symmetric division and MEN is not active in anaphase I (Jaspersen, Charles et al. 1998, Shou, Seol et al. 1999, Azzam, Chen et al. 2004, Queralt, Lehane et al. 2006).

Therefore, it is unclear why asymmetrical localisation of Cdc14 to SPBs is observed (Fig. 4. 2. 1. 3B-C). To determine whether this localisation is important for the role of Cdc14 in SPB re-duplication, I analysed a number of SPOC mutants that may regulate the Cdc14-SPB association.

4.2.3.1 Localisation of Cdc14 to SPBs is Bfa1-Bub2-dependent

I monitored Cdc14-GFP localisation in cells where SPOC components *BUB2, BFA1, KIN4* and *BMH1* were deleted. Cdc14 co-localisation with SPB signal was quantified, using SPB number and positioning, and Cdc14 nucleolar release as a marker for anaphase I. The average relative intensity of Cdc14 per SPB was calculated for each SPOC mutant, as was previously described in Fig. 4. 2. 1. 3A.

Cdc14-SPB association is significantly reduced in *bfa1Δ* and *bub2 Δ* mutants relativet to wild type cells during anaphase I (Fig. 4. 2. 3. 1A). However, deletion of upstream SPOC components *KIN4* and *BMH1* has no effect on Cdc14 abundance at SPBs ($p = 0.53$ and $p = 0.37$ respectively). Furthermore, the asymmetric localisation of Cdc14 to SPBs observed in wild type anaphase I cells is unchanged in *kin4Δ* and *bmh1Δ* mutants. Consistent with Cdc14-SPB quantification data, deletion of *BUB2* and *BFA1* results in faint or non-detectable localisation of Cdc14 to SPBs.

These findings are surprising, since Kin4 and Bmh1 control the localisation of Bfa1-Bub2 in mitosis (Caydasi, Micoogullari et al. 2014). If deletion of *KIN4* and *BMH1* affect Bfa1-Bub2 localisation similarly in meiosis, these results would suggests that the activity but not necessarily the localisation of Bfa1-Bub2 affects Cdc14 localisation to SPBs. However, it is also possible that Bfa1-Bub2 localisation is regulated independently of Kin4 and Bmh1 activity in meiosis.

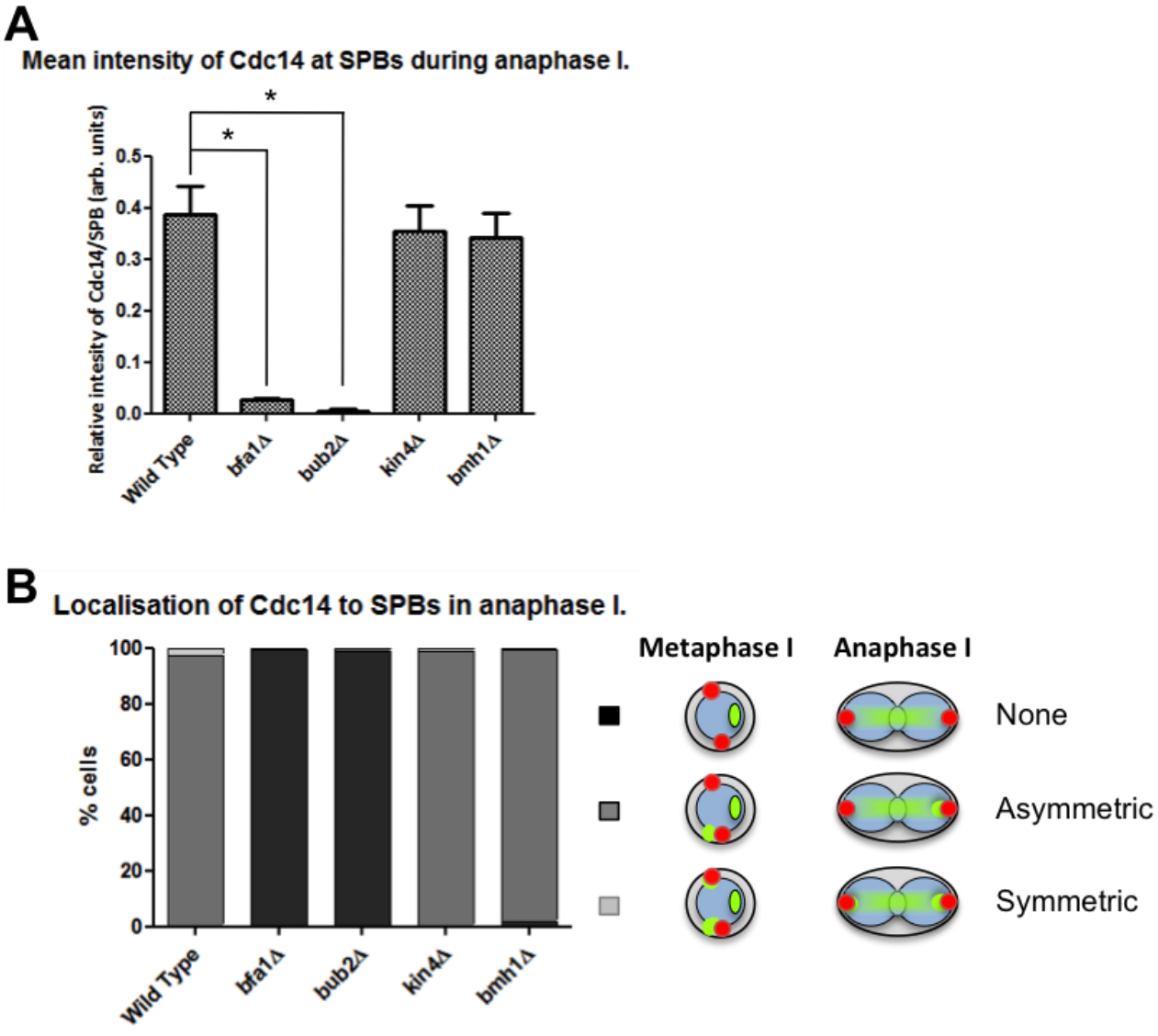

Figure 4.2.3.1: Asymmetric localisation of Cdc14 to SPBs is Bfa1/Bub2-dependent . (A) Wild type (AM11517), *bfa1Δ* (AM16079), *bub2Δ* (AM15543), *kin4Δ* (AM17134) and *bmh1Δ* (AM17341) cells containing *CDC14-GFP* and *SPC42-tomato* were induced to sporulate, released from *GAL-NDT80* block and imaged at 30 minute intervals using agarose pads. Cdc14-GFP/ Spc42-tomato signal per SPB per cell was quantified, with error bars representing standard error. Cells were classified as anaphase I through distance between SPBs foci and Cdc14 release. The two-tailed Student's *t*-test was used to calculate significance. * indicates $p<0.001$. n = 50 cells. (B) Co-localisation of Cdc14 with SPBs was scored in anaphase I cells. Asymmetric localisation of Cdc14 to SPBs in anaphase I is abolished when *BFA1* and *BUB2* are deleted. n = 100 cells.

4.2.3.2 Loss of Cdc14-SPB co-localisation prevents the timely duplication of SPBs

Since Cdc14 localisation to SPBs is significantly reduced when *BFA1* and *BUB2* are deleted in meiosis, *bfa1Δ* and *bub2Δ* mutants can be utilised to investigate the role of Cdc14-SPB co-localisation on the re-duplication of SPBs.

I monitored SPB duplication during meiosis, as was described in Fig. 4. 2. 2. 1. In *bfa1Δ* and *bub2Δ* mutants, the efficiency of tetranucleate cell formation is greatly decreased. After 6h in meiosis, 90% of wild type cells are tetranucleate whereas only 36% and ~57% of *bfa1Δ* and *bub2Δ* cells respectively contain four nuclei (Fig. 4. 2. 3. 2). A delay in the appearance of *bfa1Δ* tetranucleates is also observed. On average, cells lacking Bfa1 take ~1h longer to enter anaphase II despite the fact that timing of anaphase I entry, indicated by the appearance of binucleate cells, is unaffected.

Deletion of *BFA1* and *BUB2* during meiosis also appears to result in the accumulation of binucleate cells, as has been observed when Cdc14 activity is impaired. These binucleates persist in cell populations >4 hours longer than is observed in wild type cells (Fig. 4. 2. 3. 2). In *bfa1Δ* and *bub2Δ* mutants, ~54% and ~22% of cells respectively contain two nuclei after 6 hours in meiosis. This is compared to only ~3% observed in wild type cells. From this, it would appear that Bfa1 and Bub2 may be important for the timely and efficient transition of cells from meiosis I to meiosis II.

SPB duplication is likewise affected in the SPOC mutants. The timing of SPB re-duplication after meiosis I is delayed in *bfa1Δ* cells. Four distinct SPB foci are not observed in meiotic cells until ~30 mins after they are seen in wild type cells (Fig. 4. 2. 3. 2). This suggests that Bfa1 may be required for timely re-duplication of SPBs. Whilst

the timing of SPB duplication does not appear to be affected in *bub2Δ* mutants, the efficiency of re-duplication is. Only 58% of *bub2Δ* cells contain four SPBs compared to ~90% observed in the wild type situation. Taken together, these results imply that Bfa1-Bub2-dependent localisation of Cdc14 to SPBs may be required to ensure the proper re-duplication of SPBs for meiosis II. However, further investigation is needed to confirm such a role.

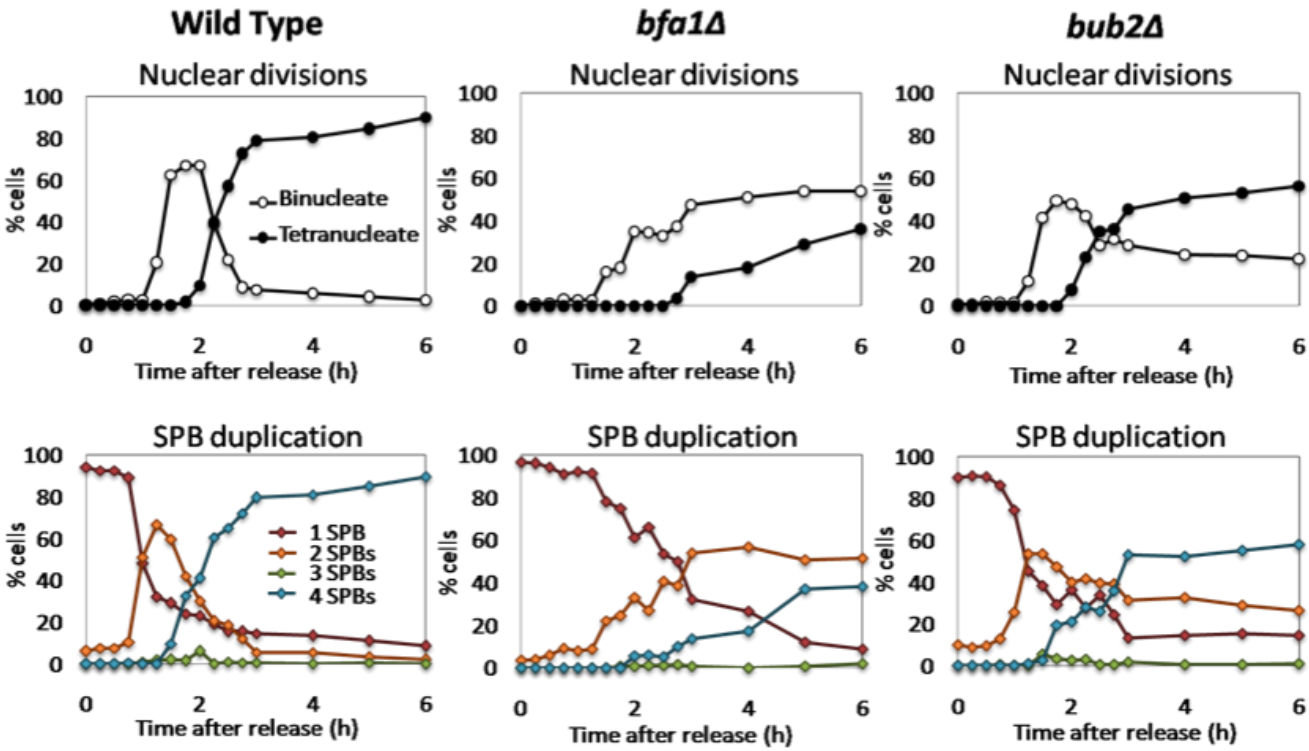

Figure 4.2.3.2: Bfa1 and Bub2 are required for timely re-duplication of SPBs in meiosis. Wild type (AM13989), *bfa1Δ* (AM16019) and *bub2Δ* (AM16080) cells containing *SPC42-tomato* were induced to sporulate and released from *GAL-NDT80* block. The percentages of binucleate and tetranucleate cells were determined. The percentages of cells that contained one, two, three and four SPB foci per cell were also calculated. n = 200 cells.

4.2.3.3 Bfa1 localises symmetrically to SPBs during meiosis I

Deletion of *BUB2* and *BFA1* results in the abolishment of Cdc14 asymmetric localisation at SPBs and delayed re-duplication of SPBs after meiosis I. This suggests that, whilst MEN in not active during meiosis I (Attner and Amon 2012), SPOC may play a role in regulating the meiosis I to meiosis II transition. During mitosis, the asymmetric localisation of Bfa1-Bub2 to SPBs indicates that mitotic spindles are correctly aligned and that SPOC is inactive. Symmetric localisation therefore correlates with SPOC activation. To investigate whether SPOC is active during meiosis, I monitored the localisation of Bfa1 within cells.

During metaphase I and anaphase I, Bfa1-tdTomato signal is evident at both SPBs in ~99% of cells (Fig. 4. 2. 3. 3A-B). This suggests that SPOC may be active during meiosis I. Since deletion of *BUB2* and *BFA1* leads to a delay in exit from meiosis I, it is possible that Bfa1-Bub2 may be required at SPBs to enable re-duplication via a MEN-independent mechanism. However, how and why symmetrically localised Bfa1 results in the asymmetric localisation of Cdc14 in anaphase I remains unclear.

When cells enter metaphase II, SPBs re-duplicate but Bfa1 signal is retained at only one of these duplicated SPBs in ~93% of cells. Upon entry into anaphase II, Bfa1-SPB co-localisation is undetectable (Fig. 4. 2. 3. 3A-B). From this observation, it could be inferred that SPOC becomes inactivated during meiosis II. This is consistent with the known role of MEN during meiosis II. Meiotic MEN signalling occurs independent of the SPB scaffold protein, Nud1 (Attner and Amon 2012). In addition, the MEN component, Cdc15, does not localise to SPBs during meiosis, implying that the pathway occurs off the SPB (Attner and Amon 2012). Bfa1-Bub2 signalling is therefore not required at the

SPB, perhaps explaining why Bfa1-tdTomato signal does not co-localise with SPBs during anaphase II.

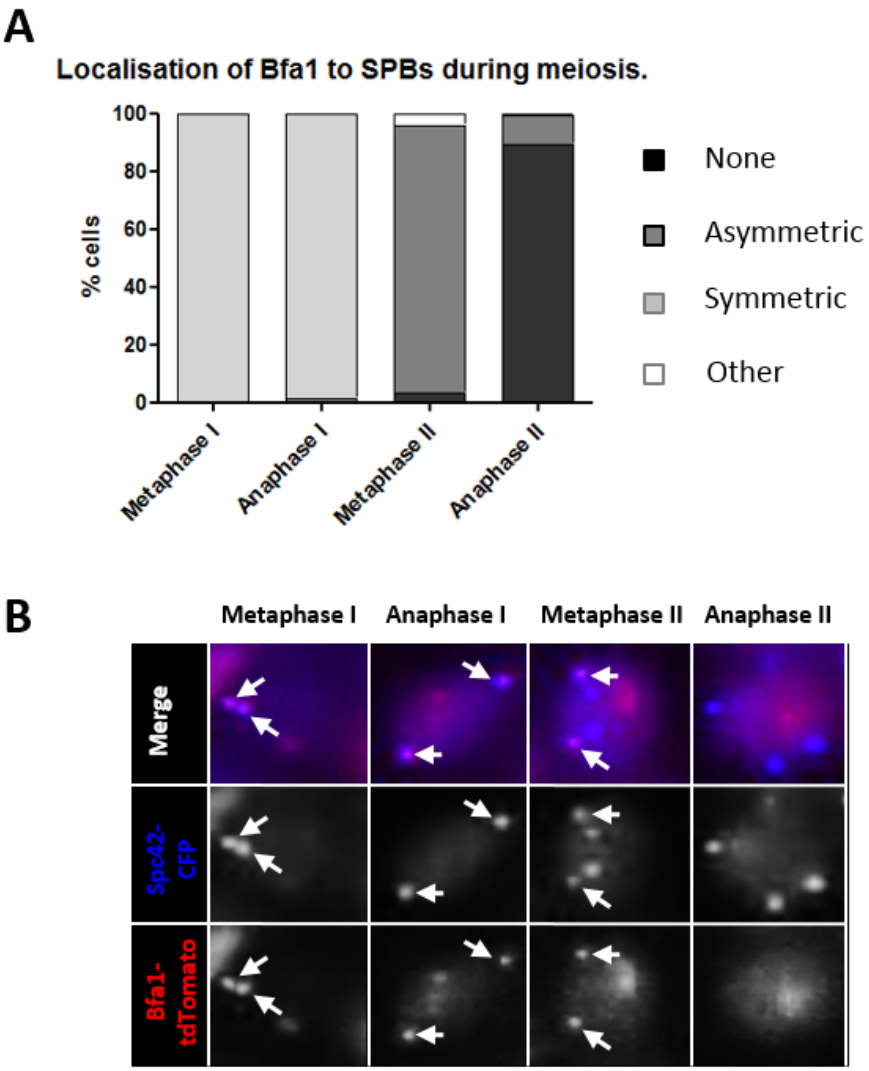

Figure 4.2.3.3: Bfa1 localises symmetrically to SPBs during meiosis I . (A) Wild type (AM17740) cells containing *SPC42-CFP, BFA1-tdTomato and CDC14-GFP* were induced to sporulate, released from *GAL-NDT80* block and imaged at 30 minute intervals using agarose pads. Cells were classified into different meiotic stages through markers such as number of SPB foci, distance between SPBs and Cdc14 nucleolar sequestration. Co-localisation of Bfa1 with SPBs was scored throughout meiosis. Symmetric localisation of Bfa1 to SPBs during meiosis I is observed. During metaphase II, Bfa1-tdTomato signal persists at only 2 SPBs. Upon entry into anaphase II, Bfa1 signal becomes diffuse within cells. n = 200 cells. (B) Representative images of Bfa1 localisation shows co-localisation with SPBs (white arrows).

* Spc42-CFP bleeds through to the GFP emissions channel so Cdc14-GFP signal is not shown. However, its nucleolar sequestration and release was used to classify meiotic stages.

4.2.3.4 Artificial tethering of Cdc14 to SPBs is lethal

To determine whether the localisation of Cdc14 to SPBs during anaphase I is essential for SPB re-duplication, I attempted to artificially tether Cdc14 to SPBs. GFP-fused proteins can be mislocalised to specific locations within the cell by coupling a GFP-binding protein (GBP) to a protein within the desired sub-cellular compartment or organelle (Rothbauer, Zolghadr et al. 2006).

I constructed Cdc14-GBP and Spc42-GFP strains. However, when I attempted to cross haploids of opposite mating types containing the two constructs, I observed that inheritance of both fusion proteins resulted in cell death (Fig. 4. 2. 3. 4). This suggests that sustained localisation of Cdc14 to SPBs is lethal during mitosis. Furthermore, the heterozygous diploids formed during the crossing displayed poor sporulation efficiency on SPO plates, indicating that regulation of Cdc14 localisation to SPBs is important for efficient meiosis.

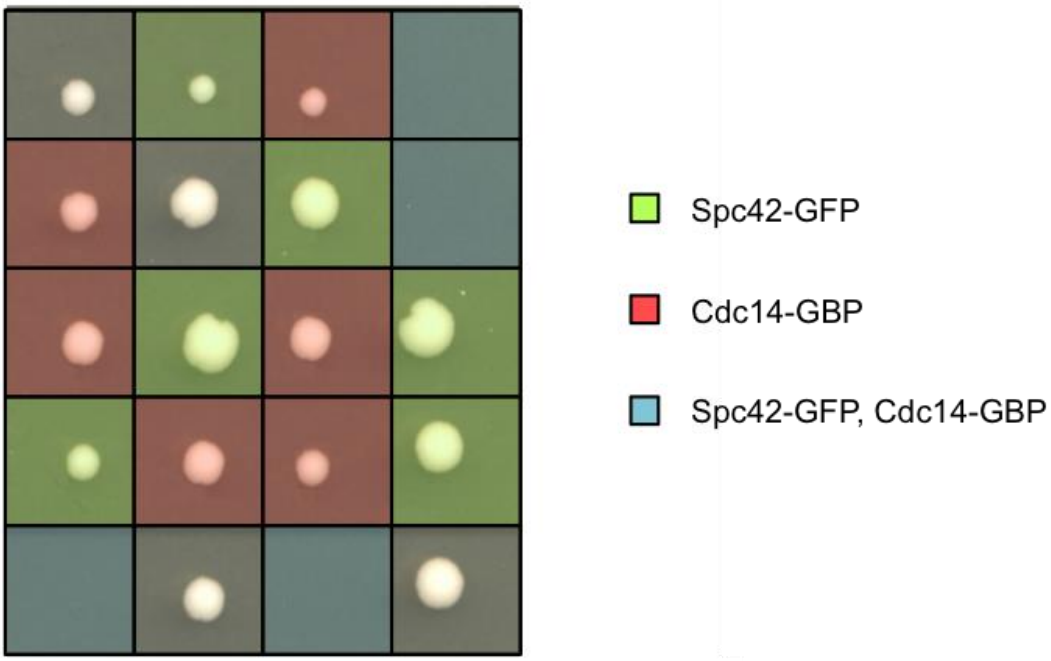

Figure 4.2.3.4: Artificial tethering of Cdc14 to SPBs is lethal. Cells containing *MATa SPC42-GFP* (AM17270) were crossed to cells containing *MATα CDC14-GBP* (AM17537). Heterozygous diploids were grown on SPO media plates. Dissection of spores revealed that the inheritance of Spc42-GFP and Cdc14-GBP was lethal to cells.

4.3 Discussion

One role of Cdc14 in mitotic exit is to reverse CDK-dependent phosphorylation (Pereira and Schiebel 2003, Higuchi and Uhlmann 2005, Woodbury and Morgan 2007, Jin, Liu et al. 2008). Dephosphorylation of multiple mitotic CDK-substrates by Cdc14 is required to enable the re-setting of cells for the next round of cell division. Similarly, for cells to exit meiosis I and transition into meiosis II, the molecular machinery within cells must be re-set in order for the proper execution of two consecutive rounds of chromosome segregation. For this reason, it is possible that Cdc14 regulates the meiosis I- meiosis II transition through reversal of CDK-phosphorylation events.

The SPB is a highly phosphorylated organelle (Wigge, Jensen et al. 1998) that has previously been identified as a target of CDK phospho-regulation (Adams and Kilmartin 1999, Kilmartin 2003, Ubersax, Woodbury et al. 2003, Jaspersen, Huneycutt et al. 2004). In meiosis I, two SPBs organise and assemble a meiosis I spindle, enabling the segregation of homologous chromosomes in anaphase I. For the segregation of sister chromatids in anaphase II, a total of four SPBs are required to assemble two meiosis II spindles. Since the SPB duplication pathway is regulated by Cdc28 (Byers and Goetsch 1974), Cdc14 may be required to oppose CDK phosphorylation to ensure proper SPB duplication and function.

I hypothesised that Cdc14 activity is required in anaphase I to dephosphorylate and re-set the SPB complex for meiosis II. When Cdc14 activity is impaired, I predicted that cells were unable to properly re-duplicate their SPBs and,

consequently, attempted to segregate sister chromatids but on a single meiosis II spindle.

To test this theory, I investigated the role of Cdc14 in SPB duplication. I found that Cdc14 associated with and localised to SPBs when released from nucleolar sequestration in anaphase I. Through quantitative fluorescence and transmission EM, I confirmed that Cdc14 is in fact required for the re-duplication of SPBs after meiosis I. As a result, *cdc14-1* cells are unable to assemble two meiosis II spindles due to an insufficient number of SPBs present in cells. Furthermore, I discovered that the early activation of Cdc14 in *cdc55mn* mutants prevents duplicated SPBs from separating in metaphase I. Since the SPBs are unable to move apart and, accordingly, migrate to opposite poles of the cell, meiotic spindle assembly is prohibited.

Interestingly, despite the fact that Cdc14 must enable re-duplication of both SPBs after meiosis I, Cdc14 localises asymmetrically to SPBs in anaphase I. Whilst during mitotic anaphase Cdc14 localises preferentially to the daughter cell-bound SPB, this localisation is linked to SPOC and MEN signalling. Active Bfa1-Bub2, part of the SPOC signalling pathway, inhibits MEN. Inhibitory phosphorylation of Bfa1-Bub2 by Cdc5 enables MEN activation and promotes mitotic exit. Bfa1-Bub2 and MEN components assemble asymmetrically on the daughter SPB, which acts as a scaffold for MEN signalling (Adams and Kilmartin 1999, Visintin and Amon 2001, Valerio-Santiago and Monje-Casas 2011), and Bub2 is required for the asymmetric localisation of Cdc14 to SPBs (Yoshida, Asakawa et al. 2002). However, in meiosis I MEN is not active (Kamieniecki, Liu

et al. 2005). Moreover, MEN signalling in meiosis II occurs off the SPB (Attner and Amon 2012). Therefore, preferential localisation of Cdc14 to one SPB is unexpected during meiosis. Currently, it is unclear which SPB Cdc14 localises to in anaphase I.

The dependency of Cdc14-SPB co-localisation on Bfa1-Bub2, despite a lack of MEN signalling in meiosis I, is surprising. One could argue that persistent SPOC activity prevents MEN activation during anaphase I. This is consistent with the finding that Bfa1 is symmetrically localised to SPBs during meiosis I. In mitosis, Cdc14 dephosphorylates Bfa1in late mitosis to re-activate the GAP following its inhibition by Cdc5 (Pereira, Manson et al. 2002). This hypophosphorylation of Bfa1 enables Tem1 inactivation and "switching off" of MEN signalling at the end of mitosis. Cdc14, therefore, may be required in anaphase I to ensure Bfa1-Bub2 remains active by opposing Cdc5-depedent phosphorylation. This would ensure MEN inactivation throughout meiosis I despite FEAR activation in anaphase I.

Another possible interpretation is that Bfa1-Bub2 is required to recruit Cdc14 to SPBs to ensure the timely re-duplication of SPBs. Deletion of *BUB2* and *BFA1* results in undetectable localisation of Cdc14 to SPBs and delays SPB re-duplication after meiosis I. Deletion of upstream SPOC regulators *KIN4* and *BMH1* had no effect on Cdc14-SPB association. Whilst Kin4 and Bmh1 play a role during mitosis in maintaining Bfa1-Bub2 activity, there is no evidence to suggest that they are required for Bfa1-Bub2 localisation to SPBs. Therefore, it is likely that in *kin4Δ* and *bmh1Δ* mutants, Bfa1 is able to recruit Cdc14 to SPBs. However, why this recruitment only occurs at one SPB is still unclear.

Chapter 5

Phospho-regulation of Sfi1 by Cdc14 enables SPB re-duplication during meiosis

5. Phospho-regulation of Sfi1 by Cdc14 enables SPB re-duplication during meiosis

5.1 Introduction

The SPB duplication pathway has been studied in detail using EM analysis of mitotic yeast cells. In G1, the half-bridge structure attached to one side of the core SPB elongates along the inner and outer faces of the nuclear envelope (Byers and Goetsch 1974, Adams and Kilmartin 1999). Central SPB components are recruited to the distal, cytoplasmic tip of the fully elongated bridge to form a small satellite, which then expands into a completely duplicated outer plaque (Adams and Kilmartin 1999). The duplicated plaque is then inserted into the nuclear envelope, after which nuclear SPB components assemble (Byers and Goetsch 1974, Winey, Goetsch et al. 1991, Winey, Hoyt et al. 1993, Schutz and Winey 1998). The result is side-by-side duplication of SPBs connected by an intact bridge. Following G1, the bridge structure is severed thus enabling SPBs to separate and form the poles of the mitotic spindle.

Daughter SPB assembly is initiated by half-bridge elongation. Whilst the half-bridge comprises of Kar1, Mps3, Cdc31 and Sfi1 proteins (Baum, Furlong et al. 1986, Rose and Fink 1987, Spang, Courtney et al. 1993, Jaspersen, Giddings et al. 2002), it is Sfi1 duplication and assembly that is the key player in bridge elongation (Li, Sandercock et al. 2006). Sfi1 molecules are attached to existing SPBs via their N-terminus. C-terminal end-to-end interactions with other Sfi1 proteins enables doubling of the half-bridge, elongating away from the

unduplicated SPB. The N-terminus of this Sfi1-dimerised bridge acts as the site for new outer plaque assembly (Li, Sandercock et al. 2006, Anderson, Prudden et al. 2007). Bridge integrity is maintained through the centrin homologue Cdc31 (Byers and Goetsch 1974, Baum, Furlong et al. 1986), which binds to Sfi1 at multiple sites and is required for the assembly of Sfi1 parallel arrays (Li, Sandercock et al. 2006, Bouhlel, Ohta et al. 2015).

Recent studies have shown that CDKs and Cdc14 regulate half -bridge elongation and fission in mitosis through phospho-regulation of the Sfi1 C-terminus (Avena, Burns et al. 2014, Elserafy, Saric et al. 2014, Bouhlel, Ohta et al. 2015). CDK-dependent phosphorylation of Sfi1 prevents C-terminal end-to-end dimerization, inhibiting half-bridge elongation. In anaphase, Cdc14 activity results in the dephosphorylation of Sfi1, which promotes half-bridge duplication. Following SPB duplication, phosphorylation of Sfi1 by CDKs enables the severing of the complete bridge structure and separation of adjacent SPBs (Avena, Burns et al. 2014, Elserafy, Saric et al. 2014, Bouhlel, Ohta et al. 2015).

I hypothesise that Cdc14 is required during meiosis for the phospho-regulation of Sfi1. This theory predicts that impairment of Cdc14 activity would result in sustained Sfi1 phosphorylation. This would prevent Sfi1 dimerization after meiosis I, which would explain why *cdc14-1* mutants display no evidence of half-bridge elongation in EM images. Furthermore, the early activation of Cdc14 in *cdc55mn* cells would result in premature Sfi1 dephosphorylation, impeding fission of the bridge and separation of SPBs.

5.2 Results

5.2.1 LFQ proteomic analysis of Spc42-3FLAG reveals reduced Sfi1 abundance at *cdc14-1* SPBs

Since half-bridge elongation initiates SPB duplication in mitosis, it is probable that accumulation and assembly of half-bridge components at the SPB is also required for re-duplication of SPBs after meiosis I. To determine whether Cdc14 activity was required for proper elongation of the half-bridge structure, I compared the protein abundance of SPB components in wild type and *cdc14-1* cells using a Spc42-FLAG construct to immunoprecipitate Spc42, harvesting cells after 4h in sporulation media. IP samples were digested with trypsin and MS was subsequently utilised to identify peptides pulled-down with Spc42 (Fig. 5. 2. 1A.). Each protein preparation and IP was performed in triplicate, resulting in a total of six data sets. Our collaborators, Juan Zou and Juri Rappsilber, using MaxQuant software, performed MS analysis. Label-Free Quantification (LFQ) intensities were calculated via spectral counting.

I normalised LFQ intensities to Spc42 and statistically analysed the MaxQuant output using Perseus software. Data sets were filtered for contaminants, logarithmised to log2(x) and grouped to compare proteins identified at SPBs in wild type and *cdc14-1* conditions. Numerical venn diagrams show the total number of proteins quantitatively identified in each sample (Fig. 5. 2. 1B-C). From the collated six data sets (Fig. 5. 2. 1B), only one protein was identified in all three wild type samples but was absent from *cdc14-1* SPBs (Leu1). Likewise, two proteins were found only in *cdc14-1* IPs (Gln1 and Pup3). These proteins are

all involved in metabolite biosynthesis and so are not relevant for investigating SPB changes when Cdc14 activity is impaired and are likely contaminants.

Since SPB structures are still present in *cdc14-1* cells, it is likely that any change to SPB composition and environment will be subtle. All 46 existing combinations of valid values identified in each sample are indicated in Fig. 5. 2. 1B. Reduction of the data matrix by filtering for valid values in at least 5 out of 6 columns, highlighted in grey in Fig. 5. 2. 1B-C, ensures that only proteins identified at SPBs in the majority of IPs were considered. 202 proteins were identified in all six samples, and a further 52 were present in 5 out of 6 samples (Fig. 5. 2. 1B-C). This filtering step reduces the total number of proteins analysed further from 740 to 254. Missing values were replaced by imputation from normal distribution.

Multi-scatter plots enabled the visual comparison of one replicate relative to another (Fig. 5. 2. 1D). SPB components are highlighted in red, Cdc14 in blue and Bfa1/Bub2 in green. The intensity distributions plotted for each data set comparison shows typically a non-uniform spread, which is slightly wider at lower intensities than at high intensities. In the majority of scatter plots, proteins plotted lie predominately on an x=y axis. This shows that protein abundances quantified in all replicates correlate well with one another. The average Pearson correlation coefficient for wild type samples is 0.73 and for *cdc14-1* is 0.90. The greater variation in relative LQF protein intensities between wild type replicates is due to greater SPB component enrichment in the first wild type sample (WT_1). This suggests that cells harvested in the first replicate experiment may

have already re-duplicated their SPBs, whereas SPBs in the other replicates, as well as in *cdc14-1* cells, are unduplicated.

Changes in SPB composition between all data sets can be quickly identified using volcano plots (Fig.5. 2. 1E). Significance (-log of pValue) is plotted against protein fold change between wild type and *cdc14-1* groups on the y- and x-axes respectively. False discovery rate (FDR) is set at 5% and s0 = 1. Whilst none of the data points are statistically divergent between wild type and c*dc14-1* grouped data sets, Cdc14 is greatly reduced at SPBs when Cdc14 activity is impaired. In addition, a number of SPB components are also reduced at *cdc14-1* SPBs. These proteins include all half-bridge and SPB peripheral components. Since half-bridge elongation initiates SPB duplication, the unduplicated SPBs in *cdc14-1* cells would likely have fewer half-bridge constituents than re-duplicating wild type SPBs.

The lack of significance in protein fold change may result from several factors. Firstly, wild type cells duplicate their SPBs from two to four poles in total. This 2-fold change may not be great enough to be detected with significance. Secondly, the variation in wild type LFQ intensities negatively affects reproducibility. Cultures grown for protein preparation are non-synchronous and, therefore, the timing of SPB re-duplication in wild type cells varies. As stated above, WT_1 cells may contain re-duplicating SPBs, whereas WT_2 and WT_3 intensity distributions are similar to those of c*dc14-1,* where SPBs are unduplicated (Fig. 5. 2. 1D).

A

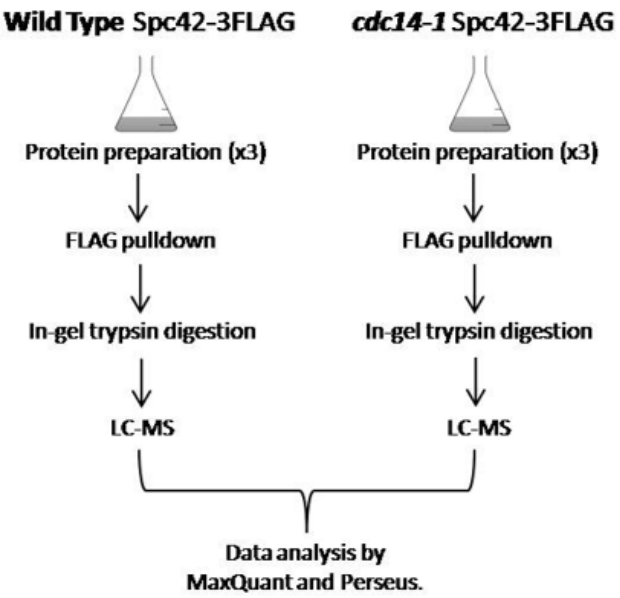

B

	Wild Type			*cdc14-1*			
	WT_1	WT_2	WT_3	CDC14_1	CDC14_2	CDC14_3	Counts
1	+	+	+	+	+	+	202
2	+	+	+	+	+		1
3	+	+	+	+		+	2
4	+	+	+		+	+	11
5	+	+		+	+	+	4
6	+		+	+	+	+	2
7		+	+	+	+	+	32
8	+	+	+		+		2
9	+	+	+			+	1
10		+	+	+	+		2
11			+	+	+	+	3
12		+		+	+	+	2
13	+			+	+	+	1
14	+	+		+	+		1
15	+	+			+	+	1
16	+		+	+	+		2
17		+	+		+	+	32
18	+		+		+	+	1
19		+	+	+		+	2
20	+	+			+		1
21			+		+	+	11
22		+	+		+		4
23		+	+			+	10
24			+	+		+	1
25			+	+	+		2
26		+			+	+	6
27				+	+	+	2
28	+	+	+				1
29	+				+	+	2
30	+		+			+	1
31		+			+		9
32			+			+	15
33					+	+	8
34			+		+		7
35		+				+	3
36	+				+		3
37	+		+				1
38		+	+				3
39				+		+	1
40						+	32
41					+		52
42				+			6
43			+				111
44		+					37
45	+						87
46							70

C

No. of columns	No. of proteins
0	70
1	325
2	50
3	41
4	50
5	52
6	202

Figure 5.2.1: LFQ Proteomic analysis of SPB composition and environment in Wild Type and *cdc14-1* cells. (A) Schematic representation of experiment. Wild type (AM11444) and *cdc14-1* (AM11443) cells containing *SPC42-3FLAG* were induced to sporulate. Cells were harvested after 4h growth for immunoprecipitation of Spc42-3FLAG. Peptides were generated by in-gel trypsin digestion and LC-MS data sets for 3 biological replicas was analysed using MaxQuant software. Statistical analysis of relative LFQ intensity output was carried out using Perseus. (B-C) Numeric venn diagrams of protein occurrence in data sets. Protein occurrence combinations (B) and totals (C) in expression columns reveal shared and unique proteins identified in grouped conditions. (D) Muti-scatter plots of log2 transformed intensity data compares biological replicas in both Wild Type and *cdc14-1* conditions. (E) Volcano plot shows –log of P values versus ratio of Wild Type/c*dc14-1* for all 254 proteins in >5 columns. No significant change in composition and environment is observed between Wild Type and *cdc14-1* SPBs. (FDR = 0.05, s0 = 1).

Red = SPB components. Blue = Cdc14. Green = Bfa1/Bub2

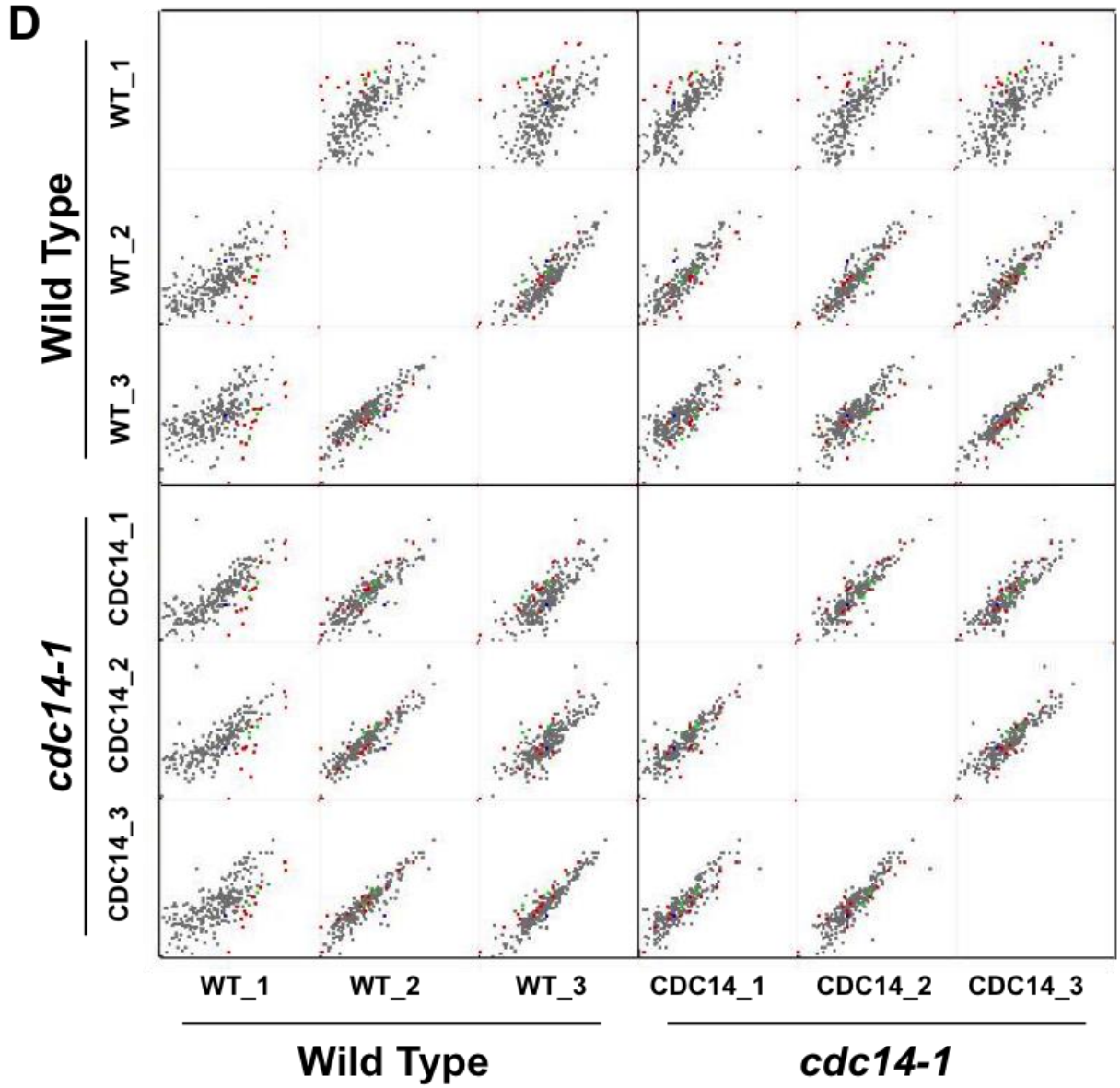
D
Wild Type
cdc14-1
WT_1
WT_2
WT_3
CDC14_1
CDC14_2
CDC14_3
Wild Type
cdc14-1

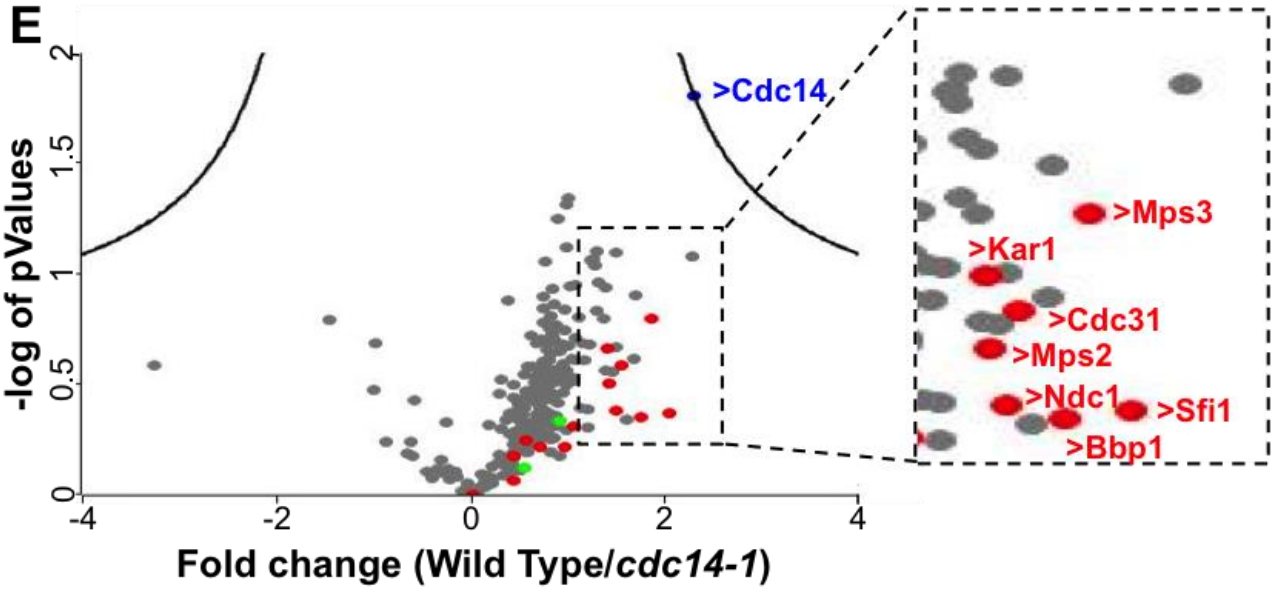
E
-log of pValues
Fold change (Wild Type/cdc14-1)
>Cdc14
>Mps3
>Kar1
>Cdc31
>Mps2
>Ndc1
>Sfi1
>Bbp1

5.2.2 Reduced Sfi1 in meiosis prevents SPB re-duplication

Since Cdc14 activity is required for Sfi1-dependent half-bridge elongation, it is possible that depletion of Sfi1 during meiosis would result in a c*dc14-1*-like phenotype. Without the accumulation of Sfi1 in prophase II, SPB re-duplication would not be initiated. To test this hypothesis, I constructed an Sfi1 meiotic null strain by putting *SFI1* under the control of the Clb2 promoter. *CLB2* is not expressed in meiosis, and this mechanism has been used previously for *cdc55mn* and *cdc20mn* strains.

I analysed SPB duplication in meiotic wild type and *sfi1mn c*ells by counting Spc42-tdTomato foci per cell. The depletion of Sfi1 during meiosis was confirmed via western blotting of 3HA-Sfi1. After 1h in sporulation media, Sfi1 is reduced ~46% and, by 3h in meiosis, it is completely undetectable (Fig. 5. 2. 2A). The percentages of binucleates and tetranucleates recorded at regular time points enabled monitoring of cell cycle progression. When Sfi1 is depleted, ~35% of cells arrest after meiosis I as binucleates (Fig. 5. 2. 2B). A further 9% of cells progress through meiosis II to form tetranucleates. The efficiency of tetranucleate formation is drastically impaired when compared to the wild type situation, which contain >82% tetranucleates after 10h in meiosis. Furthermore, tetranucleate production is severely delayed in *sfi1mn* cells, as they are only observed from 8h compared to ~4.5h in wild type cells.

The binucleates formed by *sfi1mn* cells contain two SPB foci (Fig. 5. 2. 2B). When these foci observed in binucleate *sfi1mn* cells were quantified, the total SPB F_i in cells is ~3.5 a.u. (Fig. 5. 2. 2C). This corresponds to the 3.9 a.u F_i observed in wild

type cells when two SPBs are present (Fig. 4. 2. 2. 2). This value is also roughly half the total quantitative SPB intensity per cell measured when four SPB foci are within wild type cells (~6.9 a.u.). Taken together, this data strongly suggests that depletion of Sfi1 during meiosis prevents SPB re-duplication after meiosis I.

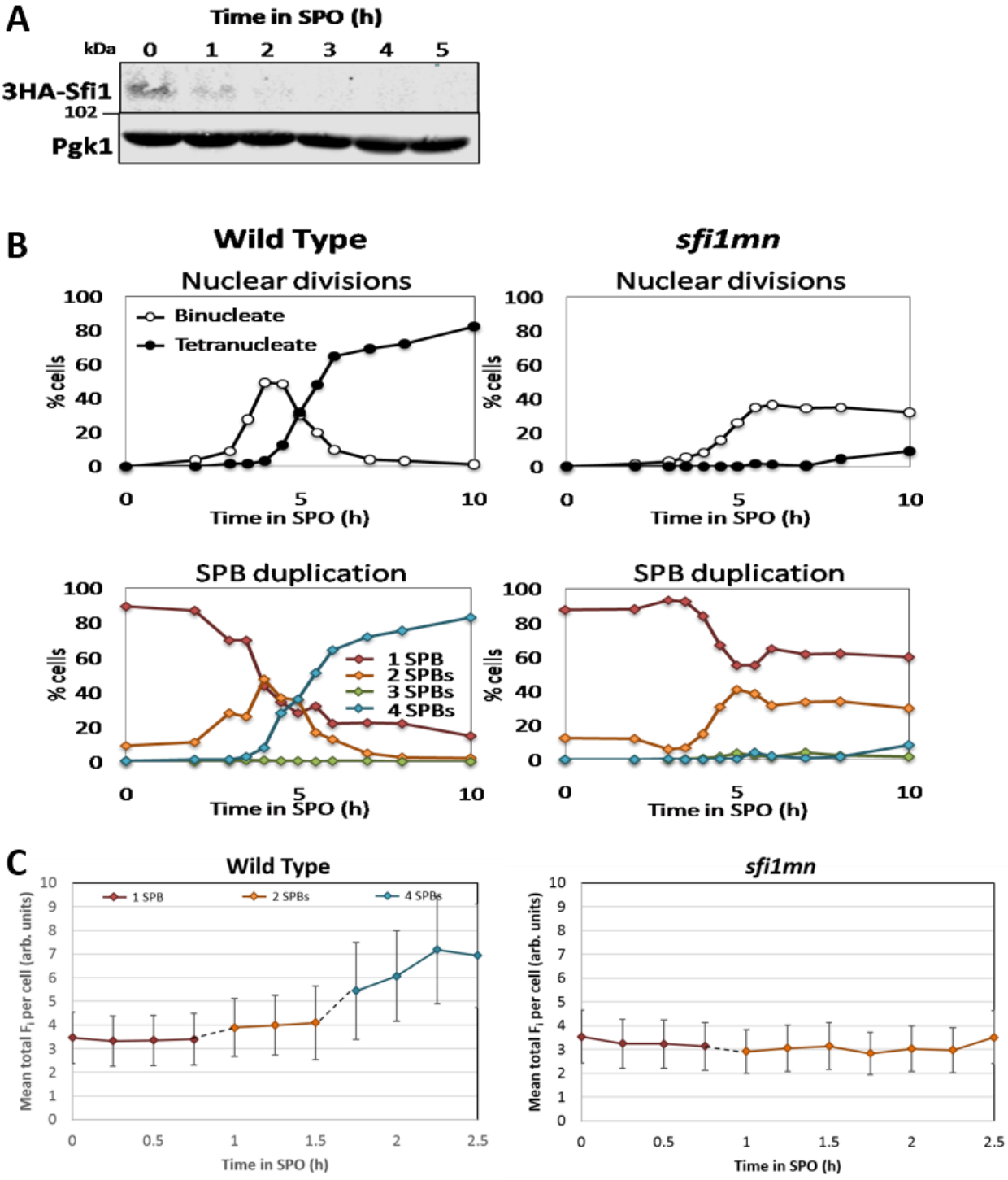

Figure 5.2.2: Depletion of Sfi1 in meiosis prevents re-duplication of SPBs. (A-C) Wild type (AM13989) and *sfi1mn* (AM16108) cells containing *SPC42-tomato* were induced to sporulate. (A) 3HA-Sfi1 andPgk1 (loading control) in *sfi1mn* cells were analysed by western blot to show *pCLB2-3HA-SFI1* expression. (B) The percentages of binucleate and tetranucleate cells were determined. The percentages of cells that contained one, two, three and four SPB foci per cell were also calculated. n = 200 cells. (C) *sfi1mn* meiotic cells were imaged at 15 minute intervals for a total of 12 hours using microfluidics. Individual SPB foci were quantified and mean total SPB fluorescence intensity (F_i) per cell was plotted, with error bars representing standard error. n = 10 cells. Wild type microfluidics experiment from Fig. 4. 2.2. 2.A

5.2.3 Cdc14 activity is required for the phospho-regulation of Sfi1

The abundance of Sfi1 fails to increase at SPBs following meiosis I when Cdc14 activity is impaired. This suggests that Cdc14 may be required to dephosphorylate Sfi1 in late anaphase I, thus relicensing SPBs for the next round of SPB duplication by enabling the assembly of the full-bridge structure. This theory would predict that Sfi1 is hyperphosphorylated in *cdc14-1* cells, when Cdc14 activity is impaired. Conversely, Sfi1 might be hypophosphorylated when Cdc14 is ectopically released in *cdc55mn* cells.

To investigate the phosphorylation state of Sfi1, I tagged the half-bridge component and monitored it throughout meiosis. Protein samples were run on a 6% SDS gel to better resolve any motility shift in Sfi1, which is characteristic of phospho-regulation. ECL development of western blots was used in preference to LiCor® due to the low abundance of Sfi1 in cells. Despite the numerous advantages of LiCor® over ECL, the latter is more sensitive and so better for detection of faint protein signal.

In wild type cells, Sfi1-6HA (~120 kDa) is present at low levels throughout meiosis (Fig. 5. 2. 3). Multiple migration bands are observed at 0.45 h after release from GAL-NDT80 block, which corresponds to the appearance of metaphase I spindles. Since SPBs separate prior to metaphase I, this observation is consistent with the idea that Sfi1 phosphorylation is required for cleavage of the full-bridge structure between SPBs. Sfi1 then accumulates in cells after exit from meiosis at 3 h, which is indicated by the disassembly of anaphase II spindles.

When Cdc14 activity is impaired, the protein bands observed for Sfi1 appear distinctly thicker from 1.45 h compared to those seen on the wild type protein gel (Fig. 5. 2. 3). This is likely due to the appearance of phosphorylated Sfi1, which migrates slower in the SDS gel. The timing of this detectable shift corresponds with the appearance of anaphase I spindles, suggesting that Sfi1 is hyperphosphorylated in *cdc14-1* cells from anaphase I onwards. Additionally, upward smearing of Sfi1 is prominent from 3 h, further arguing that impairment of Cdc14 activity prevents the dephosphorylation of Sfi1 during meiosis.

In *cdc55mn* cells, Sfi1 band thickness appears comparable to the wild type situation. There is no evidence of Sfi1 band shifting upwards, nor are there phosphorylation smears above the proteins bands, except perhaps at 5.30 h. It therefore seems that the early release of Cdc14 from inhibition prevents the hyperphosphorylation of Sfi1 seen in *cdc14-1* cells.

Whilst it is possible that the motility shift detected in *cdc14-1* is due to a posttranslational modification other than phosphorylation, the fact that it appears as a consequence of phosphatase inactivation strongly implies a role for Cdc14 in the phospho-regulation of Sfi1 during meiosis.

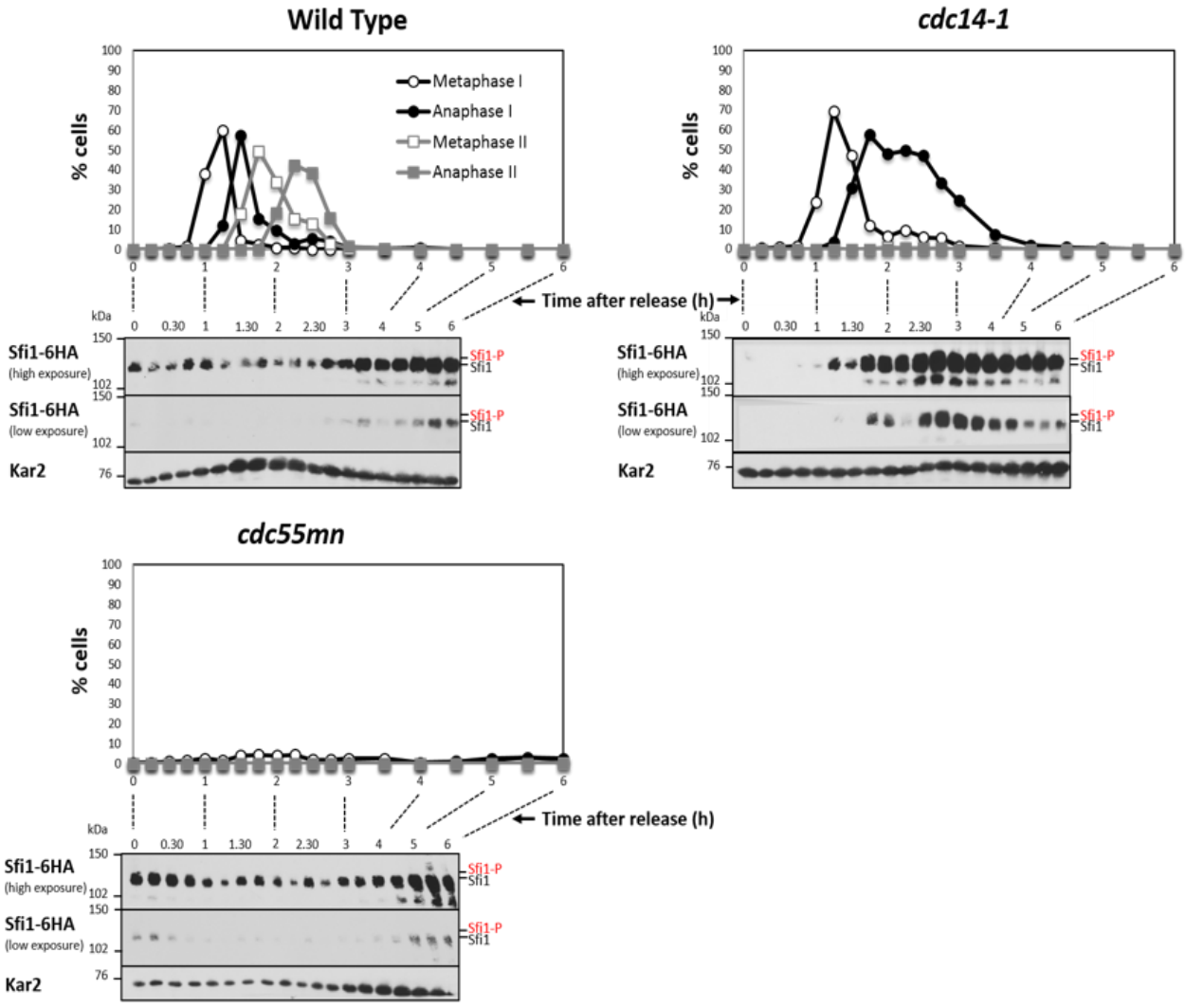

Figure 5.2.3: Impairment of Cdc14 activity results in hyperphosphorylation of Sfi1 . Wild type (AM12329) *cdc14-1* (12330) and cdc55*mn* (AM16021) cells containing *SFI1-6HA* were induced to sporulate and released from *GAL-NDT80 block.* The percentage of cells with indicated spindle morphology was determined to show meiotic progression. α-HA and α-KAR2 immunoblots show Sfi1 protein abundance and loading control. When Cdc14 activity is impaired, multiple migration bands are observed for Sfi1 from anaphase I onwards. Blots and spindle counts are representative.

5.3 Discussion

I had previously verified that Cdc14 is required for re-duplication of SPBs after meiosis I (Section 4. 2. 2). However, the exact mechanism of SPB regulation had yet to be determined. The mitotic SPB duplication pathway is regulated at many stages by CDKs (reviewed by Jaspersen and Winey 2004), and therefore it is plausible that Cdc14 is required to counteract CDK phosphorylation after meiosis I in order for progression through a second meiotic SPB duplication event. EM analysis of SPBs gave no indication of half-bridge elongation in *cdc14-1* cells after anaphase I (Fig. 4. 2. 2. 3A-B). It is therefore likely that the initiation of SPB re-duplication via half-bridge extension is a target of Cdc14 regulation.

I hypothesised that Cdc14 was required for the phospho-regulation of Sfi1 during meiosis. When Cdc14 activity is impaired, I predicted that Sfi1 became hyperphosphorylated. Since phosphorylated Sfi1 is unable to correctly dimerise during mitosis (Avena, Burns et al. 2014, Elserafy, Saric et al. 2014), this hyperphosphorylated form of meiotic Sfi1 could prevent half-bridge elongation after meiosis I and therefore inhibit SPB re-duplication. Conversely, since dephosphorylation of Sfi1 is vital for full-bridge cleavage in mitosis (Avena, Burns et al. 2014, Elserafy, Saric et al. 2014), I anticipated that ectopic release of Cdc14 lead to hypophosphorylation of Sfi1. This could perhaps explain why duplicated but unseparated SPBs are observed in *cdc55mn* cells.

To test this theory, I investigated the role of Cdc14 on SPB half-bridge extension during meiosis. Using LFQ proteomics, I identified a number of proteins that were reduced at SPBs when Cdc14 activity was impaired. These included all SPB

half-bridge components and SPB periphery proteins, suggesting that *cdc14-1* cells are unable to initiate SPB re-duplication via half-bridge elongation. I demonstrated that reduced Sfi1 protein abundance within cells prevents the re-duplication of SPBs during meiosis. Additionally, I investigated the effect of Cdc14 on Sfi1 phosphorylation. I found that impairment of Cdc14 activity resulted in multiple migrating forms of Sfi1, which is likely due to hyperphosphorylation. Furthermore, I observed that this posttranslational modification of Sfi1 is absent in cells when Cdc14 is active early. These data indicate that Cdc14 is required for the phospho-regulation of Sfi1, and suggests that this regulation is what enables re-duplication of SPBs after meiosis I and SPB separation prior to metaphase I.

This analysis of SPB duplication in *cdc14-1* and *cdc55mn* cells is currently incomplete. Without phosphatase treatment of protein samples, I cannot rule of the possibility that the motility shift observed for Sfi1 in *cdc14-1* cells is due to phosphorylation and not another type of posttranslational modification. However, the fact that the shift is only observed when Cdc14 activity is impaired and not in either wild type or *cdc55mn* situations strongly implies phospho-regulation. I attempted to address this issue by immunoprecipitating Sfi1 in wild type and *cdc14-1* cells, and treating IPs with phosphatase. Unfortunately, the low abundance of Sfi1 within cells proved to make this experiment difficult. Since Cdc14 has been shown in mitosis to regulate the phosphorylation state of Sfi1 (Avena, Burns et al. 2014, Elserafy, Saric et al. 2014), I am fairly confident to conclude that the modification made to Sfi1 is phosphorylation.

Within this study, I have not shown a direct link between Sfi1 phospho-regulation and SPB duplication/separation during meiosis. Whilst I have indicated that *cdc55mn* cells contain SPBs that are unable to cleave their full-bridge structures and that ectopic release of Cdc14 prevents hyperphosphorylation of Sfi1, I have not shown that hypophosphorylation of Sfi1 prevents SPB separation. This connection has been drawn from the data and from work carried out in mitotic cells. I am currently in the process of carrying out these crucial experiments.

Chapter 6

Final Discussion

6. Final Discussion

As discussed previously in this work, meiosis is the process through which four haploid gametes are formed from a diploid progenitor cell (reviewed by Marston and Amon 2004). It consists of one round of DNA duplication followed by two consecutive rounds of chromosome segregation, where homologous chromosomes and then sister chromatids segregate in meiosis I and meiosis II respectively. Unlike in mitosis, where each round of chromosome segregation is preceded by a DNA replication phase, an intervening round of S-phase does not occur between meiosis I and meiosis II. As a result, daughter cells exhibit a reduction in chromosome number with respect to the parental cell. The meiosis I to meiosis II transition is therefore a unique event that must be properly regulated to ensure the accurate segregation of chromosomes during meiosis.

Despite a lack of DNA re-replication between meiosis I and meiosis II, the molecular machinery required for chromosome segregation must be re-duplicated within cells. A single meiosis I spindle is needed to segregate homologous chromosomes in anaphase I. This spindle must then disassemble before the formation of two meiosis II spindles in metaphase II for the accurate segregation of sister chromatids. Both DNA replication and microtubule dynamics are regulated by cyclin-CDK activity (Ubersax, Woodbury et al. 2003, Loog and Morgan 2005). CDKs must be down-regulated at meiosis I exit to enable the disassembly of anaphase I spindles. On the other hand, some maintained CDK activity is required to prevent the re-firing of DNA origins of replication. These combined observations hint towards the need for partial down-regulation of CDKs at the meiosis I to meiosis II transition, sufficient enough to be permissive for spindle disassembly but incomplete to prohibit DNA re-replication.

The protein phosphatase, Cdc14, has been implicated in the meiosis I to meiosis II transition (Buonomo, Rabitsch et al. 2003, Marston, Lee et al. 2003). Cdc14 activity is required for the assembly of two meiosis II spindles despite the unhindered disassembly of meiosis I spindles (Bizzari and Marston 2011). Additionally, Cdc14 plays a role in CDK inactivation during mitotic exit. This CDK down-regulation is achieved through the degradation of cyclins and the stabilisation of the CDK inhibitor, Sic1 (Knapp, Bhoite et al. 1996, Toyn, Johnson et al. 1997, Verma, Annan et al. 1997, Visintin, Craig et al. 1998, Zachariae, Schwab et al. 1998, Jaspersen, Charles et al. 1999). Cdc14 has also been shown to reverse CDK-dependent phosphorylation events (Bloom, Cristea et al. 2011, Bremmer, Hall et al. 2012, Avena, Burns et al. 2014).

In the first part of this study, I aimed to determine the role of Cdc14 in meiosis I to meiosis II transition, attempting initially to address whether it was involved in the partial down-regulation of CDKs. I showed that Cdc14 is not required for cyclin degradation during meiosis. Clb1, Clb3, Clb4 and Clb5 cyclin proteolysis is unaffected when Cdc14 activity is impaired (Fig. 3. 2. 3. 2A-D). Furthermore, the early activation of Cdc14 in *cdc55mn* mutants does not result in the premature degradation of meiotic cyclins. This suggests that, if Cdc14 is required to regulate CDK activity, it is not via cyclin proteolysis. Since Clb3 and Clb5-CDK activity correlates to protein abundance (Carlile and Amon 2008), it would appear that Cdc14 does not regulate either of these CDKs. Clb1 and Clb4-CDK activities are regulated by mechanisms distinct from cyclin degradation. The posttranslational modification of Clb1, believed to be an active phosphorylated form, is observed in *cdc14-1* cells (Fig. 3. 2. 3. 1A) indicating that the phosphatase likely is not regulating Clb1-CDK either. The mechanism for Clb4-CDK

down-regulation has yet to be determined but since Clb4-CDK is active in meiosis II, it is probable that Cdc14 is not essential for its regulation at meiosis I exit. I therefore concluded that Cdc14 was not required for the down-regulation of CDKs at the meiosis I to meiosis II transition.

Next, I set out to identify potential substrates of Cdc14 during meiosis I exit. I used a non-biased approach where I pulled down Cdc14 in meiotic cells. Cells were staged so that binucleates but not tetranucleates were present in harvested populations (Fig. 4. 2. 1. 1A). The IP revealed that Cdc14 interacts with SPB components when it is not bound to its inhibitor, Cfi1/Net1 (Fig. 4. 2. 1. 1D). I further showed that Cdc14 localises to SPBs in anaphase I (Fig. 4. 2. 1. 3), and that impairment of Cdc14 activity or release prevents the appearance of four SPBs during meiosis (Fig. 4. 2. 2. 1). Through quantitative fluorescence (Fig. 4. 2. 2. 2A-B) and EM analysis (Fig. 4. 2. 2. 3A-B), I determined that *cdc14-1* mutants are unable to re-duplicate their SPBs after meiosis I. In contrast, the early activation of Cdc14 impedes SPB separation prior to metaphase I in *cdc55mn* cells (Fig. 4. 2. 2. 3C). These results suggested a role for Cdc14 in the SPB duplication pathway.

In order to build a molecular mechanism for Cdc14-dependent regulation of the SPB duplication pathway, I used LFQ proteomics to pinpoint the precise stage of SPB duplication affected in *cdc14-1* mutants. Through comparison of wild type and *cdc14-1* samples, I identified half-bridge components, Sfi1, Mps3, Cdc31 and Kar2, and SPB periphery proteins, Mps2, Ndc1 and Bbp1, as reduced at SPBs when Cdc14 activity is impaired (Fig. 5. 2. 1. 1E). Furthermore, I found that reduced Sfi1 protein abundance prevented the re-duplication of SPBs during meiosis (Fig. 5. 2. 2A-C). Through western

blot analysis, I determined that Cdc14 is required for the phospho-regulation of Sfi1. A putative hyperphosphorylated form of Sfi1 accumulates in *cdc14-1* cells (Fig. 5. 2. 3). This form is not observed when Cdc14 is active, either in wild type or *cdc55mn* cells. I speculated that Cdc14 is required during the meiosis I to meiosis II transition to dephosphorylate Sfi1, so that cells can initiate SPB re-duplication in meiosis II via half bridge elongation. Additionally, the activity of Cdc14 must be tightly regulated in early meiosis. Ectopic release of Cdc14 in *cdc55mn* mutants prevents the phosphorylation of Sfi1, which appears to be required for SPB separation via half-bridge cleavage.

6.1 Future Plans

6.1.1 Does phospho-regulation of Sfi1 affect SPB duplication/separation in meiosis?

The phospho-regulation of Sfi1 by Cdc14 appears to be vital for control of the SPB duplication pathway. However, a direct link between SPB duplication/separation and Sfi1 phosphorylation has yet to be shown in meiosis. A number of phospho-mimetic and phospho-null forms of Sfi1 were generated by (Avena, Burns et al. 2014) for SPB analysis during mitosis. To fully confirm that the SPB duplication defect observed in Cdc14-impaired cells was the result of Sfi1 hyperphosphorylation, I would need to investigate the affect of introducing an unphosphorylatable Sfi1 mutant into *cdc14-1* cells. Similarly, the integration of hyperphosphorylated form of Sfi1 in *cdc55mn* cells could help determine if Sfi1 phosphorylation is vital for SPB half-bridge cleavage. These Sfi1 phospho-forms were received from Mark Winey and could be transformed into wild type and mutant diploids containing the SPB marker, Spc42-tdTomato, to monitor their effect of SPB duplication throughout meiosis.

6.1.2 Why is Cdc14 asymmetrically localised during anaphase I?

The localisation of Cdc14 to SPBs appears to play a role in the timing of SPB duplication (Fig. 4. 2. 3. 2). However, why this localisation is asymmetric in anaphase I is unclear. The GTPase activating protein, Bfa1-Bub2, has been identified as important for Cdc14-SPB co-localisation (Fig. 4. 2. 3. 1A-B) despite Bfa1 localising to SPBs symmetrically in anaphase I (Fig. 4. 2. 3. 3A-B). Since the localisation of Bfa1 is not asymmetric, perhaps GAP activity is distinctly regulated at different poles. To gain a better understanding of the role of GAP activity on Cdc14 localisation, a GAP inactive Bub2 variant (Bub2-Q123L) (Scarfone, Venturetti et al. 2015) received from Simonetta Piatti could be introduced into cells containing Cdc14-GFP.

6.2 Conclusion

The aim of this study was to determine the role of Cdc14 during the meiosis I to meiosis II transition. My findings suggest that Cdc14 may be required to phospho-regulate the SPB half bridge, Sfi1 (Fig. 6. 2). When Cdc14 activity is impaired, SPBs are unable to re-duplicate. Sfi1 appears to be hyper-phosphorylated in *cdc14-1* cells, which could perhaps prevent the elongation of the half-bridge structure since phosphorylate Sfi1 is unable to dimerise in mitosis (Avena, Burns et al. 2014). Premature activation of Cdc14 prevents the separation of SPBs prior to metaphase I. Sfi1 appears unphosphorylated. Since Sfi1 phosphorylation is required to cleave the assembled full-bridge between duplicated SPBs (Avena, Burns et al. 2014), inhibition of Sfi1 phosphorylation therefore prevents this breakage.

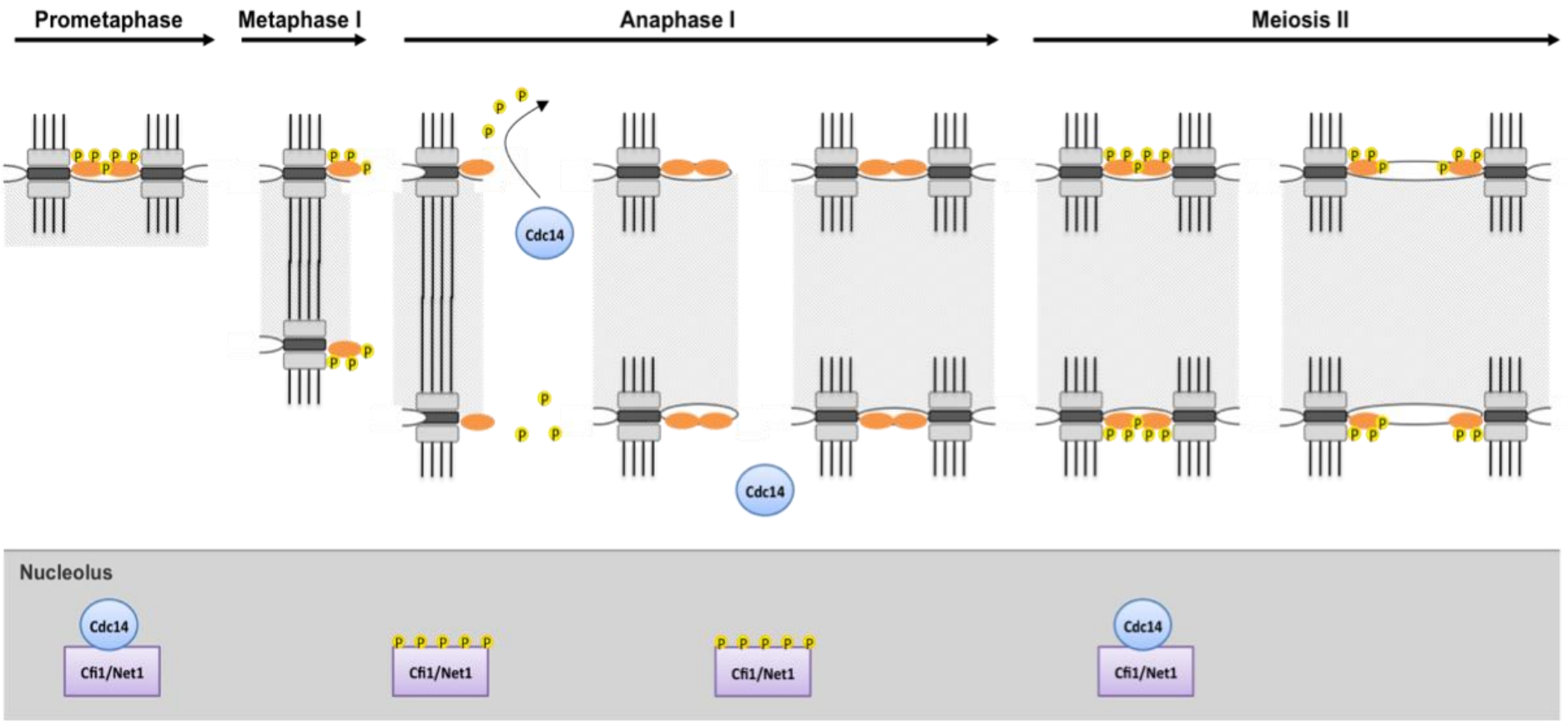

Figure 6.2: Model for Cdc14 regulation of Sfi1 during meiosis. Two duplicated SPBs are attached to one another in prometaphase by a full-bridge structure consisting primarily of dimerised Sfi1 (orange), an interaction stabilised by Cdc31. Cdc14 is sequestered in the nuclelous, preventing the dephosphorylation of Sfi1. Sfi1 phosphorylation (yellow) results in full-bridge cleavage, enabling the separation of SPBs in metaphase I. In anaphase I, release of Cdc14 from inhibition results in Sfi1 dephosphorylation. Sfi1 dimerisation occurs and two half-bridge structures elongate, initiating SPB re-duplication. When Cdc14 is resequestered in meiosis I exit, the full-bridges are severed, resulting in the separation of four distinct SPBs in meiosis II.

Bibliography

Bibliography

Adams, I. R. and J. V. Kilmartin (1999). "Localization of core spindle pole body (SPB) components during SPB duplication in Saccharomyces cerevisiae." J Cell Biol **145**(4): 809-823.

Adams, I. R. and J. V. Kilmartin (2000). "Spindle pole body duplication: a model for centrosome duplication?" Trends Cell Biol **10**(8): 329-335.

Alexandru, G., F. Uhlmann, K. Mechtler, M. A. Poupart and K. Nasmyth (2001). "Phosphorylation of the cohesin subunit Scc1 by Polo/Cdc5 kinase regulates sister chromatid separation in yeast." Cell **105**(4): 459-472.

Amon, A., S. Irniger and K. Nasmyth (1994). "Closing the cell cycle circle in yeast: G2 cyclin proteolysis initiated at mitosis persists until the activation of G1 cyclins in the next cycle." Cell **77**(7): 1037-1050.

Amon, A., M. Tyers, B. Futcher and K. Nasmyth (1993). "Mechanisms that help the yeast cell cycle clock tick: G2 cyclins transcriptionally activate G2 cyclins and repress G1 cyclins." Cell **74**(6): 993-1007.

Anderson, V. E., J. Prudden, S. Prochnik, T. H. Giddings, Jr. and K. G. Hardwick (2007). "Novel sfi1 alleles uncover additional functions for Sfi1p in bipolar spindle assembly and function." Mol Biol Cell **18**(6): 2047-2056.

Attner, M. A. and A. Amon (2012). "Control of the mitotic exit network during meiosis." Mol Biol Cell **23**(16): 3122-3132.

Avena, J. S., S. Burns, Z. Yu, C. C. Ebmeier, W. M. Old, S. L. Jaspersen and M. Winey (2014). "Licensing of yeast centrosome duplication requires phosphoregulation of sfi1." PLoS Genet **10**(10): e1004666.

Azzam, R., S. L. Chen, W. Shou, A. S. Mah, G. Alexandru, K. Nasmyth, R. S. Annan, S. A. Carr and R. J. Deshaies (2004). "Phosphorylation by cyclin B-Cdk underlies release of mitotic exit activator Cdc14 from the nucleolus." Science **305**(5683): 516-519.

Bardin, A. J. and A. Amon (2001). "Men and sin: what's the difference?" Nat Rev Mol Cell Biol **2**(11): 815-826.

Bardin, A. J., R. Visintin and A. Amon (2000). "A mechanism for coupling exit from mitosis to partitioning of the nucleus." Cell **102**(1): 21-31.

Baro, B., J. A. Rodriguez-Rodriguez, I. Calabria, M. L. Hernaez, C. Gil and E. Queralt (2013). "Dual Regulation of the mitotic exit network (MEN) by PP2A-Cdc55 phosphatase." PLoS Genet **9**(12): e1003966.

Barral, Y., S. Jentsch and C. Mann (1995). "G1 cyclin turnover and nutrient uptake are controlled by a common pathway in yeast." Genes Dev **9**(4): 399-409.

Baum, P., C. Furlong and B. Byers (1986). "Yeast gene required for spindle pole body duplication: homology of its product with Ca2+-binding proteins." Proc Natl Acad Sci U S A **83**(15): 5512-5516.

Benjamin, K. R., C. Zhang, K. M. Shokat and I. Herskowitz (2003). "Control of landmark events in meiosis by the CDK Cdc28 and the meiosis-specific kinase Ime2." Genes & development **17**(12): 1524-1539.

Berchowitz, L. E., A. S. Gajadhar, F. J. van Werven, A. A. De Rosa, M. L. Samoylova, G. A. Brar, Y. Xu, C. Xiao, B. Futcher, J. S. Weissman, F. M. White and A. Amon (2013). "A developmentally regulated translational control pathway establishes the meiotic chromosome segregation pattern." Genes Dev **27**(19): 2147-2163.

Berdougo, E., M. V. Nachury, P. K. Jackson and P. V. Jallepalli (2008). "The nucleolar phosphatase Cdc14B is dispensable for chromosome segregation and mitotic exit in human cells." Cell Cycle **7**(9): 1184-1190.

Bizzari, F. and A. L. Marston (2011). "Cdc55 coordinates spindle assembly and chromosome disjunction during meiosis." The Journal of cell biology **193**(7): 1213-1228.

Blat, Y. and N. Kleckner (1999). "Cohesins bind to preferential sites along yeast chromosome III, with differential regulation along arms versus the centric region." Cell **98**(2): 249-259.

Bloom, J., I. M. Cristea, A. L. Procko, V. Lubkov, B. T. Chait, M. Snyder and F. R. Cross (2011). "Global analysis of Cdc14 phosphatase reveals diverse roles in mitotic processes." The Journal of biological chemistry **286**(7): 5434-5445.

Bloom, J. and F. R. Cross (2007). "Multiple levels of cyclin specificity in cell-cycle control." Nat Rev Mol Cell Biol **8**(2): 149-160.

Bouhlel, I. B., M. Ohta, A. Mayeux, N. Bordes, F. Dingli, J. Boulanger, G. Velve Casquillas, D. Loew, P. T. Tran, M. Sato and A. Paoletti (2015). "Cell cycle control

of spindle pole body duplication and splitting by Sfi1 and Cdc31 in fission yeast." J Cell Sci.

Brar, G. A., B. M. Kiburz, Y. Zhang, J. E. Kim, F. White and A. Amon (2006). "Rec8 phosphorylation and recombination promote the step-wise loss of cohesins in meiosis." Nature **441**(7092): 532-536.

Bremmer, S. C., H. Hall, J. S. Martinez, C. L. Eissler, T. H. Hinrichsen, S. Rossie, L. L. Parker, M. C. Hall and H. Charbonneau (2012). "Cdc14 phosphatases preferentially dephosphorylate a subset of cyclin-dependent kinase (Cdk) sites containing phosphoserine." J Biol Chem **287**(3): 1662-1669.

Buonomo, S. B., K. P. Rabitsch, J. Fuchs, S. Gruber, M. Sullivan, F. Uhlmann, M. Petronczki, A. Toth and K. Nasmyth (2003). "Division of the nucleolus and its release of CDC14 during anaphase of meiosis I depends on separase, SPO12, and SLK19." Developmental Cell **4**(5): 727-739.

Byers, B. and L. Goetsch (1974). "Duplication of spindle plaques and integration of the yeast cell cycle." Cold Spring Harb Symp Quant Biol **38**: 123-131.

Calzada, A., M. Sanchez, E. Sanchez and A. Bueno (2000). "The stability of the Cdc6 protein is regulated by cyclin-dependent kinase/cyclin B complexes in Saccharomyces cerevisiae." J Biol Chem **275**(13): 9734-9741.

Carlile, T. M. and A. Amon (2008). "Meiosis I is established through division-specific translational control of a cyclin." Cell **133**(2): 280-291.

Caydasi, A. K., B. Ibrahim and G. Pereira (2010). "Monitoring spindle orientation: Spindle position checkpoint in charge." Cell division **5**: 28.

Caydasi, A. K., M. Lohel, G. Grunert, P. Dittrich, G. Pereira and B. Ibrahim (2012). "A dynamical model of the spindle position checkpoint." Mol Syst Biol **8**: 582.

Caydasi, A. K., Y. Micoogullari, B. Kurtulmus, S. Palani and G. Pereira (2014). "The 14-3-3 protein Bmh1 functions in the spindle position checkpoint by breaking Bfa1 asymmetry at yeast centrosomes." Mol Biol Cell **25**(14): 2143-2151.

Caydasi, A. K. and G. Pereira (2009). "Spindle alignment regulates the dynamic association of checkpoint proteins with yeast spindle pole bodies." Dev Cell **16**(1): 146-156.

Cenamor, R., J. Jimenez, V. J. Cid, C. Nombela and M. Sanchez (1999). "The budding yeast Cdc15 localizes to the spindle pole body in a cell-cycle-dependent manner." Molecular cell biology research communications : MCBRC **2**(3): 178-184.

Chen, C. T., M. P. Peli-Gulli, V. Simanis and D. McCollum (2006). "S. pombe FEAR protein orthologs are not required for release of Clp1/Flp1 phosphatase from the nucleolus during mitosis." J Cell Sci **119**(Pt 21): 4462-4466.

Cho, H. P., Y. Liu, M. Gomez, J. Dunlap, M. Tyers and Y. Wang (2005). "The dual-specificity phosphatase CDC14B bundles and stabilizes microtubules." Mol Cell Biol **25**(11): 4541-4551.

Chu, S. and I. Herskowitz (1998). "Gametogenesis in yeast is regulated by a transcriptional cascade dependent on Ndt80." Mol Cell **1**(5): 685-696.

Ciosk, R., W. Zachariae, C. Michaelis, A. Shevchenko, M. Mann and K. Nasmyth (1998). "An ESP1/PDS1 complex regulates loss of sister chromatid cohesion at the metaphase to anaphase transition in yeast." Cell **93**(6): 1067-1076.

Clement, A., L. Solnica-Krezel and K. L. Gould (2011). "The Cdc14B phosphatase contributes to ciliogenesis in zebrafish." Development **138**(2): 291-302.

Clift, D., F. Bizzari and A. L. Marston (2009). "Shugoshin prevents cohesin cleavage by PP2A(Cdc55)-dependent inhibition of separase." Genes & development **23**(6): 766-780.

Cohen-Fix, O., J. M. Peters, M. W. Kirschner and D. Koshland (1996). "Anaphase initiation in Saccharomyces cerevisiae is controlled by the APC-dependent degradation of the anaphase inhibitor Pds1p." Genes Dev **10**(24): 3081-3093.

Crasta, K., H. H. Lim, T. H. Giddings, M. Winey and U. Surana (2008). "Inactivation of Cdh1 by synergistic action of Cdk1 and polo kinase is necessary for proper assembly of the mitotic spindle." Nature cell biology **10**(6): 665-675.

Crasta, K. and U. Surana (2006). "Disjunction of conjoined twins: Cdk1, Cdh1 and separation of centrosomes." Cell Division **1**.

Cueille, N., E. Salimova, V. Esteban, M. Blanco, S. Moreno, A. Bueno and V. Simanis (2001). "Flp1, a fission yeast orthologue of the s. cerevisiae CDC14 gene, is not required for cyclin degradation or rum1p stabilisation at the end of mitosis." J Cell Sci **114**(Pt 14): 2649-2664.

Culotti, J. and L. H. Hartwell (1971). "Genetic control of the cell division cycle in yeast. 3. Seven genes controlling nuclear division." Exp Cell Res **67**(2): 389-401.

D'Amours, D. and A. Amon (2004). "At the interface between signaling and executing anaphase--Cdc14 and the FEAR network." Genes & development **18**(21): 2581-2595.

D'Amours, D., F. Stegmeier and A. Amon (2004). "Cdc14 and condensin control the dissolution of cohesin-independent chromosome linkages at repeated DNA." Cell **117**(4): 455-469.

Dahmann, C. and B. Futcher (1995). "Specialization of B-type cyclins for mitosis or meiosis in S. cerevisiae." Genetics **140**(3): 957-963.

Dalton, S. (1998). "Cell cycle control of chromosomal DNA replication." Immunol Cell Biol **76**(5): 467-472.

Darieva, Z., A. Pic-Taylor, J. Boros, A. Spanos, M. Geymonat, R. J. Reece, S. G. Sedgwick, A. D. Sharrocks and B. A. Morgan (2003). "Cell cycle-regulated transcription through the FHA domain of Fkh2p and the coactivator Ndd1p." Curr Biol **13**(19): 1740-1745.

Dirick, L., L. Goetsch, G. Ammerer and B. Byers (1998). "Regulation of meiotic S phase by Ime2 and a Clb5,6-associated kinase in Saccharomyces cerevisiae." Science **281**(5384): 1854-1857.

Dischinger, S., A. Krapp, L. Xie, J. R. Paulson and V. Simanis (2008). "Chemical genetic analysis of the regulatory role of Cdc2p in the S. pombe septation initiation network." J Cell Sci **121**(Pt 6): 843-853.

Donaldson, A. D. and J. V. Kilmartin (1996). "Spc42p: a phosphorylated component of the S. cerevisiae spindle pole body (SPD) with an essential function during SPB duplication." J Cell Biol **132**(5): 887-901.

Dryden, S. C., F. A. Nahhas, J. E. Nowak, A. S. Goustin and M. A. Tainsky (2003). "Role for human SIRT2 NAD-dependent deacetylase activity in control of mitotic exit in the cell cycle." Mol Cell Biol **23**(9): 3173-3185.

Duro, E. and A. L. Marston (2015). "From equator to pole: splitting chromosomes in mitosis and meiosis." Genes Dev **29**(2): 109-122.

Elsasser, S., F. Lou, B. Wang, J. L. Campbell and A. Jong (1996). "Interaction between yeast Cdc6 protein and B-type cyclin/Cdc28 kinases." Mol Biol Cell **7**(11): 1723-1735.

Elserafy, M., M. Saric, A. Neuner, T. C. Lin, W. Zhang, C. Seybold, L. Sivashanmugam and E. Schiebel (2014). "Molecular mechanisms that restrict yeast centrosome duplication to one event per cell cycle." Curr Biol **24**(13): 1456-1466.

Epstein, C. B. and F. R. Cross (1992). "CLB5: a novel B cyclin from budding yeast with a role in S phase." Genes Dev **6**(9): 1695-1706.

Faust, A. M., C. C. Wong, J. R. Yates, 3rd, D. G. Drubin and G. Barnes (2013). "The FEAR protein Slk19 restricts Cdc14 phosphatase to the nucleus until the end of anaphase, regulating its participation in mitotic exit in Saccharomyces cerevisiae." PLoS One **8**(9): e73194.

Feldman, R. M., C. C. Correll, K. B. Kaplan and R. J. Deshaies (1997). "A complex of Cdc4p, Skp1p, and Cdc53p/cullin catalyzes ubiquitination of the phosphorylated CDK inhibitor Sic1p." Cell **91**(2): 221-230.

Fernius, J. and K. G. Hardwick (2007). "Bub1 kinase targets Sgo1 to ensure efficient chromosome biorientation in budding yeast mitosis." PLoS genetics **3**(11): e213.

Fink, A. L. (1998). "Protein aggregation: folding aggregates, inclusion bodies and amyloid." Folding & design **3**(1): R9-23.

Fitch, I., C. Dahmann, U. Surana, A. Amon, K. Nasmyth, L. Goetsch, B. Byers and B. Futcher (1992). "Characterization of four B-type cyclin genes of the budding yeast Saccharomyces cerevisiae." Mol Biol Cell **3**(7): 805-818.

Fu, C., J. J. Ward, I. Loiodice, G. Velve-Casquillas, F. J. Nedelec and P. T. Tran (2009). "Phospho-regulated interaction between kinesin-6 Klp9p and microtubule bundler Ase1p promotes spindle elongation." Dev Cell **17**(2): 257-267.

Funabiki, H., H. Yamano, K. Kumada, K. Nagao, T. Hunt and M. Yanagida (1996). "Cut2 proteolysis required for sister-chromatid seperation in fission yeast." Nature **381**(6581): 438-441.

Furuno, N., M. Nishizawa, K. Okazaki, H. Tanaka, J. Iwashita, N. Nakajo, Y. Ogawa and N. Sagata (1994). "Suppression of DNA replication via Mos function during meiotic divisions in Xenopus oocytes." EMBO J **13**(10): 2399-2410.

Gambus, A., R. C. Jones, A. Sanchez-Diaz, M. Kanemaki, F. van Deursen, R. D. Edmondson and K. Labib (2006). "GINS maintains association of Cdc45 with MCM in replisome progression complexes at eukaryotic DNA replication forks." Nat Cell Biol **8**(4): 358-366.

Geiser, J. R., E. J. Schott, T. J. Kingsbury, N. B. Cole, L. J. Totis, G. Bhattacharyya, L. He and M. A. Hoyt (1997). "Saccharomyces cerevisiae genes required in the absence of the CIN8-encoded spindle motor act in functionally diverse mitotic pathways." Molecular Biology of the Cell **8**(6): 1035-1050.

Geymonat, M., A. Spanos, G. de Bettignies and S. G. Sedgwick (2009). "Lte1 contributes to Bfa1 localization rather than stimulating nucleotide exchange by Tem1." J Cell Biol **187**(4): 497-511.

Ghiara, J. B., H. E. Richardson, K. Sugimoto, M. Henze, D. J. Lew, C. Wittenberg and S. I. Reed (1991). "A cyclin B homolog in S. cerevisiae: chronic activation of the Cdc28 protein kinase by cyclin prevents exit from mitosis." Cell **65**(1): 163-174.

Grava, S., F. Schaerer, M. Faty, P. Philippsen and Y. Barral (2006). "Asymmetric recruitment of dynein to spindle poles and microtubules promotes proper spindle orientation in yeast." Dev Cell **10**(4): 425-439.

Gruneberg, U., K. Campbell, C. Simpson, J. Grindlay and E. Schiebel (2000). "Nud1p links astral microtubule organization and the control of exit from mitosis." EMBO J **19**(23): 6475-6488.

Gruneberg, U., M. Glotzer, A. Gartner and E. A. Nigg (2002). "The CeCDC-14 phosphatase is required for cytokinesis in the Caenorhabditis elegans embryo." J Cell Biol **158**(5): 901-914.

Guo, Y., C. Kim and Y. Mao (2013). "New insights into the mechanism for chromosome alignment in metaphase." Int Rev Cell Mol Biol **303**: 237-262.

Haase, S. B., M. Winey and S. I. Reed (2001). "Multi-step control of spindle pole body duplication by cyclin-dependent kinase." Nature cell biology **3**(1): 38-42.

Hartwell, L. H. (1991). "Twenty-five years of cell cycle genetics." Genetics **129**(4): 975-980.

Hassold, T. and P. Hunt (2001). "To err (meiotically) is human: the genesis of human aneuploidy." Nature reviews. Genetics **2**(4): 280-291.

He, X., S. Asthana and P. K. Sorger (2000). "Transient sister chromatid separation and elastic deformation of chromosomes during mitosis in budding yeast." Cell **101**(7): 763-775.

Heller, R. C., S. Kang, W. M. Lam, S. Chen, C. S. Chan and S. P. Bell (2011). "Eukaryotic origin-dependent DNA replication in vitro reveals sequential action of DDK and S-CDK kinases." Cell **146**(1): 80-91.

Henderson, K. A., K. Kee, S. Maleki, P. A. Santini and S. Keeney (2006). "Cyclin-dependent kinase directly regulates initiation of meiotic recombination." Cell **125**(7): 1321-1332.

Hentges, P., B. Van Driessche, L. Tafforeau, J. Vandenhaute and A. M. Carr (2005). "Three novel antibiotic marker cassettes for gene disruption and marker switching in Schizosaccharomyces pombe." Yeast **22**(13): 1013-1019.

Higuchi, T. and F. Uhlmann (2005). "Stabilization of microtubule dynamics at anaphase onset promotes chromosome segregation." Nature **433**(7022): 171-176.

Hildebrandt, E. R. and M. A. Hoyt (2001). "Cell cycle-dependent degradation of the Saccharomyces cerevisiae spindle motor Cin8p requires APC(Cdh1) and a bipartite destruction sequence." Mol Biol Cell **12**(11): 3402-3416.

Hoffman, D. B., C. G. Pearson, T. J. Yen, B. J. Howell and E. D. Salmon (2001). "Microtubule-dependent changes in assembly of microtubule motor proteins and mitotic spindle checkpoint proteins at PtK1 kinetochores." Mol Biol Cell **12**(7): 1995-2009.

Holt, L. J., J. E. Hutti, L. C. Cantley and D. O. Morgan (2007). "Evolution of Ime2 phosphorylation sites on Cdk1 substrates provides a mechanism to limit the effects of the phosphatase Cdc14 in meiosis." Molecular Cell **25**(5): 689-702.

Honigberg, S. M. and K. Purnapatre (2003). "Signal pathway integration in the switch from the mitotic cell cycle to meiosis in yeast." J Cell Sci **116**(Pt 11): 2137-2147.

Hornig, N. C., P. P. Knowles, N. Q. McDonald and F. Uhlmann (2002). "The dual mechanism of separase regulation by securin." Curr Biol **12**(12): 973-982.

Hu, F., Y. Wang, D. Liu, Y. Li, J. Qin and S. J. Elledge (2001). "Regulation of the Bub2/Bfa1 GAP complex by Cdc5 and cell cycle checkpoints." Cell **107**(5): 655-665.

Ishiguro, T., K. Tanaka, T. Sakuno and Y. Watanabe (2010). "Shugoshin-PP2A counteracts casein-kinase-1-dependent cleavage of Rec8 by separase." Nature cell biology **12**(5): 500-506.

Iwabuchi, M., K. Ohsumi, T. M. Yamamoto, W. Sawada and T. Kishimoto (2000). "Residual Cdc2 activity remaining at meiosis I exit is essential for meiotic M-M transition in Xenopus oocyte extracts." The EMBO journal **19**(17): 4513-4523.

Jaspersen, S. L., J. F. Charles and D. O. Morgan (1999). "Inhibitory phosphorylation of the APC regulator Hct1 is controlled by the kinase Cdc28 and the phosphatase Cdc14." Curr Biol **9**(5): 227-236.

Jaspersen, S. L., J. F. Charles, R. L. Tinker-Kulberg and D. O. Morgan (1998). "A late mitotic regulatory network controlling cyclin destruction in Saccharomyces cerevisiae." Mol Biol Cell **9**(10): 2803-2817.

Jaspersen, S. L., T. H. Giddings, Jr. and M. Winey (2002). "Mps3p is a novel component of the yeast spindle pole body that interacts with the yeast centrin homologue Cdc31p." J Cell Biol **159**(6): 945-956.

Jaspersen, S. L., B. J. Huneycutt, T. H. Giddings, Jr., K. A. Resing, N. G. Ahn and M. Winey (2004). "Cdc28/Cdk1 regulates spindle pole body duplication through phosphorylation of Spc42 and Mps1." Developmental Cell **7**(2): 263-274.

Jaspersen, S. L. and D. O. Morgan (2000). "Cdc14 activates cdc15 to promote mitotic exit in budding yeast." Current biology : CB **10**(10): 615-618.

Jaspersen, S. L. and M. Winey (2004). "The budding yeast spindle pole body: structure, duplication, and function." Annual review of cell and developmental biology **20**: 1-28.

Jin, F., H. Liu, F. Liang, R. Rizkallah, M. M. Hurt and Y. Wang (2008). "Temporal control of the dephosphorylation of Cdk substrates by mitotic exit pathways in budding yeast." Proc Natl Acad Sci U S A **105**(42): 16177-16182.

Juang, Y. L., J. Huang, J. M. Peters, M. E. McLaughlin, C. Y. Tai and D. Pellman (1997). "APC-mediated proteolysis of Ase1 and the morphogenesis of the mitotic spindle." Science **275**(5304): 1311-1314.

Kaiser, B. K., M. V. Nachury, B. E. Gardner and P. K. Jackson (2004). "Xenopus Cdc14 alpha/beta are localized to the nucleolus and centrosome and are required for embryonic cell division." BMC Cell Biol **5**: 27.

Kaiser, B. K., Z. A. Zimmerman, H. Charbonneau and P. K. Jackson (2002). "Disruption of centrosome structure, chromosome segregation, and cytokinesis by misexpression of human Cdc14A phosphatase." Mol Biol Cell **13**(7): 2289-2300.

Kamieniecki, R. J., L. Liu and D. S. Dawson (2005). "FEAR but not MEN genes are required for exit from meiosis I." Cell cycle **4**(8): 1093-1098.

Kamieniecki, R. J., R. M. Shanks and D. S. Dawson (2000). "Slk19p is necessary to prevent separation of sister chromatids in meiosis I." Curr Biol **10**(19): 1182-1190.

Kao, L., Y. T. Wang, Y. C. Chen, S. F. Tseng, J. C. Jhang, Y. J. Chen and S. C. Teng (2014). "Global analysis of cdc14 dephosphorylation sites reveals essential regulatory role in mitosis and cytokinesis." Molecular & cellular proteomics : MCP **13**(2): 594-605.

Kassir, Y., D. Granot and G. Simchen (1988). "IME1, a positive regulator gene of meiosis in S. cerevisiae." Cell **52**(6): 853-862.

Katis, V. L., M. Galova, K. P. Rabitsch, J. Gregan and K. Nasmyth (2004). "Maintenance of cohesin at centromeres after meiosis I in budding yeast requires a kinetochore-associated protein related to MEI-S332." Curr Biol **14**(7): 560-572.

Katis, V. L., J. J. Lipp, R. Imre, A. Bogdanova, E. Okaz, B. Habermann, K. Mechtler, K. Nasmyth and W. Zachariae (2010). "Rec8 phosphorylation by casein kinase 1 and Cdc7-Dbf4 kinase regulates cohesin cleavage by separase during meiosis." Dev Cell **18**(3): 397-409.

Kerr, G. W., S. Sarkar, K. L. Tibbles, M. Petronczki, J. B. Millar and P. Arumugam (2011). "Meiotic nuclear divisions in budding yeast require PP2A(Cdc55)-mediated antagonism of Net1 phosphorylation by Cdk." The Journal of cell biology **193**(7): 1157-1166.

Khmelinskii, A., J. Roostalu, H. Roque, C. Antony and E. Schiebel (2009). "Phosphorylation-dependent protein interactions at the spindle midzone mediate cell cycle regulation of spindle elongation." Dev Cell **17**(2): 244-256.

Kilmartin, J. V. (2003). "Sfi1p has conserved centrin-binding sites and an essential function in budding yeast spindle pole body duplication." J Cell Biol **162**(7): 1211-1221.

Kilmartin, J. V. and P. Y. Goh (1996). "Spc110p: assembly properties and role in the connection of nuclear microtubules to the yeast spindle pole body." EMBO J **15**(17): 4592-4602.

Kim, J., G. Luo, Y. Y. Bahk and K. Song (2012). "Cdc5-dependent asymmetric localization of bfa1 fine-tunes timely mitotic exit." PLoS Genet **8**(1): e1002450.

Kim, S., R. Meyer, H. Chuong and D. S. Dawson (2013). "Dual mechanisms prevent premature chromosome segregation during meiosis." Genes Dev **27**(19): 2139-2146.

Kitajima, T. S., S. A. Kawashima and Y. Watanabe (2004). "The conserved kinetochore protein shugoshin protects centromeric cohesion during meiosis." Nature **427**(6974): 510-517.

Kitajima, T. S., T. Sakuno, K. Ishiguro, S. Iemura, T. Natsume, S. A. Kawashima and Y. Watanabe (2006). "Shugoshin collaborates with protein phosphatase 2A to protect cohesin." Nature **441**(7089): 46-52.

Klein, F., P. Mahr, M. Galova, S. B. Buonomo, C. Michaelis, K. Nairz and K. Nasmyth (1999). "A central role for cohesins in sister chromatid cohesion, formation of axial elements, and recombination during yeast meiosis." Cell **98**(1): 91-103.

Knapp, D., L. Bhoite, D. J. Stillman and K. Nasmyth (1996). "The transcription factor Swi5 regulates expression of the cyclin kinase inhibitor p40SIC1." Molecular and cellular biology **16**(10): 5701-5707.

Knop, M. and E. Schiebel (1997). "Spc98p and Spc97p of the yeast gamma-tubulin complex mediate binding to the spindle pole body via their interaction with Spc110p." EMBO J **16**(23): 6985-6995.

Knop, M. and K. Strasser (2000). "Role of the spindle pole body of yeast in mediating assembly of the prospore membrane during meiosis." EMBO J **19**(14): 3657-3667.

Krapp, A., S. Schmidt, E. Cano and V. Simanis (2001). "S. pombe cdc11p, together with sid4p, provides an anchor for septation initiation network proteins on the spindle pole body." Curr Biol **11**(20): 1559-1568.

Krasinska, L., G. de Bettignies, D. Fisher, A. Abrieu, D. Fesquet and N. Morin (2007). "Regulation of multiple cell cycle events by Cdc14 homologues in vertebrates." Exp Cell Res **313**(6): 1225-1239.

Labib, K. (2010). "How do Cdc7 and cyclin-dependent kinases trigger the initiation of chromosome replication in eukaryotic cells?" Genes Dev **24**(12): 1208-1219.

Labib, K., J. F. Diffley and S. E. Kearsey (1999). "G1-phase and B-type cyclins exclude the DNA-replication factor Mcm4 from the nucleus." Nat Cell Biol **1**(7): 415-422.

Laloraya, S., V. Guacci and D. Koshland (2000). "Chromosomal addresses of the cohesin component Mcd1p." J Cell Biol **151**(5): 1047-1056.

Lee, B. H. and A. Amon (2003). "Role of Polo-like kinase CDC5 in programming meiosis I chromosome segregation." Science **300**(5618): 482-486.

Lee, S. E., L. M. Frenz, N. J. Wells, A. L. Johnson and L. H. Johnston (2001). "Order of function of the budding-yeast mitotic exit-network proteins Tem1, Cdc15, Mob1, Dbf2, and Cdc5." Current biology : CB **11**(10): 784-788.

Levin, M. (2005). "Left-right asymmetry in embryonic development: a comprehensive review." Mechanisms of development **122**(1): 3-25.

Li, L., B. R. Ernsting, M. J. Wishart, D. L. Lohse and J. E. Dixon (1997). "A family of putative tumor suppressors is structurally and functionally conserved in humans and yeast." The Journal of biological chemistry **272**(47): 29403-29406.

Li, L., M. Ljungman and J. E. Dixon (2000). "The human Cdc14 phosphatases interact with and dephosphorylate the tumor suppressor protein p53." J Biol Chem **275**(4): 2410-2414.

Li, P., Y. Shao, H. Jin and H. G. Yu (2015). "Ndj1, a telomere-associated protein, regulates centrosome separation in budding yeast meiosis." The Journal of cell biology **209**(2): 247-259.

Li, R. (2013). "The art of choreographing asymmetric cell division." Developmental cell **25**(5): 439-450.

Li, S., A. M. Sandercock, P. Conduit, C. V. Robinson, R. L. Williams and J. V. Kilmartin (2006). "Structural role of Sfi1p-centrin filaments in budding yeast spindle pole body duplication." J Cell Biol **173**(6): 867-877.

Liakopoulos, D., J. Kusch, S. Grava, J. Vogel and Y. Barral (2003). "Asymmetric loading of Kar9 onto spindle poles and microtubules ensures proper spindle alignment." Cell **112**(4): 561-574.

Liang, F., F. Jin, H. Liu and Y. Wang (2009). "The molecular function of the yeast polo-like kinase Cdc5 in Cdc14 release during early anaphase." Mol Biol Cell **20**(16): 3671-3679.

LiCor Biosciences, L.-U. (2015). "Quantitative Infrared Western Blots." Retrieved 26 Feb, 2015, from http://www.licor.com/bio/applications/quantitative_western_blots/index.html.

Listovsky, T., A. Zor, A. Laronne and M. Brandeis (2000). "Cdk1 is essential for mammalian cyclosome/APC regulation." Exp Cell Res **255**(2): 184-191.

Longtine, M. S., A. McKenzie, 3rd, D. J. Demarini, N. G. Shah, A. Wach, A. Brachat, P. Philippsen and J. R. Pringle (1998). "Additional modules for versatile and economical PCR-based gene deletion and modification in Saccharomyces cerevisiae." Yeast **14**(10): 953-961.

Loog, M. and D. O. Morgan (2005). "Cyclin specificity in the phosphorylation of cyclin-dependent kinase substrates." Nature **434**(7029): 104-108.

Maekawa, H., C. Priest, J. Lechner, G. Pereira and E. Schiebel (2007). "The yeast centrosome translates the positional information of the anaphase spindle into a cell cycle signal." J Cell Biol **179**(3): 423-436.

Mailand, N., C. Lukas, B. K. Kaiser, P. K. Jackson, J. Bartek and J. Lukas (2002). "Deregulated human Cdc14A phosphatase disrupts centrosome separation and chromosome segregation." Nat Cell Biol **4**(4): 317-322.

Manzoni, R., F. Montani, C. Visintin, F. Caudron, A. Ciliberto and R. Visintin (2010). "Oscillations in Cdc14 release and sequestration reveal a circuit underlying mitotic exit." The Journal of cell biology **190**(2): 209-222.

Marston, A. L. and A. Amon (2004). "Meiosis: cell-cycle controls shuffle and deal." Nature reviews. Molecular cell biology **5**(12): 983-997.

Marston, A. L., B. H. Lee and A. Amon (2003). "The Cdc14 phosphatase and the FEAR network control meiotic spindle disassembly and chromosome segregation." Developmental Cell **4**(5): 711-726.

Marston, A. L., W. H. Tham, H. Shah and A. Amon (2004). "A genome-wide screen identifies genes required for centromeric cohesion." Science **303**(5662): 1367-1370.

Masumoto, H., S. Muramatsu, Y. Kamimura and H. Araki (2002). "S-Cdk-dependent phosphorylation of Sld2 essential for chromosomal DNA replication in budding yeast." Nature **415**(6872): 651-655.

Masumoto, H., A. Sugino and H. Araki (2000). "Dpb11 controls the association between DNA polymerases alpha and epsilon and the autonomously replicating sequence region of budding yeast." Mol Cell Biol **20**(8): 2809-2817.

Matos, J., J. J. Lipp, A. Bogdanova, S. Guillot, E. Okaz, M. Junqueira, A. Shevchenko and W. Zachariae (2008). "Dbf4-dependent CDC7 kinase links DNA replication to the segregation of homologous chromosomes in meiosis I." Cell **135**(4): 662-678.

Megee, P. C., C. Mistrot, V. Guacci and D. Koshland (1999). "The centromeric sister chromatid cohesion site directs Mcd1p binding to adjacent sequences." Mol Cell **4**(3): 445-450.

Meitinger, F., M. E. Boehm, A. Hofmann, B. Hub, H. Zentgraf, W. D. Lehmann and G. Pereira (2011). "Phosphorylation-dependent regulation of the F-BAR protein Hof1 during cytokinesis." Genes & development **25**(8): 875-888.

Mendenhall, M. D. and A. E. Hodge (1998). "Regulation of Cdc28 cyclin-dependent protein kinase activity during the cell cycle of the yeast Saccharomyces cerevisiae." Microbiol Mol Biol Rev **62**(4): 1191-1243.

Menssen, R., A. Neutzner and W. Seufert (2001). "Asymmetric spindle pole localization of yeast Cdc15 kinase links mitotic exit and cytokinesis." Curr Biol **11**(5): 345-350.

Miller, M. P., E. Unal, G. A. Brar and A. Amon (2012). "Meiosis I chromosome segregation is established through regulation of microtubule-kinetochore interactions." Elife **1**: e00117.

Miller, R. K. and M. D. Rose (1998). "Kar9p is a novel cortical protein required for cytoplasmic microtubule orientation in yeast." J Cell Biol **140**(2): 377-390.

Mimura, S., T. Seki, S. Tanaka and J. F. Diffley (2004). "Phosphorylation-dependent binding of mitotic cyclins to Cdc6 contributes to DNA replication control." Nature **431**(7012): 1118-1123.

Mocciaro, A., E. Berdougo, K. Zeng, E. Black, P. Vagnarelli, W. Earnshaw, D. Gillespie, P. Jallepalli and E. Schiebel (2010). "Vertebrate cells genetically deficient for Cdc14A or Cdc14B retain DNA damage checkpoint proficiency but are impaired in DNA repair." J Cell Biol **189**(4): 631-639.

Moens, P. B. and E. Rapport (1971). "Spindles, spindle plaques, and meiosis in the yeast Saccharomyces cerevisiae (Hansen)." J Cell Biol **50**(2): 344-361.

Mohl, D. A., M. J. Huddleston, T. S. Collingwood, R. S. Annan and R. J. Deshaies (2009). "Dbf2-Mob1 drives relocalization of protein phosphatase Cdc14 to the cytoplasm during exit from mitosis." The Journal of cell biology **184**(4): 527-539.

Molk, J. N., S. C. Schuyler, J. Y. Liu, J. G. Evans, E. D. Salmon, D. Pellman and K. Bloom (2004). "The differential roles of budding yeast Tem1p, Cdc15p, and Bub2p protein dynamics in mitotic exit." Mol Biol Cell **15**(4): 1519-1532.

Monje-Casas, F. and A. Amon (2009). "Cell polarity determinants establish asymmetry in MEN signaling." Dev Cell **16**(1): 132-145.

Morgan, D. O. (1997). "Cyclin-dependent kinases: engines, clocks, and microprocessors." Annu Rev Cell Dev Biol **13**: 261-291.

Morgan, D. O. (1999). "Regulation of the APC and the exit from mitosis." Nat Cell Biol **1**(2): E47-53.

Mueller, P. R., T. R. Coleman, A. Kumagai and W. G. Dunphy (1995). "Myt1: a membrane-associated inhibitory kinase that phosphorylates Cdc2 on both threonine-14 and tyrosine-15." Science **270**(5233): 86-90.

Musacchio, A. and K. G. Hardwick (2002). "The spindle checkpoint: structural insights into dynamic signalling." Nat Rev Mol Cell Biol **3**(10): 731-741.

Nalepa, G. and J. W. Harper (2004). "Visualization of a highly organized intranuclear network of filaments in living mammalian cells." Cell Motil Cytoskeleton **59**(2): 94-108.

Nasmyth, K., L. Dirick, U. Surana, A. Amon and F. Cvrckova (1991). "Some facts and thoughts on cell cycle control in yeast." Cold Spring Harb Symp Quant Biol **56**: 9-20.

Nerusheva, O. O., S. Galander, J. Fernius, D. Kelly and A. L. Marston (2014). "Tension-dependent removal of pericentromeric shugoshin is an indicator of sister chromosome biorientation." Genes Dev **28**(12): 1291-1309.

Nguyen, V. Q., C. Co and J. J. Li (2001). "Cyclin-dependent kinases prevent DNA re-replication through multiple mechanisms." Nature **411**(6841): 1068-1073.

Niepel, M., C. Strambio-de-Castillia, J. Fasolo, B. T. Chait and M. P. Rout (2005). "The nuclear pore complex-associated protein, Mlp2p, binds to the yeast spindle pole body and promotes its efficient assembly." The Journal of cell biology **170**(2): 225-235.

O'Toole, E. T., M. Winey and J. R. McIntosh (1999). "High-voltage electron tomography of spindle pole bodies and early mitotic spindles in the yeast Saccharomyces cerevisiae." Mol Biol Cell **10**(6): 2017-2031.

Ovejero, S., P. Ayala, A. Bueno and M. P. Sacristan (2012). "Human Cdc14A regulates Wee1 stability by counteracting CDK-mediated phosphorylation." Mol Biol Cell **23**(23): 4515-4525.

Palmer, A., A. Gavin and A. Nebreda (1998). "A link between MAP kinase and $p34^{cdc2}$/cyclin B during oocyte maturation: $p90^{rsk}$ phosphorylates and inactivates the $p34^{cdc2}$ inhibitory kinase Myt1." EMBO J **17:** 5037-5047.

Park, C. J., J. E. Park, T. S. Karpova, N. K. Soung, L. R. Yu, S. Song, K. H. Lee, X. Xia, E. Kang, I. Dabanoglu, D. Y. Oh, J. Y. Zhang, Y. H. Kang, S. Wincovitch, T. C. Huffaker, T. D. Veenstra, J. G. McNally and K. S. Lee (2008). "Requirement for the budding yeast polo kinase Cdc5 in proper microtubule growth and dynamics." Eukaryot Cell **7**(3): 444-453.

Pellman, D., M. Bagget, Y. H. Tu, G. R. Fink and H. Tu (1995). "Two microtubule-associated proteins required for anaphase spindle movement in Saccharomyces cerevisiae." J Cell Biol **130**(6): 1373-1385.

Pereira, G., T. Hofken, J. Grindlay, C. Manson and E. Schiebel (2000). "The Bub2p spindle checkpoint links nuclear migration with mitotic exit." Mol Cell **6**(1): 1-10.

Pereira, G., C. Manson, J. Grindlay and E. Schiebel (2002). "Regulation of the Bfa1p-Bub2p complex at spindle pole bodies by the cell cycle phosphatase Cdc14p." J Cell Biol **157**(3): 367-379.

Pereira, G. and E. Schiebel (2003). "Separase regulates INCENP-Aurora B anaphase spindle function through Cdc14." Science **302**(5653): 2120-2124.

Pereira, G., T. U. Tanaka, K. Nasmyth and E. Schiebel (2001). "Modes of spindle pole body inheritance and segregation of the Bfa1p-Bub2p checkpoint protein complex." EMBO J **20**(22): 6359-6370.

Petronczki, M., M. F. Siomos and K. Nasmyth (2003). "Un menage a quatre: the molecular biology of chromosome segregation in meiosis." Cell **112**(4): 423-440.

Queralt, E., C. Lehane, B. Novak and F. Uhlmann (2006). "Downregulation of PP2A(Cdc55) phosphatase by separase initiates mitotic exit in budding yeast." Cell **125**(4): 719-732.

Reimann, J. and P. Jackson (2002). "Emi1 is required for cytostatic factor arrest in veterbrate eggs." Nature **416:** 850-854

Reynolds, D., B. J. Shi, C. McLean, F. Katsis, B. Kemp and S. Dalton (2003). "Recruitment of Thr 319-phosphorylated Ndd1p to the FHA domain of Fkh2p requires Clb kinase activity: a mechanism for CLB cluster gene activation." Genes Dev **17**(14): 1789-1802.

Richardson, H., D. J. Lew, M. Henze, K. Sugimoto and S. I. Reed (1992). "Cyclin-B homologs in Saccharomyces cerevisiae function in S phase and in G2." Genes Dev **6**(11): 2021-2034.

Richardson, H. E., C. Wittenberg, F. Cross and S. I. Reed (1989). "An essential G1 function for cyclin-like proteins in yeast." Cell **59**(6): 1127-1133.

Riedel, C. G., V. L. Katis, Y. Katou, S. Mori, T. Itoh, W. Helmhart, M. Galova, M. Petronczki, J. Gregan, B. Cetin, I. Mudrak, E. Ogris, K. Mechtler, L. Pelletier, F. Buchholz, K. Shirahige and K. Nasmyth (2006). "Protein phosphatase 2A protects centromeric sister chromatid cohesion during meiosis I." Nature **441**(7089): 53-61.

Rigaut, G., A. Shevchenko, B. Rutz, M. Wilm, M. Mann and B. Seraphin (1999). "A generic protein purification method for protein complex characterization and proteome exploration." Nature biotechnology **17**(10): 1030-1032.

Roccuzzo, M., C. Visintin, F. Tili and R. Visintin (2015). "FEAR-mediated activation of Cdc14 is the limiting step for spindle elongation and anaphase progression." Nat Cell Biol.

Rock, J. M. and A. Amon (2009). "The FEAR network." Current biology : CB **19**(23): R1063-1068.

Rodier, G., P. Coulombe, P. L. Tanguay, C. Boutonnet and S. Meloche (2008). "Phosphorylation of Skp2 regulated by CDK2 and Cdc14B protects it from degradation by APC(Cdh1) in G1 phase." EMBO J **27**(4): 679-691.

Rose, M. D. and G. R. Fink (1987). "KAR1, a gene required for function of both intranuclear and extranuclear microtubules in yeast." Cell **48**(6): 1047-1060.

Rothbauer, U., K. Zolghadr, S. Tillib, D. Nowak, L. Schermelleh, A. Gahl, N. Backmann, K. Conrath, S. Muyldermans, M. C. Cardoso and H. Leonhardt (2006). "Targeting and tracing antigens in live cells with fluorescent nanobodies." Nat Methods **3**(11): 887-889.

Rout, M. P. and J. V. Kilmartin (1990). "Components of the yeast spindle and spindle pole body." J Cell Biol **111**(5 Pt 1): 1913-1927.

Sacristan, M. P., S. Ovejero and A. Bueno (2011). "Human Cdc14A becomes a cell cycle gene in controlling Cdk1 activity at the G(2)/M transition." Cell Cycle **10**(3): 387-391.

Saito, R. M., A. Perreault, B. Peach, J. S. Satterlee and S. van den Heuvel (2004). "The CDC-14 phosphatase controls developmental cell-cycle arrest in C. elegans." Nat Cell Biol **6**(8): 777-783.

Saunders, W. S. and M. A. Hoyt (1992). "Kinesin-related proteins required for structural integrity of the mitotic spindle." Cell **70**(3): 451-458.

Scarfone, I., M. Venturetti, M. Hotz, J. Lengefeld, Y. Barral and S. Piatti (2015). "Asymmetry of the Budding Yeast Tem1 GTPase at Spindle Poles Is Required for Spindle Positioning But Not for Mitotic Exit." PLoS Genet **11**(2): e1004938.

Schmidt, A., N. R. Rauh, E. A. Nigg and T. U. Mayer (2006). "Cytostatic factor: an activity that puts the cell cycle on hold." J Cell Biol **119:** 1213-1218.

Schutz, A. R. and M. Winey (1998). "New alleles of the yeast MPS1 gene reveal multiple requirements in spindle pole body duplication." Mol Biol Cell **9**(4): 759-774.

Schuyler, S. C., J. Y. Liu and D. Pellman (2003). "The molecular function of Ase1p: evidence for a MAP-dependent midzone-specific spindle matrix. Microtubule-associated proteins." J Cell Biol **160**(4): 517-528.

Schwob, E., T. Bohm, M. D. Mendenhall and K. Nasmyth (1994). "The B-type cyclin kinase inhibitor p40SIC1 controls the G1 to S transition in S. cerevisiae." Cell **79**(2): 233-244.

Schwob, E. and K. Nasmyth (1993). "CLB5 and CLB6, a new pair of B cyclins involved in DNA replication in Saccharomyces cerevisiae." Genes Dev **7**(7A): 1160-1175.

Sharon, G. and G. Simchen (1990). "Centromeric regions control autonomous segregation tendencies in single-division meiosis of Saccharomyces cerevisiae." Genetics **125**(3): 487-494.

Sharon, G. and G. Simchen (1990). "Mixed segregation of chromosomes during single-division meiosis of Saccharomyces cerevisiae." Genetics **125**(3): 475-485.

Shirayama, M., Y. Matsui, K. Tanaka and A. Toh-e (1994). "Isolation of a CDC25 family gene, MSI2/LTE1, as a multicopy suppressor of ira1." Yeast **10**(4): 451-461.

Shirayama, M., W. Zachariae, R. Ciosk and K. Nasmyth (1998). "The Polo-like kinase Cdc5p and the WD-repeat protein Cdc20p/fizzy are regulators and substrates of the anaphase promoting complex in Saccharomyces cerevisiae." EMBO J **17**(5): 1336-1349.

Shou, W., R. Azzam, S. L. Chen, M. J. Huddleston, C. Baskerville, H. Charbonneau, R. S. Annan, S. A. Carr and R. J. Deshaies (2002). "Cdc5 influences phosphorylation of Net1 and disassembly of the RENT complex." BMC Mol Biol **3**: 3.

Shou, W., J. H. Seol, A. Shevchenko, C. Baskerville, D. Moazed, Z. W. Chen, J. Jang, H. Charbonneau and R. J. Deshaies (1999). "Exit from mitosis is triggered by Tem1-dependent release of the protein phosphatase Cdc14 from nucleolar RENT complex." Cell **97**(2): 233-244.

Siegmund, R. F. and K. A. Nasmyth (1996). "The Saccharomyces cerevisiae Start-specific transcription factor Swi4 interacts through the ankyrin repeats with the mitotic Clb2/Cdc28 kinase and through its conserved carboxy terminus with Swi6." Mol Cell Biol **16**(6): 2647-2655.

Skowyra, D., K. L. Craig, M. Tyers, S. J. Elledge and J. W. Harper (1997). "F-box proteins are receptors that recruit phosphorylated substrates to the SCF ubiquitin-ligase complex." Cell **91**(2): 209-219.

Smith, H. E., S. S. Su, L. Neigeborn, S. E. Driscoll and A. P. Mitchell (1990). "Role of IME1 expression in regulation of meiosis in Saccharomyces cerevisiae." Mol Cell Biol **10**(12): 6103-6113.

Spang, A., I. Courtney, U. Fackler, M. Matzner and E. Schiebel (1993). "The calcium-binding protein cell division cycle 31 of Saccharomyces cerevisiae is a component of the half bridge of the spindle pole body." J Cell Biol **123**(2): 405-416.

Stark, M. J. (1996). "Yeast protein serine/threonine phosphatases: multiple roles and diverse regulation." Yeast **12**(16): 1647-1675.

Stegmeier, F. and A. Amon (2004). "Closing mitosis: the functions of the Cdc14 phosphatase and its regulation." Annu Rev Genet **38**: 203-232.

Stegmeier, F., J. Huang, R. Rahal, J. Zmolik, D. Moazed and A. Amon (2004). "The replication fork block protein Fob1 functions as a negative regulator of the FEAR network." Curr Biol **14**(6): 467-480.

Stegmeier, F., R. Visintin and A. Amon (2002). "Separase, polo kinase, the kinetochore protein Slk19, and Spo12 function in a network that controls Cdc14 localization during early anaphase." Cell **108**(2): 207-220.

Stuart, D. and C. Wittenberg (1998). "CLB5 and CLB6 are required for premeiotic DNA replication and activation of the meiotic S/M checkpoint." Genes Dev **12**(17): 2698-2710.

Sullivan, M. and F. Uhlmann (2003). "A non-proteolytic function of separase links the onset of anaphase to mitotic exit." Nat Cell Biol **5**(3): 249-254.

Sundberg, H. A. and T. N. Davis (1997). "A mutational analysis identifies three functional regions of the spindle pole component Spc110p in Saccharomyces cerevisiae." Mol Biol Cell **8**(12): 2575-2590.

Sundberg, H. A., L. Goetsch, B. Byers and T. N. Davis (1996). "Role of calmodulin and Spc110p interaction in the proper assembly of spindle pole body compenents." J Cell Biol **133**(1): 111-124.

Tanaka, T., M. P. Cosma, K. Wirth and K. Nasmyth (1999). "Identification of cohesin association sites at centromeres and along chromosome arms." Cell **98**(6): 847-858.

Taxis, C., C. Maeder, S. Reber, N. Rathfelder, K. Miura, K. Greger, E. H. Stelzer and M. Knop (2006). "Dynamic organization of the actin cytoskeleton during meiosis and spore formation in budding yeast." Traffic **7**(12): 1628-1642.

Tibbles, K. L., S. Sarkar, B. Novak and P. Arumugam (2013). "CDK-dependent nuclear localization of B-cyclin Clb1 promotes FEAR activation during meiosis I in budding yeast." PLoS One **8**(11): e79001.

Tomson, B. N., R. Rahal, V. Reiser, F. Monje-Casas, K. Mekhail, D. Moazed and A. Amon (2009). "Regulation of Spo12 phosphorylation and its essential role in the FEAR network." Curr Biol **19**(6): 449-460.

Towbin, H., T. Staehelin and J. Gordon (1979). "Electrophoretic transfer of proteins from polyacrylamide gels to nitrocellulose sheets: procedure and some applications." Proc Natl Acad Sci U S A **76**(9): 4350-4354.

Toyn, J. H., A. L. Johnson, J. D. Donovan, W. M. Toone and L. H. Johnston (1997). "The Swi5 transcription factor of Saccharomyces cerevisiae has a role in exit from mitosis through induction of the cdk-inhibitor Sic1 in telophase." Genetics **145**(1): 85-96.

Trautmann, S., B. A. Wolfe, P. Jorgensen, M. Tyers, K. L. Gould and D. McCollum (2001). "Fission yeast Clp1p phosphatase regulates G2/M transition and coordination of cytokinesis with cell cycle progression." Curr Biol **11**(12): 931-940.

Tsumoto, K., M. Umetsu, I. Kumagai, D. Ejima and T. Arakawa (2003). "Solubilization of active green fluorescent protein from insoluble particles by guanidine and arginine." Biochemical and biophysical research communications **312**(4): 1383-1386.

Ubersax, J. A., E. L. Woodbury, P. N. Quang, M. Paraz, J. D. Blethrow, K. Shah, K. M. Shokat and D. O. Morgan (2003). "Targets of the cyclin-dependent kinase Cdk1." Nature **425**(6960): 859-864.

Uhlmann, F., F. Lottspeich and K. Nasmyth (1999). "Sister-chromatid separation at anaphase onset is promoted by cleavage of the cohesin subunit Scc1." Nature **400**(6739): 37-42.

Uhlmann, F. and K. Nasmyth (1998). "Cohesion between sister chromatids must be established during DNA replication." Curr Biol **8**(20): 1095-1101.

Uhlmann, F., D. Wernic, M. A. Poupart, E. V. Koonin and K. Nasmyth (2000). "Cleavage of cohesin by the CD clan protease separin triggers anaphase in yeast." Cell **103**(3): 375-386.

Umetsu, M., K. Tsumoto, S. Nitta, T. Adschiri, D. Ejima, T. Arakawa and I. Kumagai (2005). "Nondenaturing solubilization of beta2 microglobulin from inclusion bodies by L-arginine." Biochemical and biophysical research communications **328**(1): 189-197.

Valerio-Santiago, M. and F. Monje-Casas (2011). "Tem1 localization to the spindle pole bodies is essential for mitotic exit and impairs spindle checkpoint function." J Cell Biol **192**(4): 599-614.

Vallen, E. A., W. Ho, M. Winey and M. D. Rose (1994). "Genetic interactions between CDC31 and KAR1, two genes required for duplication of the microtubule organizing center in Saccharomyces cerevisiae." Genetics **137**(2): 407-422.

van Werven, F. J. and A. Amon (2011). "Regulation of entry into gametogenesis." Philosophical transactions of the Royal Society of London. Series B, Biological sciences **366**(1584): 3521-3531.

Verma, R., R. S. Annan, M. J. Huddleston, S. A. Carr, G. Reynard and R. J. Deshaies (1997). "Phosphorylation of Sic1p by G1 Cdk required for its degradation and entry into S phase." Science **278**(5337): 455-460.

Visintin, R. and A. Amon (2001). "Regulation of the mitotic exit protein kinases Cdc15 and Dbf2." Mol Biol Cell **12**(10): 2961-2974.

Visintin, R., K. Craig, E. S. Hwang, S. Prinz, M. Tyers and A. Amon (1998). "The phosphatase Cdc14 triggers mitotic exit by reversal of Cdk-dependent phosphorylation." Molecular Cell **2**(6): 709-718.

Visintin, R., E. S. Hwang and A. Amon (1999). "Cfi1 prevents premature exit from mitosis by anchoring Cdc14 phosphatase in the nucleolus." Nature **398**(6730): 818-823.

Visintin, R., S. Prinz and A. Amon (1997). "CDC20 and CDH1: a family of substrate-specific activators of APC-dependent proteolysis." Science **278**(5337): 460-463.

Visintin, R., F. Stegmeier and A. Amon (2003). "The role of the polo kinase Cdc5 in controlling Cdc14 localization." Molecular Biology of the Cell **14**(11): 4486-4498.

Vogel, J., B. Drapkin, J. Oomen, D. Beach, K. Bloom and M. Snyder (2001). "Phosphorylation of gamma-tubulin regulates microtubule organization in budding yeast." Dev Cell **1**(5): 621-631.

Waizenegger, I., J. F. Gimenez-Abian, D. Wernic and J. M. Peters (2002). "Regulation of human separase by securin binding and autocleavage." Curr Biol **12**(16): 1368-1378.

Wigge, P. A., O. N. Jensen, S. Holmes, S. Soues, M. Mann and J. V. Kilmartin (1998). "Analysis of the Saccharomyces spindle pole by matrix-assisted laser desorption/ionization (MALDI) mass spectrometry." J Cell Biol **141**(4): 967-977.

Winey, M. and K. Bloom (2012). "Mitotic spindle form and function." Genetics **190**(4): 1197-1224.

Winey, M., L. Goetsch, P. Baum and B. Byers (1991). "MPS1 and MPS2: novel yeast genes defining distinct steps of spindle pole body duplication." J Cell Biol **114**(4): 745-754.

Winey, M., M. A. Hoyt, C. Chan, L. Goetsch, D. Botstein and B. Byers (1993). "NDC1: a nuclear periphery component required for yeast spindle pole body duplication." J Cell Biol **122**(4): 743-751.

Wolfe, B. A., W. H. McDonald, J. R. Yates and K. L. Gould (2006). "Phospho-regulation of the Cdc14/Clp1 phosphatase delays late mitotic events in S-pombe." Developmental Cell **11**(3): 423-430.

Woodbury, E. L. and D. O. Morgan (2007). "Cdk and APC activities limit the spindle-stabilizing function of Fin1 to anaphase." Nature cell biology **9**(1): 106-112.

Woodruff, J. B., D. G. Drubin and G. Barnes (2012). "Spindle assembly requires complete disassembly of spindle remnants from the previous cell cycle." Mol Biol Cell **23**(2): 258-267.

Wu, J., H. P. Cho, D. B. Rhee, D. K. Johnson, J. Dunlap, Y. Liu and Y. Wang (2008). "Cdc14B depletion leads to centriole amplification, and its overexpression prevents unscheduled centriole duplication." J Cell Biol **181**(3): 475-483.

Xu, S., H. K. Huang, P. Kaiser, M. Latterich and T. Hunter (2000). "Phosphorylation and spindle pole body localization of the Cdc15p mitotic regulatory protein kinase in budding yeast." Current biology : CB **10**(6): 329-332.

Yellman, C. M. and D. J. Burke (2006). "The role of Cdc55 in the spindle checkpoint is through regulation of mitotic exit in Saccharomyces cerevisiae." Molecular Biology of the Cell **17**(2): 658-666.

Yeong, F. M., H. H. Lim, C. G. Padmashree and U. Surana (2000). "Exit from mitosis in budding yeast: biphasic inactivation of the Cdc28-Clb2 mitotic kinase and the role of Cdc20." Mol Cell **5**(3): 501-511.

Yoshida, M., H. Kawaguchi, Y. Sakata, K. Kominami, M. Hirano, H. Shima, R. Akada and I. Yamashita (1990). "Initiation of meiosis and sporulation in Saccharomyces cerevisiae requires a novel protein kinase homologue." Mol Gen Genet **221**(2): 176-186.

Yoshida, S., K. Asakawa and A. Toh-e (2002). "Mitotic exit network controls the localization of Cdc14 to the spindle pole body in Saccharomyces cerevisiae." Curr Biol **12**(11): 944-950.

Yoshida, S. and A. Toh-e (2002). "Budding yeast Cdc5 phosphorylates Net1 and assists Cdc14 release from the nucleolus." Biochemical and biophysical research communications **294**(3): 687-691.

Zachariae, W., M. Schwab, K. Nasmyth and W. Seufert (1998). "Control of cyclin ubiquitination by CDK-regulated binding of Hct1 to the anaphase promoting complex." Science **282**(5394): 1721-1724.

Appendices

Appendices

Appendix 1: Mass Spectrometry results for Cdc14-TAP IP in meiosis

	Wild Type		*cdc55mn*	
Name	No tag	Cdc14-TAP	No tag	Cdc14-TAP
SPC110		**73**	**33**	**89**
CNM67		**45**	**14**	**53**
ACS1	18	33	21	32
POM152		52		51
EFT1	20	33	13	32
TDH3	20	30	19	28
ATP1	20	28	22	26
SPC42		**36**	**19**	**40**
PGK1	21	26	17	29
PCK1	21	27	15	30
CDC19	20	27	15	31
FAS1	8	32	13	36
NET1		**43**	**15**	**29**
BFA1		42	8	37
FOX2	9	33	8	37
CDC14	**12**	**30**	**16**	**28**
SSA1	18	25	14	28
URA2	13	29	13	29
ALD4	18	25	15	22
PET9	19	25	13	22
TEF1	18	21	19	19
FAS2	8	27	10	29
ENO2	16	22	13	21
MLS1	12	20	9	30
SSB1	16	27		25
SPC97		**28**		**38**
QCR2	13	19	7	22
GUT2	12	19	11	18
ACH1	11	20	10	19
SPC29		**20**	**8**	**31**
ICL1	16	17	10	15
SPC72		**27**		**30**
ADH1	11	18	12	15
PDC1	11	17	8	20
SPC98		**25**		**30**
GDH2	12	20		23
FAA2		21		33
ACC1		23	7	22
IDP2	9	17	6	19

Table A1: All protein identified by Mass Spectrometry.

	Wild Type		*cdc55mn*	
Name	No tag	Cdc14-TAP	No tag	Cdc14-TAP
MPS3		**26**	**4**	**20**
PMA2	10	15	8	17
ADH2	7	18	10	14
SFC1	11	15	6	17
MPS2		**19**	**3**	**26**
HSL7		25		23
RPL3	7	15	7	18
POR1	12	14	7	14
CAT2	6	12	6	21
COR1	10	14	9	11
HSP60	10	17	5	12
BBP1		**22**	**3**	**18**
RPS3	7	12	10	14
HSP82		20		23
YEF3	12	11	4	16
ADY3		18		24
SIK1	16	11		15
NOP58	9	14	8	10
BUB2		16	7	17
GPH1	4	20		16
KGD1	8	14	7	10
FBA1	10	13	5	11
GFA1		14	7	17
TPI1	7	13	6	11
CIT1	11	10	6	10
PFK2	8	15		14
ACO1	8	13		16
RPS1A	3	19	12	2
SDH1	7	15	4	10
MIR1	5	14	4	13
NDC1		**18**		**18**
PFK1		13	6	16
ACT1	3	9	9	14
RPS5	10	10	5	10
KAR1		**17**		**18**
NDI1	9	10	4	12
ERG6	6	12	5	11
RPS18A	7	9	6	11
RPP0	8	10	5	10
CDC31		**12**	**5**	**15**
CDC48		14	5	12
CIT2		11	2	18
ATP5	8	10	4	9
SFI1		**15**		**16**

Table A1 (Continued): All protein identified by Mass Spectrometry.

	Wild Type		*cdc55mn*	
Name	No tag	Cdc14-TAP	No tag	Cdc14-TAP
RPL8A	7	12	1	11
SSC1	11	19		
HSC82	14	3	11	2
FAA1		11	4	15
IDH1	7	8	6	9
ENO1	7	11	3	9
TUB4		**14**		**16**
PDH1		14	5	10
RPL4A		11	6	12
PEP4	5	8	8	8
VMA2		16		13
CAR2		11	5	12
TUB2		9	6	13
RPS6A	6	10	4	8
TIF1	5	10	4	9
RPS1B	10	3	1	14
GPM1	7	13	7	
ILV5	9	12	6	
NOP1	12	8	7	
CHC1		14		13
PGI1	7	8	3	9
KAR2		13	4	9
ASC1	3	12	5	6
RPL10	7	9		10
LPD1	5	14	6	
CIT3		11	4	10
TDH1	3	9	7	6
TEF4	6	7	6	6
FBP1		14		11
FMP13	7	10		8
ATP3	8	9		8
TUB1		10	3	10
RPL7A	8		4	11
TOF2		22		
DNM1		11		10
LSC2		11		10
LSP1	7	10	3	
RPL23A	5	10	5	
RPS13	5	8	7	
SPS19		9		11
DLD1	5	14		
PRP43	10		9	
RPL1A		8	3	8
IPP1		9	2	8

Table A1 (Continued): All protein identified by Mass Spectrometry.

	Wild Type		*cdc55mn*	
Name	No tag	Cdc14-TAP	No tag	Cdc14-TAP
HTB1	3	5	4	7
YEL020C		8		11
RPL19A	5		5	9
OM45	7	11		
SEC53	6	7	5	
BMH1	8		5	5
ATP4	3	8		7
RPL20A	5	8	4	
RPS14A	6	8	3	
TSA1	5	6	6	
RPL14A	4	6	2	5
CMD1		**9**		**8**
NDJ1		8		9
NUD1		**8**		**9**
RPS22A	3		6	8
PYC1	5		4	8
HXK1	5	8	3	
RPL27A	5	6	4	
RPL30		6	4	5
TDH2	3	6	2	4
RPS17A	4		3	8
IDP3		4		11
IDH2	5		2	8
GLK1			3	12
PSA1	4	5		6
RPL6A	6			9
ARO1				15
CST9				15
MDH1	3	11		
MET6		14		
RPL6B		8	6	
DMC1		9		5
PIL1	4			10
MDH3				14
PDB1	3	8	2	
HHF1	4	6		3
NCP1			4	9
ARF2	5	3		5
CTA1				13
POX1				13
NBP1		12		
QCR7	6	6		
RPL2A	7		5	
SSB2			12	
RIP1		5		7

Table A1 (Continued): All protein identified by Mass Spectrometry.

	Wild Type		*cdc55mn*	
Name	No tag	Cdc14-TAP	No tag	Cdc14-TAP
SSA3	2		1	9
RPS11A	6		5	
RPS4A	11			
SSA2	1	6	1	3
PEX11			4	7
PCS60				11
MDH2		10		
RPL28	6		4	
SNU13	5		5	
BGL2	3			7
HMG1				10
ARF1		5	4	
KGD2	5	4		
RPS12	5	4		
RPS24A	5		4	
RPS25A	5		4	
RPS31	5		4	
SAH1	6		3	
STE23				9
UGP1				9
ARG1		8		
DED81		8		
HYP2		5	3	
MCR1		8		
MPC54		**8**		
PAB1	4		4	
SAR1	8			
RPL8B		1	6	1
RPS8A	2			6
PGM2				8
COX2		4	3	
DPS1		7		
MKT1	7			
RPL13A	7			
RPL18A	7			
RPL5	7			
VPH1		7		
ERG10			3	4
RNQ1			3	4
RPS2				7
ATP7	4		2	
DEF1	6			
RPL12A			6	
AAT2				6
PMU1				6

Table A1 (Continued): All protein identified by Mass Spectrometry.

	Wild Type		*cdc55mn*	
Name	No tag	Cdc14-TAP	No tag	Cdc14-TAP
RPN1				6
RPT3				6
VPS1				6
HXK2		5		
IDP1		5		
RPL17A	2		3	
RPS20	5			
GLC7				5
RVB2				5
COX5A	4			
DPM1			4	
FUM1			4	
GND1			4	
GSF2			4	
PET10	4			
RAS2		4		
RIM4	4			
RPL24A			4	
RPL36A	4			
RPS0A			4	
RPS19A	4			
RPS9A			4	
SAM2			4	
SIS1			4	
ERV25				4
GPD1			3	
OM14	3			
PPN1			3	
RPL17B		3		
RPL21A	3			
RPL9A	3			
RPL9B			3	
SOD2	3			
SSA4		2		1
POT1				3
DED1			2	
FUR1			2	
RFS1			2	
RPL38	2			
TUB3		2		
YCP4	2			
YHM2			2	
AAC1				2
ADY2			1	
BMH2	1			

Table A1 (Continued): All protein identified by Mass Spectrometry.

	Wild Type		*cdc55mn*	
Name	No tag	Cdc14-TAP	No tag	Cdc14-TAP
COX1			1	
GAS5			1	
YJL045W		1		

Table A1 (Continued): All protein identified by Mass Spectrometry.
Red = SPB components Blue = Cdc14 Purple = Cfi1/Net1

Appendix 2: Cdc14-TAP IP interactions in metaphase-arrested cells

A2.1: Mass Spectrometry results for Cdc14-TAP IP in metaphase I

	Wild Type	*cdc55mn*
Name	Cdc14-TAP	Cdc14-TAP
SPC110	**35**	**45**
CNM67	**24**	**45**
ACS1	26	39
NET1	**54**	**6**
SPC42	**27**	**31**
FAS1	19	35
HSP82	22	32
ATP1	25	29
CDC19	17	34
CDC14	**27**	**23**
ENO1	18	31
SSA1	20	29
TEF1	21	28
EFT1	20	28
FOX2	16	31
TDH3	19	28
PET9	20	27
PGK1	14	29
ALD4	17	24
FAS2	12	26
MLS1	8	28
ADH1	15	21
TOF2	35	
PCK1	15	19
QCR2	15	17
PDC1	9	22
POR1	13	18
RPS3	11	19
SPC29	**13**	**16**
SSC1	14	14
URA2	7	20
COR1	9	18
RPS1B	11	15
ICL1	6	19
GPM1	8	17
GUT2	13	12
GDH2	3	21
ACH1	4	20
FAA1	9	15
GPH1	5	18
RPL7A	7	16

	Wild Type	*cdc55mn*
Name	Cdc14-TAP	Cdc14-TAP
RPS4A	7	16
ACO1	8	15
GFA1	8	15
PMA2	9	14
NDI1	12	11
MPS2	**7**	**15**
BFA1	8	14
PIL1	8	14
IDP2	7	14
ADH2	6	14
FBA1	7	13
TPI1	7	13
OM45	8	12
RPS6A	8	12
RPS5	9	11
KAR2	5	14
CIT1	8	11
HSP60	10	9
HSP104	4	14
MDH1	5	13
ACT1	7	11
MIR1	8	10
SSB1		17
ACC1	4	13
CDC48	5	12
CHC1	5	12
RPL4A	5	12
CAR2	6	11
HHF1	6	11
RPL26A	6	11
KGD1	9	8
RPL8B		16
UGP1	1	15
RPS11A	5	11
SDH1	5	11
ILV5	6	10
PGI1	6	10
RPL2A	6	10
RPP0	7	9
SFC1	7	9
PFK1	1	14

Table A2.1: All protein identified by Mass Spectrometry.

	Wild Type	*cdc55mn*
Name	Cdc14-TAP	Cdc14-TAP
RPL3	3	12
SPS2	3	12
IDH1	5	10
RPS17A	5	10
BUB2	6	9
RPS16A	6	9
FAA2	2	12
HXK1	2	12
PGM2	2	12
FBP1	3	11
GLK1	3	11
TSA1	3	11
VMA2	3	11
ENO2	4	10
RPL1A	4	10
RPL19A	5	9
TUB2	5	9
RPL23A	6	8
LEU1	10	4
SSB2	14	
BMH1		13
SPO21		**13**
POX1	1	12
GND1	3	10
MDH2	3	10
ADY3	4	9
RPS18A	4	9
RPS25A	4	9
TKL1	4	9
ATP5	5	8
RPS8A	6	7
ERG6	7	6
HEF3		12
LSP1	2	10
PAB1	2	10
RPL16B	2	10
WTM1	2	10
FMP13	3	9
PES4	3	9
DPM1	4	8
RPL10	4	8
RPS0B	4	8
RPS24A	4	8
RPS9A	4	8
SDH2	4	8

	Wild Type	*cdc55mn*
Name	Cdc14-TAP	Cdc14-TAP
RPS14A	5	7
SPC72	**5**	**7**
TDH1	5	7
IDH2	7	5
SIR2	12	
RPN2	1	10
SSE1	1	10
CAT2	2	9
LPD1	2	9
CAR1	3	8
CIT2	3	8
IPP1	3	8
RPL18A	3	8
TUB1	3	8
ATP4	4	7
RPL24B	4	7
RPS13	4	7
TEF4	4	7
ATP7	5	6
RPL21A	5	6
RPL33A	5	6
SEC53	5	6
RPL6B		10
YSW1		10
RPN1	2	8
RPL5	3	7
RPS12	3	7
RPS19A	3	7
TIF1	3	7
ARF1	4	6
ATP3	4	6
MRP8	4	6
RPL27A	4	6
RPS20	4	6
RPS31	4	6
CIT3	6	4
RPL8A	7	3
BFR1		9
ETR1		9
HTB2		9
LSC2		9
PCS60		9
RPL13B		9
TAL1		9
CLU1	1	8

Table A2.1 (Continued): All protein identified by Mass Spectrometry.

	Wild Type	*cdc55mn*
Name	Cdc14-TAP	Cdc14-TAP
GUS1	1	8
POT1	1	8
RPL15A	1	8
DNM1	2	7
DPS1	2	7
FUM1	2	7
MIP6	2	7
RPL36B	2	7
VPH1	2	7
BBP1	**3**	**6**
CDC31	**3**	**6**
DAK1	3	6
DMC1	3	6
ERG10	3	6
PDH1	3	6
QCR7	3	6
RPL11B	3	6
RPL17A	3	6
RPL20A	3	6
RPT1	3	6
RTN1	3	6
YDJ1	3	6
COX2	4	5
FAA4	4	5
KGD2	4	5
OLA1	4	5
RPS1A	4	5
ODC1	6	3
APE2		8
CYS4		8
EMI2		8
MDH3		8
MET6		8
CPR1	1	7
ERG13	1	7
BAT2	2	6
RPL12A	2	6
RPL30	2	6
RVB2	2	6
SAH1	2	6
SEC14	2	6
TMA19	2	6
YAL018C	2	6
CYT1	3	5
PDI1	3	5

	Wild Type	*cdc55mn*
Name	Cdc14-TAP	Cdc14-TAP
PET10	3	5
PYC1	3	5
RPL14A	3	5
RPL35A	3	5
SSA2	3	5
COX6	4	4
RIP1	4	4
RPS15	4	4
HTB1	7	1
ABF2		7
NQM1		7
PDB1		7
RPL9B		7
RPS2		7
SHM2		7
TOM70		7
AAT2	1	6
CDC5	1	6
CRC1	1	6
GLC3	1	6
PSA1	1	6
RPS7A	1	6
SPS19	1	6
SUB2	1	6
UBA1	1	6
BGL2	2	5
CCT8	2	5
CWP1	2	5
GAS1	2	5
HXK2	2	5
PEX11	2	5
PST2	2	5
RPL38	2	5
SAM2	2	5
TPS1	2	5
YAT2	2	5
GPD1	3	4
LSC1	3	4
NCE102	3	4
NDC1	**3**	**4**
RPT3	3	4
SIK1	3	4
VTC4	3	4
HYP2	4	3
MPS3	**4**	**3**

Table A2.1 (Continued): All protein identified by Mass Spectrometry.

	Wild Type	*cdc55mn*		Wild Type	*cdc55mn*
Name	Cdc14-TAP	Cdc14-TAP	**Name**	Cdc14-TAP	Cdc14-TAP
ADE17		6	RPS23A	1	4
CAM1		6	RPT4	1	4
GDB1		6	RVB1	1	4
RPN8		6	SPO74	1	4
SEC24		6	YAT1	1	4
AMS1	1	5	ASC1	2	3
PEP4	1	5	AYR1	2	3
PFK2	1	5	DED1	2	3
SSA4	1	5	ERG20	2	3
THS1	1	5	GSP1	2	3
TMA29	1	5	GVP36	2	3
URA1	1	5	LEU4	2	3
YCP4	1	5	PHB2	2	3
YNK1	1	5	RPL31A	2	3
DON1	2	4	SOD2	2	3
RPL25	2	4	SSO1	2	3
RPS10A	2	4	RPA190	3	2
SEC4	2	4	RPS7B	3	2
SSA3	2	4	SAR1	3	2
TFP1	2	4	BMH2	4	1
YFR032C	2	4	RPL13A	5	
ARG1	3	3	ADE13		4
MCR1	3	3	ADE16		4
PHB1	3	3	ADE2		4
RNR4	3	3	ADK1		4
RPS27A	3	3	APE3		4
ADE6		5	ARP2		4
COF1		5	GUA1		4
CTA1		5	HMG1		4
CYS3		5	LAP3		4
FRS1		5	LAP4		4
KAP123		5	LAT1		4
NCP1		5	MBF1		4
SCP160		5	PRS3		4
SER1		5	RPL28		4
SMC3		5	RPN5		4
THR4		5	SEC61		4
ARP3	1	4	SUC2		4
CDC60	1	4	TCB3		4
HFD1	1	4	TUF1		4
HHT1	1	4	VMA13		4
HSC82	1	4	YEF3		4
NPL3	1	4	YEL020C		4
PUP2	1	4	ADE52C7	1	3
RPG1	1	4	ARC35	1	3

Table A2.1 (Continued): All protein identified by Mass Spectrometry.

	Wild Type	*cdc55mn*
Name	Cdc14-TAP	Cdc14-TAP
COX5A	1	3
CYB2	1	3
HOM2	1	3
MSC1	1	3
PHO88	1	3
PRX1	1	3
RPN10	1	3
RPN11	1	3
RPN9	1	3
RPT5	1	3
SES1	1	3
SOD1	1	3
SPR1	1	3
STO1	1	3
SUI2	1	3
TDH2	1	3
TUB4	**1**	**3**
VPS1	1	3
IME2	2	2
INO1	2	2
NUD1	**2**	**2**
PDA1	2	2
RHO1	2	2
RPS22A	2	2
SPC97	**2**	**2**
YMR031C	2	2
YOP1	2	2
RPL9A	3	1
ALA1		3
ARB1		3
ARO9		3
CCT3		3
CCT4		3
CDC28		3
CDC3		3
CDC33		3
CPR6		3
CYC1		3
DHH1		3
DUG1		3
FDH1		3
FET5		3
GRE3		3
GRX2		3
HOM6		3

	Wild Type	*cdc55mn*
Name	Cdc14-TAP	Cdc14-TAP
IDP3		3
IMD4		3
MET17		3
MUC1		3
PHO86		3
POL30		3
PRE5		3
PRE6		3
PRE7		3
PTC3		3
PUP3		3
QRI1		3
RIB4		3
RIM1		3
RPL32		3
RPN13		3
RPN7		3
RPS26A		3
RPT2		3
RPT6		3
SEC23		3
SER3		3
SPR3		3
SPS22		3
SSZ1		3
STI1		3
UGA1		3
WBP1		3
YET3		3
YHR202W		3
YNR034W		3
YPT7		3
ADE4	1	2
ADH3	1	2
CDC10	1	2
CMD1	**1**	**2**
HSP42	1	2
KRS1	1	2
LSB3	1	2
LYS20	1	2
NAP1	1	2
PRO3	1	2
RAS2	1	2
RPL43A	1	2
RTN2	1	2

Table A2.1 (Continued): All protein identified by Mass Spectrometry.

	Wild Type	*cdc55mn*
Name	Cdc14-TAP	Cdc14-TAP
SAC6	1	2
SBP1	1	2
SDH3	1	2
TRP5	1	2
YOR285W	1	2
YPT1	1	2
ACS2	2	1
ARG4	2	1
DEF1	2	1
DLD1	2	1
NBP1	2	1
PMT1	2	1
RHO3	2	1
RIM4	2	1
RPS29A	2	1
YRA1	2	1
NDE2	3	
AAC1		2
ADE3		2
AGX1		2
AHP1		2
ALD2		2
ARA1		2
ARC1		2
ARO1		2
ARO8		2
BAT1		2
BCY1		2
CCC1		2
CCT2		2
CCT6		2
CCT7		2
CDA2		2
CDC12		2
COP1		2
COX7		2
COX9		2
CPR3		2
DBP1		2
DCS1		2
DED81		2
ECM4		2
EFB1		2
EGD2		2
EHD3		2

	Wild Type	*cdc55mn*
Name	Cdc14-TAP	Cdc14-TAP
EMP24		2
ERG26		2
ERG9		2
ERV25		2
FPR3		2
GAD1		2
GCD11		2
GCV1		2
GET3		2
GND2		2
GSF2		2
GSY2		2
HEM2		2
HHO1		2
HMG2		2
HRR25		2
HSP12		2
HTA1		2
HTS1		2
HTZ1		2
ICL2		2
IFA38		2
KAP95		2
LYS1		2
MCK1		2
MPC54		2
NHP6B		2
NIP1		2
NUG1		2
NUS1		2
OST1		2
OYE2		2
PBI2		2
PCM1		2
PDS5		2
PFS1		2
PHO8		2
PMC1		2
PMT4		2
PRE1		2
PRE4		2
PRP43		2
PRS2		2
PUB1		2
QCR8		2

Table A2.1 (Continued): All protein identified by Mass Spectrometry.

	Wild Type	*cdc55mn*
Name	Cdc14-TAP	Cdc14-TAP
RFA1		2
RHR2		2
RKI1		2
RPL33B		2
RPL34A		2
RPL39		2
RPS28A		2
RPS30A		2
RRP5		2
RSP5		2
SAC1		2
SAM4		2
SCL1		2
SDS23		2
SEC21		2
SEC26		2
SEC31		2
SHE10		2
SIS1		2
SOL4		2
SPC98		**2**
SPR28		2
SSD1		2
SSP1		2
STE23		2
STE24		2
STT3		2
SUI3		2
SYP1		2
TGL4		2
TIF5		2
TOM22		2
TPD3		2
TPK1		2
TRR1		2
TSL1		2
TYS1		2
VAC8		2
VMA4		2
VPS21		2
YCK2		2
YET1		2
YHR113W		2
YIL108W		2
YKR018C		2

	Wild Type	*cdc55mn*
Name	Cdc14-TAP	Cdc14-TAP
YKT6		2
YMR099C		2
YMR196W		2
YNL045W		2
YNL134C		2
YOR251C		2
YPL225W		2
YPT31		2
ZUO1		2
ZWF1		**2**
ADH5	1	1
ADY2	1	1
CDA1	1	1
COX1	1	1
COX4	1	1
FMP10	1	1
FMP45	1	1
FPR1	1	1
GCD6	1	1
GSY1	1	1
HSL7	1	1
HYR1	1	1
ILV2	1	1
NHP2	1	1
NOP58	1	1
OM14	1	1
RPL17B	1	1
RPL6A	1	1
RPN6	1	1
RPP1B	1	1
RPP2A	1	1
SRP1	1	1
SUP45	1	1
TIM11	1	1
TOM40	1	1
VMA6	1	1
VMA8	1	1
YHB1	1	1
YPL260W	1	1
ALO1	2	
ATP17	2	
ILV3	2	
MDJ1	2	
PAA1	2	
RPS26B	2	

Table A2.1 (Continued): All protein identified by Mass Spectrometry.

	Wild Type	*cdc55mn*
Name	Cdc14-TAP	Cdc14-TAP
ACB1		1
ADO1		1
AFG3		1
AHA1		1
AIP1		1
ALG12		1
APT1		1
ARC18		1
ARE2		1
ARF2		1
ATG8		1
ATO3		1
ATP16		1
BDH1		1
BNA4		1
CAP2		1
CBF5		1
COX13		1
CRG1		1
CRP1		1
CST9		1
DBP5		1
DBP9		1
DOP1		1
DPB11		1
DPL1		1
ECM11		1
ECM33		1
ECM38		1
EGD1		1
ELP2		1
ENT3		1
ERV14		1
ERV29		1
FES1		1
FMP26		1
FPR2		1
GAS4		1
GAS5		1
GCV3		1
GCY1		1
GET1		1
GGC1		1
GID7		1
GIP4		1

	Wild Type	*cdc55mn*
Name	Cdc14-TAP	Cdc14-TAP
GLC7		1
GLO1		1
GNA1		1
GOR1		1
GPT2		1
GRS1		1
GRX4		1
GUK1		1
HEK2		1
HIM1		1
HOP1		1
HSP26		1
IDI1		1
IDP1		1
ILV6		1
IRC24		1
IST2		1
KAP120		1
KAR1		**1**
LSM1		1
LYS12		1
MAM3		1
MAM33		1
MCA1		1
MCM7		1
MEF1		1
MEK1		1
MET12		1
MGM101		1
MKT1		1
MLC1		1
MMF1		1
MNN10		1
MNN9		1
MPD1		1
MSR1		1
MSS4		1
MSS51		1
MTD1		1
MVD1		1
NAT1		1
NDE1		1
NDJ1		1
NSP1		1
NTF2		1

Table A2.1 (Continued): All protein identified by Mass Spectrometry.

	Wild Type	*cdc55mn*		Wild Type	*cdc55mn*
Name	Cdc14-TAP	Cdc14-TAP	**Name**	Cdc14-TAP	Cdc14-TAP
NUP120		1	SPE3		1
OST3		1	SPO73		1
PBP2		1	SPS4		1
PDR11		1	SSE2		1
PET100		1	SSH1		1
PEX8		1	SSO2		1
PFY1		1	SSS1		1
PIC2		1	STN1		1
PIR3		1	STU2		1
PMI40		1	SUP35		1
PNC1		1	SVF1		1
PPN1		1	SVP26		1
PRE3		1	TFP3		1
PRE8		1	TFS1		1
PRE9		1	TGL1		1
PRP19		1	THI20		1
PRS5		1	THR1		1
PRT1		1	TIF4631		1
PXA2		1	TKL2		1
REC8		1	TMA17		1
RET2		1	TOM20		1
RFS1		1	TOP2		1
RLI1		1	TPK2		1
RMD1		1	TRP3		1
RNQ1		1	TRX1		1
RNR2		1	UBP6		1
ROK1		1	UTR2		1
RPB4		1	VAS1		1
RPC40		1	VMA5		1
RPL24A		1	YBL029CA		1
RPN12		1	YBR285W		1
RPS30B		1	YCL057C-A		1
SBH2		1	YDL086W		1
SDH4		1	YDL144C		1
SEC17		1	YDL237W		1
SEC27		1	YGR054W		1
SEC62		1	YGR130C		1
SEC63		1	YGR250C		1
SEC66		1	YHR087W		1
SFT2		1	YLR225C		1
SGT2		1	YMR148W		1
SMC1		1	YNL115C		1
SMK1		1	YNL208W		1
SNA2		1	YNR021W		1
SNF4		1	YOR152C		1

Table A2.1 (Continued): All protein identified by Mass Spectrometry.

	Wild Type	***cdc55mn***
Name	Cdc14-TAP	Cdc14-TAP
YOR289W		1
YPL009C		1
YPR004C		1
YPR172W		1
YPT52		1
YSA1		1
ZSP1		1
ALT1	1	
ARG5%2C6	1	
ATP18	1	
ATP20	1	
ATP6	1	
BSC1	1	
CAF16	1	
CYB5	1	
GAL11	1	
GDE1	1	
GRX3	1	
GTT1	1	
HIS5	1	
ILS1	1	
IMD3	1	
PRB1	1	
SEC13	1	
SNU13	1	
SPO19	1	
YHM2	1	
YPL205C	1	
YPR010C-A	1	
YSH1	1	

Table A2.1 (Continued): All protein identified by Mass Spectrometry.

A2.2: Comparison of Cdc14-TAP IPs

	Meiotic cells					Metaphase I-arrested cells				
Name	Wild Type	*cdc55mn*	Norm. Wild Type	Norm. *cdc55mn*	Wild Type/ *cdc55mn*	Wild Type	*cdc55mn*	Norm. Wild Type	Norm. *cdc55mn*	Wild Type/ *cdc55mn*
CDC14	30	28	1.00	1.00	1.00	27.00	23.00	1.00	1.00	1.00
NET1	43	29	1.43	1.04	1.38	54.00	6.00	2.00	0.26	7.66
TUB4	14	16	0.47	0.57	0.82	1.00	3.00	0.04	0.13	0.28
SPC98	25	30	0.83	1.07	0.78	0.00	2.00	0.00	0.09	0.00
SPC97	28	38	0.93	1.36	0.69	2.00	2.00	0.07	0.09	0.85
SPC72	27	30	0.90	1.07	0.84	5.00	7.00	0.19	0.30	0.61
NUD1	8	9	0.27	0.32	0.83	2.00	2.00	0.07	0.09	0.85
CNM67	45	53	1.50	1.89	0.79	24.00	45.00	0.89	1.96	0.45
SPC42	36	40	1.20	1.43	0.84	27.00	31.00	1.00	1.35	0.74
SPC29	20	31	0.67	1.11	0.60	13.00	16.00	0.48	0.70	0.69
CMD1	9	8	0.30	0.29	1.05	1.00	2.00	0.04	0.09	0.43
SPC110	73	89	2.43	3.18	0.77	35.00	45.00	1.30	1.96	0.66
NDC1	18	18	0.60	0.64	0.93	3.00	4.00	0.11	0.17	0.64
MPS2	19	26	0.63	0.93	0.68	7.00	15.00	0.26	0.65	0.40
BBP1	22	18	0.73	0.64	1.14	3.00	6.00	0.11	0.26	0.43
KAR1	17	18	0.57	0.64	0.88	0.00	1.00	0.00	0.04	0.00
MPS3	26	20	0.87	0.71	1.21	4.00	3.00	0.15	0.13	1.14
CDC31	12	15	0.40	0.54	0.75	3.00	6.00	0.11	0.26	0.43
SFI1	15	16	0.50	0.57	0.88	0.00	0.00	0.00	0.00	1.00
MPC54	8	0	0.27	0.00	2667.67	0.00	2.00	0.00	0.09	0.00
SPO21	0	0	0.00	0.00	1.00	0.00	13.00	0.00	0.57	0.00

Table A2.2: Normalisation and comparison of Cdc14-TAP IP experiments.

Appendix 3: Mass Spectrometry results for LFQ proteomic analysis of Spc42-3FLAG IP

Label-free quantitation (LFQ) algorithms in MaxQuant were utilised by Juan Zou in the Juri Rappsilber lab (University of Edinburgh) to calculate the LFQ intensities indicated in Table A3. I normalized LFQ intensities for each protein to Spc42 LFQ intensity in the same sample. I then input the normalised data into Perseus software.

*Contaminant hits are excluded from Table A3.

	Wild Type samples			***cdc14-1* samples**		
Name	WT_1	WT_2	WT_3	CDC14_1	CDC14_2	CDC14_3
AAC1	0	172960000	221260000	101170000	0	176810000
AAT2	0	227930000	223080000	81213000	128810000	167800000
ABF2	0	0	0	0	0	35748000
ABP1	0	0	0	0	0	9656000
ACC1	19965000	48724000	34692000	0	48418000	25805000
ACH1	382850000	3271900000	2564400000	791310000	1635600000	1964400000
ACO1;ACO2	566870000	856310000	2823200000	886780000	1523600000	2229700000
ACS1	2041700000	1166900000	1178400000	3894400000	8110600000	7434000000
ACS2	713430000	557120000	321170000	799470000	639930000	572200000
ACT1	663230000	1836200000	1754200000	1239400000	2270100000	2730200000
ADA2	0	0	2164400	0	0	0
ADD66	0	0	0	12510000	0	0
ADE1	0	0	67202000	0	0	30095000
ADE12	0	0	13852000	0	0	0
ADE13	0	0	0	0	54632000	68418000
ADE17	0	42104000	53795000	0	32513000	116890000
ADE2	0	0	19944000	0	0	0
ADE3;MIS1	0	0	0	0	0	70359000
ADE5%2C7	0	0	0	0	40880000	28439000
ADE6	0	0	4983800	0	0	0
ADH1;ADH5	4451000000	1132500000	1463700000	4770800000	5992300000	1010500000

Table A3: LFQ intensities of Wild Type and *cdc14-1* samples.

	Wild Type samples			*cdc14-1* samples		
Name	WT_1	WT_2	WT_3	CDC14_1	CDC14_2	CDC14_3
ADH2	897910000	326380000	1072400000	194580000	285980000	511070000
ADH3	0	0	35134000	0	0	0
ADK1	0	0	65403000	0	41956000	41860000
ADO1	0	67732000	50946000	0	49843000	33921000
ADP1	0	14661000	0	0	0	0
ADY2	0	0	172260000	0	0	0
ADY3	0	225910000	144260000	0	170440000	0
AGX1	0	94624000	93909000	0	0	109020000
AHA1	0	0	8792200	0	0	0
AHC1	0	0	611630000	0	0	0
AHP1	0	75866000	70977000	88736000	77545000	127890000
ALA1	0	0	43155000	0	24650000	26916000
ALD2;ALD3	0	0	0	0	6730100	0
ALD4;ALD5	1833600000	4911200000	9625500000	2729100000	5104900000	5535100000
ALD6	0	0	19515000	0	0	0
AMS1	0	33441000	0	0	89760000	0
APA1	0	0	7196000	0	0	0
APE3	0	70028000	96111000	76346000	73565000	0
APL6	0	0	34260000	0	0	0
ARA1	0	0	144580000	77285000	0	103080000
ARB1	0	0	0	0	4139100	0
ARC1	0	0	0	0	41757000	0
ARC18	0	0	0	0	0	0
ARE2	10650000	0	0	0	0	0
ARF1	0	57818000	104200000	49899000	69629000	62897000
ARF2	0	0	24077000	0	0	0
ARG1	0	50054000	774030000	0	18313000	36551000
ARG3	0	0	21802000	0	0	0
ARG4	0	0	90718000	0	0	0
ARO1	0	0	0	0	0	33036000
ARO4;ARO3	0	43994000	32606000	0	0	41977000
ARO8	0	0	10797000	0	0	0
ARP2	0	0	25259000	20111000	24049000	0
ARP3	0	0	0	0	0	0
ARP4	22481000	0	0	0	0	0
ASC1	366920000	253510000	549360000	254820000	368080000	482230000

Table A3 (Continued): LFQ intensities of Wild Type and *cdc14-1* samples.

	Wild Type samples			*cdc14-1* samples		
Name	WT_1	WT_2	WT_3	CDC14_1	CDC14_2	CDC14_3
ASK10	0	0	0	0	18289000	0
ASN2;ASN1	0	0	0	0	0	32963000
ATO2	0	0	0	0	0	28404000
ATO3	0	0	0	0	0	2213600
ATP1	1627000000	3405600000	4134600000	2104600000	3185400000	3856600000
ATP15	0	0	19468000	0	0	0
ATP17	0	129930000	102490000	0	85097000	82500000
ATP20	0	27959000	0	0	0	0
ATP3	162170000	252630000	403170000	201630000	260660000	294330000
ATP4	0	73100000	286050000	47965000	67549000	216140000
ATP5	0	163930000	387080000	0	196570000	206330000
ATP7	0	129000000	382710000	0	166270000	203690000
AVO1	0	4560300	0	0	0	0
AXL1	0	0	0	0	0	0
BAT1	0	0	35908000	0	0	0
BAT2	0	0	158820000	46388000	102950000	165300000
BBP1	2530100000	0	161830000	289590000	38416000	186590000
BCY1	0	0	48190000	0	0	26107000
BFA1	2320200000	354950000	75314000	312550000	831560000	374040000
BFR1	0	0	0	0	0	10617000
BGL2	55318000	0	97300000	92903000	48352000	66401000
BLM10	0	0	2866900	0	0	0
BMH1	216760000	732400000	601030000	510110000	1543800000	569240000
BMH2	0	155100000	122130000	0	253530000	91144000
BNA4	0	0	10868000	0	0	0
BOS1	0	0	0	0	0	0
BRE1	114700000	0	0	0	0	0
BRL1	0	0	0	0	0	0
BRX1	0	6023300	0	0	0	0
BUB2	3863000000	714520000	463000000	843220000	1274300000	873870000
CAR1	0	0	98050000	0	95948000	0
CAR2	0	454790000	799810000	63132000	216230000	358600000
CAT2	64645000	318400000	304320000	129400000	226660000	226760000
CBF5	360750000	310520000	40317000	187370000	207190000	261140000

Table A3 (Continued): LFQ intensities of Wild Type and *cdc14-1* samples.

	Wild Type samples			*cdc14-1* samples		
Name	WT_1	WT_2	WT_3	CDC14_1	CDC14_2	CDC14_3
CBR1	0	0	0	0	0	0
CCT2	0	0	10517000	0	0	0
CCT3	0	0	0	0	7275400	0
CCT4	12190000	0	0	0	0	0
CCT6	0	0	0	0	14075000	0
CCT7	0	0	0	0	0	9480500
CCT8	0	0	8388000	0	0	0
CDC10	0	0	0	0	28501000	0
CDC12	0	0	9156700	0	0	0
CDC14	476970000	116680000	400840000	175120000	261380000	198920000
CDC19;PYK2	3185200000	4556100000	6324200000	3483400000	3116400000	6488400000
CDC28	0	0	0	0	0	9862600
CDC31	3250100000	477760000	291120000	614730000	343790000	413720000
CDC33	188070000	58246000	0	235810000	73628000	105030000
CDC48	0	72950000	277530000	60544000	80950000	139190000
CDC5	0	0	0	0	81499000	19910000
CDC60	0	0	11660000	0	0	0
CHC1	0	42268000	0	0	28526000	38869000
CHL4	5770600	0	0	0	0	0
CIC1	3698400	0	0	0	0	0
CIT1	484310000	1748000000	2372700000	888410000	1388300000	1957100000
CIT2	42585000	385600000	239450000	56838000	100750000	161200000
CIT3	0	236340000	144800000	83570000	85881000	180460000
CLU1	0	0	0	0	0	19407000
CMD1	18114000	0	0	0	0	0
CNM67	2314700000	6608900000	3925000000	1206000000	1321600000	5838900000
COF1	0	0	75309000	0	0	0
COG6	0	0	19460000	0	0	0
COP1	0	0	0	0	0	0
COR1	210160000	455200000	724190000	234420000	362950000	566940000
COX1	0	0	121590000	0	0	0
COX13	0	0	4318100	0	0	0
COX2	120960000	289050000	442430000	167140000	228100000	337870000
COX4	0	0	5984500	0	0	0
COX5A	0	0	21242000	0	0	55250000
COX9	0	0	43776000	0	0	0
CPA2	0	0	28110000	0	0	0

Table A3 (Continued): LFQ intensities of Wild Type and *cdc14-1* samples.

	Wild Type samples			*cdc14-1* samples		
Name	WT_1	WT_2	WT_3	CDC14_1	CDC14_2	CDC14_3
CPR1	0	119480000	148730000	51330000	89353000	218040000
CPR3	0	0	0	0	8884100	0
CPR6	0	0	0	0	0	0
CPS1	58875000	0	46975000	37288000	61054000	0
CRC1	0	34963000	64816000	0	24201000	24691000
CRN1	0	0	0	0	0	0
CST9	0	151460000	0	0	45644000	0
CTA1	0	102250000	53558000	0	82675000	0
CTF3	10995000	0	0	0	0	0
CUP5	17309000	0	0	0	0	0
CYB2	0	0	131490000	0	0	0
CYC1;CYC7	27741000	158330000	159260000	0	149770000	122090000
CYS3	0	0	18880000	0	42866000	0
CYS4	0	0	72279000	0	0	0
CYT1	0	0	74523000	0	0	29206000
DBF20;DBF2	44592000	0	0	0	0	0
DBP1	0	0	0	0	37608000	0
DBP3	175820000	0	0	0	0	0
DBP9	14708000	0	0	0	0	0
DCS1	0	27229000	50402000	0	0	42611000
DCS2	0	0	0	0	0	0
DDI1	0	0	8590200	0	0	0
DED1	279670000	169270000	119690000	120190000	1010900000	202230000
DED81	0	0	0	0	0	0
DHH1	0	0	4838400	0	0	0
DIP2	0	0	0	0	0	0
DLD1	0	0	20240000	0	40765000	11337000
DMC1	0	105420000	62708000	43513000	227610000	0
DNM1	0	6836500	0	0	0	0
DOT5	0	0	0	0	0	0
DPM1	73164000	83787000	50689000	0	80818000	41664000
DPS1	0	53688000	120480000	0	48909000	49416000
DUG1	0	0	40854000	0	0	0
ECM14	18112000	109900000	119160000	299430000	385850000	208360000
ECM8	0	0	0	0	0	0
EFB1	0	0	67952000	0	0	0
EFT1;EFT2	1991000000	2558800000	3409500000	2377700000	3205100000	3334600000

Table A3 (Continued): LFQ intensities of Wild Type and *cdc14-1* samples.

	Wild Type samples			*cdc14-1* samples		
Name	WT_1	WT_2	WT_3	CDC14_1	CDC14_2	CDC14_3
EGD1	0	0	9287200	0	0	0
EGD2	0	0	57789000	0	0	0
EHD3	0	7011900	0	0	0	0
EMG1	29552000	0	0	0	0	0
EMI2	0	0	0	0	0	0
ENO1	2114100000	9302200000	1326000000	4474800000	4505200000	1015400000
ENO2	1399800000	2921300000	5127800000	2882200000	2347400000	5074900000
ERB1	0	34178000	0	0	0	29659000
ERG10	66583000	186310000	492860000	138700000	308020000	298770000
ERG13	74055000	210020000	198610000	0	260760000	232550000
ERG2	0	0	37920000	0	0	0
ERG20	0	0	29178000	0	41439000	33480000
ERG28	0	0	1441100	0	0	0
ERG6	65033000	61483000	98594000	0	122300000	89043000
ERG9	0	0	23849000	0	0	0
ERP1	12598000	0	0	0	0	0
ERV14	0	0	0	0	0	0
ERV25	0	23290000	0	0	0	0
ETR1	0	0	59881000	0	0	0
FAA1	0	47904000	0	0	61579000	0
FAA2	53073000	535630000	72801000	0	208240000	289740000
FAA4;FAA3	0	0	0	0	0	0
FAR8	87656000	861160000	185040000	633450000	233600000	960200000
FAS1	275520000	379490000	527510000	171360000	322120000	541730000
FAS2	120610000	215420000	305380000	149970000	181860000	298080000
FBA1	1176600000	3019300000	7390000000	2879500000	2912000000	5219700000
FBP1	0	559430000	815720000	265750000	368630000	439350000
FIG1	0	0	0	0	0	0
FMP13	0	0	54036000	0	0	0
FMP29	0	0	11535000	0	0	0
FOX2	54627000	960060000	364930000	0	454310000	295880000
FPR1	0	0	30783000	0	0	0
FPR3;FPR4	126670000	0	0	0	0	0
FRS1	0	6053200	0	0	0	0
FUM1	112970000	258720000	369820000	192490000	193340000	351260000

Table A3 (Continued): LFQ intensities of Wild Type and *cdc14-1* samples.

	Wild Type samples			*cdc14-1* samples		
Name	WT_1	WT_2	WT_3	CDC14_1	CDC14_2	CDC14_3
FUR1	0	0	18747000	0	0	0
FYV6	0	0	0	0	0	0
GAR1	29360000	0	0	0	0	0
GAS1	0	25612000	40074000	23464000	55317000	19402000
GCD11	0	0	15092000	0	0	46435000
GCV1	0	0	56730000	0	22491000	34603000
GDH1	85921000	0	243080000	75544000	55647000	0
GDH2	0	0	0	0	56748000	34130000
GDI1	0	0	0	0	0	31409000
GFA1	93329000	91653000	88277000	60513000	173590000	71504000
GLC3	0	0	0	0	26110000	0
GLC7	0	0	35171000	0	0	0
GLE2	8352500	0	0	0	0	0
GLK1	52760000	243220000	475610000	183560000	142740000	354790000
GLN1	0	0	0	115680000	111770000	111480000
GLR1	0	0	0	0	16160000	11252000
GND1	0	0	0	0	27195000	0
GPD1	0	301430000	297550000	201420000	287340000	368190000
GPD2	25966000	102390000	16703000	71727000	88441000	55531000
GPH1	0	229610000	281740000	170640000	155220000	298700000
GPM1	1249200000	2904500000	3368100000	1623000000	1738800000	2961100000
GPR1	0	0	2482400000	0	0	0
GRE3	0	0	9401300	0	0	0
GRS1;GRS2	0	0	5443900	0	0	0
GRX2	0	63399000	0	0	26763000	0
GRX4;GRX3	0	0	150340000	0	0	0
GSC2;FKS1	0	0	0	0	18775000	0
GSP2;GSP1	134660000	174550000	80945000	113070000	219130000	67604000
GSY2;GSY1	0	0	27042000	0	0	23650000
GUK1	0	0	37612000	0	0	0
GUS1	79251000	120320000	152340000	60362000	106690000	154290000
GUT2	0	158900000	333990000	33504000	65752000	156290000
GVP36	0	0	38849000	0	0	0
HAP1	0	0	0	0	0	0

Table A3 (Continued): LFQ intensities of Wild Type and *cdc14-1* samples.

	Wild Type samples			*cdc14-1* samples		
Name	WT_1	WT_2	WT_3	CDC14_1	CDC14_2	CDC14_3
HAS1	0	0	0	0	0	0
HEM2	0	0	43240000	0	0	0
HFD1	0	0	24666000	0	0	0
HHF1;HHF2	804050000	1826400000	926790000	3122800000	391600000	594710000
HHT1;HHT2	279840000	1001400000	151750000	609440000	270040000	115550000
HIS1	0	0	27137000	0	0	0
HIS5	0	0	7421600	0	0	0
HMF1	0	0	0	0	0	1402800
HMG1;HMG2	64668000	0	0	0	0	0
HOM2	33752000	84185000	393950000	53759000	33786000	92784000
HOM6	0	74931000	95691000	61355000	56423000	100740000
HRB1	0	4792100	0	0	0	0
HRK1	8676800	0	0	0	0	0
HSC82	698810000	1350200000	1943900000	940760000	1590300000	1412900000
HSL7	227950000	412870000	93041000	470730000	575930000	719880000
HSP104	0	0	51052000	0	45290000	38190000
HSP42	0	191000000	69366000	52096000	149210000	43171000
HSP60	262470000	465190000	728570000	325210000	622750000	621220000
HSP82	0	78047000	145880000	0	67623000	75223000
HTA1;HTA2	298520000	1404700000	811050000	1457500000	550950000	434990000
HTB1	0	0	29521000	0	0	0
HTB2	659070000	2512000000	954630000	248780000	111900000	897310000
HTZ1	0	0	0	0	19825000	0
HUA2	0	901210000	126600000	0	0	37291000
HXK1	101920000	687590000	968490000	221220000	250820000	583270000
HXK2	0	0	69982000	0	58649000	84291000
HXT5;HXT4	21461000	0	110850000	0	0	55645000
HYP2;ANB1	140590000	395050000	689020000	176720000	461040000	585800000
HYR1;GPX2	0	0	0	0	0	0
ICL1	834500000	2964900000	3338500000	1350200000	2819300000	2680700000
ICL2	0	0	0	0	0	34556000
IDH1	280450000	546810000	590540000	462540000	515990000	568370000

Table A3 (Continued): LFQ intensities of Wild Type and *cdc14-1* samples.

	Wild Type samples			*cdc14-1* samples		
Name	WT_1	WT_2	WT_3	CDC14_1	CDC14_2	CDC14_3
IDH2	393860000	528790000	1064300000	423180000	409370000	737800000
IDP1	0	110400000	167690000	0	66767000	148200000
IDP2;IDP3	103650000	563430000	1135000000	519520000	638130000	1073300000
IFM1	0	0	0	0	0	0
ILS1	0	5119800	0	0	0	0
ILV1	0	0	24406000	0	0	0
ILV2	105800000	100910000	379890000	0	51598000	89337000
ILV3	0	0	41457000	0	0	0
ILV5	223590000	344150000	630780000	262120000	186580000	317140000
ILV6	0	0	431150000	0	0	56794000
IMD4;IMD3	0	0	33113000	0	0	0
IMP3	21864000	0	0	0	0	0
IMP4	22630000	0	0	0	0	0
INO1	0	158790000	198030000	196910000	144340000	301010000
INP1	0	0	0	0	0	0
IPP1	93509000	173520000	546840000	176810000	255210000	303500000
IRC24	0	0	20344000	0	0	0
IRC3	0	0	0	0	0	0
IVY1	33650000	0	0	0	0	0
KAP123	0	48912000	76545000	0	0	46137000
KAP95	0	0	0	0	14407000	0
KAR1	1622100000	409160000	209460000	524260000	262360000	263960000
KAR2	455280000	265420000	339710000	498850000	506360000	344890000
KES1	0	0	24166000	0	0	0
KGD1	191470000	377620000	629760000	545250000	293910000	538840000
KGD2	76633000	248290000	300730000	166030000	213020000	264540000
KIN2;KIN1	165690000	0	0	0	0	0
KOG1	0	174590000	0	0	37790000	68316000
KRE33	12134000	0	0	0	0	0
KRI1	15276000	0	0	0	0	0
KRR1	19817000	0	0	0	0	0
KRS1	0	0	52716000	0	0	62075000
KSP1	0	16852000	0	0	0	0
KTR3	0	0	619980000	0	0	0

Table A3 (Continued): LFQ intensities of Wild Type and *cdc14-1* samples.

	Wild Type samples			*cdc14-1* samples		
Name	WT_1	WT_2	WT_3	CDC14_1	CDC14_2	CDC14_3
LAP3	0	43207000	65208000	0	65705000	64765000
LAP4	0	0	0	0	50124000	0
LAT1	0	0	56474000	0	0	0
LEU1	168560000	99653000	609880000	0	0	0
LEU4;LEU9	0	73024000	117710000	0	46883000	78293000
LPD1	45763000	267000000	338990000	203650000	222170000	286780000
LRO1	0	0	0	0	0	0
LSB3	0	0	0	0	23045000	17626000
LSC1	0	85160000	186600000	0	94425000	149920000
LSC2	0	136170000	254270000	148460000	172520000	194630000
LSP1	49904000	117230000	168720000	121150000	194190000	172900000
LST8	0	176470000	13036000	0	0	80782000
LUG1	105220000	0	0	0	0	0
LYS12	0	0	15097000	0	0	0
LYS21;LYS20	0	0	61100000	0	0	0
MAK21	11721000	0	0	0	0	0
MAM33	0	0	0	0	0	14742000
MBF1	0	36679000	25275000	29486000	78607000	33213000
MCM21	0	0	0	0	0	0
MCR1	0	101310000	310170000	0	88313000	243200000
MDH1	156660000	695700000	1167800000	315000000	640940000	912470000
MDH2	320630000	1035600000	1506100000	741000000	979430000	771630000
MDH3	0	0	202540000	0	0	0
MDJ1	16124000	0	0	0	0	0
MEK1	0	0	0	0	92107000	0
MEP2	0	0	0	0	8030700	0
MET17	0	0	196290000	0	63864000	63161000
MET6	0	0	130930000	36736000	114940000	137010000
MFT1	0	0	0	0	0	0
MGM101	0	37701000	0	0	0	0
MIR1	376470000	375900000	969040000	468410000	451250000	463570000
MKT1	0	75304000	58209000	0	0	48130000
MLC1	0	0	0	0	0	0
MLP1	100340000	0	0	0	0	0

Table A3 (Continued): LFQ intensities of Wild Type and *cdc14-1* samples.

	Wild Type samples			*cdc14-1* samples		
Name	WT_1	WT_2	WT_3	CDC14_1	CDC14_2	CDC14_3
MLP2	14865000	0	0	0	0	0
MLS1;DAL7	894990000	3066900000	2660100000	981040000	2474100000	1941100000
MOB1	10905000	0	0	0	0	0
MPC54	0	0	0	0	49674000	0
MPP10	0	0	0	0	0	0
MPS2	2898400000	321340000	663720000	1107300000	226780000	625480000
MPS3	1011200000	305890000	261820000	116920000	205860000	341120000
MRH1;YRO2	36345000	0	0	0	49768000	27709000
MRPL20	16703000	0	0	0	0	0
MRPL31	0	0	0	41973000	0	0
MRPL32	10102000	0	0	0	0	0
MRPL36	31348000	0	0	0	0	0
MSH4	0	0	0	0	0	0
MSS116	101820000	67789000	64381000	104440000	66218000	118190000
MSS51	0	0	0	0	0	0
MUC1	62282000	0	0	0	0	0
MVD1	0	6200200	0	0	0	0
MYO2	0	1112100000	0	40391000	30113000	779360000
MYO4	0	0	0	0	0	0
NAM7	0	0	0	0	0	3575000
NAN1	37976000	0	0	0	0	0
NAP1	0	0	4516500	0	0	0
NAT1	0	0	2270600	0	0	0
NBP1	789870000	0	0	0	0	0
NCE102	14909000	0	0	0	13719000	0
NCP1	0	0	19366000	0	0	0
NDC1	1355200000	81465000	57227000	130570000	67360000	157360000
NDI1	0	52444000	128340000	0	55359000	64755000
NDJ1	0	25843000	0	0	16405000	0
NET1	185380000	1257000000	256600000	0	68721000	0
NHP2	223510000	170940000	71302000	118970000	128410000	61974000
NIC96	96460000	0	13921000	0	0	0
NIP7	9719700	0	0	0	0	0
NMA1;NMA2	0	0	0	0	0	14795000
NOP1	5315600000	1766100000	739020000	3567300000	2803100000	1679700000
NOP10	16466000	0	0	0	0	0

Table A3 (Continued): LFQ intensities of Wild Type and *cdc14-1* samples.

	Wild Type samples			*cdc14-1* samples		
Name	WT_1	WT_2	WT_3	CDC14_1	CDC14_2	CDC14_3
NOP13	4039600	0	0	0	0	0
NOP15	0	0	0	0	0	0
NOP4	0	0	0	0	0	0
NOP58	1060700000	735030000	205990000	698380000	580000000	452170000
NOP8	10738000	0	0	0	0	0
NPL3	5257000000	3483200000	1795300000	3443000000	7139700000	2542400000
NSP1	15938000	0	0	0	0	0
NUD1	1852700000	134530000	52715000	141200000	291980000	211590000
NUM1	0	0	0	0	0	0
NUP170	34252000	0	0	0	0	0
NUP57	58619000	0	0	0	0	0
NUP82	0	0	0	0	0	0
NUP84	10775000	0	0	0	0	0
ODC1	0	0	54281000	0	0	0
OLA1	167910000	123180000	148760000	68176000	75907000	168810000
OM14	0	76909000	247530000	0	0	120180000
OM45	0	75014000	44508000	0	61021000	43265000
ORC6	0	0	80357000	0	0	0
OYE2	0	24345000	68641000	0	0	0
PAB1	185500000	2463000000	557540000	213840000	816720000	596180000
PBI2	0	0	9931300	0	0	0
PBP1	4926300	0	0	0	0	0
PBP2	0	1773800	0	0	0	0
PCA1	0	0	0	0	0	0
PCH2	0	0	0	0	9765100	0
PCK1	1206900000	6417400000	6490500000	2648400000	4017700000	5366900000
PCS60	0	0	0	0	34220000	0
PDA1	0	0	54549000	0	0	33351000
PDB1	71613000	210230000	246940000	78446000	126430000	203950000
PDC1;PDC6;THI3	3231000000	3842400000	4845500000	3978600000	3206200000	4030000000
PDC5	0	0	0	0	0	0
PDH1	105940000	522100000	522790000	213810000	264450000	456260000
PDI1	0	0	0	0	27533000	0
PDR10	0	71811000	0	0	0	0
PDR11	0	0	0	0	0	0
PEP4	0	0	78969000	0	0	0
PET10	0	0	78591000	0	0	104880000

Table A3 (Continued): LFQ intensities of Wild Type and *cdc14-1* samples.

	Wild Type samples			*cdc14-1* samples		
Name	WT_1	WT_2	WT_3	CDC14_1	CDC14_2	CDC14_3
PET123	0	0	70975000	0	0	0
PET9;AAC3	987190000	1294600000	2868700000	888650000	1366500000	2347400000
PEX11	0	41244000	0	0	0	0
PFK1	51390000	70059000	116780000	57988000	98412000	148420000
PFK2	98602000	240790000	133890000	129510000	244660000	158780000
PFY1	0	0	0	0	0	37773000
PGI1	202180000	503790000	771910000	393350000	367580000	692460000
PGK1	1674900000	7691800000	12714000000	3899600000	4806600000	7617600000
PGM2;PGM1	0	139610000	214350000	88271000	143120000	161380000
PHB1	0	0	0	0	0	0
PHB2	3593000	0	0	0	0	0
PHO8	0	0	30670000	0	0	0
PHO86	9594300	0	0	0	0	0
PHO88	0	64659000	23827000	0	0	0
PIH1	0	0	0	25724000	0	0
PIL1	313400000	734750000	549400000	367310000	525920000	707400000
PMA2	2589600000	1525800000	2033200000	1269100000	3124100000	2784700000
PMI40	0	0	0	0	3966200	0
PMT2	0	2684000	0	0	0	0
POL30	0	0	11575000	0	0	0
POM152	100900000	0	0	0	0	0
POR1	1525500000	2952700000	3240100000	1073900000	1855500000	2000100000
POT1	0	24560000	31091000	0	41354000	40395000
POX1	0	128530000	26624000	0	889360000	0
PPN1	0	103830000	87256000	180320000	173260000	115620000
PRB1	27595000	43213000	42119000	15610000	120820000	21680000
PRE1	71270000	107830000	80871000	131760000	128320000	96222000
PRE10	0	57199000	0	0	148150000	32458000
PRE2	0	22421000	4776600	0	30454000	5728300
PRE3	0	57453000	72373000	92021000	85417000	91900000
PRE4	0	72589000	52882000	128890000	164440000	106740000
PRE5	92871000	129320000	103970000	239830000	118730000	147210000
PRE6	43341000	66556000	100550000	102100000	0	108100000

Table A3 (Continued): LFQ intensities of Wild Type and *cdc14-1* samples.

	Wild Type samples			*cdc14-1* samples		
Name	WT_1	WT_2	WT_3	CDC14_1	CDC14_2	CDC14_3
PRE7	0	0	0	62756000	0	95132000
PRE9	93849000	160950000	161280000	305830000	264260000	250550000
PRO3	0	0	0	0	0	0
PRP43	254560000	0	0	0	27639000	0
PRT1	0	0	0	0	0	0
PRX1	0	0	45490000	0	63487000	0
PSA1	55566000	56449000	250970000	0	36696000	90573000
PSP2	0	22318000	0	0	25348000	0
PST2	72162000	112110000	261120000	125460000	129290000	201800000
PUP1	0	16615000	0	0	0	17949000
PUP2	0	58177000	0	104970000	77696000	71491000
PUP3	0	0	0	67068000	69333000	32576000
PWP2	8780200	0	0	0	0	0
PXA2	0	11661000	0	0	0	0
PXR1	108290000	0	0	0	0	0
PYC2;PYC1	51000000	182350000	236220000	116340000	195670000	141800000
QCR10	0	0	1631200	0	0	0
QCR2	336650000	709760000	1249500000	436090000	507430000	841520000
QCR7	0	0	105110000	0	0	0
QCR8	0	0	51791000	0	0	0
RAD52	0	18019000	0	0	13892000	6850400
RAP1	0	8524500	0	0	0	0
RCL1	4484400	0	0	0	0	0
RER1	0	0	0	0	0	0
RET2	6496900	0	0	0	0	0
RHO1	0	0	25779000	0	0	0
RIB4	0	63802000	126880000	0	48581000	61623000
RIM1	0	0	0	0	25935000	0
RIM4	0	1441700000	134220000	232750000	385580000	104760000
RIO1	2071400	0	0	0	0	0
RIP1	0	140730000	267870000	0	185270000	106410000
RKI1	0	48625000	118170000	0	50575000	118330000
RKR1	0	0	0	0	0	1327900000
RMD1	0	10632000	0	0	0	0
RNA1	0	0	9435500	0	0	0

Table A3 (Continued): LFQ intensities of Wild Type and *cdc14-1* samples.

	Wild Type samples			*cdc14-1* samples		
Name	WT_1	WT_2	WT_3	CDC14_1	CDC14_2	CDC14_3
RNR4	0	0	96552000	0	0	0
ROK1	0	0	0	0	0	0
RPA34	230180000	0	0	0	0	0
RPA49	0	0	0	0	0	0
RPG1	0	0	0	0	7369200	0
RPL10	1758100000	1488300000	1212900000	975680000	1492500000	1135700000
RPL11B; RPL11A	821120000	378620000	465980000	353910000	825440000	457200000
RPL12A; RPL12B	367030000	390060000	755780000	456440000	476800000	629670000
RPL13A; RPL13B	961560000	876440000	465780000	732360000	1092000000	473190000
RPL14A; RPL14B	699030000	346930000	816950000	508320000	558700000	578920000
RPL15A; RPL15B	198810000	141380000	97637000	144740000	0	103130000
RPL16B	764480000	398190000	413210000	743850000	367390000	405440000
RPL17A	0	0	0	0	295840000	0
RPL17B	1072200000	749870000	708670000	882490000	1379000000	826590000
RPL18A; RPL18B	318890000	221670000	144430000	346170000	153020000	120670000
RPL19A; RPL19B	1114800000	626690000	396240000	909460000	322650000	341240000
RPL1A;RPL1B	692580000	537330000	807240000	531540000	736060000	631390000
RPL20A; RPL20B; UTP20	799430000	727770000	1004800000	781880000	882090000	1004800000
RPL21A	0	0	150420000	0	0	0
RPL21B	1515600000	655590000	361510000	588070000	917380000	352730000
RPL22A; RPL22B	0	0	77529000	0	54718000	0
RPL23A; RPL23B	460720000	312910000	435470000	383690000	346990000	452030000
RPL24A	0	0	0	109460000	0	0
RPL24B	892770000	346440000	138050000	833790000	270250000	225930000
RPL25	632920000	630600000	571570000	667460000	710090000	655940000
RPL26A; RPL26B	2389600000	4381700000	4274800000	1512600000	8943500000	5636100000
RPL27A; RPL27B	1206200000	456240000	603570000	738020000	860830000	519150000
RPL28	768280000	381200000	310880000	370210000	346540000	263290000

Table A3 (Continued): LFQ intensities of Wild Type and *cdc14-1* samples.

	Wild Type samples			*cdc14-1* samples		
Name	WT_1	WT_2	WT_3	CDC14_1	CDC14_2	CDC14_3
RPL29	22848000	0	0	0	3097000	0
RPL2A;RPL2B	1939000000	1312000000	1048500000	1667900000	1612000000	1015200000
RPL3	1810100000	1181500000	4945000000	6821400000	1084900000	4813500000
RPL30	36144000	29453000	46170000	31367000	37841000	34017000
RPL31A; RPL31B	30237000	16396000	15466000	16549000	30167000	17094000
RPL32	994400000	549750000	221070000	443000000	643230000	268410000
RPL33A	39810000	37098000	27539000	34146000	25771000	28080000
RPL34A; RPL34B	26666000	17053000	11144000	24415000	17426000	12216000
RPL35A; RPL35B	20997000	10508000	66888000	20374000	42205000	16315000
RPL36B; RPL36A	38446000	18285000	21946000	47677000	24350000	23656000
RPL37A	13154000	0	0	0	0	0
RPL37B	0	11489000	3923900	0	13345000	7758500
RPL38	881500000	709120000	1174300000	1504400000	1005900000	959860000
RPL39	1376000000	567690000	436680000	1665100000	928270000	590300000
RPL40A; RPL40B; UBI4	0	0	5192600	0	0	0
RPL42A; RPL42B	234800000	94230000	11329000	59680000	55168000	48716000
RPL43A; RPL43B	114640000	62621000	58010000	55815000	191460000	36984000
RPL4A;RPL4B	2148200000	1413900000	1861000000	1325200000	1856500000	1743100000
RPL5	172910000	212810000	184190000	191680000	184410000	233960000
RPL6A	0	0	158580000	77485000	93406000	115850000
RPL6B	220190000	238260000	320930000	195260000	307700000	279450000
RPL7A;RPL7B	590410000	501440000	558280000	594770000	549780000	531850000
RPL8A	45532000	81162000	77494000	49764000	89108000	79127000
RPL8B	499770000	701950000	594380000	525150000	990810000	618020000
RPL9A	446120000	135360000	169810000	255350000	268690000	141670000
RPL9B	2554000000	852050000	1591000000	2744200000	1181500000	1156500000
RPN1	0	64630000	0	0	39062000	0
RPN10	0	0	0	0	0	0
RPN11	0	0	0	0	13888000	0

Table A3 (Continued): LFQ intensities of Wild Type and *cdc14-1* samples.

	Wild Type samples			*cdc14-1* samples		
Name	WT_1	WT_2	WT_3	CDC14_1	CDC14_2	CDC14_3
RPN2;ECM17	0	0	17319000	0	21322000	0
RPN3	0	14515000	0	0	28012000	14557000
RPN5	0	18868000	0	0	75727000	0
RPN6	0	0	0	0	60684000	0
RPN8	0	0	13516000	0	0	0
RPP0	950600000	830040000	1224800000	648040000	1054900000	976850000
RPP1B	8628700	0	0	0	0	0
RPS0B;RPS0A	563080000	565500000	969070000	571290000	653050000	856670000
RPS10A;RPS10B	92808000	0	77814000	0	95951000	75264000
RPS11A;RPS11B	2073600000	1050100000	880610000	1268600000	1496800000	967500000
RPS12	295150000	300360000	376430000	176650000	437640000	403090000
RPS13	1245500000	726510000	851400000	932890000	957450000	799430000
RPS14A	1083300000	688220000	652680000	633230000	872960000	589130000
RPS14B	0	0	5999500	0	0	0
RPS15	406890000	482760000	387750000	523710000	657810000	563630000
RPS16A;RPS16B	653510000	403690000	600970000	427800000	776040000	591650000
RPS17A;RPS17B	432670000	212510000	291490000	415110000	285860000	244040000
RPS18A;RPS18B	751920000	443070000	496730000	402460000	630190000	432560000
RPS19B;RPS19A	276030000	338690000	577570000	314380000	586410000	578890000
RPS1A	1358700000	799590000	1026700000	1085300000	1096000000	792620000
RPS1B	191630000	139290000	138820000	158180000	174430000	172740000
RPS2	251000000	198080000	190930000	215030000	167460000	165610000
RPS20	506890000	435320000	610740000	476490000	489810000	659530000
RPS22A;RPS22B	189530000	224460000	391820000	181420000	285940000	367290000
RPS23A;RPS23B	363230000	209190000	106550000	166520000	214520000	141220000
RPS24A;RPS24B	648820000	496560000	363680000	417300000	691380000	414220000
RPS25A;RPS25B	462670000	498670000	498810000	500720000	599490000	567490000
RPS26A	555200000	205690000	89946000	184010000	181620000	131710000
RPS26B	0	1996400	0	0	0	0
RPS27A;RPS27B	448170000	237660000	295750000	245640000	315710000	420120000

Table A3 (Continued): LFQ intensities of Wild Type and *cdc14-1* samples.

	Wild Type samples			*cdc14-1* samples		
Name	WT_1	WT_2	WT_3	CDC14_1	CDC14_2	CDC14_3
RPS28A; RPS28B	0	0	0	0	58738000	0
RPS29A	832230000	159060000	95575000	186770000	439310000	141640000
RPS29B	270310000	34232000	19619000	53011000	88582000	31788000
RPS3	734340000	868530000	1077600000	733400000	1210200000	969700000
RPS30A; RPS30B	16558000	15256000	0	0	14446000	18939000
RPS31	756340000	391440000	795320000	441270000	654010000	403730000
RPS4A;RPS4B	2026100000	949680000	559880000	925630000	1372100000	711950000
RPS5	673900000	629550000	687110000	732740000	752990000	940690000
RPS6A;RPS6B	1281300000	1039700000	883850000	1329300000	934100000	959500000
RPS7A	660990000	540690000	515790000	448530000	918670000	741490000
RPS7B	111980000	90218000	140080000	69339000	110510000	137720000
RPS8A;RPS8B	571780000	472090000	262940000	386940000	364000000	402190000
RPS9B;RPS9A	589310000	242710000	443470000	476320000	451270000	360630000
RPT1	0	0	0	0	42921000	0
RPT2	0	0	0	0	0	0
RPT3	0	0	0	0	24128000	0
RPT4	0	89927000	35174000	27084000	63981000	54252000
RPT5	0	0	0	0	41846000	0
RPT6	0	0	2075900	0	0	0
RRN5	0	41568000	0	0	0	0
RRP12	7326300	0	0	0	0	0
RRP15	0	2096800	0	0	0	0
RRP5	137580000	25975000	32119000	0	26150000	0
RRP9	15031000	0	0	0	0	0
RSC1	0	0	0	0	0	0
RSF2	0	0	0	0	0	0
RSM18	0	0	0	0	10170000	0
RSP5	0	0	0	0	0	0
RTN1	0	83019000	223800000	0	52622000	132320000
RVB1	0	0	0	20604000	0	0
RVB2	0	0	0	32027000	0	0
SAC1	18190000	0	0	0	0	0
SAH1	196060000	210850000	289590000	226520000	386670000	555860000
SAM1	207900000	88315000	113320000	197150000	194870000	189310000

Table A3 (Continued): LFQ intensities of Wild Type and *cdc14-1* samples.

	Wild Type samples			*cdc14-1* samples		
Name	WT_1	WT_2	WT_3	CDC14_1	CDC14_2	CDC14_3
SAM2	0	0	0	0	25236000	0
SAP1	0	0	0	0	0	0
SAR1	0	63341000	58856000	86232000	0	72348000
SBP1	0	36835000	7830700	0	48581000	9343800
SCH9	16729000	0	0	0	0	0
SCL1	0	86555000	85560000	162030000	134250000	156510000
SDH1	328760000	379660000	666030000	435050000	416460000	567580000
SDH2	60260000	130950000	214000000	73344000	131420000	227680000
SDH3	0	0	64839000	0	0	69700000
SEC14	0	0	19305000	0	0	0
SEC21	0	0	0	0	37634000	11933000
SEC23	0	0	38453000	0	31917000	30285000
SEC26	0	0	0	0	0	0
SEC28	0	0	0	0	0	9722700
SEC4	0	0	0	0	29877000	0
SEC53	110310000	81043000	136380000	91057000	136130000	128620000
SEC61	29224000	0	0	0	0	0
SEC63	0	0	0	0	0	0
SED5	0	0	0	0	0	0
SEH1	0	0	0	0	0	0
SEN1	0	247200000	0	0	0	0
SER1	0	0	24303000	0	0	0
SER3	0	0	0	0	0	0
SER33	0	0	0	0	0	0
SES1	0	0	83976000	0	0	66602000
SFC1	282660000	193790000	352690000	246970000	200600000	226790000
SFI1	595850000	30878000	3199800	24740000	8725800	0
SGN1	0	0	11004000	0	0	0
SHE9	0	184850000	0	0	0	0
SHM2;SHM1	110360000	98453000	98484000	64978000	164590000	151450000
SIK1	3789600000	1657700000	657180000	2426700000	1833100000	1211100000
SIS1	0	0	0	0	0	6368000
SNA2	0	0	24992000	0	0	0
SNF1	7262800	0	0	0	0	0
SNF4	37611000	0	0	0	0	0
SNU13	1013000000	330370000	731270000	696510000	983750000	548720000
SOD1	0	163900000	162960000	0	133790000	92251000

Table A3 (Continued): LFQ intensities of Wild Type and *cdc14-1* samples.

	Wild Type samples			*cdc14-1* samples		
Name	WT_1	WT_2	WT_3	CDC14_1	CDC14_2	CDC14_3
SOD2	51764000	140450000	346470000	95204000	164220000	155310000
SOF1	0	0	0	0	0	0
SPC110	2576800000	2736800000	1515900000	4005900000	4373400000	3366800000
SPC29	4715200000	1378600000	619780000	3256100000	2076700000	1177800000
SPC42	**2.2103E+11**	**3.1789E+11**	**2.4207E+11**	**6.8588E+11**	**4.0572E+11**	**2.9532E+11**
SPC72	2840200000	475040000	266840000	541040000	1244900000	603610000
SPC97	1306900000	0	0	0	130730000	47713000
SPC98	1460200000	25596000	0	52252000	280340000	97825000
SPE3	0	0	0	0	0	0
SPO14	0	0	92486000	0	0	0
SPO21	0	0	0	0	27155000	0
SPO23	0	0	0	0	9681000	0
SPR3	0	0	0	0	33500000	0
SPS19	0	383680000	62152000	0	105860000	22282000
SPS4	0	0	0	0	30049000	0
SPT15	0	0	10323000	0	0	0
SPT5	40027000	73114000	49627000	85430000	72968000	51756000
SPT7	0	0	53745000	0	0	0
SRO9	72446000	0	0	0	0	0
SRP1	0	0	2744700	0	0	0
SRP40	108380000	46795000	0	0	46326000	0
SSA1	2400500000	3924400000	4192800000	4107200000	4779900000	3993600000
SSA2	512830000	243600000	165220000	644130000	484240000	465360000
SSA3	0	11851000	0	0	0	0
SSA4	0	31004000	0	0	0	0
SSB1	0	0	0	0	0	117940000
SSB2	6858600000	6652800000	5281100000	1315100000	9876300000	9870400000
SSC1;ECM10	1074900000	2894000000	2843200000	4051000000	3697900000	2994600000
SSD1	51585000	83592000	0	15989000	33461000	17496000
SSE1;SSE2	0	106770000	224810000	130450000	156630000	342050000
SSF1;SSF2	23249000	0	0	0	0	0
SSO1;SSO2	0	0	24562000	0	0	0
SSS1	0	0	22271000	0	0	0
SSZ1	0	0	0	0	0	7543500

Table A3 (Continued): LFQ intensities of Wild Type and *cdc14-1* samples.

	Wild Type samples			*cdc14-1* samples		
Name	WT_1	WT_2	WT_3	CDC14_1	CDC14_2	CDC14_3
STE6	0	1335300	0	0	0	0
STI1	0	0	27414000	0	0	0
STM1	0	30499000	24330000	0	0	65049000
STO1	0	0	0	0	6432100	0
SUB2	0	0	27052000	0	0	0
SUI1	0	0	15501000	0	0	0
SUI2	0	0	0	0	0	27813000
SWT1	0	0	0	0	101090000	0
TAL1	0	83180000	164040000	60917000	141870000	153610000
TCO89	0	76876000	0	0	0	86177000
TCP1	0	4933000	0	0	0	0
TDH1	0	661740000	861120000	0	43375000	132090000
TDH2	327420000	1018880000	1700800000	621230000	940130000	985660000
TDH3	104980000000	222830000000	265410000000	147550000000	220640000000	225660000000
TEF1;TEF2	9590400000	9724500000	1030700000000	7720500000	1061100000000	1029100000000
TEF4	146680000	174460000	263670000	170330000	197720000	267350000
TEM1	13523000	0	0	0	0	0
TES1	138730000	360850000	246500000	0	337730000	182320000
TFP1	32923000	45567000	22787000	0	60858000	25453000
TGL3	0	37871000	0	0	0	0
TGL4	0	35174000	0	0	0	0
THR1	0	0	76666000	0	13547000	26439000
THR4	0	0	69778000	0	0	40038000
THS1	0	0	0	0	36106000	0
TIF1;TIF2	339590000	575960000	779500000	464160000	509480000	723360000
TIF5	0	0	0	0	0	10471000
TIF6	0	0	50283000	56882000	52443000	0
TKL1	142780000	219990000	434070000	264280000	291890000	428100000
TMA19	0	64076000	111010000	52393000	48096000	114430000
TMA29	0	0	141840000	0	0	0
TNA1	0	0	0	0	0	0
TOF2	0	17466000	0	0	0	0
TOM40	0	0	0	0	12128000	0
TOM70	0	0	0	0	15506000	8213000
TOR1	0	233430000	0	0	40055000	77180000

Table A3 (Continued): LFQ intensities of Wild Type and *cdc14-1* samples.

	Wild Type samples			*cdc14-1* samples		
Name	WT_1	WT_2	WT_3	CDC14_1	CDC14_2	CDC14_3
TOR2	0	105410000	0	0	0	0
TPD3	0	0	19920000	0	24504000	0
TPI1	604590000	1909000000	3853200000	1010000000	2072700000	2483700000
TPS1	109500000	172910000	197640000	102630000	158140000	172980000
TPS2	0	0	0	0	0	0
TRA1	39781000	0	0	0	0	0
TRP3	13412000	0	0	0	0	0
TRP5	0	0	13176000	0	0	0
TRX2;TRX1	0	0	0	0	20087000	0
TSA1;TSA2	317760000	493810000	976810000	586500000	461360000	654850000
TSC11	0	0	0	0	0	0
TUB1;TUB3	89538000	67847000	0	83794000	76283000	0
TUB2	287470000	344760000	235640000	258350000	109800000	275650000
TUB4	1926200000	0	0	45930000	196000000	77740000
TUF1	0	110120000	138880000	101780000	132940000	161030000
TUS1	0	0	389050000	0	0	0
UBA1	0	0	0	0	0	23299000
UBA4	68808000	1656400000	3114400000	5892600000	7424700000	3583900000
UBP13	0	0	0	0	0	0
UGP1	0	296890000	173200000	97142000	198530000	114220000
URA1	0	79292000	117080000	0	89090000	105630000
URA2	496290000	450270000	600290000	819590000	376790000	1166300000
URB1	25975000	0	0	0	0	0
URB2	0	0	0	0	0	0
UTP10	62280000	0	0	0	0	0
UTP13	27730000	0	0	0	0	0
UTP15	75204000	0	0	0	0	0
UTP21	10143000	0	0	0	0	0
UTP22	9607600	0	0	0	0	0
UTP4	20862000	0	0	0	0	0
UTP5	16059000	0	0	0	0	0
UTP6	12194000	0	0	0	0	0
UTP8	31655000	0	0	0	0	0
UTP9	34295000	0	0	0	0	0
UTR2	0	0	0	0	0	2573900

Table A3 (Continued): LFQ intensities of Wild Type and *cdc14-1* samples.

	Wild Type samples			*cdc14-1* samples		
Name	WT_1	WT_2	WT_3	CDC14_1	CDC14_2	CDC14_3
VAC8	0	0	0	0	0	0
VAS1	0	0	0	0	0	31251000
VID22	0	0	0	0	0	126240000
VMA2	94681000	176650000	120000000	94285000	223600000	87162000
VMA5	0	0	13963000	0	0	0
VNX1	0	6472200	0	0	0	0
VPH1	0	448260000	142580000	0	77667000	148400000
VPS1	0	0	0	0	21998000	0
VTC4	0	156070000	73212000	0	36935000	51447000
WBP1	12352000	0	0	0	0	0
WRS1	0	0	0	0	0	0
WTM1	0	58691000	113660000	33880000	132550000	46524000
YAP5	85933000	0	0	0	0	0
YAT1	79814000	120480000	104850000	0	0	66781000
YAT2	0	31707000	55739000	0	0	61387000
YBL028C	0	0	0	0	0	18823000
YCK2	0	0	0	0	0	0
YCL057C-A	0	0	0	0	0	42142000
YCP4	0	0	67652000	0	31789000	56917000
YCS4	0	0	0	0	0	0
YDJ1	0	0	0	0	0	16539000
YDL086W	0	0	0	0	0	0
YDL237W	0	0	0	0	0	0
YDR051C	213890000	0	0	0	0	0
YDR374C	0	0	0	0	52356000	0
YEF3;HEF3	437480000	385310000	319950000	432520000	599030000	662310000
YER078C	7547100000	1586300000	926810000	3405500000	3021900000	1351000000
YFL052W	0	0	0	0	0	0
YGL059W	8804600	0	0	0	0	0
YGL194C-A	31262000	0	0	0	0	0
YGR130C	0	0	0	0	42550000	0
YGR207C	0	0	15815000	0	0	0
YGR250C	0	0	7732100	0	0	0
YGR283C	0	0	0	0	0	0
YHB1	0	0	10965000	0	0	0

Table A3 (Continued): LFQ intensities of Wild Type and *cdc14-1* samples.

	Wild Type samples			*cdc14-1* samples		
Name	WT_1	WT_2	WT_3	CDC14_1	CDC14_2	CDC14_3
YHM2	0	0	13757000	0	0	0
YHR020W	0	0	19051000	0	0	0
YHR097C	0	4202400	0	0	0	0
YIL057C	6383400	28637000	0	17887000	10261000	14417000
YIP3	0	0	0	0	0	0
YJL043W	0	0	0	0	27159000	0
YJL045W	0	0	0	0	0	0
YJR008W	0	31225000	11401000	0	12992000	0
YKL018C-A	0	35978000	0	0	37878000	0
YMR031C	0	0	0	0	0	0
YMR099C	0	0	44604000	0	0	37991000
YMR31	0	11827000	0	0	0	0
YMR310C	0	0	0	0	8787200	0
YMR315W	0	0	0	0	0	0
YNK1	0	207230000	427640000	170990000	181710000	409330000
YNL134C	0	0	17673000	0	0	0
YNR036C	0	0	0	0	13802000	0
YOL083W	0	0	0	0	232480000	0
YOP1	0	81279000	111990000	0	83716000	98709000
YOR029W	0	0	0	0	0	0
YOR285W	0	0	49435000	0	0	0
YPK1	0	0	0	0	4354800	0
YPK2	3123200	0	0	0	0	0
YPL225W	0	0	0	0	0	0
YPL260W	0	0	0	0	1410300	0
YPR004C	0	17169000	0	0	0	0
YPR089W	0	0	0	0	0	0
YPR115W	0	0	0	0	0	0
YPS5	0	0	0	0	0	0
YRA1	0	0	55034000	0	48213000	0
YSP3	0	0	0	0	0	0
YSW1	0	78885000	23024000	0	0	0
ZIP2	0	29510000	0	0	0	0

Table A3 (Continued): LFQ intensities of Wild Type and *cdc14-1* samples.

	Wild Type samples			***cdc14-1* samples**		
Name	WT_1	WT_2	WT_3	CDC14_1	CDC14_2	CDC14_3
ZUO1	0	0	33828000	0	0	53429000
ZWF1	0	0	0	0	23328000	0

Table A3 (Continued): LFQ intensities of Wild Type and *cdc14-1* samples.